Security Impact Assessment of Active Distributed Network (ADN) on the Future Grid Operations

Ifedayo Oladeji

A thesis submitted to
Auckland University of Technology – (AUT)
in fulfilment of the requirements for the degree of
Doctor of Philosophy
(PhD)

2023

School of Engineering, Computer, and Mathematical Sciences

Abstract

Fossil fuel-based power generation contributes significantly to global warming. To decarbonize the electric power generation, a significant amount of renewable energy sources (RES) based-distributed generation (DG) units will be connected to the grid. High penetration of RES-DG units connected at different grid levels will provide technical merits if properly planned and operated. The concern, however, is how to guarantee the security of the grid with high penetration of RES-DG, considering the characteristics of the power grid and the behaviours of the connected RES-DG units under both steady-state and transient conditions. Penetration of DG units creates an active distribution system (ADN) with several impacts within the ADN and the transmission-distribution network boundary nodes. Variability of the grid load levels and power generation from RES-DG units will also impact the grid security. Voltage fluctuations, reverse power flow, power intermittency, and harmonics increase are some of the effects of high penetration of RES-DG units on the distribution network. The absence of mechanical inertia support from the RES-DG units during grid disturbance reinforces the need to be concerned about the penetration level. It is therefore important to understand the specific impact of high penetration of RES-DG units on the security of the different levels of the grid. The knowledge obtained will help operators plan toward increasing the penetration level of RES-DG units and apply appropriate measures and suitable control schemes to mitigate arising stability issues due to the high penetration.

This PhD research aims to assess the security impact of high penetration of RES-DG units on modern grid operations. The security assessment and proposed models border three key integrated grid sections: the transmission network, the distribution network, and the transmission-distribution network boundary. The results of investigating the impacts of RES-DG unit operations on the identified grid sections are presented in separate chapters. Two chapters are dedicated to the offline and online assessment and prediction of the security of the transmission grid.

Chapter 1 provides the background of this thesis. Also, it contains the research gaps, objectives, and specific contributions of the thesis. Chapter 2 provides a comprehensive literature review of the security impact of active distribution networks on modern grid operation. Chapter 2 also reviews the technical impacts of RES-DG penetration into the grid and discusses the role of renewable energy source generation in the grid transition. It also presents a comprehensive review of proposed techniques to limit the security impacts on the three identified grid sections. Lastly, it identifies several research gaps and drawbacks that eventually formed part of the research question in this thesis.

The proposed methods start with the optimal placement of RES-DG units in a distribution network in Chapter 3. The method in Chapter 3 involves developing a decision tree classification

technique to optimize the network's security indices under the nodal hosting capacity and PVDG capacity constraints. The security indices considered in this paper are the branches' risk index (RI) and power loss (PL). The proposed method is a robust machine learning approach with deterministic and probabilistic security indices to determine the optimal placement of PVDG units. Chapter 3 also analyses the impacts of the different PVDG units' voltage control modes on the performance of the distribution network.

Chapter 4 presents a method to assess, classify and predict the security of the integrated grid using varying grid parameters with an offline machine learning approach. Firstly, an adaptive neuro-fuzzy inference system (ANFIS) suitable for real-time applications is developed to predict the critical clearing time considering varying load levels and grid inertia. Then, a continuous transient stability assessment technique is developed to generate the training dataset. A density-based clustering via classification approach is proposed to label the dataset. Finally, a predictive model was obtained from the labelled dataset using a Naïve-Bayes (NB) probabilistic classifier. The advantage of the proposed technique in this chapter lies in considering the impact of the penetration of RES-DG units on the grid’s security and the wide range of contingencies considered. Also, prior knowledge of the grid’s security state is not required with the proposed clustering approach.

After establishing the offline security assessment and prediction method in Chapter 4, Chapter 5 presents a framework for online security prediction and control for modern power grids. System operators must assess the grid's security for specific levels of inertia, load, RES-DG penetration, and fault location to plan, control, and operate the network securely. Unlike offline methods, an online security prediction framework can establish potential grid security in a reasonable time ahead. Thus, this chapter proposes an incremental machine learning training technique and intelligent security control system to ensure the grid's security. An incremental Naïve Bayes algorithm is applied to the training dataset developed from the responses of the grid to transient stability simulations. The intelligent security control system consists of a Gaussian process regression-based load shed value estimator. The proposed intelligent security control system ensures the grid's security for predicted insecure scenarios by estimating the load shed value to keep the operation of the grid in a security state.

The coordinated operation between the transmission and distribution networks is necessary to ensure the security of the modern grid. Interaction must exist between transmission and distribution systems operators acting independently to maintain grid voltage within the individual networks. The operation of the modern grid involves the utilization of the flexibilities of the active distribution network to achieve voltage supports during grid disturbance. It is therefore vital to ensure security at the transmission-distribution network boundary during flexibility operations. Consequently, Chapter 6 develops a bi-level model (economic and technical objective levels) to achieve optimal flexibility operation. The economic objective is

achieved through a robust distribution network reconfiguration technique to minimize network losses. An improved decision tree classification technique is proposed for level two to determine the amount of flexibility in MW for optimal voltage support. The optimization problem in the first level is solved using a fmincon solver algorithm considering deterministic and probabilistic constraints. The proposed algorithm minimizes the power loss and optimizes the voltage support for specific grid operations. The thesis closes with Chapter 7, which presents the conclusion from the PhD research drawn from Chapters 2 to 6 and the future work and prospects to broaden the subjects addressed in this study.

Contents

List of Figures

List of Tables

Attestation of Authorship

I hereby declare that this submission is my work and that, to the best of my knowledge and belief, it contains no material previously published or written by another person (except where explicitly defined in the acknowledgements), nor material which to a substantial extent has been submitted for the award of any other degree or diploma of a university or other institution of higher learning.

Chapters 2 – 6 of this doctoral thesis comprise separate several rounds of peer-reviewed manuscripts. Manuscripts in Chapters 2 – 5 are journal manuscripts (either published or submitted), while Chapter 6 is a manuscript submitted to a conference. All co-authors have approved the inclusion of the joint work in this doctoral thesis.

10/10/ 2022

Signature

Date

Co-Authored Articles and Contributions

Chapter Title	Author	Contribution (%)
Chapter 2: Security Impacts Assessment of Active Distribution Network on the Modern Grid Operation - A Review	I. Oladeji P. Makolo M. Abdillah J. Shi R. Zamora	80 2 5 5 8
Chapter 3: Security Constrained Optimal Placement of Renewable Energy Sources Distributed Generation for Modern Grid Operations	I. Oladeji R. Zamora T.T. Lie	85 10 5
Chapter 4: Density-based clustering and probabilistic classification for integrated transmission-distribution network security state prediction	I. Oladeji P. Makolo R. Zamora T.T. Lie	82 3 10 5
Chapter 5: An online security prediction and control framework for modern power grids	I. Oladeji R. Zamora T.T. Lie	85 10 5
Chapter 6: A Bi-Level Security Constrained Model for Optimal Flexibility Operation	I. Oladeji R. Zamora T.T. Lie	85 10 5

We, the undersigned, hereby agree to the participation percentages and contribution to the chapters identified in the table above.

Dr Ramon Zamora
(Primary Supervisor)

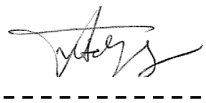

Prof Tek-Tjing Lie
(Secondary Supervisor)

Dr Peter Makolo
(Collaborator)

Dr Muhammad Abdillah
(Collaborator)

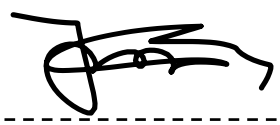

Dr Jian Shi
(Collaborator)

Publications During the PhD Programme

Articles in peer-reviewed journals

Oladeji, I.; Makolo, P.; Abdillah, M.; Shi, J.; Zamora, R. Security Impacts Assessment of Active Distribution Network on the Modern Grid Operation—A Review. Electronics 2021, 10(16), 2040; https://doi.org/10.3390/electronics10162040 **(Published).**

Oladeji, I.; Zamora, R.; Lie, T. An Online Security Prediction and Control Framework for Modern Power Grids. Energies 2021, 14(20), 6639; https://doi.org/10.3390/en14206639 **(Published).**

Oladeji, I., et al. " Security Constrained Optimal Placement of Renewable Energy Sources Distributed Generation for Modern Grid Operations ", Sustainable Energy, Grids and Networks, vol. 32, 2022, https://doi.org/10.1016/j.segan.2022.100897 (**Published**).

Oladeji, I., et al. " Density-based clustering and probabilistic classification for integrated transmission-distribution network security state prediction ", Electric Power Systems Research, vol. 211, p. 108164, 2022. ISSN 0378-7796, doi.org/10.1016/j.epsr.2022.108164 (**Published**).

Conference contributions

Oladeji, I., et al. (2021). Optimal Placement of Renewable Energy Sources Distributed Generation in an Unbalanced Network for Modern Grid Operations. 2021 International Conference on Smart Energy Systems and Technologies (SEST) **(Published).**

Franklin Nkado, **Oladeji, I**., et al. (2022). Data clustering for Optimal Photovoltaic-Distributed Generation Placement in an Active Distribution Network (Nigercon) **(Published).**

Oladeji, I., et al. "Instance-based model-driven technique for online critical clearing time prediction for the modern power grid ", SPIES 2022 **(Accepted).**

Preface

This thesis has been prepared at the School of Engineering, Computer and Mathematical Sciences, Auckland University of Technology, New Zealand, in fulfilment of the requirements for a Doctor of Philosophy (PhD) degree award. The work has been carried out from February 2019 to September 2022 under the supervision of Dr Ramon Zamora and Prof Tek-Tjing Lie.

The main goal of this thesis is to develop models to monitor and ensure the security of the modern power system with high penetration of renewable energy sources. A holistic approach to modern power system security is implemented by considering the security implications of RES-DG operations on the active distribution network, the transmission network, and the transmission-distribution boundary. An optimal RES-DG placement model was proposed for the distribution network to optimize the risk index and power loss while considering the hosting capacity. Offline and online security assessment techniques are developed for the integrated transmission distribution network. The impact of RES-DG operations at the T-D boundary during voltage support operation was also studied. The optimization models and security assessment techniques are intended to ensure the integrated transmission-distribution network's security with increased RES-DG penetration in the quest for a 100% renewable energy power grid.

This PhD thesis follows the Auckland University of Technology (AUT) institution's doctoral thesis Format Two, also referred to as the “Manuscript Format”. The thesis comprises seven chapters. Apart from Chapters 1 and 7, which contain the thesis introduction and conclusion, Chapters 2 – 6 contain manuscripts either already published in a journal or submitted for publication. Consequently, some repetitions in the general introductions and technical discussions may be observed across some chapters within this thesis. Preambles are included between Chapters 2 – 6 to enhance the synthesis of the chapters of the thesis. The rest of each chapter is identical to the published journal article or submitted manuscript. Finally, Chapter 7 contains the conclusion and major discussion of Chapters 2 - 6 and provides future work related to the security of the low inertia in modern and future networks.

Acknowledgments

This doctoral thesis represents the compilation of the research output during my time as a research student at Auckland University of Technology (AUT), Auckland, New Zealand. Many people have contributed to the success of the PhD research in one way or another to help and support the realization of this thesis. I glorify the Almighty God, the giver of life, for providing me with strength, knowledge, and sustenance throughout my PhD research.

I express my heartfelt gratitude to my primary supervisor, Dr Ramon Zamora who has significantly supported me in this PhD journey even from the application process. Dr Ramon's incredible vision and pursuit of excellence raised the bar, and I would like to express my deep acknowledgment of your mentorship style. Also, I appreciate your invaluable time in reviewing all the manuscripts written along the way to the culmination of this thesis. This thesis would not be possible without your useful comments and suggestions for each manuscript. My sincere thanks also go to my co-supervisor, Prof Tek Lie, for providing me with invaluable insights, inspiration, and support.

I would also like to express my sincere appreciation to Dr Peter Makolo for the fruitful collaboration on three journal articles and one conference paper. His contributions and productive discussions during the research group meetings are also highly appreciated. The contributions of past, present, and honorary members of the research group: Dr Nicholas Mukisa, Dr Leo Yazhou Jiang, Xin Lin, Asaad Mohammad, and Uvini Perera, are well appreciated.

Special thanks go to the New Zealand government through the Ministry of Foreign Affairs and Trade (MFAT) for providing me with the Scholarship opportunity to pursue my PhD research in New Zealand. I thank the AUT Manaaki scholarship team for their encouragement and support during difficult times. I also wish to appreciate the efforts of all staffs of the School of Engineering, Computer, and Mathematical Sciences, AUT for creating a conducive atmosphere for learning and research.

I am also indebted to my family. I am deeply grateful to my lovely wife, Iyanuoluwa Mercy, and our son Temidayo. Your unwavering love and prayers are my primary source of energy and strength. To my dear Mother, Alaba Mary, thank you for the sacrifices you made for me and the opportunities those sacrifices have given me. Thanks to my dear brothers and sister, Olawale, David, and Adeola, your prayers kept me moving in the PhD journey. May God bless you abundantly. I also appreciate my in-laws, the Awojoodu's, for all their prayers, support, and encouragement throughout all these years. May our love continue to grow stronger.

I am also grateful to the Abolarinwa, Martins, and the Apostolic faith mission church in Australia. They have been a source of happiness and extended their brotherly hands whenever I needed them during my challenging times in New Zealand. May God bless you.

1 Introduction

1.1 Background and motivation

Numerous driving factors influence the interest in renewable energy sources (RES)-based power generation systems. These factors include the demand for clean energy, demands for new electricity market policies for decentralization, and the demand for improved technical performances with new operating constraints [1]. In response to these demands, the shares of renewable energy sources-based power generation systems such as solar photovoltaic (PV) and wind turbine (WT) systems have significantly increased within the grid over the past few decades. The energy policies from several countries aim to achieve 100% power generation from renewable energy sources-based power generation units [2]. Consequently, many synchronous generators in the grid will be replaced with RES-distributed generation (DG) units connected to all grid levels [3]. However, as the penetration of the RES-DG units increases, several security concerns emerge due to the characteristics of the RES-DG units regarding the power production unpredictability and the lack of a non-mechanical connection to the grid. [4].

The concerns of high penetrations of RES-DG units into the grid can be summed up into intermittency, availability, and security challenges. The power output from the RES-DG units mostly depends on variable sources. The variability of the sources results in the intermittency of power generation, which could result in over-generation and under-generation. The RES-DG units are connected electronically to the grid and do not have mechanical inertia to support the grid during major disturbances. Mechanical inertia is important to resist the sudden change in the grid frequency during power imbalances caused by a disturbance in the network. Consequently, replacing traditional synchronous generators with RES-DG units reduces the effective rotational inertia in the grid [5, 6]. Grids with high penetration levels of RES-DG units and reduced effective inertia are referred to as low inertia grids. Low inertia grids are vulnerable to several operational and security challenges [7], as recorded in recent partial and total blackouts events in [8-10]. In order to meet modern society's demands for increased energy efficiency and system security, the modern low inertia grid framework includes critical capabilities such as bidirectional power flow, inter-device communication, cyber and physical protection, automatic fault detection, and resilience. Upgrading the existing high-inertia traditional grid requires modernization of components as well as the development of new operation optimization and control techniques. Table 1.1 compares the traditional grid and the modern low-inertia grid.

Table 1.1: Comparison between traditional and modern grid

Traditional Grid	**Modern low-inertia Grid**
Limited demand-side participation	Advance demand-side participation
Uni-directional communication	Bi-directional communication
Centralized bulk generation	Decentralized distributed generation
Low penetration of RES-DG and ESS	High penetration of RES-DG and energy storage systems
Mechanical inertia	Synthetic inertia
Low ROCOF	High ROCOF
Limited sensors	Abundant sensor
High short circuit current	Low short circuit current

Modern system operators are committed to adopting effective techniques to mitigate the impact of disturbances in low inertia grids. The solutions will include techniques to estimate, monitor, and predict insecurities in the grid and determine appropriate control actions to ensure the grid's security for insecure states. Although many grid security challenges emerge at high penetrations of RES-DG units into the grid, RES-DG units are also an essential part of several existing control techniques to enhance security and improve the grid's resilience. The control techniques, however, are applied at the alert/asecure system state as corrective measures to prevent the grid from entering the insecure states. Intelligent load shedding, demand-side participation, synthetic inertia, virtual power plant system, and flexibilities from an active distribution network are among the established control strategies employed to address the underlying operational and stability challenges in low inertia grids [11, 12].

The demands for the operation of the generation units connected to the distribution network increase with the demand for the distribution network's participation in grid's security. The RES-DG units are the main components for power generation within the modern distribution network. The schemes to support the grid's security for long- and short-term ranges can be categorized into planning, operation, and enhancement schemes. For the modern grid, more emphasis should be on optimal planning of RES-DG units within the distribution network and optimal operation during flexibility services. The capabilities of the developed models should include multi-RES-DG penetration level assessments and dynamic network reconfiguration for effective flexibility operation during voltage support.

The reduced equivalent inertia values and varying total power generation in the grid due to the high penetration of RES-DG units is a new concern for modern network operators. Also, the constant changes in grid load and occurrences of contingencies are other attributes considered during grid planning and operations. The grid attributes, which used to be relatively constant, are now time-varying, making the grid's security state a time-varying phenomenon. If the system attributes can significantly change with time, then the security states will fluctuate between the defined security states with high unpredictability [13]. The varying security state of the modern grids is a new challenge facing modern grid operators. Consequently, there is a growing need for effective and accurate techniques for estimating, classifying, and hence, predicting the security states of the grid

for security control and enhancement [14]. An accurate grid's security state prediction for every grid operating scenario can ensure the grid's security for the current RES-DG penetration level and increments in future penetration levels.

Offline techniques have been established for the estimation of the security of the grid through the knowledge of the grid's response to transient disturbances with increased penetration levels of RES-DG units. The techniques involve algorithms to identify the state of the power system using identified pre-fault, during-fault, and post-fault parameters. For instance, offline methods such as in [15-17] classify the grid's security using assessed and historical voltage values during events in the grid. Offline transient security assessment requires computations and often involves tedious steady and transient stability simulations. Therefore, offline security assessment and estimation techniques are not suitable for grid protection and control measures required for real-time operations. Consequently, online security assessment and classification techniques such as in [18, 19] are proposed using establishing algorithms that can monitor the security states of the grid and, therefore, can be used for protection and control in real-time.

As security is becoming highly volatile in the modern grid, it is vital to consider a holistic view to ensure the security of the modern grid. Independent solutions may no longer be effective as the modern grid is highly integrated and characterized by a bi-directional power flow and information flow. A holistic and comprehensive solution will include models at the transmission and distribution network levels of the grid and at the boundary to ensure and enhance the security of the modern grid. Solutions for transmission networks would include security assessment, classification, and prediction models with varying grid attributes. Solutions for the distribution network would consist of active distribution network planning and operation models considering specific security objectives and constraints. At the boundary between the transmission and distribution networks, the solutions would include models for optimal flexibility operations for voltage, considering the boundary elements' security constraints.

1.2 Research gaps

The review of recent literature related to the security of modern grids with high penetration of RES-DG units indicates that:

- There is a lack of security-based probabilistic objectives and constraints in the RES-DG placement problem formulation for the unbalanced distribution network in the literature.

Most existing approaches only considered the steady-state voltage security of the grid. Many proposed transient security assessment techniques are computationally complex [19-21]. It is evident from the literature review that there is a need for an improved, less computationally complex model for optimal distribution network with RES-DG planning and operation. The new techniques should

be more effective, computationally less complex and considering both deterministic and probabilistic variables.

- The roles of probabilistic security prediction models as a solution to the arising security challenges of grids with high penetration of RES-DG units have not been adequately explored.

Although many techniques to assess the security of the emerging power grids exist in the literature, the impact of high penetration of RES-DG units on the time-changing equivalent inertia in the modern grid has not been thoroughly covered in the literature. For the secured operation of the modern grid with high penetration of RES-DG units, it is essential to have the capability to predict the security with respect to the transmission network, distribution network, and boundary elements during flexibility operations. The successful offline and online classification and prediction of the frequency and voltage response of the modern grid enables the grid operators to activate appropriate control measures as proposed in this thesis to ensure the security of the grid [11, 22-24]

- Very little attempt to extend the online security predictor determinants to include varying parameters critical to the grids with high penetration of non-synchronous generators.

Modern grid operators aim to securely increase the power generation from RES-DG units in order to achieve a close to 100% renewable energy grid. Therefore, there is a need to develop a new online security prediction and intelligent security control technique. The developed technique for ensuring the grid's security with respect to the transmission network should consider time-varying inertia, load changes, contingencies, and the impact of different types of RES-DGs while limiting the computation burden and time during predictions. Also, the security prediction model should consider easily computed grid features such as post-disturbance voltage, frequency, and power transfer.

- There is need for more research to include probabilistic and security constraints in the reconfiguration problem formulation for optimal flexibility support from the distribution network.

Many of the existing techniques focus only on economic considerations to minimize the cost of flexibility operation. Also, there are no models to mitigate the negative impact of flexibility operations on the grid’s security. New probabilistic security indices should be considered for RES-DG penetration planning and flexibility operation to minimize the risk of insecurity associated with aggregated distributed energy resources operations. Enhanced interaction between the transmission and distribution network operators through optimal flexibility operations will ensure the security of the grid with RES-DG units.

1.3 Research questions and objectives

Based on the challenges of the modern network due to reduced effective inertia, variabilities in power output, and increase in flexibility demand, this research work aims to develop models to assess, predict and ensure the security of the modern grid considering the high penetration of RES-DG and operations of the active distribution networks. The models are proposed to address research questions concerning ensuring the security of the modern grid with high penetration of RES-DG units and enhancing the interaction between the future transmission and distribution system (TSs and DSs) for voltage controls. The proposed models are designed for the distribution network, transmission network, and the boundary between the two networks.

The research questions addressed in this research are as follows:

- How to assess and ensure the power grid's security under high penetration of RES-DG units, network contingencies, and other grid components?
- How to enhance the interaction between the future transmission and distribution system (TSs and DSs) for voltage control?

The specific research objectives developed from the research questions are listed below:

- To develop a RES-DG optimal placement technique in an unbalanced distribution network considering novel security objectives. The developed method helps to assess the impact of penetration of RES-DG units on the voltage risk and to minimize the network power loss.
- To develop an offline security clustering and classification technique using grid post-contingency response information. The developed technique considers different RES-DG types, several RES-DG penetration levels, and different contingencies and faulted elements.
- To develop an online security prediction technique with varying grid attributes compared to existing security classification. The technique predicts the grid's security with varying inertia, load level, fault locations, and dispatch from RES-DG units.
- To develop a technique to optimize the flexibility of the active distribution network for voltage support at the transmission and distribution boundary. The developed method will help DSO to determine the best distribution network reconfiguration to obtain the optimal impact during flexibility operations.

1.4 Contributions

The work presented in this Ph.D. thesis is in the form of manuscripts, where each manuscript has unique contributions to the body of knowledge related to the security of the modern grid with the varying penetration of RES-DG units. In response to the research gaps identified in the literature, the contributions of this thesis are highlighted as follows:

- A security-constrained optimal RES-DG placement technique using a decision tree classification approach with novel indices. The technique considers deterministic and probabilistic variables and the impact of various RES-DG local voltage control modes, which have not been considered in the literature.
- A novel grid security state prediction technique using density-based clustering and a probabilistic machine learning approach. The technique proposes an algorithm for dataset development that considers the penetration levels of different types of DGs and contingencies on the elements in the network.
- A state-of-art online security prediction and control method using an incremental machine learning model training process. The method uses time-varying grid attributes which are not considered in the literature for online grid security prediction.
- A novel bi-level security-constrained method for optimal flexibility operation for voltage support. The proposed method considers the economic and technical objectives at separate levels to determine the optimal voltage flexibility operation points.

1.5 Thesis outline

This PhD thesis follows the Auckland University of Technology (AUT) institution's doctoral thesis Format Two, also referred to as the “Manuscript Format”. Chapter 1 presents the overall thesis introduction. Chapter 2 covers a literature review on the existing technique for assessing the security impact of increased penetration of RES-DGs into the grid and methods to ensure the grid's security considering the modern grid's new dynamics. An optimal RES-DG placement technique is presented in Chapter 3. Chapter 4 consists of the offline security clustering and classification for the integrated transmission-distribution network. A framework for online security prediction with varying grid attributes is presented in Chapter 5. Furthermore, Chapter 6 presents the optimization of flexibility operation for voltage support in modern networks. Finally, the summary of the conclusions from each chapter and considerations for future research related to the security of the modern grid are presented in Chapter 7. **Error! Reference source not found.** below shows the thesis structure, the chapter titles, and the titles of the manuscripts for Chapters 2 - 6.

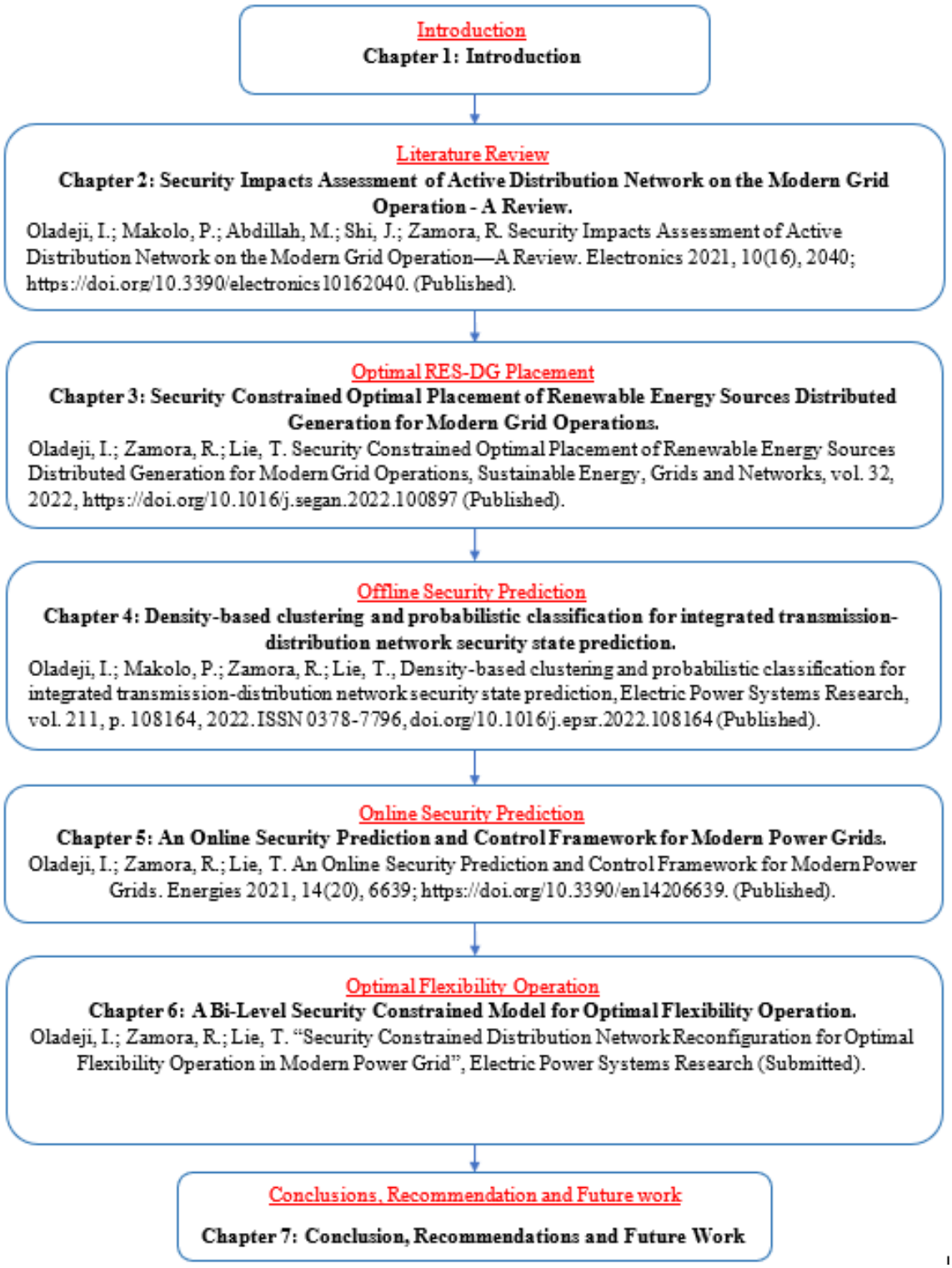

Figure 1.1: Thesis structure

2 Manuscript 1: Literature Review

Preamble

Chapter 2 presents the motivation for undertaking this research, focusing on the discussions and studies presented in subsequent chapters. As the effective inertia in the modern grid becomes a varying attribute due to changing penetration levels of renewable energy sources-based distributed generation (RES-DG) units, effective grid security assessment, prediction, and enhancement techniques are needed. The chapter opens with a discussion of the role of RES-DG in the emerging power grid. The review of the technical impacts of RES-DG is presented afterward. The chapter also reviews and discusses existing recommendations to limit the negative impacts of high penetration of RES-DG units and maximize the benefits of the RES-DG units. Also, it examines existing research trends to support high penetration of RES-DG with a focus on components and interaction between the integrated transmission and distribution networks to achieve a 100% renewable energy grid. The survey emphasizes the significance of interaction of models for ensuring the grid's security at both distribution and transmission levels. Lastly, Chapter 2 also reinforces the need to develop offline and online security prediction models considering artificial intelligence algorithms.

Security Impacts Assessment of Active Distribution Network on the Modern Grid Operation—A Review

Ifedayo Oladeji[1]*, Peter Makolo[1], Muhammad Abdillah[2], Jian Shi[3] and Ramon Zamora[1]

[1]Department of Electrical and Electronic Engineering, Auckland University of Technology, Auckland 1010, New Zealand
[2]Department of Electrical Engineering, Universitas Pertamina, Jakarta 12220, Indonesia;
[3]Department of Engineering Technology, University of Houston, Houston, TX 77204, USA

Abstract: The future grid will include a high penetration of distributed generation, which will have an impact on its security. This paper discusses the latest trends, components, tools, and frameworks aimed at 100% renewable energy generation for the emerging grid. The technical and economic impacts of renewable energy sources (RES)-based distributed generation (DG) on the emerging grid security are also discussed. Moreover, the latest approaches and techniques for allocating RES-DG into the distribution networks using specific performance indices based on recent literature were reviewed. Most of the methods in recent literature are based on metaheuristic optimization algorithms that can optimally allocate the RES-DGs based on the identified network variables. However, there is a need to extend these methods in terms of parameters considered, objectives, and possible ancillary support to the upstream network. The limitations of existing methods in recent literature aimed at ensuring the security of the integrated transmission-active distribution network under high RES-DG penetration were identified. Lastly, the existing interaction methods for voltage and frequency control at the transmission and active distribution system interface were also investigated. Relevant future research areas with a focus on ensuring the security of the emerging grid with high RES-DG penetration into the distribution networks are also recommended.

Keywords: Renewable energy; Security assessment; Distributed generation; Emerging grid

*Corresponding Author: Tel.: +64225331241
E-mail address: ifedayo.oladeji@aut.ac.nz

2.1 Introduction

Fossil fuel-based power generation has raised serious global environmental concerns due to the excessive amount of emission it contributed, thereby depleting the ozone layer and resulting in many more consequences. The increase in CO2, which is a major greenhouse gas (GHG), has been predicted to hit 45 billion metric tons by 2040 [25] [1]. About 77% of GHG comes from power systems and industries. Some power systems are driven by safety while some are driven by economics. Economics-driven power systems are occasionally operated close to their security limits. Occasional overloading of the transmission lines, voltage stability issues, system frequency fluctuations, power quality issues, and large active and reactive power losses are some of the

challenges faced by the present grid. Many blackouts have been reported as a result of insufficient generation and transmission capacities coupled with the weakened transmission infrastructure and aging components [26][2]. With the global power demand being estimated at around 770 TW by the year 2050 [27][3], the present grid may be incapable of supporting the future power system requirements and dynamic load growth within the required security limits.

In addition to reducing the carbon footprint of the power generation, the incorporation of renewable energy generation into the present grid can significantly improve its performance and reliability. Policies have been adopted by several countries in line with the millennium development goals regarding the environment and global warning to significantly increase the amount of power generation from renewable energy sources. The successes claimed by many countries on high penetration of renewable energy power generation may be attributed to small and isolated grids with relatively small loads. In addition, in many scenarios, power is generated through big hydro and geothermal plants. These power generation systems may be considered as a central generation where penetration of distributed generation (DGs) systems will have no significant impact on the security of the grid. Major security challenges emerge at high penetration of renewable energy sources distributed generation (RES-DG) into the grid.

The benefits of RES-DGs are contingent on the optimal planning and operation of the appropriate type of RES-DG. With advancements in power electronics, modern RES-DGs do not only generate energy but also provide the system operators with new capabilities to support the transmission system. Several RES-DGs can be aggregated and operated as virtual power plants (VPP) to provide frequency control under contingencies. Optimal planning of RES-DG involves the allocation and penetration levels into the distribution systems. Optimal allocation of RES-DGs reduces the power loss within the distribution system and also improves the distribution network voltage profile.

Unlike the conventional distribution network, which merely receives power from a transmission or sub-transmission network, an active distribution network has a power generation within it. The active distribution network operators proactively manage medium and small-scale renewable energy and non-renewable energy source DGs to achieve efficient operation. High penetration of RES-DG may increase power quality issues and protection challenges within the active distribution system. Considering that the emerging power grids will contain high penetrations of RES-DGs, it is therefore important to employ support technologies and schemes to limit the negative security impacts. Enabling and support technologies include improved energy storage systems (ESS) and enhanced communication systems. Interaction schemes between the transmission network and active distribution networks for voltage and frequency controls will ensure the security of the emerging grid. Through these support tools and schemes, the emerging grid may be able to operate securely under high penetrations of RES-DG.

To this end, this paper is focused on issues surrounding the high penetration of small renewable energy generation into the distribution systems where the impacts on the grid's security are significant. The contributions of this paper include:

- A comprehensive technical discussion on the trends of energy storage systems (ESS) and other supporting components in the quest for a 100% renewable energy grid.
- A review of the existing techniques, optimization objectives, and algorithms for optimal RES-DG allocation in the literature within the last 10 years.
- A review and analysis of existing voltage and frequency flexibility interaction techniques to support the increased penetration of RES-DGs.

The rest of this paper is organized as follows. Section 2.2 discusses the role of renewable energy sources in the power grid transition. In Section 2.3, the technical impacts of high penetration of RES-DG into the grid are discussed. The review of existing methods and techniques to limit the impact of RES-DG penetrations is presented in Section 2.4. Section 2.5 discusses and reviews the trends in technology and tools to ensure the security of the grid under high penetrations of RES-DG. Section 2.6 contains the conclusions from the reviews and the recommendations for future research areas based on the limitations of the existing techniques.

2.2 Grid Transition

Over the last two decades, the number of power system blackouts has continuously increased [9, 26]. This increase is a result of continuous load growth and the challenges in the transmission/distribution systems. One of the immediate solutions to reducing the number of blackouts is to increase investments in all the subsystems of the grid. Consequently, deregulation and decentralization policies were adopted to encourage private sector participation, thereby increasing investments in the power grid. Deregulation of the electricity market is aimed at improving the reliability and efficiency of the grid from the network planning stage to network operations. Before decentralization, central generation (CG) and centralized control have been the major power generation and control methods, respectively. Under the CG method, large generating stations are sited remotely from bulk consumers but close to their turbine drive source due to environmental and economic constraints. The power generated is instantaneously transported via long transmission lines to the consumers. Although not a new concept, distributed generation (DG) methods have acquired extensive acceptance due to grid decentralizing as well as the disadvantages of CG in terms of high power loss and investment cost. DG methods are therefore intended to reduce the cost of power delivery and enhance the reliability of power despite the load growth. The pros and cons of the CG and DG methods considering technical and economic impacts are extensively discussed in [28]

2.2.1 The Emerging Power Grid

The emerging grid is envisioned as an integration of smart components, networks, and subsystems under decentralized control to provide benefits for consumers and utilities. At the subsystem level, the emerging grid may be realized or classified into smart infrastructure subsystem, smart information subsystem, smart protection subsystem, management subsystem, and smart data communication subsystems. The infrastructure subsystem is responsible for the secured bi-directional flow of power and information between the producers, consumers, and control systems. The major unit in this subsystem is the smart energy which consists of the smart generation, transmission, and distribution units [29]. The smart generation units will harness the potentials of renewable energy sources distributed generation systems. The aggregation of RES-DGs advances the concept and feasibility of virtual power plants (VPP). Virtual power plants are DGs with an aggregated capacity equivalent to the large CG systems. The concept of VPPs provides extra benefits such as reliability, flexibility, and quick response to fluctuations compared to CGs. However, the operation and control of VPPs require complex techniques to become beneficial [30].

The emerging power grid will include high penetration of RES-DGs due to economic, environmental, and technical reasons. RES-DGs are classified from small (micro) to large-sized renewable energy source power generators sited close to the consumers, thereby eliminating the need for long transmission, and significantly reducing power losses. RES-DG are tied to the grid through electronic converter systems due to the absence of rotating mechanical inertia. Consequently, they are often regarded as non-synchronous generators. Table 2.1 gives a summary of the types of DGs with related characteristics of the RES type, energy storage, and compensation systems by unit capacities.

Table 2.1: Summary of distributed generation by Capacity [31]

Classification	**Capacity**	**RES Type**	**Active Power (P)**	**Reactive Power (Q)**	**Example**
Micro DG	1 W to < 5 kW	A	+	0	PV, Battery, and Fuel cell
Small DG	5 kW to < 5 MW	B	0	±	Condensers and capacitors
Medium DG	5 MW to < 50 MW	C	+	+	Mini hydro
Large DG	50 MW to < 300 MW	D	+	−	Wind turbine

+ Generate − Absorb.

The strong correlation between global power demand and CO2 emission forecasts necessitates the shift in the power generation framework. This framework change is aimed at reducing the fossil fuel-based power supply to achieve the global vision in response to climate change. Renewable energy sources (RES)-based distributed generation (DG) provides the best solution for future power generation considering the technical and environmental challenges. Several countries have designed and adopted policies to gradually increase the penetration of the RES-DG in respective power systems. Figure 2.1 shows the total global installed and available capacity of power generation from RES-DG by leading countries, as of 2017. Despite China, Germany, and

Japan having the largest installed and available capacities, Spain and India have the relative highest proportion of available-to-installed capacity. The persistent question, however, is how to ensure the security of the emerging grids with significantly increased levels of RES-DG clusters into the distribution networks.

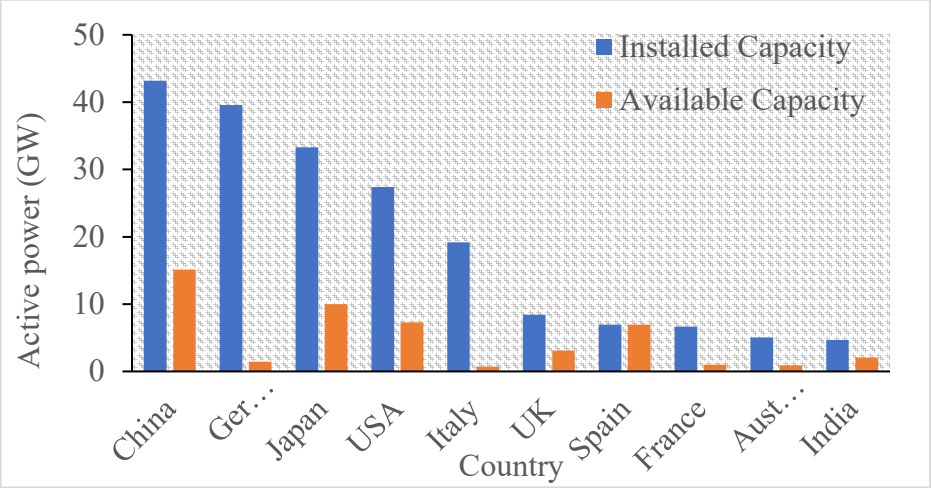

Figure 2.1: DGs installed and available capacities by countries [32]

Several terms such as smart grid, future grid, and intelligent grid have been used to describe the emerging power system. Simply put, the emerging grid entails a transformation from the conventional grid framework to an information-controlled, data-enabled, and highly interconnected network between producers and consumers of electric power embracing new technologies in transmission, distribution, and generation [33]. The objective is to operate a network to provide abundant, affordable, clean, efficient, and reliable power. The expected benefits of the emerging grid are not limited to reliability and efficiency improvements, but also include a strategic contribution to reduce global carbon emissions. The drivers of the emerging power grid can be categorized into network decentralization, generation decarbonization, and information digitalization, as shown in Figure 2.2.

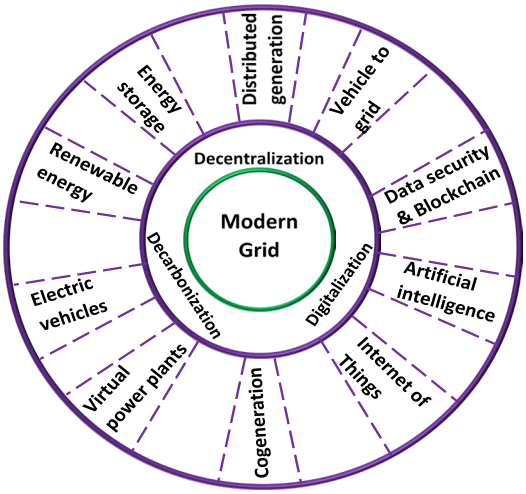

Figure 2.2: Drivers of the future power grid.

Decentralization of power generation through distributed generation systems and energy storage systems reduces the power losses and subsequently the cost of power delivery. Renewable energy systems and electric vehicles are aimed at reduction of greenhouse gases contribution from power generation and transportation, respectively. However, indiscriminate and uncontrolled charging of large numbers of electric vehicles increases the load on the network and causes stress on the grid. Charging models and algorithms have thereby been proposed to limit the impact of EVs on the grid [34]. The modern grid will also take advantage of the availability of IoT devices and advancements in artificial intelligence algorithms for operation prediction. The security problems of the grid due to threats and attacks will also be limited due to modern security and blockchain technologies. The physical components of the emerging grid must be well integrated and coordinated through the distributed control centers. The control centers of the modern grids will be capable of ultrafast data acquisition, processing, and command redistribution. Also, the control modules will be expandable, scalable, and adaptable to changing architecture, services, and tools [35].

Another description of the emerging grid is the concept of a digital grid. The grid is divided into smaller units called grid cells which will be connected by digital routers. This is similar to the energy ethernet model. The following three key technology capabilities are crucial for these models to be feasible: the plug-and-play interface, information router, and an open-ended utility program [36, 37]. While there is significant progress in the applications of solid-state transformers (SSTS) as energy routers, the RES-DGs must also be able to operate in the plug-and-play mode. The ability of small, distributed resources and storage systems to operate in the plug-and-play mode will improve the resilience of the grid in terms of demand response, grid resilience, and restoration. The multi-criteria optimization problems proposed for grid restoration after major blackouts will also be significantly simplified if the major grid components can operate in the plug and play mode.

Power delivery will be achieved through an integrated transmission system–distribution system (TS/DS) consisting of FACTS devices, HVDC systems, voltage control devices, synchro phasors, and communication devices. The operators for each network within the integrated grid must operate within guidelines and code specific to the responsibilities which are aimed at achieving efficient power delivery. Figure 2.3 shows an example of the emerging grid consisting of large renewable energy generations, distributed renewable energy generation, and electric vehicles. The electric vehicles can also interact with the active distribution networks in the vehicle to grid (V2G) mode, thereby supporting the grid during peak load demand periods. The coupling point for the renewable energy generation systems to the grid depends on the type and generation capacity.

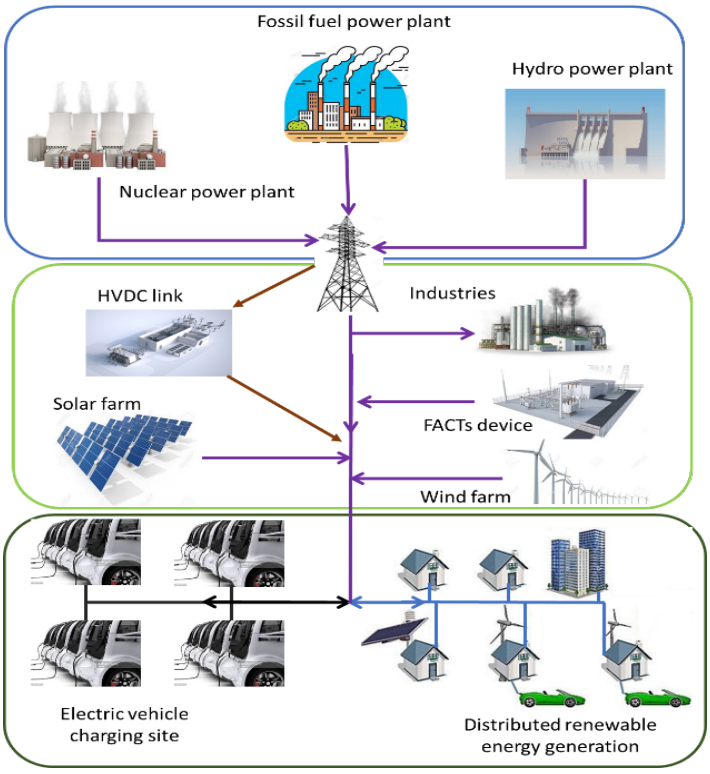

Figure 2.3: Model for the emerging power grid.

The function of the emerging grid includes bi-directional power flow between multiple voltage levels within a highly meshed network structure consisting of integrated AC and DC networks. Voltage and frequency control strategies in this multi-level model will be more complex compared to the single-voltage level AC-AC network within a grid. Research has been done to improve the efficiency of converters for this meshed model including HVDC and super grids [38]. A large part of the papers examined in [39] aimed to enhance the converters for bi-directional power flow control to ensure security and to improve the power quality in a high RES-DG penetrated environment. The distribution systems already have distribution FACTs devices (D-FACTS) designed to provide voltage support and power flow control at the medium voltage (MV) and low voltage (LV) levels. Therefore, as the idea of an integrated AC-DC grid develops, it is necessary to have the DC version of flexible AC transmission systems (DC-FACTS) [40]. The meshed AC-DC grid will be configured to operate in a fully accessible model for small-scale RES-DGs and storage technologies for cost-effectiveness and effective consumer participation. To ensure the efficient operation of emerging integrated networks, and to achieve the goal of RES-DG and energy storage penetration, there is a need to develop a reliable integrated network management system for hybrid AC-DC power flow.

2.2.2 The Role of Renewable Energy Source in the Emerging Power Grid Architecture

As the demand for clean and efficient energy increases, a significant amount of renewable energy source (RES)-based distributed generation (DG) will be added to the grid. The model of the

modern grid is based on the architecture of highly interconnected networks with the underlying component of the penetration of RES-DG systems. Synchronizing the operations of the RES-DG systems with the grid will ensure the future grid's security. Solar PV, wind turbine, and hydro (mini) systems represent the bulk of RES-DG that is significantly viable for power generation. Figure 2.4 provides a characteristic comparison of RES-DG using availability factors, environmental impact, and cost-benefit considerations. The unlimited supply and the cleanliness of the renewable energy sources are underlying positive factors across the types of renewable energy systems. However, the high construction cost of units of renewable energy systems is also a common factor to be considered at the active distribution network planning stage.

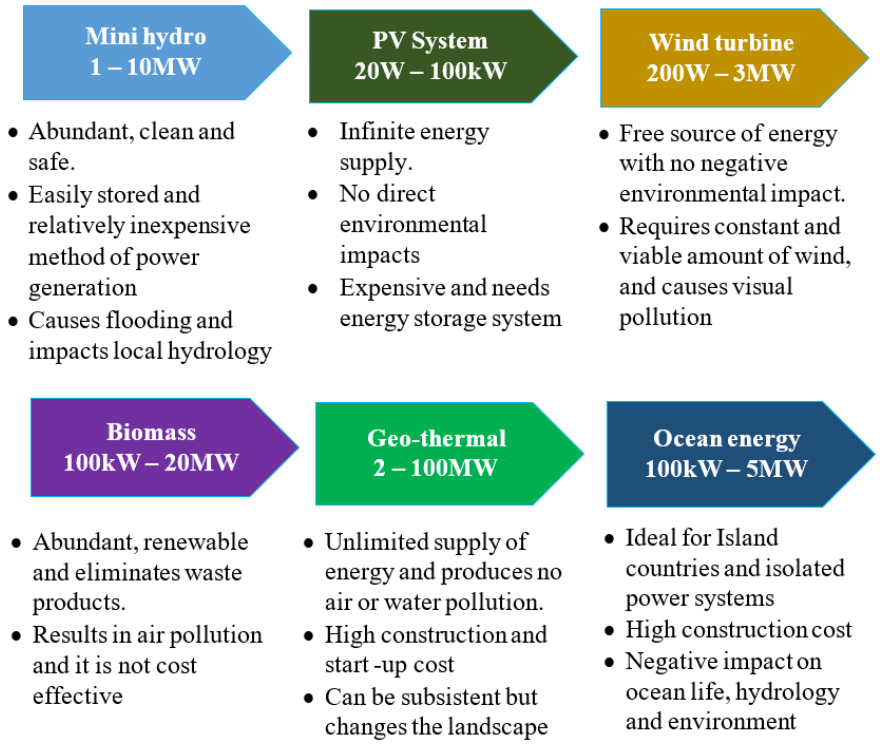

Figure 2.4: Renewable energy considerations [41].

The applicability of RES-DG on the emerging grid considering scenario peculiarities is summarized in the model in Figure 2.5 showing a wide range of factors influencing the role of DG in future power systems. The security for a grid determined by the RES-DG penetration level, network configuration, and operation will be influenced by the weight attached to the choice factors.

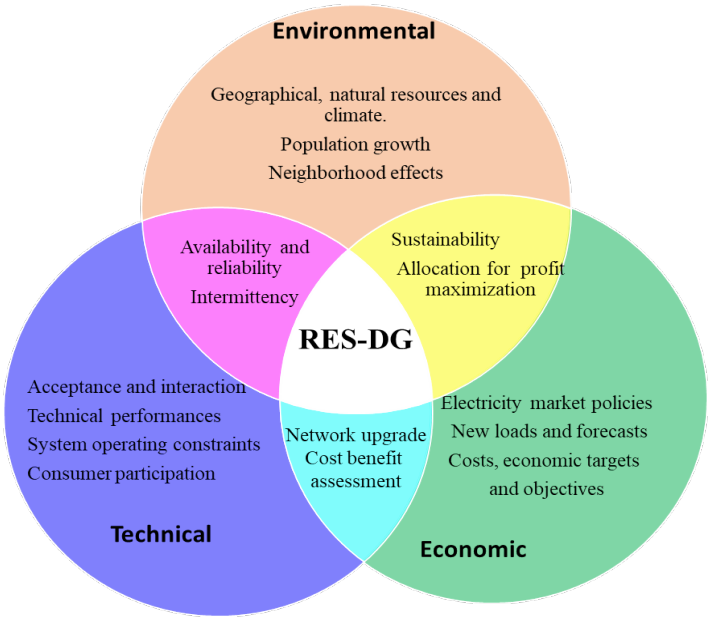

Figure 2.5: Factors influencing RES-DG penetration.

While it is certain that renewable energy systems will significantly reduce the power generation from fossil fuel-based generating plants, thereby reducing the greenhouse gases emissions, there are other environmental factors to be considered. Animals are removed from their natural habitats to acquire large landmasses for both PV and wind systems. The usage of a large area of land for PV and wind systems to generate a considerable amount of power also distorts the landscape. Furthermore, several bird species have been declared endangered after being killed by the rotors of wind turbines. Activities on the rivers and oceans have also been noted to disturb the ocean lives and may unbalance the natural order of life. The main economic factors considered among several others are the cost of power generation and the purchasing power of the consumers. In addition, incentives from governments and the subsidization of the initial construction costs and price of energy are taken into consideration. The technical factors considered are the impacts of renewable energy systems on the grid's security, reliability, and protection. The decisions based on the technical factors are vital due to the inherent characteristics of the renewable energy sources generation systems.

The power output of RES-DG clusters depends on the efficiency of the units. With the efficiencies of wind turbine generators now significantly improved, the efficiencies of the solar PV panel will also increase from 12-19 % to about 30-35% under favorable conditions [42]. The total installed capacity from renewable energy sources globally has increased by 50% between 2019 and 2020 [43]. The European Union has revised its proposed renewable energy source penetration target from 27% to 32% by 2030. These values are expected to increase with the global increase in load demand. In line with the global millennium developmental goals concerning climate change, ref. [44] discusses cases of substantial levels of RES-DG penetration and arguments for a proposed increment in the future.

Many existing small and isolated power systems have already integrated renewable energy source generation. Penetration levels above 30% have been reported for many isolated power systems (IPS) [45]. The high penetration level is due to the certainty of achieving significant technical and economic benefits from a relatively small investment in renewable energy. Renewable energy generation has been employed in scenarios where electrification of islands through the HVAC and HVDC transmission system are not economically viable. With diesel generators as backup, many islands from developed countries are powered solely by renewable energy sources. Countries with large power grids like China, the USA, Brazil, and many countries in Europe including France, Germany have established policies supporting the penetration of renewable energy generation into their respective grids. China is the leading country with policies enhancing the rapid penetration of small and large renewable energy generation systems. One of the several policies is to encourage individual consumer rooftop PV installations. China's total rooftop solar capacity was reported at 5.27 GW in 2020, with total solar installations expected to reach 28-34 GW by the end of 2021 [46].

A leading country in rooftop solar photovoltaics (PVs) manufacturing, Germany has proposed increasing its solar and wind capacity from 120 to 215–237 GW after the withdrawal from the nuclear energy program. The renewable energy generation program has committed to 65% and 80% renewable energy of the total electricity demand by the year 2030 and 2050, respectively [2]. To realize this level of penetration, the German government has continued to subsidize the costs associated with the installation of RES-DG for consumers [47]. The installed generation capacity of Brazil reached a total of 162.8 GW in the year 2018 out of which 83.3% is renewable energy. From the total installed renewable energy generation, 22.6% are penetrated into the low voltage networks. With the electricity demand forecast at about 300% increase of the demand from the year 2013 to 2050, the penetration levels of wind power and solar power are projected to increase to 13.4% and 97% respectively by the year 2026 [48]. For smaller power grids, the highest renewable energy sources distributed generation penetration of over 45% is recorded for Denmark. Renewable energy distributed generation also accounts for about 20% of the total electricity generation in Spain and Sweden [49].

2.3 Technical Impacts of RES-DG Penetration

The high penetration of RES-DG integration into the distribution network will significantly alter the structure of the network. Renewable energy sources distributed generation system transforms a traditionally passive distribution network into a multi-source active distribution network. The right RES-DG penetration into the distribution networks will reduce the overall network losses and enhance the voltage profile. The utilization of RES-DG by distribution system operators to manage the variability and uncertainty of demand and supply across different timescales is another advantage. This demand-supply management process is referred to as grid flexibility [50]. These flexibilities include network peak load shaving, load shifting, and valley filling [51]. The impacts of RES-DGs' penetration in the active distribution network and the connected upstream

network are shown in Figure 2.6. The positive impacts of RES-DGs in this paper are discussed under the performance index. The most considered performance indices are voltage stability, reliability, and power loss. The negative impacts of RES-DGs are discussed under the power quality and protection challenges. Power quality challenges are mostly due to the variability of solar irradiance and wind velocity as well as the absence of mechanical inertia in RES-DG systems. Protection challenges are due to the absence of fault current limiting capability of RES-DG converters.

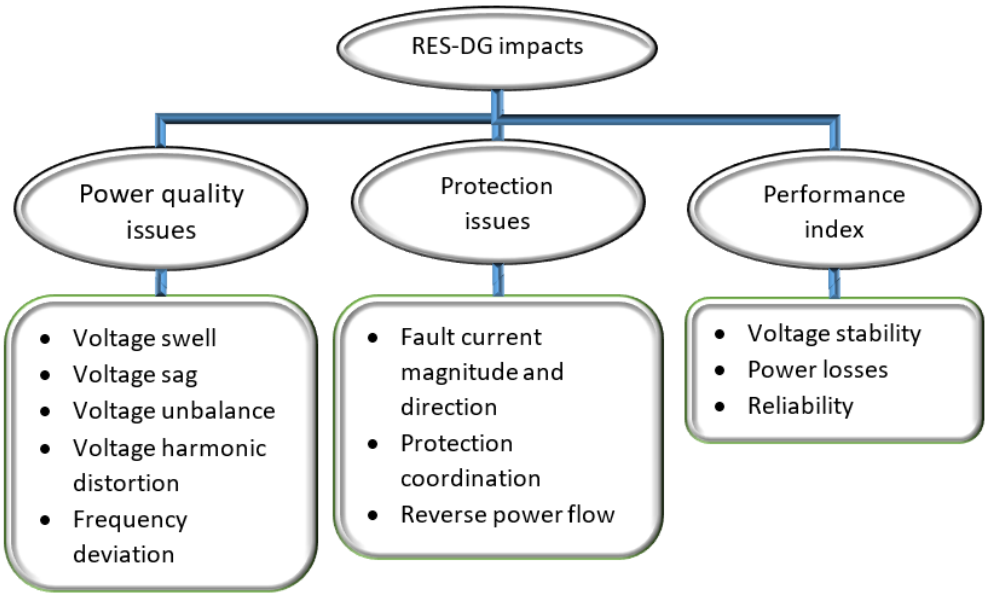

Figure 2.6: Technical impacts of DG penetration.

2.3.1 Power Quality Issues

Penetration of RES-DG reduces the overall system inertia as the synchronous generators are replaced by non-synchronous generators. Although the frequency of the network and its derivatives are rarely affected at low penetrations of RES-DG, some results in the literature have proved that the rotor speed deviation, rotor speed oscillation duration, and deviation of electrical frequency increase due to the reduced inertia [6, 52, 53]. Research on the penetration of RES-DG is mostly developed under power loss and voltage objectives. Modern wind turbines are equipped with voltage control features through sophisticated power electronics which enables them to function as a conventional utility generator regarding voltage support for distribution and transmission systems. Consequently, the focus should be on frequency response which is significantly impacted due to the reduced overall mechanical inertia. The stochastic characteristics of RES-DG and load variability necessitate the consideration of the local voltage and frequency constraints during active distribution network planning. To minimize the occurrences of local frequency instability, the penetration of RES-DG into the distribution network should be based on the grid's power-frequency characteristics. Also, the boundary of penetration of RES-DG should be defined under different scenarios of generation fluctuation and reserve capacity [54].

Another Another challenge of the high penetration of RES-DG on the active distribution network is its impact on the voltage and its waveform. The impact on voltage can be grouped into temporary voltage change and voltage step change. Temporary voltage change which includes voltage sags and swells is caused by the sudden drop in the root mean square (RMS) voltage and is characterized by a slow recovery to a new steady-state voltage magnitude. Voltage sags and swells mostly occur during the fault period in the distribution network with large loads. The voltage step is the rapid changes in RMS voltage levels due to changes in active and reactive power levels. Voltage step usually follows a system switching, unintentional islanding, unplanned outage of loads, unplanned outage of reactive power compensators, and line contingencies [55]. The overall power factor from a cluster depends on the instantaneous power scheduled from the different RES-DG types. Voltage step constraints have the greatest impact at lagging RES-DG cluster power factors, while operation at leading power factor tends to minimize the voltage problems [56]. Under the requirements of ANSI C84.1-2011 1995 from the IEEE Standards Coordinating Committee 21, the operations of DG should not cause voltage instabilities within the distribution network, at the point of common coupling (PCC) of clustered RES-DGs, and the TS-DS interface [57]. This is critical for time-varying voltage-dependent loads which are usually ignored by most studies. The impact of high penetration of DG on the voltage waveform is discussed under the voltage harmonics distortion. Voltage harmonics distortion which is caused usually by the electronic converters in the network has also been predicted to increase with load growth. The voltage step is an important index that has been overlooked by studies focused on the allocation of RES-DGs. Harmonic distortion levels also limit high RES-DG penetration. Little attention has been given to the harmonic injection into the transmission network through the TS-DS interface occurring at the point of common coupling (PCC). The permissible level of harmonics distortion caused by inverter-based DGs is regulated in IEEE-519-1992 standards.

To overcome voltage stability issues limiting maximum RES-DG penetration, several practical scenario-based methods may be employed. These methods include adjusting the secondary winding of LV transformers, giving priority to reactive power absorbing DGs, RES-DG power curtailment, reducing line impedances, and storage of the excess power [58]. Due to engineering and physical design constraints, some of the techniques may not be practicable and applicable to all distribution networks. Therefore, it is desirable to develop a generic approach that integrates the network dynamic limits for active distribution network planning and operations. Such an approach will include parameters that will be categorized into one or more of the following limits: static element limits, generation, and demand seasonal limits, static and dynamic system stability limits, as well as operator-specific limits. Some of these limits are obtainable through real-time systems, while others are obtainable using forecast models. For example, the impacts of passing clouds and sudden changes in wind parameters should be considered in the inter-hour scheduling under the seasonal generation limits.

The overpenetration of RES-DG within an active distribution network occurs when more power is generated from RES-DG than scheduled. Power curtailment and storage are traditional approaches that have been used to limit the amount of power from DGs. Flexibility utilization techniques are also becoming common for managing RES-DGs generation levels by system operators. The flexibility obtained through RES-DG penetration may be extended to the transmission system through the aggregators. The challenge here lies in the complex computation involved in the inter-network-operation modeling, and the representation of the flexibility operating region due to generation variability and network limitations [59].

2.3.2 Protection Challenges

The impact on the protection system depends on whether the DG is synchronous or non-synchronous, as well as the DG penetration level. The challenge for the protection systems is the unintended reverse power flow from the active distribution network to the upstream medium voltage network when the RES-DG is at peak power generation during off-peak load demand periods. The surplus current is perceived by the relays as fault current within the network. This misinterpretation of fault current may cause unintended islanding within the network. Different types of DGs have different short circuit characteristics to which the protection systems must effectively respond under predictable and unpredictable fault conditions. In addition, the degree of protective failure is determined by the DG's size. Refs. [39,40] demonstrated the changes in short circuit current due to different DG penetration levels for a three-phase short circuit fault at different positions from the DG.

Traditionally, distribution networks are radial by design, and the protection schemes are designed for a single-source power supply from the transmission system. The penetration of DGs is more promising in loop network configurations. Therefore, the functioning of modern protection schemes is inclined toward loop applications over radial applications [41]. In the loop protection schemes, a relay may malfunction due to tie switch operations and bidirectional current flow. A new protection scheme capable of fast fault location and fault section isolation in a loop network is proposed in [42] to achieve the protection of the modern power grid. Protection devices with a simple design and time-current characteristics have effectively performed the tasks of protection from overcurrent in both radial and loop configurations. However, with the RES-DGs also contributing to the fault currents in the emerging distribution network, the traditional protection, which assumed unidirectional flow of current, will no longer be effective. The variability and unpredictability of DGs may increase the loss of coordination of the existing protection devices. Moreover, fault levels will be increased, and varying fault currents will further compromise the protection coordination. Ref. [43] concluded that the deviations in the local node frequencies increase with the high RES-DG, thereby reducing the precision of the fault location algorithms.

The loss of protection coordination has negative impacts on the reliability of the distribution system. The study in [44] shows that the reliability of the traditional distribution system is degraded significantly by the loss of protection coordination resulting from the high penetration of RES-DGs. Protection blinding and sympathetic or false tripping have been identified as the two most common causes of miscoordination. Blinding occurs when the sensitivity of a protective relay is reduced. The fault currents seen by the upstream protective devices will be reduced by the presence of a RES-DG located downstream. The equivalent fault current will depend on the short circuit impedances of the main source and the RES-DG as well as the impedance of the feeder to the point of fault. Sympathetic tripping occurs when a protective device in a feeder operates for a fault outside its protection zone mostly in another feeder. This tripping happens when the protection device's precision is lost as a result of reverse current from the RES-DG toward the fault location [45].

Several techniques for new protection devices' design for the emerging grid have been recommended in [46]. These techniques can be classified under non-traditional fault identification and new relay characteristics development. Communications-based solutions that attempt to detect and locate faults within the active distribution network are becoming common. The appropriate circuit breakers are then identified to trip and clear the fault. A new relay characteristic for the protection system was proposed in [30] based on the inverse operating time vs. line admittance characteristics. This new characteristic enhances the sensitivity of the relay for precise fault location on the feeder. These new relays can also be coordinated similarly to the existing simple time–overcurrent relays [46,47].

2.3.3 Performance Indicators

Voltage instability, which occurs frequently as a result of increasing load demands and limited transmission capacity, is alarming and has been a source of concern for power system operators [60]. Voltage stability is the ability of networks to maintain acceptable voltages at all network nodes under normal operating conditions and after being subjected to disturbances. The inability of a network to supply the reactive power demand is a major contributor to voltage instability. The assessment of voltage stability is done under dynamic and static stability studies. Dynamic voltage assessment produces the voltage response of a system to a sequence of discrete events in the time domain [61]. Static voltage assessment involves the identification of critical network nodes, evaluation of load margins, and estimation of reactive power compensation [62]. Voltage instability is a local challenge to distribution system operators as it is a global challenge to transmission system operators.

Several voltage stability indices (VSIs) have been proposed in the literature for voltage stability assessment. Some of these indices may be used to detect the weak lines and buses in the network as well as to achieve optimal RES-DGs allocation. The available voltage stability indices can be grouped into the Jacobian matrix-based indices and system variable-based indices [63]. The

system variables-based indices can be generalized into the line voltage stability indices (LVSIs) and bus voltage stability indices (BVSI). The LVSIs are based on the reduced two bus network representation and are used to evaluate the weak links with potential voltage problems in the network. The BVSIs are indices derived from nodes' voltage deviation, which is caused by reactive power demand and supply imbalance [64].

The penetration of RES-DG units into the distribution networks provides several benefits like improving voltage profiles and load factors. To achieve these benefits, the RES-DG must be optimally sized and sited on a specific node in the network. Installing RES-DGs units in non-optimal locations may lead to voltage instability of the network. The proposed techniques and algorithms for optimal placements of RES-DGs are discussed in section 4.1.

The bulk of power loss from generation to utilization has been attributed to the transmission and distribution networks. Therefore, power loss reduction is considered a key objective during the planning of active distribution networks considering RES-DG penetration. Since high power loss contributes to the high cost of power delivery, there has been a considerable increase in research aimed at reducing active power loss in the distribution network employing RES-DGS. It is economically and technically impractical to have active and reactive power support on every node in the distribution network. Therefore, an optimal site and size of RES-DG must be selected to maximize the benefits. Because the relationship between the RES-DG penetration level and power loss follows an inverse quadratic function trajectory [65], a non-optimal allocation may therefore lead to an increase in power loss. Although it is usual to combine power loss objective with other performance indices in a multi-objective RES-DG allocation problem, techniques for power loss minimization as a single objective optimization problem is also common. The benefits of existing techniques in a single objective problem over a multiobjective problem for power loss minimization using RES-DGs are unclear and highly doubtful [66]. With a focus on power loss minimization, heuristic techniques were proposed in [67-69] in a multi-objective optimization model.

Reliability is another important index in measuring the performance of an active distribution network with RES-DG penetration. Traditional methods of evaluating reliability are based on deterministic conditions which rely on past system experiences. These methods do not consider the probabilistic nature of outages that may be caused by RES-DGs. It is also impractical for new active distribution networks due to the lack of historical reliability data. In addition, deterministic methods are focused on specific reliability indices. However, with these indices, it may be impossible to explicitly express the performance of the network [70]. Research has consequently moved from deterministic approaches to stochastic approaches which are based on the summary of statistical data on the individual components within the system.

Deterministic reliability assessment methods such as the Markov process involve simplified and linearized representation of the power grid while ignoring the grid's probabilistic characteristics. Although deterministic methods are useful for conventional grid operations, electricity market deregulation and the introduction of variabilities from renewable energy generation sources make

deterministic methods insufficient and obsolete. The responsibilities of the modern emerging grid operators include ensuring the grid's reliability under probabilistic conditions. Probabilistic reliability assessment methods such as the Monte Carlo simulations become significantly helpful for probabilistic conditions. The probabilistic reliability assessments consider randomness and uncertainty using the probability distributions, hence, modeling a real system. Since the reliability assessment is performed with random data within the distribution, the results may vary for different assessments. However, the standard deviations of the results are usually small. The average of the result conclusively represents the reliability of the grid. Improved deterministic reliability assessment methods such as the advanced Markov process, where several possible reliability states of the grid can be monitored, are also useful for the reliability assessment of modern power grids.

The Markov process and Monte Carlo simulation are the two common methods available for reliability assessment of systems. A large amount of simulation and time needed to estimate the average of the reliability in the Monte Carlo method makes it less preferable to the Markov process. In Markov method, several reliability indices may be quickly evaluated using the systems' state space [71]. The reliability of an active distribution network varies with the point of connection of the RES-DG on the feeder. Under the emerging deregulated system with increased competition for market share from operators, it is highly important to ensure good reliability. Refs. [72-74] focused on the distribution network planning and expansion using optimal RES-DG placement to maximize the distribution network reliability. At lower penetration, RES-DG improves the reliability of the distribution networks, specifically when reliability is evaluated using the availability index. However, the overall reliability of the grid could be compromised at high penetration levels [75].

2.4 Recommendations to Limit Security Impacts

2.4.1 Active Distribution Network Planning

Probabilistic active distribution network planning techniques which enable a better risk assessment under realistic conditions for optimal RES-DG penetration level assessment are becoming common [76]. Probabilistic modeling methods were proposed in [77, 78] based on solar PV generation and load uncertainties. An effective probabilistic planning model will be adaptable to several RES-DG types and network configurations. Also, it should consider the impact of environmental factors on the performance of the RES-DGs. The study in [79] shows that wind turbines generate more energy in a year when compared with solar generation of the same capacity. The concept in recent literature combines the technical and economic benefits for optimal RES-DG penetration level assessment. Using techno-economic analysis of a PV-WT hybrid system, ref. [80] claimed 32.75% to be the secured penetration level. Ref. [81] reviews the impact of RES-DGs output variation caused by short-time weather changes. The proposed approaches in [82, 83] are the steps to developing a more realistic probabilistic model for RES-DG penetration level estimation using

solar radiation, wind speed, and panel cost variations. An ideal model will include dynamic RES-DG clusters planning with complex network architecture under systems security constraints.

By considering the impacts of an unconstrained increase in RES-DG penetration into the grid as discussed in the previous section, it is important to optimally allocate the appropriate RES-DG type. The impact of capacity, types, and operating power factors of different RES-DGs on the grid was investigated in [84]. Analytical approaches based on loss sensitivity factor, voltage stability factor and selection index for optimal RES-DG allocation are common in recent literature. The approaches are effective and require less time due to the less complex computations involved. The proposed method may be extended to include more power quality and security Indices. Focusing on the power quality, a regulator for PV systems voltage fluctuations and reactive power flow control was proposed in [85, 86].

It is also important to consider the steady and rapid load changes during RES-DG penetration planning for different RES-DG types under deterministic annual load growth. Probabilistic methods based on the load shifting technique are considered effective to analyze the network under highly flexible loading conditions. Optimal RES-DG penetration can enhance the system loading factor, line stability, and voltage stability [87]. Table 2.2 describes the classification of the commonly used optimization objectives for distribution network planning with RES-DG allocation. The optimization objectives are classified as technical, financial, and index-based. Based on the optimization objectives classified in Table 2.2, the best nodes to allocate RES-DGs within distribution networks can be decided. It is common to combine two or more objectives to form a multi-objective optimization problem for the planning of active distribution networks. For safety-driven power systems, priority is given to the technical and index-based objectives, while financial objectives are considered more important in economy-driven power systems.

Hybrid optimization algorithms may be more suitable for RES-DG allocation particularly for large systems considering the impacts of other network components when a specific performance index needs to be assessed [88]. Hybrid optimization approaches are generally robust in handling the complex mathematical modeling of large unbalanced systems under load and RES-DG output variations. Refs. [65, 89] discussed several RES-DG allocation methods with emphasis on the objective functions, constraints, and proposed algorithms. For smaller distribution systems, analytical methods may be effective to obtain the optimal allocation based on simple performance indices. The impact of power exchange at the transmission system-active distribution system (TS-ADS) interface has always been neglected in the formulation of the problem considering that most RES-DG allocation techniques are focused on isolated systems without interaction beyond the substation. The operation of the emerging grid will be dynamic with flexible services and power exchange at the TS-ADS interface and between multi-voltage meshed networks. This dynamic operation may require optimal reconfiguration of the active distribution system in the future depending on the prevailing condition.

Table 2.2: Distribution network planning with RES-DG allocation objectives.

Technical Objectives	Financial Objectives	Index-Based Objectives
Specific line and total active, reactive power loss	DG capacity and efficiency maximization	Power loss index
Voltage profile and stability	Energy harvest maximization	Voltage index
Energy losses	DG costs minimization	Current index
Specific line and total power transfer maximization	Profitability, NPV optimization	Short circuit index

2.4.1.1 Renewable Energy Source-DG Optimal Allocation

Many proposed RES-DG allocation methods have been focused on a single RES-DG type, which may not fully characterize the behavior of a realistic multi-RES DGs system in an integrated grid. The methods are implemented on isolated networks with no comprehensive security assessment index to validate the claims. Consequently, there is a need for more research to develop new objectives and enhanced optimization techniques to dynamically allocate RES-DGs based on peculiar system needs and flexibility supports. Additionally, the tools to implement the new objectives under network security indices should be expandable and adaptable for reliability assessments under dynamic conditions for active distribution network and transmission network interactions. Figure 2.7 highlights the existing optimization techniques used to allocate RES-DGs to achieve high levels of penetration under prevailing system security constraints. The common metaheuristic algorithms and optimization objectives for RES-DG allocation in recent literature (2010–2020) are summarized in Table 2.3. While new algorithms such as the Harris hawk optimizer (2019) are being developed, particle swarm optimization algorithm has been applied extensively to obtain the global optima from the fitness/objective functions. Voltage profile enhancement and/or power loss reduction are the most common objective(s) for a single or multi-objective RES-DG allocation optimization problem.

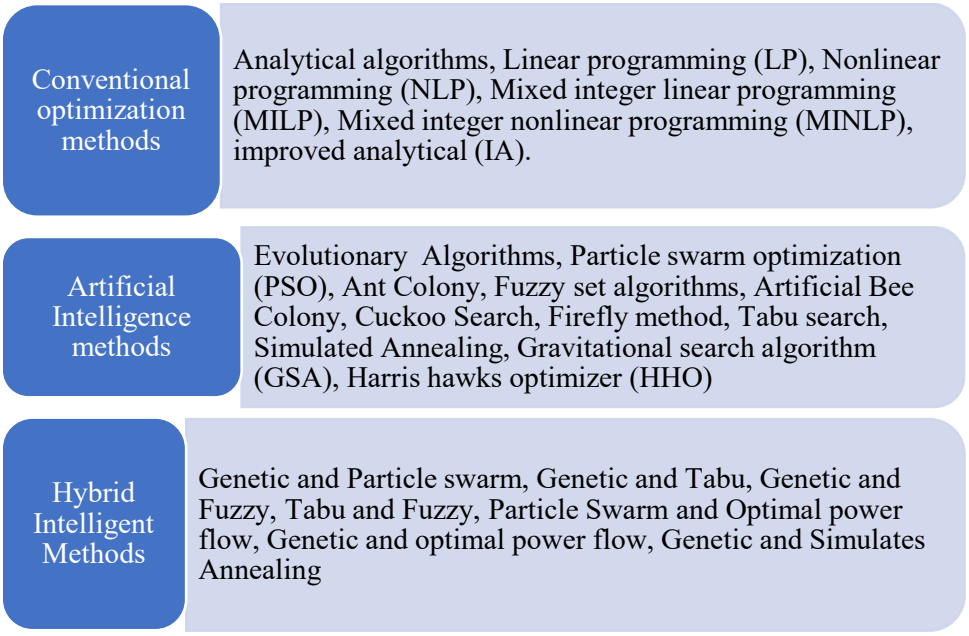

Figure 2.7: Optimization algorithm/techniques for RES-DG allocation.

Table 2.3: Common metaheuristic algorithms with optimization objectives.

Reference(s)	Objective(s)	Method
[67, 90-92]	Power loss reduction and voltage enhancement [31]. Power loss reduction [53, 55]. Loadability enhancement [54].	Particle swarm optimization (PSO)
[69, 93, 94]	Power loss reduction and voltage stability improvement [33]. Power loss reduction and voltage enhancement and system stability improvement [56]. Power loss reduction [57].	PSO and GSA [33]. PSO and HHO [56]. PSO and IA [57]
[95, 96]	Power loss reduction and reliability improvement [58]. Power loss reduction and voltage enhancement [59].	Sorting genetic algorithm [58]. Genetic algorithm [59]
[97]	Power loss reduction and voltage enhancement	Genetic algorithm with fuzzy logic
[98, 99]	Power loss reduction and voltage enhancement [61]. Power loss reduction [62].	Ant lion optimization
[100-102]	Power loss reduction and voltage enhancement [63, 65]. Voltage stability improvement [64].	Improved bee algorithm [63]. Artificial bee colony [64]. Improved honey bee mating [65]
[103-105]	Power loss reduction and voltage enhancement [66, 68]. Power loss reduction [67].	Differential evolutionary
[106]	Power loss reduction.	Whale optimization algorithm
[107]	Power loss reduction and voltage enhancement.	Dragonfly algorithm

2.4.1.2 Hosting Capacity Enhancement

The allocation of RES-DG within a network must be per IEEE 1547.1 standard. This standard provides relevant requirements regarding the distribution network hosting capacity and DGs penetration for secured network operations [108]. The hosting capacity (HC) is defined as the amount of DGs that can penetrate the distribution network while ensuring that the network security constraints are maintained within acceptable ranges without any physical changes in the network topology. The common constraints considered for the estimation of the HC are the thermal, voltage, power quality, and protection constraints [109, 110]. The HC concept enables DSOs to quantify the impact of DG units on the performance of the distribution network using a specific set of security indices. Given the global and local constraints, HC values may be assigned to the distribution network and individual node separately. The HC for the node is referred to as locational or nodal HC. Nodal HC is more prevalent for modern distribution networks considering the impact of geographical distance on the voltage constraint, which is one of the major constraints considered in the HC evaluation. The node HC is expressed analytically as the ratio of the power from the DG units to the average load connected to the node.

To accommodate more RES-DGs securely, the HC must be enhanced as shown in Figure 2.8. Hosting capacity enhancement may be achieved through distribution network reconfiguration and expansion. With higher nodal HCs, more RES-DGs may be penetrated securely into the active distribution network. Under low nodal HCs and high penetration of RES-DG, the operation of the network will lie within the unacceptable region. Network expansion requires extensive planning, significant investment, and time to implement. Therefore, it is only suitable for long-term HC enhancement. Distribution network reconfiguration is simply achieved by the opening and closing of sectional and tie switches that already exist within the network. Hence, it is suitable for short-term and medium-term HC enhancement.

The distribution network reconfiguration scheme whose primary objective is to reduce the power losses within the network has been extended to enhance the hosting capacities of the distribution network nodes [109, 111]. Also, to ensure the security limits are not violated in the occurrence of a contingency, dynamic distribution network reconfiguration methods have been proposed in the literature to redirect power flow throughout the network [112, 113]. With dynamic network reconfiguration, the continuity of service across the network zones and areas is ensured. A multi-period optimal power flow technique with active network management (ANM) architecture for dynamic reconfiguration was proposed in [114]. Under thermal and voltage constraints, the proposed approach attempts to obtain the optimal location that maximizes the penetration size of RES- DGs in the distribution network.

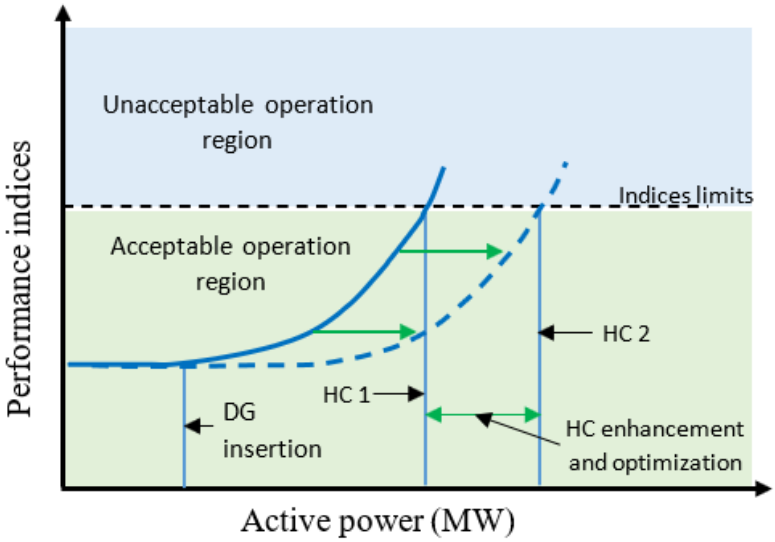

Figure 2.8: Distribution network hosting capacity.

2.4.2 Integrated Grid Security Assessment

Methods for system security assessment are broadly categorized into deterministic and probabilistic methods [115]. Under deterministic methods, there must be some pre-existing list of contingencies and expected responses to be satisfied by the system. Similarly, under probabilistic methods, a secured power system should exhibit a high probability of residing in the secured and alerts states under probabilistic network scenarios. A simple and common technique for voltage

stability assessment is the continuous power flow (CPF) with distribution-equivalencing-based predictor and corrector with a step length regulator [116]. Grid-wide security state and RES-DGs performance monitoring models are also common techniques in literature [117].

The security assessment is a major concern in the planning, design, and operation stages of electric power systems. This assessment could be done under static, transient, and dynamic modes depending on the state of the system, type of contingencies, system parameters, and dynamics focus [118]. The process of detecting the instant state of a power system is referred to as a security assessment. The security of the electric power system with RES-DGs should be tracked constantly using appropriate security indices. Normal state implies that the load is satisfied, and no limit violations occur under prevailing operating constraints and in the presence of unforeseen contingencies. Assessment of these indices may be carried out within a small area network or wide area network. More so, with the likelihood of contingencies, the security tracking process should be adaptable and extended to the alert and emergency states of the system.

In order to properly assess the security of grids with RES-DG, each step of the traditional grid security assessment process must incorporate both the steady state and dynamic RES-DG models. For steady-state assessment, the variable power output from the RES-DG units must be modeled correctly. For the dynamic and transient security assessment with RES-DG units, the steps involve monitoring the system frequency, observing the RES-DG units' synchronization units, and assessing the small signal stability. The step also involves assessing the effectiveness of the frequency response of the RES-DG units to be able to activate the appropriate dynamic frequency response. The small signal stability assessment is essential to determine if the oscillation of the system can be effectively damped. During disturbances, the frequency nadir and the rate of change of frequency (ROCOF) are tracked for the entire grid. Since it is common for RES-DG units and synchronous generation units to be impacted by large and sudden disturbances, practical risk-based security assessment methods are used in real power system operations. For the risk-based security assessment, the transient stability assessment is performed using large disturbances for N-1 and, in some cases, N-2. If the grid is stable for the large disturbance for N-1 or N-2, then the grid is dynamically stable, and the transient security can be guaranteed.

The security of the present grid has been challenged due to several technical and economic reasons. Several techniques including analytical methods and heuristic optimization techniques have been applied to solve the optimal load flow problems for the emerging power systems [119, 120]. These techniques are aimed at obtaining the best operating states of such networks considering the prevailing constraints. The security of the grid may be easily perturbed under the high penetration of RES-DG into the distribution network due to the characteristics of the generation, future loading, and the network itself. The objectives of a power system include ensuring the required amount of power is delivered to the customers at an acceptable standard and quality at the normal and alert states of the system. The N-1 and N-2 security criteria are used to evaluate the abilities to operate within permissible standards at the loss of one and two system elements [121]. This is ensured during

the planning, development, and reinforcement of such a network. While the future grid with high RES-DG penetration may present a high degree of adequacy, security is not guaranteed.

The non-linear property of RES-DG power output creates challenges in forecasting and scheduling for system operators. The energy obtained is greater at certain periods and may lead to voltage rises on nodes near the RES-DG site if not promptly curtailed. The impact of excess or surplus power generation from RES-DG systems may be limited through reliable forecasting models considering the prevailing weather factors. A reliable model will include probabilistic load growth and possible network contingencies for dynamic network architectures. Modern transmission network expansion planning (TNEP) has generated concerns about the security and reliability of the emerging grid. These concerns are increased with the proliferation of aggregators into the power trading markets. Most research has been done on the day-ahead market in the planning horizon due to the quantity of energy being traded in this market compared to other markets. The security solution model proposed in [122] is restricted to wind power integration.

To maximize the potentials of active distribution network flexibilities, new models for the integrated grid operation and efficient market structure must be developed. Several articles have been published on the impacts of an active distribution network on the integrated grid with several proposed assessment and enhancement techniques. Ref. [123] presents a review on the impact of flexible resources on the distribution systems in recent literature from the emerging grids' security perspective using three criteria. The criteria include indicators for the security of supply, modelling assumptions made, and flexibility impact assessment methods. The assumptions made for flexibility operations, the trade-off between different flexibility services, and distribution network fault handling are the major assumption considered.

The intensified investigation of voltage and frequency stability issues is prompted by the challenge posed by high RES-DG penetration. The grid frequency may attain a magnitude outside the statutory range during load demand and supply imbalance. Depending on the distribution network configuration and the RES-DG site, this imbalance may also cause voltage instability [124]. While voltage can be easily controlled at any level within the integrated grid using transformer tap changers and compensators, frequency stability using secondary controls for fast frequency regulation may be difficult to implement considering the several components involved [125]. The importance of transient stability cannot be overemphasized under power system protection. To ensure system security in these conditions, the critical clearing time (CCT) for which each relay would be activated must be predetermined through dynamic stability studies [126]. Existing conventional and non-conventional frequency stability control techniques have been applied to analyze the characteristics of disturbances and to determine the optimal response that ensures the grid's frequency stability. The conventional method includes the primary, secondary, and tertiary frequency response models. The non-conventional frequency control is mostly realized using synchronous and/or non-synchronous DG systems [127].

2.4.3 Interaction between Transmission and Active Distribution Networks

The interaction between future transmission and active distribution network operators will determine the grid's security in the future. Interaction is required between transmission and active distribution network components that were originally designed to operate independently. The coordinated control between the components which include the AVRs, FACTS devices, reactors/compensation, tap changers, and virtual power plants will be essential to maintain grid voltage and frequency within and across the transmission and active distribution networks [128]. Distributed control of RES-DGs can provide frequency regulation services to relieve the frequency control burden on traditional online automatic governor control (AGC) units. Ref. [129] discussed existing demand-side frequency control techniques for the power grid. The frequency control methods include centralized and decentralized control for demand flexibility. With demand flexibility, specific residential and industrial loads can be automatically switched off when there is insufficient generation. For the existing control methods to be viable for the future grid, the challenges associated with demand flexibility needs to be addressed. One of these challenges is the unpredictable changing diversity of loads which may lead to more load being switched off than the required amount [130].

The major operation control methods include centralized, hierarchical, decentralized, and distributed [131]. Decentralized and distributed controls are proposed as preferred control methods for the modern integrated grid in [132]. Optimal ancillary service utilization from the active distribution network through a decentralized control scheme could guarantee a maximum control of the nominal voltage. Under decentralized controls, equilibrium points at which the grids' stability may be guaranteed are discussed in [23]. In modern grid operations, distributed control schemes with exclusively localized algorithms are becoming common [133]. With distributed control, all devices and protocols are distributed, localized, and belongs to a unit, while communication is achieved between the local units and control centers. Optimal control decisions can be achieved using key information about the global power imbalance from local frequency deviations on each node. Figure 2.9 shows the interaction between the TS and DS in an active distributed system for secured future operations. The interaction between the transmission and active distribution networks may be achieved through interaction for inter-network powerflow control, network states variables, and flexibility services. Individual network operator manages the assets to achieve optimal power flow control. The system aggregator regulates the allocation and pricing for the normal powerflow and flexibility services.

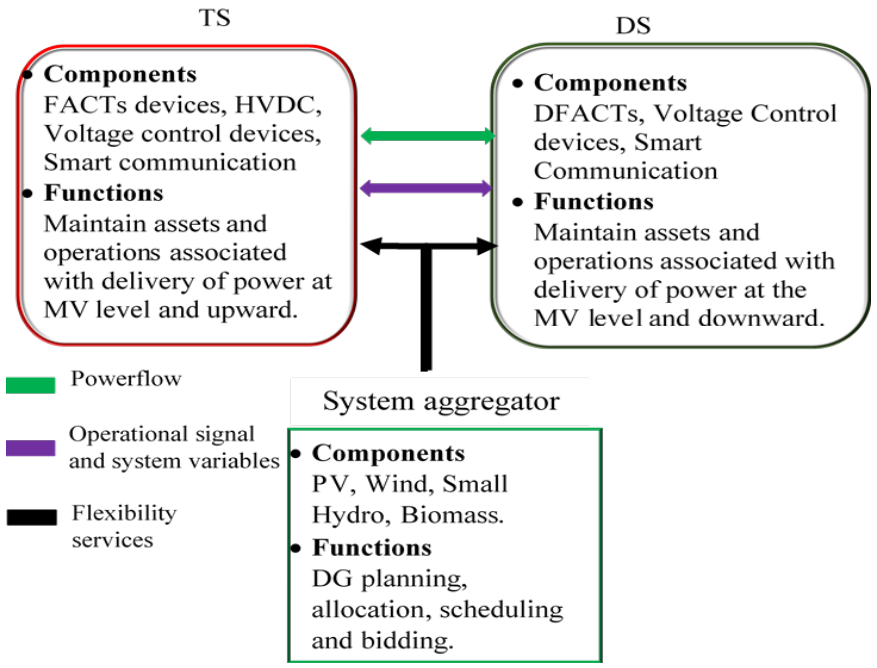

Figure 2.9: Conceptual interaction between the future TS and DS.

Through coordinated distributed demand-side control with distributed generation for primary frequency regulation, stability may be guaranteed. The objective of good interaction includes achieving fast frequency response through demand response as demonstrated in [134-136]. The proposed demand response optimal load control technique was improved in [137] by introducing a gain-tuning variable into the multi-objective optimization algorithm

It is necessary to study the effects of probabilistic and dynamic system loading for efficient generation-load matching. A scheme that consists of continuous fast-acting distributed load control algorithms for primary frequency regulation implemented at several system nodes can effectively achieve frequency control under dynamic load. A method for the optimal supply and load control for primary frequency stability using the combined passive dynamics of the generation and load scenarios was proposed in [138]. The proposed method can achieve power rebalance and localized frequency resynchronizations with significant improvement in transient conditions.

The impact of generation uncertainty of RES-DGs is critical to the development of flexible market schemes. It is therefore important to study the impact of RES-DG variability on major flexibility services such as energy balancing and congestion management. Enhanced interaction between the TS and DS is important during multiple flexibility services activation. Integration of the TS and DS flexibility control models for optimal control at the TS-DS interface to achieve global optimization will ensure the secured operation of the grid at high RES-DG penetration levels. Three market designs for TS, DS, and retailers were proposed for flexibility trading in [139]. Flexibility cost estimation and energy sharing were achieved using a series-linked optimization approach in [140, 141]. The major drawbacks of the proposed approaches for optimized interaction are the limits of optimization parameters and system security trade-offs.

Coordinating the voltage and frequency controls for the integrated transmission and active distribution network may be a major challenge in the future grid. The operation of the grid must be within the given voltage and frequency constraints while maintaining the adequacy of the power supply. While it is common to operate the PV and wind turbine systems independently with energy storage systems, a combination of the two systems within a cluster may be predominant in the future to obtain a range of ancillary support. System control, load following, supplement reserve, real power loss replacement, energy imbalance, dynamic scheduling, network stability, and system restoration are some of the ancillary services that will be considered [142]. The efficient operations of RES-DGs clusters depend on the ability of distribution network operators to instantly control the resultant power factor. Ref. [100] discussed several methods for optimal RES-DG types mix within a cluster to achieve the best responses considering different load types and different load profiles. According to [91], RES-DG types capable of generating both active and reactive power would significantly enhance the grid's loadability and reduce network total losses. Table 2.4 shows the grid ancillary services from the RES-DG types and battery storage.

Table 2.4: Renewable energy resource and energy storage system ancillary services.

Ancillary Service	Solar PV	Wind Turbine	Hydro	Battery Storage
Reactive and Voltage Support	***	***	***	***
Frequency Regulation (steady-state)	**	**	***	***
Frequency Arrest (transient state)	**	**	**	**
Frequency Support (Rebound Period)	**	**	***	**
Frequency Support (Recovery Period)	**	**	***	**
Dispatchability/Flexibility	*	*	***	***

Good *, Very good **, Excellent ***.

2.5 Research Trends for High RES-DG Penetration Support

2.5.1 Supporting Technologies

This section discusses the recent smart technology devices and concepts that support the penetration of RES-DG into the grids. A growing concept among scholars is the idea of an AC-DC nanogrid, which is suggested to become the basic building block of the future grid. This idea is directed toward the residential networks at the lowest power and voltage levels. Although the idea may imply a purely off-grid RES-DG system, the advantages of the nanogrid include fewer power converters, higher overall system efficiency, and easier interfacing between DC supply and DC load. Additionally, there is no frequency stability and reactive power issues, and the power losses are very minimal [143]. The nanogrid model will be supported through advancements in small-capacity energy storage systems (SCESS), high-temperature superconducting (HTS) materials, and smart home energy management systems (SHEMS).

2.5.1.1 Energy Storage Systems

In the future, storage systems will be more enhanced and easily handled, using predominantly modular power flow technologies. Supercapacitors, batteries, and magnetic energy storage will be readily available and easily accessible. Consumers will have access to storage devices with high power and energy densities at efficiencies over 90% [144]. Table 2.5 shows the characteristics of available energy storage devices.

Table 2.5: Energy storage types and characteristics.

ES Systems	Power Rating (MW)/Unit	Energy Density Wh/l	Power Density Wh/l	Response Time	Discharge Time	Efficiency (%)
Pumped Hydro	100–2500	0.2–2	0.1–0.2	10 s–12 min	4–16 h	70–85
CAES	100–1000	2–6	0.2–0.6	12 min	2–30 h	79–90
BESS	0.001–100	150–300	120–160	seconds	1 min–8 hrs	80–90
Flywheel	0.005–20	20–80	5000	seconds	sec-min	80–95
SMES	0.01–100	~6	~2600	milliseconds	millisec-seconds	80–95
Super Cap	0.01–1	10–20	40–120,000	milliseconds	millisec-min	80–95

Availability of high-capacity energy storage systems will mitigate the technical issues caused by variabilities of the RES-DG output in a high penetrated distribution system. The energy storage systems will also support power generation during transient and sustained load spikes resulting from electric vehicles. Recently, energy storage systems and mobile distributed generation systems have been utilized as virtual power plants (VPP) and inertia emulators for grids' voltage and frequency support. The impact of electric vehicle (EV) loads on the grid must also be considered during active distribution network planning. The models for EV load forecast should be developed for real-life charging scenarios (home, office, and trip) and drivers' schedules (work, leisure, and shopping). Future models will consider from long-term to inter-hour EV load forecasting to achieve the minimum distribution network load-generation imbalance. To obtain reliable energy management models, the models should be extended beyond the common EV parameters such as arrivals and departure time, state of charge (SOC) at the beginning and end of the trip to include location, and specific EV user behaviors, which may only be stochastically modeled.

2.5.1.2 Communication and Data Security

The grid is designed to operate in a hierarchical operational structure consisting of several layers. The five common layers to most power grids are the control application, network services, network measuring and monitoring, physical and communication layers. These layers are embedded and coordinated to ensure the continued grid operability [145]. An enhanced real-time grid-wide monitoring system has been proposed to monitor the security of the grid. The application of a real-time monitoring system can be extended to the distribution network with synchro phasors on nodes

with RES-DGs to monitor generation output and local demand fluctuations. The smart communication system is also essential for the coordinated operations of CGs and DGs protection systems, tracking of disturbance for quick islanding action, and resynchronization functions [146]. The wide-area monitoring analysis protection-control system (WARMAP) is one of the existing systems designed to ensure the safe operation of the integrated transmission and active distribution networks across these layers [147]. The communication layer, which is the key to the emerging grid operation is equally critical to the WARMAP system. The communication layer describes the information exchange among actors in the different layers according to the services to be managed and provided for both long-term and short-term operational services. Communication interruption as a result of high channel latency reduces the reliability of existing security monitoring systems [148]. To prevent the breakdown between the layers, it is necessary to review and regularise the information communication systems standards, codes, and requirements.

The communication layer is also important to the realization of the energy internet through the possibility of grid components to operate in the plug-and-play model. Although the implementation of energy internet will improve the system reliability and energy efficiency [149], several concerns must be considered. Some of these concerns include challenges in components standardization, stability issues, cyber-attacks vulnerability, and scalability [150]. Consequently, the goal of recent research in the area of energy internet has been focused on addressing these concerns [151]. Smart sensing systems and remote IoT devices have been developed to monitor energy flows at the system nodes. These devices will have the capability to automatically re-route power based on the programmed criterion for optimal operation of the grid [152]. Several architectures including the Future Renewable Electric Energy Delivery and Management (FREEDM) in the USA and Global Energy Interconnection Development and Cooperation Organization (GEIDCO) in China have been implemented to achieve the vision of the energy internet through the integration of RES-DGs with standardized plug and play interfaces [153].

A review of smart grid communication technologies was presented in [154] focusing on the use of power line communication (PLC). It was concluded that PLC with medium access control (MAC) and time domain multiple access (TDMA) protocols are effective for smart grid communication due to their flexibility. However, their applicability for real-time operation monitoring between the transmission and active distribution operators is uncertain due to their low coexistence efficiencies. Ref. [155] demonstrated that the frequency stability of the emerging power system may be enhanced through the utilization of the appropriate data communication topology for RES-DG control to achieve fast secondary frequency response. Data transferred through the PLC can be used for effective voltage control by the transmission system operators. Data nodes which are referred to as control agents are installed on the transmission system nodes to stores the voltage states of the nodes. In [156], the control agents were employed to make operational decisions by optimizing the present and future voltage state within the network constraints.

The integrity of transients and RMS network data transfer is crucial to the protection systems. A backup protection scheme for traditional protection using fast data exchange approach for interfaced islanded RES-DGs is demonstrated in [157]. The IEC 61850 standard emphasizes the importance of integration and unification of communication standards between different network components and models. Ref. [158] achieved the interfacing of the distributed energy sources testbed in the smart grid energy research center (SMERC) from the USA with the Korean institute of energy research (KIER) testbed. The interface aims to develop a communication-supported microgrid digital protection relay for fast fault detection across the two testbeds. The method involves the application of a distributed microgrid digital protection relay which communicates with the microgrid central protection manager (MCPM).

The ability to accurately model active distribution systems with smart grid components and associated characteristics will require existing tools to significantly adapt to meet the new conditions. Enhanced and faster computing methods will be key for tool development in active distribution system analysis to support the emerging grid. The integrity of system data and information is crucial to the operation of the emerging grid. Despite its many advantages, the emerging grid is characterized by various security attacks since it combines several components. Some of these components which include synchrophasors, the internet of things (IoT), wireless devices, and industrial components are susceptible to a variety of attacks. Device attacks, data attacks, privacy attacks, and network availability attacks are some of the existing and potential attacks. Furthermore, the existing technologies for protection against these attacks have not integrated modern security solutions, therefore, may not be effective [159]. The capacity to sense and prevent an attack at different network layers and levels under dynamic system architecture through advanced information security devices is critical to the grid's security. The consideration of these attacks increases the complexity of planning and grid restoration models for the emerging grid [160].

2.5.2 RES-DG Penetration Level

Renewable energy sources DG penetration increases the scope and complexity of active distribution network planning and operation due to the variables that are considered. Attempts to define RES-DG penetration have been about the space utilization for PV and WT installation to the total space, the annual energy from DG systems, and the total energy consumption relative to the transformer capacity. More specifically, RES-DG penetration can be defined as the ratio of the total RES-DG power to the peak load demand on a specific feeder in a distribution network [161]. It is indeed necessary to make reasonable assumptions to develop a feasible RES-DG penetration modeling considering several parameters involved. The parameters include the number and types of clustered RES-DG connected to a point, the power factors of the DGs, physical upgrades and investments on network elements, and the variations of wind and solar irradiance. These parameters will be combined and optimized to obtain several best operation stochastic scenarios for a specific active distribution network at specific times. To optimize the operating state of a network, the

approaches proposed by scholars can be categorized into the distribution power flow approach, scenario-based approach, engineering approach, and network planning approach.

The maximum allowable RES-DG penetration can be determined by constantly observing the networks' security limits as the penetration is steadily increased. Many traditional rules and guidelines including the rule of thumb will no longer be applicable. New guidelines and techniques, therefore, need to be developed. According to the thumb rule, a RES-DG can be penetrated up to 15% without having any significant technical impact on the distribution system [162]. Whereas the zero-point analysis focuses on the point on the feeder where power flow is zero, due to the RES-DG unit aggregated output. The secured increase in the RES-DG penetration lies in the capabilities of the grid-following inverters to support frequency and voltage using local distributed and decentralized frequency and voltage regulation strategies.

Operating a zero-inertia system with grid-following inverters, where it is unclear which grid components are responsible for frequency and voltage regulations in an emergency state is at the moment hypothetical. The future power grid models a system with a very low inertia requirement since many synchronous generators will be replaced with non-synchronous generators. This model may be feasible with the guarantee of only small and steady power imbalances. However, to ensure the security of the emerging grid during fault conditions, a significant level of inertia proportional to the capacity of the grid is required. While the possibility of a 100% renewable energy grid was discussed for small and large power systems in [163], a safe RES-DG penetration level of 20% - 30% for the grid security to be guaranteed was recommended in [164]. This secure penetration level is recommended given that traditional frequency control methods may not be suitable for the integrated transmission and active distribution network operation under normal and contingency conditions. To this end, new tools to dynamically assess the safe RES-DG penetration level into the distribution network for secure operation under normal and N-1 states considering changing network architecture are needed.

The allocation of RES-DG is dependent on the structure and load concentration of the distribution network. Allocation of RES-DG simply means to determine the size of the RES-DG and the siting of the RES-DGs within the distribution network. The size of the RES-DGs is determined from the distribution network feeders' hosting capacity [109]. The hosting capacity is used to describe the RES-DG penetration level below which the grid is secured without network reconfiguration or reinforcements. Since the hosting capacity of the node reduces with distance from the substation, reconfiguration of the distribution network is useful to ensure high hosting capacities at certain network nodes [165]. The future active distribution networks will be highly meshed to obtain higher feeders' hosting capacities. However, solutions to the difficulties of operation of the protection devices need to be developed. Since the relation between the maximum penetration of clustered RES-DGs and the distance from the TS-DS substation has been established, the objectives of allocation techniques and methods include determining the level of generation scheduled to these RES-DGs considering security constraints.

2.5.3 Integrated Transmission-Active Distribution Security

The discussions on emerging grid security have been focused on the impact of high RES-DG penetrations on the transient stability of the grid [166]. An attempt was made in [167] to include probabilistic characteristics of wind DG into the grid's oscillatory stability margin (OSM) using random modeling and quantitative statistical analysis. It was claimed that the location and existence of high wind DG penetration are detrimental to the OSM of the active distribution network. Enhanced real-time system monitoring can be achieved with phasor measurement units (PMUs) combined with artificial intelligence-based state estimation during normal and contingencies states. A heuristic technique-based quantitative assessment of dynamic and transient stability using PMU and wide-area monitoring (WAM) techniques to analyze various stability concerns in the smart power grid caused by DG was proposed in [168].

The optimal distributed power flow control within the emerging grid will depend on reliable network component modeling. The modeling and assessment of the impacts of RES-DG on the emerging grid are mostly stochastic due to the generation and load variabilities. However, to develop functional and reliable models, some degree of certainty will be assumed. New techniques that combine deterministic and probabilistic methods have been developed in recent literature. A hybrid method was proposed in [169]_ENREF_96 to study the impact of PV-based DG units on the distribution system. The impact of wind generation uncertainties on the generation and transmission expansion planning was also studied in [170] using hybrid quantitative and heuristic modeling.

Models for efficient bidirectional power flow control between the transmission networks and active distribution networks are important to ensure the reliability of the protection systems. Two hierarchy levels of optimal power flow were proposed in [171] to achieve decentralized optimal operation between the TS and DS. While many deterministic or probabilistic techniques have been proposed in the literature for the security assessment of grid with RES-DG, few considered the N-1 and N-2 security criteria for a given system operating state. Developing deterministic security assessment methods for the grid is straightforward and also easy to implement. However, generalizing the results of the worst-case scenarios obtained using such a deterministic model may not fully represent the response of the network during contingencies. Few other papers considered probabilistic approaches for reliability assessment using indices like the Loss of Load Probability (LOLP) and Loss of Load Frequency (LOLF) to evaluate security under steady and transient states. However, to deal with the frequently occurring RES-DG and EV variations, as well as occasional network contingencies, such a security assessment approach requires extensive computation and simulation. Hence, the security of the emerging grid may be ensured using dynamic security assessment tools for the integrated grid considering several deterministic and probabilistic conditions in the transmission network, active distribution network, and the TS/DS interface.

2.6 Conclusions and Future Work

2.6.1 Conclusions

High penetration of RES-DG into the distribution networks creates many operational benefits as well as some technical concerns. The flexibilities of DG systems will increase grid resilience and enhance grid stability through ancillary services support if properly planned and operated. The latest trends for the emerging grid operation, framework, components, tools, and techniques were discussed in this paper. Renewable energy sources DG penetration allocation using various techniques, which include analytical, conventional, and AI-based optimization methods, were reviewed. Technical impacts of high RES-DG penetration on the distribution systems were investigated using various indices (power losses, voltage, and transient stability index) under various deterministic and probabilistic approaches. Reliable tools for RES-DG clusters generation schedule may be achieved through enhanced prediction models for RES-DG generation forecast considering short time planning, weather conditions, load forecast, and network constraints.

Conventional relays are unreliable for system protection due to variations in the direction and level of fault currents. Excess current is generated during the off-peak demand period and peak generation period from RES-DG causing unintended reverse power flow. The protection system selectivity is impacted by the reverse power flow, thereby, occasionally resulting in false tripping. Advancements in alternative protection systems such as directional overcurrent relays will improve the coordination of protection devices within the grid under high RES-DG penetration.

This review showed that the present grid relies on the independent frequency and voltage controls within the transmission and active distribution systems using central and hierarchical approaches. In conclusion, the major limiting factors for high RES-DG are voltage instability issues, protection challenges, and reduced resultant system inertia. The proposed techniques for voltage control and new protection schemes in the literature are promising to be considered for practical applications. However, until synthetic and virtual inertia emulation systems, as well as upgraded energy storage systems, are fully deployed in the TS and DS, the question of how much RES-DG penetration into the active distribution system is safe remains unresolved to a considerable extent.

2.6.2 Recommendations for Future Research

This paper presented a discussion about the emerging grid framework and the technical issues regarding its security. Various tools and techniques proposed to assess the impact of high penetration of RES-DG into the grid were also reviewed. Observations were made concerning the limitations of the proposed approaches aimed at ensuring the security of the emerging grid with high penetration of RES-DGs. Following these reviews and conclusions, more research to address limitations in these areas is needed:

- Dynamic and adaptable RES-DG clusters allocation technique considering system ancillary services.
- Security assessment of integrated TS-DS considering active distribution network architecture reconfiguration scenarios.
- Enhanced interaction for voltage and frequency control schemes in an integrated TS-DS with demand-side management.

Author Contributions: Conceptualization, I.O and R.Z; methodology, I.O and R.Z; validation, R.Z, M.A and J.S; formal analysis, I.O and R.Z; writing—original draft preparation, I.O; writing—review and editing, I.O, R.Z, P.M, M.A and J.S; visualization, R.Z, P.M, M.A and J.S; supervision, R.Z. All authors have read and agreed to the published version of the manuscript.

Funding: The authors acknowledge the financial support provided by the Ministry of Foreign Affairs and Trade (MFAT), New Zealand in the form of New Zealand Scholarship for Doctoral Degree to conduct this research.

Institutional Review Board Statement: Not applicable.

Informed Consent Statement: Not applicable.

Data Availability Statement: Not applicable.

Conflicts of Interest: The authors declare no conflict of interest.

3 Manuscript 2: Optimal RES-DG Placement

Preamble

One of the review's conclusions in Chapter 2 is the need to extend the optimization objective and constraints for distribution network planning for the optimal placement of RES-DG units to include probabilistic security variables. The variability in the power output from RES-DG units results in probabilistic scenarios that can only be accommodated with probabilistic security indices and constraints. Also, limiting the effects of the bi-directional power flow caused by the occasional over-generation from RES-DG units would require the inclusion of probabilistic security objectives and constraints in the optimal allocation problem formulation of RES-DG units. Consequently, Chapter 3 presents a method for optimal RES-DG units allocation using deterministic and probabilistic variables using the decision tree classification approach. The variables considered are the grid power loss, voltage risk index, and hosting capacity. The power loss and hosting capacity are the deterministic variables, while the voltage risk index is the probabilistic variable. The impact of the different inverter voltage control modes on the optimal RES-DG allocation is also discussed in Chapter 3.

Security Constrained Optimal Placement of Renewable Energy Sources Distributed Generation for Modern Grid Operations

Ifedayo Oladeji*, Ramon Zamora and Tek-Tjing Lie

Department of Electrical and Electronic Engineering, Auckland University of Technology, Auckland 1010, New Zealand

Abstract: In modern distribution network planning and operation, optimal distribution generation (DG) placement has become increasingly important. Consequently, extending the optimal DG placement objectives beyond the commonly used deterministic indices to include probabilistic security indices is essential. This paper proposes a decision tree (DT) classification approach for multiple photovoltaic DG (PVDG) units' placements using specific indices in an unbalanced distribution network. The security indices considered in this paper are the branches' risk index (RI) and power loss (PL). The optimal branch(es) for PVDG units' placements are determined through the branches' RI and PL, and the optimal nodes are determined using the nodal hosting capacity (HC) and zero-point (𝔛). The proposed technique was tested on the IEEE 33 and 69 node radial distribution networks considering three common PV voltage control modes, namely, constant voltage (CV) mode, reactive power-voltage (QV) mode, and reactive power-power factor (Q-PF) mode. After the optimal placement of the PVDG units under the constant voltage control technique, the worst case of the average probabilistic voltage was improved from 0.798 and 0.941 to 0.94 and 0.975 for IEEE 33 and 69 node distribution networks, respectively. The steady-state power loss was also reduced by 78% and 32.72% for the IEEE 33 and 69 node distribution networks, respectively. The proposed technique was also compared with recent and existing methods in the literature. The proposed technique performs better in terms of power loss reduction and voltage enhancement.

Keywords: Hosting capacity, Modern grid, Optimal placement, Photovoltaic, Risk index.

Nomenclature

$\boldsymbol{I_{br}^{p}}$	Total branch current.
$\boldsymbol{V_{i}^{p}}$	Phases voltages magnitude.
$\boldsymbol{V_{T}^{h}}$	Voltage harmonics distortion.
$\boldsymbol{RI}$	Risk index.
$\boldsymbol{PL}$	Power loss.
$\boldsymbol{HC}$	Hosting capacity.
$\boldsymbol{V_{cr}}$	Nodal critical voltage.
$\boldsymbol{S_{tg}}$	Total DG apparent power generation.
$\boldsymbol{P_{g}}$	DG active power generation at the $\boldsymbol{i}$-th node.
$\boldsymbol{P_{li}}$	Active load of the $\boldsymbol{i}$-th node.
$\boldsymbol{Q_{l}}$	Reactive load of the $\boldsymbol{i}$-th node.
$\boldsymbol{P_{r}}$	Probability of $\boldsymbol{i}$-th node voltage outside limits.
$\boldsymbol{A}$	Severity of voltage deviation.
$\boldsymbol{V_{cr}}$	Critical node voltage.
$\boldsymbol{B}$	Branch.

$\boldsymbol{\sigma}$	Branch load deficit
ϰ	Zero-point
CV	Constant voltage
QV	Reactive power – voltage
Q-PF	Reactive power – power factor
PVDG	Photovoltaic distributed generator
DT	Decision tree
$\boldsymbol{P_t}$	Parent node
$\boldsymbol{C_t}$	Child node

*Corresponding Author: Tel.: +64225331241
E-mail address: ifedayo.oladeji@aut.ac.nz

3.1 Introduction

3.1.1 Background and motivation

The power grid's topology is transitioning from centralized generation to distributed generation (DG) within distribution networks. Traditionally, distribution networks are passive networks and are considered a load to the transmission/sub-transmission networks. Distributed generation (DG) units in a distribution network create an active distribution network (ADN), which, if not optimally allocated, may cause security challenges within such distribution networks. The change in distribution network topology from a passive to an active distribution network occasionally causes voltage limit violations, insufficient-excessive generation, and insecurity across the transmission and distribution systems [172].

When optimally allocated, DG can improve the distribution network's security and reliability while significantly reducing the power loss. Non-optimal high penetration of DG, on the other hand, may impact power quality and protection systems coordination, and cause congestion in some network zones [173]. Also, the amount of power generated by renewable energy source (RES) based DG units is strongly correlated with stochastic variables such as weather, temperature, and time. Therefore, the integration of DG into modern distribution systems, as shown in Figure 3.1, necessitates a proper planning framework to ensure that the performance of the distribution network can meet the expected power supply quality, security, reliability, and profitability [14]. Modern distribution network planning and operation includes reconfiguration schemes through available tie-lines and section lines to achieve dynamic DG allocation. Dynamic DG allocation is necessary to enhance network reliability and resilience during planned and unplanned outages. Modern distribution networks are designed to manage bi-directional power flow and inter-area power transfer via tie-lines. Excess power flows into the sub-transmission network through grid exit points for flexibility support from the distribution network during off-peak hours.

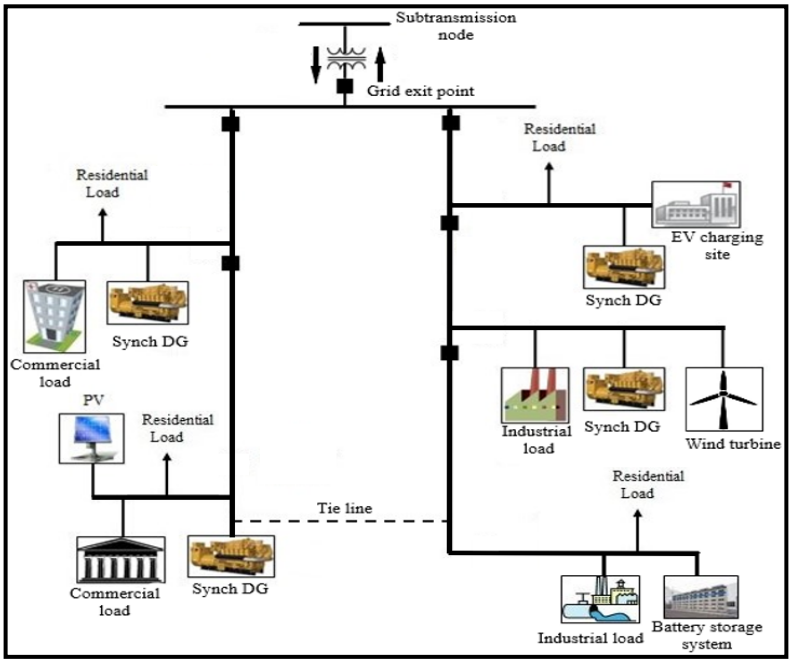

Figure 3.1: Modern distribution network

The allocation of DG units in modern distribution networks is considered an optimization problem that may be solved using appropriate algorithms. Analytical, heuristic or a combination of both have been proposed in the literature to solve optimization problems. The factors that impact algorithms' choice under the prevailing network operation conditions include the combination of possible sites, the type, and the size of the proposed DG units. The combination of factors will increase the complexity of the optimization process and the computational requirements of the tools required to obtain optimal solutions, especially for large distribution networks. Given that some recent grid blackouts were caused by DG system failures [26], the DG placement objectives must be expanded to incorporate security and risk indices in addition to voltage profile, costs, and power loss (PL) indices for normal network conditions. The security and risk indices should also consider probabilistic approaches that combine the generation's uncertainties, load variations, and network contingencies.

3.1.2 Literature survey

Techniques for the allocation of renewable and non-renewable energy sources DG units in distribution networks have been discussed and proposed in several articles. Refs. [51, 174] present reviews on issues including approaches for optimal DG allocation, ancillary support from DGs, applications, prospects, and the impact of DG units on the distribution network. Recent optimal allocation techniques, objectives, and constraints for the DG units have been thoroughly investigated in [65, 175, 176]. The technique proposed in [176] extends beyond placement objectives and constraints to include suitable allocation techniques for the existing ancillary market and potential challenges in DGs management. Ref. [65] presents a comprehensive and systemic analysis of techniques for voltage enhancement and power loss reduction considering several network planning

variables and types of loads. Although modeling the DG unit allocation problem as a deterministic and single-objective problem is valid, as shown in [177], a practical approach to optimal DG allocation should be created using a stochastic multi-objective model. Refs. [90, 93, 178] proposed techniques for optimal DGs allocation considering generation and load uncertainties under several scenarios. The method in [178] involves Monte-Carlo simulation-based particle swarm optimization techniques with multiple DG units and battery storage. It focuses on economic objectives that may be extended to include technical objectives.

The allocation of DG units has primarily been achieved through analytical models based on specific performance metrics. Solutions are relatively easy to obtain with analytical models, and the conclusions are consistent under the conditions and assumptions given. Additionally, analytical models can minimize the computational complexity of unbalanced systems. Recent articles have explored analytical methods for allocating DGs in a distribution network. Refs. [84, 93] propose methodologies based on the loss sensitivity, voltage stability, and DG selection index. The voltage profile was improved using the probabilistic load flow (PLF)-based voltage stability evaluation technique and varied DGs operational power factors.

The optimal DG units allocation problem is a multi-constraint and non-linear problem. Therefore, heuristic optimization algorithms are widely utilized over conventional optimization solving techniques. The preference for heuristic optimization techniques is due to the ability of heuristic algorithms to achieve better convergence with complex and non-linear problems. Like analytical methods, conventional optimization methods can be employed for problems with small networks and problems with fewer constraints, as shown in [179, 180]. Hybrid non-linear programming and metaheuristic algorithms are proposed in [181, 182] to enhance the performance of the conventional optimization methods. The problem-independent characteristic of metaheuristic algorithms makes it excellent for DG unit optimal allocation problems. Metaheuristic methods based on swarm intelligence are widely employed in the literature for optimal DG unit allocation. Swarm intelligence algorithms can adapt to changing constraint spaces and are immensely flexible and robust [98, 99]. Using several swarm intelligent-based algorithms, ref. [69] demonstrated the feasibility of achieving optimal allocation of multi DG units with different types. The objective includes voltage deviation and power loss minimization using the weak bus and loss sensitivity factor. Hybrid swarm intelligence techniques were also proposed in [21, 22] in order to enhance the performance of the swarm intelligent-based algorithms.

The need for more robust and intelligent techniques leads to an increase in the applications of machine learning algorithms to power system problems. Machine learning algorithms have been applied to solve distribution system planning and DG allocation problems [183, 184]. A technique for optimal sizing of the PVDG sources in the unbalanced distribution network using reinforcement learning was proposed in [185]. The proposed reinforcement learning with a single regressor technique in [186] is helpful for the allocation of DGs in a network by anticipating voltage violations

for several generation scenarios. However, the suitability of the proposed technique to detect violations due to load changes cannot be established.

3.1.3 Contributions and paper organization

The proposed method in this paper involves optimizing the network's probabilistic risk index (RI) and power loss (PL) under the nodal hosting capacity and PVDG capacity constraints, using the decision tree classification technique. The RI is estimated using the probability of a node voltage existing outside the security limit and the severity of the deviation of the node voltage from the nominal value. The voltage probability is derived using a probabilistic unbalanced power flow technique based on Monte-Carlo simulations with normal distributions for load variations. The risk of undervoltage or overvoltage caused by the high penetration of DG can be reduced using the proposed allocation technique. Also, in this paper, the optimal RES-DG allocation was studied under three common RES-DG units voltage control modes: constant voltage (CV), reactive power-voltage (QV), and reactive power-power factor (Q-Pf).

The literature survey shows that the security-based objectives and constraints have not been adequately addressed during the distribution network planning and expansion of existing networks. Therefore, there is a need to incorporate security-based probabilistic objectives and constraints in the DG placement problem formulation while considering the unbalanced state of the distribution network. Consequently, the main contributions of this paper include:

1) applying network risk index (RI) variables to determine the optimal branch for PVDG(s) placement,
2) applying a hosting capacity and branch zero-point approach to obtain the optimal node for PVDG(s) placement,
3) implementing a decision tree (DT) classification technique for optimal PVDG placement in an unbalanced distribution network and
4) analysing the impacts of the different PVDG units' voltage control modes on the performance of the distribution network.

The rest of this paper is organized in the following order. Section 3.2 discussed the modern distribution network planning focusing on the impact of non-optimal DG allocation, the network's hosting capacity, and PV system modeling. The proposed approaches for RI evaluation, the DG placement problem formulation, and the decision tree (DT) classification model implementation are presented in Section 3.3. The results obtained from testing the proposed technique on IEEE 33 and 69 nodes distribution networks are presented and discussed in Section 3.4, while the conclusions are presented in Section 3.5.

3.2 Modern Distribution Network Planning

The penetration of DG systems and energy storage systems (ESS) in modern distribution systems will be substantial. As these systems become more widely used, the conventional role of distribution system operators in terms of planning and operation will change. When significant DG penetrations are to be anticipated for a distribution network in the future, the complexity of the planning models is also increased. Distribution networks should be analyzed for maximum allowable penetration of these systems, especially the RES-DG, to prevent jeopardizing grid security. Photovoltaic distributed generation (PVDG) and wind turbine distributed generation (WTDG) are the two most promising and common RES-DG systems. PVDG and WTDG units' output intermittency and variability exacerbate distribution system operators' forecasting, planning, and power scheduling challenges. The likelihood of contingencies within the distribution system, which can occur for various factors, increases the complexity of distribution network planning. Consequently, deterministic methods for distribution network planning may be ineffective for modern networks.

Considering the capacities of the proposed DG units to be connected to the distribution network, the unit's peak power output, particularly the PVDG unit, is occasionally greater than the immediate local load demand. The excess power results in overvoltages and reverse power flow within the distribution network. Power curtailment, power exporting, storage technologies, and reactive power control techniques are solutions that have been explored to achieve power flow control. A PVDG unit reactive power local control technique based on the capabilities of the PV inverters is employed to maintain the local voltage within the acceptable range. The constant voltage (CV) mode, reactive power-voltage (QV) mode, and reactive power-power factor (Q-Pf) mode are three common types of local voltage control modes of PV inverter systems.

3.2.1 Impact of non-optimal placement of DG units

Distributed generation units convert a traditionally passive distribution network into a multi-source active distribution network. The major advantages of proper penetration of DG into distribution networks include the reduction of overall network losses and improvement of the voltage profile. Another advantage is that distribution system operators can utilize the generation from specific DG units to control demand and supply fluctuation across different timelines and seasons [37].

Overpenetration of DG causes negative impacts, mostly discussed under power quality and protection problems. When the DG units generate more power than scheduled, it is referred to as overpenetration of DG within an active distribution network. The main causes of power quality issues are a lack of mechanical inertia in RES-DG units as well as unpredictability of solar irradiance and wind velocity. Likewise, the lack of fault current limiting capacity in RES-DG unit converters creates significant protection challenges [93].

Sudden changes to the root mean square (RMS) voltage are caused by the solar irradiance and wind velocity changes. In a distribution network with significant loads, voltage sags and swells are common during fault periods and are accompanied by a prolonged restoration to a new steady-state voltage magnitude. Several realistic scenario-based strategies, including improving the dispatchability of RES-DG units and prioritizing DG units with reactive power absorption capabilities, may be adopted to address voltage stability concerns that limit optimal DG penetration [11].

3.2.2 Hosting capacity

The allocation and operation of distributed generation unit and other related components within a distribution network must conform to the IEEE Std 1547.1 standard. This standard specifies important distribution network hosting capacity requirements and DG operations [108]. The hosting capacity (HC) is estimated as the amount of power generation from DG that can penetrate the distribution network while maintaining acceptable network security limitations without requiring network reinforcements or expansion. Following a change in distribution network architecture, such as reconfiguration or expansion, a new HC value must be established for the network.

The HC framework allows distribution system operators (DSOs) to assess the impact of DG units on the distribution network's performance by using specific sets of security indices. According to global and local constraints, HC values are assigned to the distribution network and individual nodes. Locational or nodal HC refers to the HC for the node. Because of the impact of geographical distance on the voltage profile, which is one of the critical constraints in HC evaluation, nodal HC is more popular for modern distribution networks. If S_{DG} is the total power from the DG units and S_{Load} is the load connected to the node, then the nodal HC may be expressed analytically using (1).

$$HC(i) = \frac{S_{DG}}{S_{Load}} \tag{1}$$

The three major steps used to determine the HC for each node in the distribution network in this paper are as follows:

Step 1 - Constraints selection

The key constraints for hosting capacity evaluation are the thermal loading, voltage, power quality, and protection constraints.

Step 2 – Constraints definition and HC estimation

Local or global constraints are specified during the constraints definitions for nodal and global HC, respectively. The HC is subsequently estimated using normal power flow analysis considering the specified constraints.

Step 3 – Security limits violation check

The final step in determining the nodal HC is to compare the estimated HC to the existing security limit. This step is required to assess the additional DG capacity that can be accommodated.

3.2.3 Constraints definition

The thermal limit is used to constrain the current flow in each phase (p) of the network branches as given in (2). The voltage constraint for HC estimation is given in (3). Individual harmonic distortion (IHD) constraints are used in (4) to ensure compliance with harmonic standards. The nodal fault current contribution and reverse power flow are the common protection constraints available for the HC estimation. The fault current contribution constraint is modeled as (5). Also, the reverse current representing the reverse power flow constraint is modeled as (6).

$$I_{br}^{p} \leq I_{br,max}^{p} \tag{2}$$

$$V_{i,min}^{p} \leq V_{i}^{p} \leq V_{i,max}^{p} \tag{3}$$

$$V_{i,T}^{m} \leq IHD^{m} \tag{4}$$

$$I_{f}^{p} \leq I_{f,max}^{p} \tag{5}$$

$$I_{r}^{p} \leq I_{r,max}^{p} \tag{6}$$

where $I_{br,max}^{p}$ is the current carrying capacity of the branch, V_{i}^{p} is the node phase voltage, $V_{i,T}^{h}$ is the voltage distortion at node i for the harmonic order m for period T. I_{f}^{p} and I_{r}^{p} are the fault and reverse currents for each phase.

3.2.4 PV modeling and inverter voltage control

The power output of photovoltaic DG (PVDG) systems depends on the environmental conditions around the installation site. Environmental conditions, precisely the ambient temperature and solar irradiance vary every time and season. Several methods have been proposed to model the solar irradiance characteristics [187, 188]. Increased penetration of PVDG into the distribution networks will undoubtedly affect the system's operation in the normal state due to the stochastic nature of the PVDG output. This paper, therefore, proposes a technique aimed at reducing the voltage risk during normal and probabilistic operation states where all the security conditions are always met with varying levels of power generation from PVDGs. Optimal allocation and operation of PVDG will support the network to remain in the normal state or recover from the alert and emergency states in terms of flexibility services. Peak load shaving, valley filling, load shifting, frequency support, and voltage support are examples of obtainable flexibility supports from distribution networks with PVDG [189].

The PVDG unit's performance depends on the season, time of day, and PVDG inverter efficiency. The power output from PV generators is modeled in (7). The PV cell temperature (T_c) is represented in (8), while the variation of the power output from PV (P_{pv}) is represented by the function in (9) [190, 191].

$$P_{pv} = P_{stc}\left[\frac{G}{1000}(1 + \delta[T_c - 25])\right] \tag{7}$$

$$T_c = T_{amb} + \left(\frac{T_{c-n}-20}{800}\right)G \tag{8}$$

$$f(P_{pv}) = \frac{1}{\sigma\sqrt{2\pi}}Exp\left[-\frac{1}{2}\frac{(P_{pv}-\mu)^2}{\sigma^2}\right] \tag{9}$$

where μ and σ are the expected mean value and standard deviations of the power output from the PVDG units, T_{amb} and T_{c-n} are the ambient temperature, cell temperature at nominal operating conditions in ℃, respectively, G is the solar irradiance in (W/m^2), δ is the power-temperature coefficient (%/℃), and P_{stc} is the power under standard conditions.

3.2.4.1 Constant voltage (CV) mode

The constant voltage (CV) mode for local voltage control is one of the most commonly used voltage control techniques in PV systems. The CV mode enables the PV system to generate optimal power using a suitable maximum power point tracking (MPPT) method. The output voltage of the PV system is kept constant irrespective of the changes in environmental conditions (solar irradiance and temperature) [192]. The CV technique ensures that the difference between a reference voltage and the output voltage of the PV converter is below a certain threshold. The output voltage (V_o) modeled by (10) is maintained at a constant value by altering the converter's duty cycle D [193].

$$V_o = \frac{V_{in}(K+1)}{1-D} \tag{10}$$

where V_o is the output voltage, V_{in} is the voltage before the PV converter, and K is a constant representing the PV converter turn ratio.

3.2.4.2 Reactive power-voltage (QV) control mode

In the reactive power-voltage (QV) control mode, the active power from the PV system is kept constant, while the reactive power Q_V is determined according to the voltage at the node to which the PV is connected. If Q^i_{max} is the maximum reactive power generation limit of the PV system, then the reactive power at the PV inverter node can be modeled using (11) to (13) [194].

$$Q_V^i = \begin{cases} Q_i^{max} & V_i < V_1 \\ \alpha & V_1 \le V_i \le V_2 \\ 0 & V_2 \le V_i \le V_3 \\ \beta & V_3 \le V_i \le V_4 \\ -Q_i^{max} & V_i > V_4 \end{cases} \quad (11)$$

$$\alpha = \frac{Q_i^{max}}{V_1 - V_2(V_i - V_1)} + Q_i^{max} \quad (12)$$

$$\beta = \frac{Q_i^{max}}{V_3 - V_4(V_i - V_3)} + Q_i^{max} \quad (13)$$

where V_1 and V_4 are the lower and upper voltage limits respectively, V_2 and V_3 are the lower and upper voltage limits of the dead zone, respectively.

3.2.4.3 Reactive power-power factor (Q-PF) control mode

In the variable reactive power-power factor characteristic mode, the active power from the PVDG unit is determined by varying the unit's power factor. The PVDG unit's operating power factor translated linearly within a predefined minimum and maximum active power limits, as shown in Figure 3.2. When the active power delivered by the PVDG unit is lesser than a predefined minimum limit which is the PVDG unit rated active power (P_r), the PVDG power factor is unity. As P approaches P_r, the power factor also approaches the minimum power factor pf_{min}. The effective operating power factor (pf) and the reactive power (Q_i) of the PVDG unit can be modeled using (14) to (16).

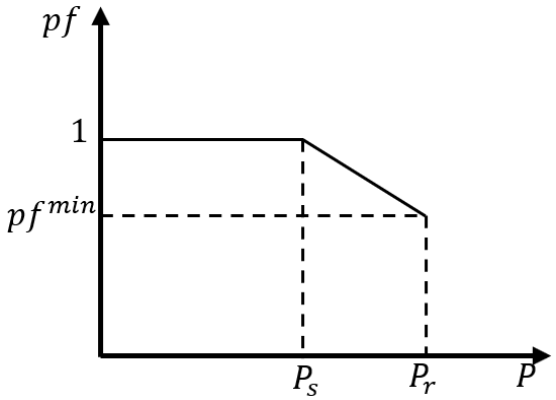

Figure 3.2: Power factor-active power curve

$$pf = \begin{cases} 1 & 0 \le P < P_s \\ 1 + \gamma & P_s \le P \le P_r \\ pf_{min} & P = P_r \end{cases} \quad (14)$$

$$\gamma = 1 - \frac{pf_{min}}{P_s} - P_r \quad (15)$$

$$Q_i = \frac{\sqrt{1 - pf^2}}{pf} P_r \quad (16)$$

3.3 Methodology

The allocation of RES-DG in a modern distribution network is a probabilistic network planning problem that must account for uncertainties. Possible contingencies as well as variations in the output of the PVDG units and node loads are among the uncertainties that must be considered for the modern distribution network. The variations in the node load are modeled using appropriate distribution functions. However, given that the distribution network's topology remains constant before implementing reconfiguration schemes, a degree of certainty can be anticipated. This paper, therefore, seeks to determine the optimal PVDG units placement through the deterministic and stochastic variables-based decision tree (DT) model. The network risk index (RI) and power loss (PL) are considered probabilistic indices, whereas hosting capacity (HC) and zero-point are considered deterministic indices.

3.3.1 Modeling the voltage risk index

The risk index (RI) represents a quantitative risk level assessment of the node voltage of the distribution network. In this paper, the voltage RI is estimated based on the probability that the voltage at the node will exist outside the permissible limits. The algorithm proposed for the modeling of a distribution network RI is based on the Monte-Carlo simulation-based probabilistic load flow (MCSPLF) method as shown in (17) and (18) [195, 196]. The loads' active and reactive power variations are modeled using the normal probability distribution functions (pdfs) as shown in (19).

$$P_{li}\left(s\langle\mu_{P_{li}},\sigma_{P_{li}}\rangle\right) = G\left(f(P_l),h(s),\mu_{P_{li}},\sigma_{P_{li}}\right) \tag{17}$$

$$Q_{li}\left(s\langle\mu_{Q_{li}},\sigma_{Q_{li}}\rangle\right) = G\left(f(Q_l),h(s),\mu_{Q_{li}},\sigma_{Q_{li}}\right) \tag{18}$$

$$f(P_l,Q_l) = \frac{1}{\sqrt{2\pi\sigma(P_l,Q_l)}}\,exp\left(-\frac{((P_l,Q_l)-\mu(P_l,Q_l))^2}{2\sigma^2_{(P_l,Q_l)}}\right) \tag{19}$$

where h is the random sample in the set of possible samples for the s-th scenario, μ and σ are the expected value and standard deviations of the active (P_l) and reactive (Q_l) loads, respectively.

If A is the severity of the average node voltage deviation after the s-th probabilistic load flow, the RI can be modeled as (20). The probability $P_r(i)$ that the voltage at the i-th node will exist outside the permissible limit can be modeled as (21), and $A(i)$ is defined as (22), where $\overline{V}$ is the average voltage for the set of s-th sample instances, N is the total number of simulations, n_1 is the total number of $\overline{V}$ lesser than 0.95 p.u., and n_2 is the total number of $\overline{V}$ greater than 1.05 p.u.

$$RI(i) = P_r(i) * A(i) \tag{20}$$

$$P_r(i) = \lim_{N\to\infty}\frac{(n_1)}{N} + \lim_{N\to\infty}\frac{(n_2)}{N} \tag{21}$$

$$A(i) = \left|1 - \overline{V}(i)\right| \tag{22}$$

3.3.2 Unbalanced distribution network power loss modeling

The radial network topology is the common distribution network topology for several reasons. Several branches are connected to a substation's feeder. Unless any voltage control measure is implemented within the network, the node voltage magnitude is proportional to the node's distance from the substation, assuming the node loads are equal. The operation of DGs in a radial distribution network topology is less complicated. Therefore, since the distribution network is realistically unbalanced due to asymmetric line characteristics and load imbalance in the network phases, accurate network assessment is mainly obtainable through unbalanced assessment mode. In addition, more reliable data for DG allocation techniques may be obtained from the unbalanced network modeling and assessment [197]. A three-phase unbalanced network may be modeled using a single branch, as shown in Figure 3.3 [198].

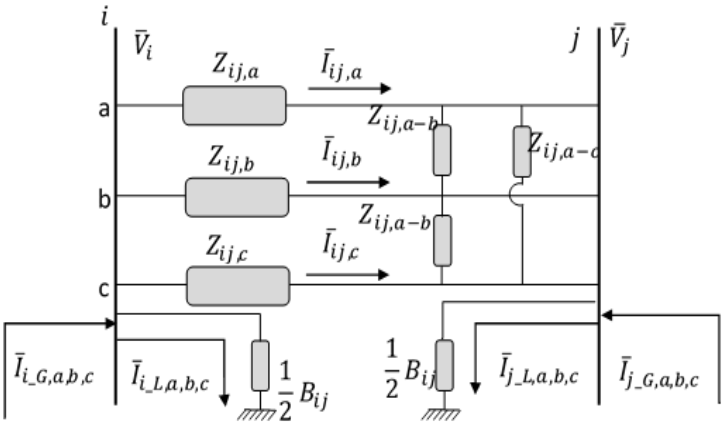

Figure 3.3: Unbalance network model

From Figure 3.3, if $Z_{ij,a}$, $Z_{ij,b}$ and $Z_{ij,c}$ are the line impedances for each phase between the nodes, and $\bar{I}_{ij,a}$, $\bar{I}_{ij,b}$, $\bar{I}_{ij,c}$ are the vector line currents, then the total current at node i and voltage drops across each phase in the branch ij are given as (23) and (24), respectively. Hereafter, the network is assessed to determine the nodes' voltage deviation and power loss. The total power loss in an unbalanced distribution network is modeled in (25). The power loss is evaluated considering the active and reactive power flow constraints per phase, as shown in (26) and (27), respectively.

$$\underbrace{\bar{I}_i}_{a,b,c} = \underbrace{\bar{I}_{i,L}}_{a,b,c} + \underbrace{\bar{I}_{iG}}_{a,b,c} \tag{23}$$

$$\begin{bmatrix} \Delta\bar{V}_{ij,a} \\ \Delta\bar{V}_{ij,b} \\ \Delta\bar{V}_{ij,c} \end{bmatrix} = \begin{bmatrix} Z_{ij,a} & Z_{ij,a-b,} & Z_{ij,a-c} \\ Z_{ij,a-b} & Z_{ij,b} & Z_{ij,b-c} \\ Z_{ij,a-c} & Z_{ij,b-c} & Z_{ij,c} \end{bmatrix} = \begin{bmatrix} \bar{I}_{ij,a} \\ \bar{I}_{ij,b} \\ \bar{I}_{ij,c} \end{bmatrix} \tag{24}$$

$$PL = \sum_{k=1}^{m} (Z_{ij,a}\bar{I}_{ij,a}{}^2 + Z_{ij,b}\bar{I}_{ij,b}{}^2 + Z_{ij,c}\bar{I}_{ij,c}{}^2) \tag{25}$$

$$P_i^p = P_i^p + V_i^p \sum_{j=1} \sum_{n=1} V_j^n \left[G_{ij}^p \cos \theta_{ij}^p + B_{ij}^p \sin \theta_{ij}^p \right] \quad (26)$$

$$Q_i^p = Q_i^p + V_i^p \sum_{j=1} \sum_{n=1} V_j^n \left[G_{ij}^p \sin \theta_{ij}^p - B_{ij}^p \cos \theta_{ij}^p \right] \quad (27)$$

where P_i^p and Q_i^p are the active and reactive power generation per phase at node *i,* respectively; G_{ij} is the conductance between nodes *i* and *j*; B_{ij} is the node susceptance between nodes *i* and *j;* n is the number of phases (p); *m* is the number of branches; V_i and V_j are the voltage magnitudes of the nodes *i* and *j,* respectively; and θ_{ij} is the angle of the admittance between nodes *i* and *j*.

3.3.3 Optimal PVDG placement problem formulation

The allocation of DG for modern distribution networks is often regarded as an optimization problem. This paper proposes a classification decision tree (DT) model for optimal DG allocation. The variables considered for optimization are the branches' risk index and power loss. If α and β represent the unitless voltage risk index (RI) and power loss (PL) variables, respectively, then the optimal location (Y) for the DG can be obtained from the problem formulated in (28) constrained by the total considered PVDG units' capacity.

$$Y = \min (\alpha + \beta) \quad (28)$$

Subject to:

$$S_{tg}^{min} \leq S_{tg} \leq S_{tg}^{max}$$

3.3.4 Decision tree-based classification

Decision trees (DT) have been proven to be effective for classification optimization problems. A DT is constructed from nodes and edges that are arranged in a hierarchical pattern. In order to create the DT structure, a data instance is classified as yes or no based on predefined conditions. The classification is progressed from top to bottom until a conclusion that corresponds to the optimization objective is obtained. The DT algorithm was adopted in this paper because of its flexibility, capability to handle numerical and categorical data, and excellent performance with small and large datasets. For some problems, a DT can be developed without a dataset in some cases.

As shown in Figure 3.4, there are three types of nodes in a DT. The dots represent the number of instances in a given dataset, while the colors represent the instances with similar intrinsic properties to be used for classification. The root node is normally at the top of the hierarchy, with only outgoing edges and no incoming edges. Internal or parent nodes have both incoming and outgoing edges, whereas leaf nodes have only incoming edges and no outgoing edges. The sum of all the instances in child nodes derived from the same parent node must equal the number of instances

in the parent node. The generic structure of a DT is developed following a recursive application of Hunt's algorithm [199].

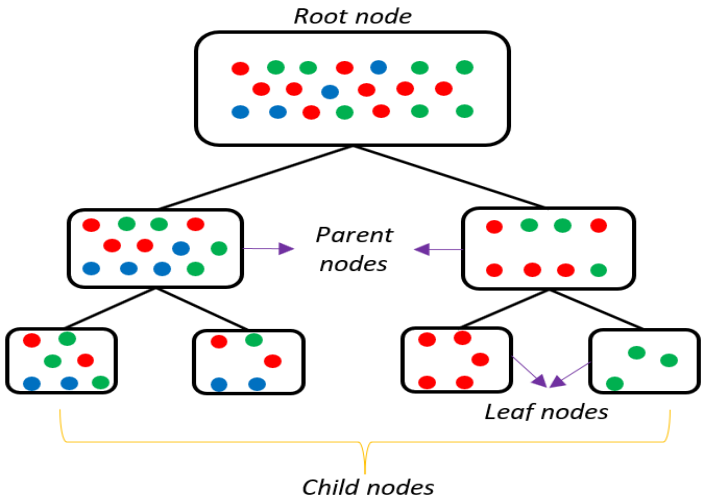

Figure 3.4: Decision tree model

The decision tree algorithm is preferred due to its capability to perform well on several data types. The DT algorithm is implemented by splitting the parent node into child nodes. The process is repeated on each child node until a homogenous node known as the leaf node is obtained. Node splitting may be achieved using several techniques based on the type of class variable. If R_t is a collection of records from which a logical conclusion for a node t can be derived, and all of the records in R_t belong to the same class, the node t is considered a child node and is labeled C_t. On the other hand, R_t is considered a parent node P_t if it contains records from several classes. Only internal nodes can be both the parent and the child node simultaneously. The records of R_t are subsequently distributed to the children based on the classification outcome [200]. This procedure is repeated for each child node until further classification is no longer possible. In this paper, the set R_t comprises of RI, HC, and branch load deficit (σ) for all the branches in the distribution network. The classifications based on the capacity of the proposed DG and zero-point ($\mathbb{X}$) are done at the internal nodes. Finally, the leaf nodes determine whether or not to install a DG at a distribution network node based on the value of HC.

3.4 Results and discussion

3.4.1 IEEE 33 Nodes test case results

The results and discussions of testing the proposed approach on the modified IEEE 33 node distribution network obtained from [201] are presented in this section. The network is a radial network consisting of 33 nodes and 32 branches, as shown in Figure 3.5. The IEEE 33-node radial distribution network is common for testing and comparing proposed DG unit placements algorithms. It has a voltage of 12.66 kV, load size of 3.715 MW and 2.3 Mvar. The total active and reactive power losses for the base network are 210.01 kW and 142.45 kvar, respectively, before PVDG(s)

placement. The sizes of the PVDG unit used are 50%, 75%, and 95% of the total load for the simulation case 1, case 2, and case 3, respectively. The unbalanced phase load distributions for nodes 30 and 24 represent the worst-case phase load distribution in the network, as shown in Figure 3.6. The normal and probabilistic power flow assessments, hosting capacity evaluation, and PVDG voltage control modes are simulated using the Powerfactory 2021.

The highest normal state and probabilistic loadings of 34% and 44.6% are recorded for branch 2. A worst-case voltage magnitude of 0.96 p.u. was obtained for the unbalanced distribution network under the normal state. Figure 3.7 shows the base network's normal and probabilistic voltage profile obtained from 10,000 simulation instances. The standard deviation of the probabilistic voltage profile is highly correlated with the mean voltage magnitude, and it increases with node distance from the substation. Under the probabilistic assessment with 10,000 simulation scenarios, 25 nodes have average voltage magnitudes below the permissible limit of 0.95 p.u.

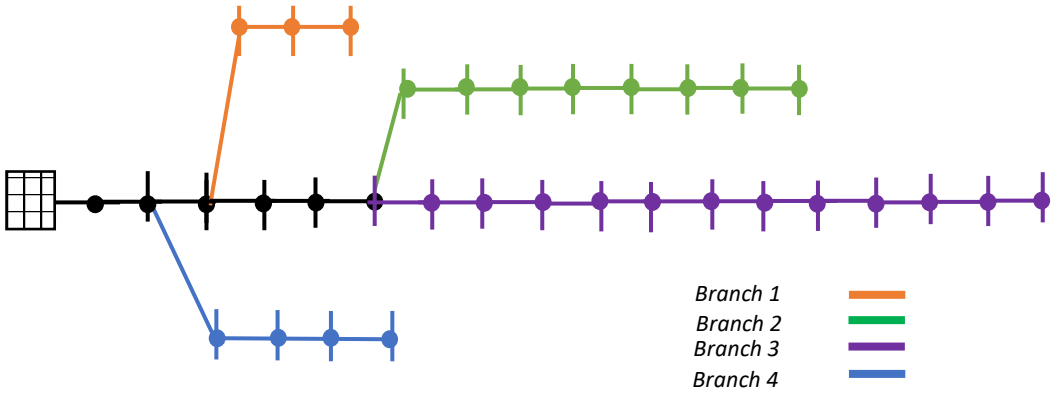

Figure 3.5: IEEE 33 Node distribution network

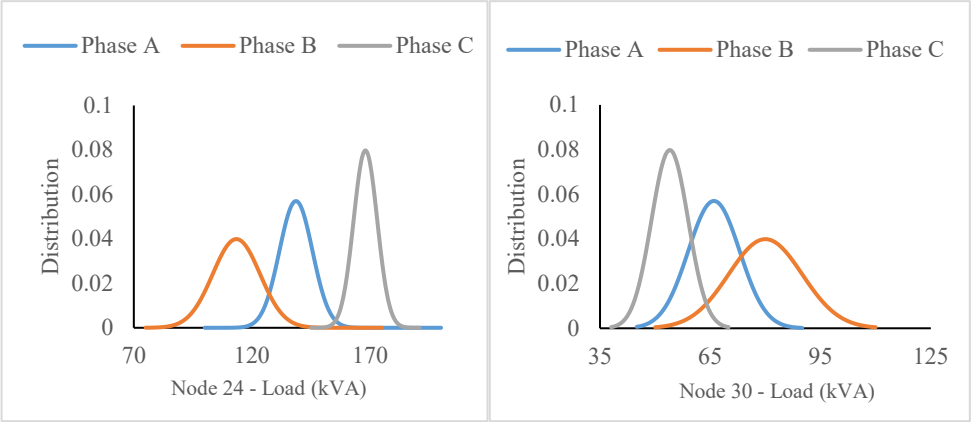

Figure 3.6: Phase load distributions

Figure 3.8 shows the branches' power losses and line loadings under normal and probabilistic assessments for the IEEE 33-nodes distribution network base case. The total probabilistic active power losses obtained from the summation of the branch losses is 215 kW. The highest losses and loading are recorded for lines 27-28 and 6-26, respectively. The nodal RI and the voltage standard deviation are shown in Figure 3.9. The worst nodal RIs correspond to nodes with significant average

voltage magnitude deviation from the standard value of 1 p.u. The RI and voltage standard deviation increase with distance from the branch or generator. Depending on the capacity and local control technique adopted for the proposed DG within a distribution network, high RI and voltage standard deviation may be recorded around the DG connected node(s).

The nodal hosting capacities (HC) and the corresponding minimum voltage for each node and critical voltage ($\boldsymbol{V_{cr}}$) are shown in Figure 3.10. The final minimum HC voltage values may be used to determine the optimal nodes for HC enhancement. Also, each node's fault current contribution constraint is set at 10% of the total fault current. The nodal fault current is obtained from a three-phase short circuit analysis using the equivalent synchronous machine model. Branch 2 had the lowest average hosting capacity value of 3.03 MVA. Because the nodal HC is constrained by the node voltage, which would be increased after installing DG on a branch, it is expected that the new HC will be slightly improved. However, this may not be the case for all the DG types and local voltage control techniques. Therefore, the optimal node for the DG allocation should generate the greatest HC improvement or retain the highest HC after installing the DG. In addition, an average critical voltage of 0.66 p.u. was obtained for the base network, corresponding to a maximum network capacity of 18.4 MW.

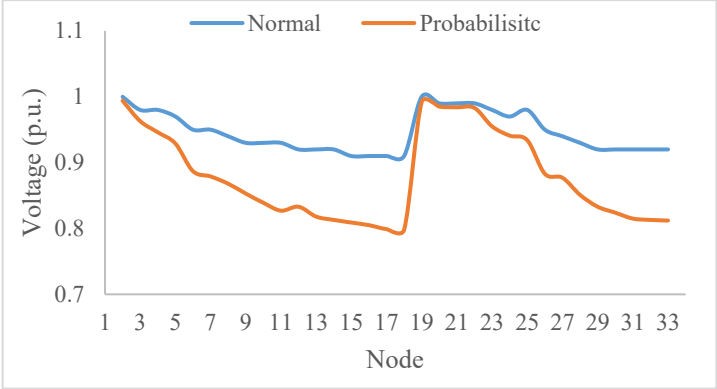

Figure 3.7: Network normal and probabilistic voltage profiles

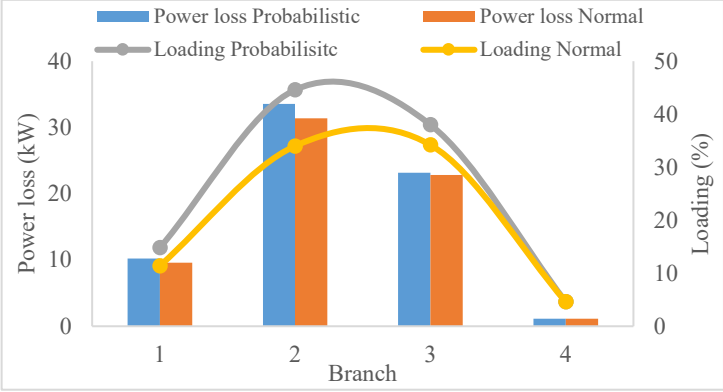

Figure 3.8: Base network losses and loading

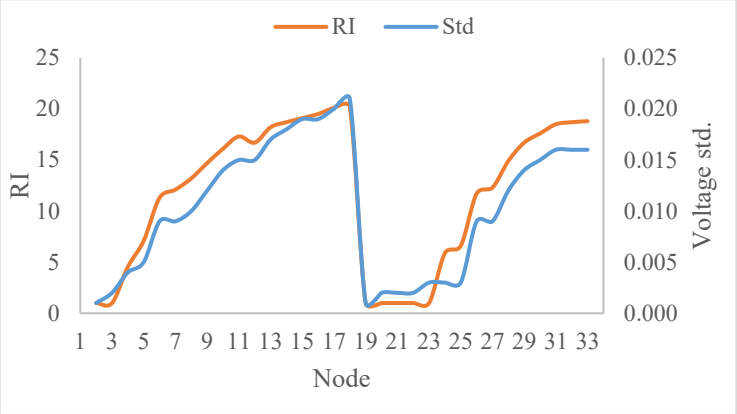

Figure 3.9: Base network risk index and voltage std

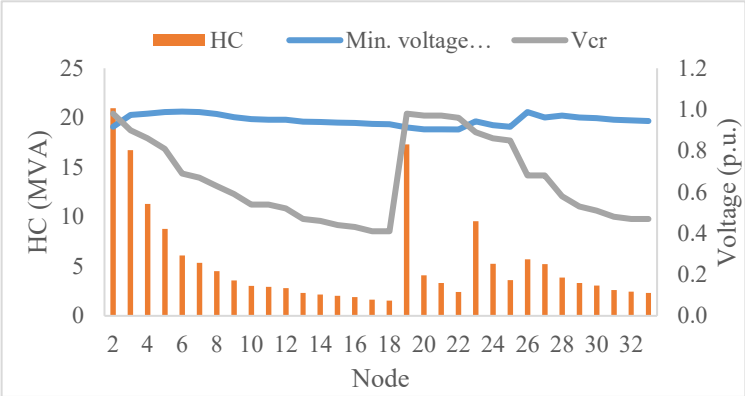

Figure 3.10: Network hosting capacity and voltage parameters

3.4.1.1 Decision tree classification results

This section presents the implementation of the proposed DT model to obtain the optimal node(s) to minimize the power loss and risk index. In addition to being effective for network branches without existing DGs, the proposed method is extended to network branches with DGs already installed. The proposed DT model is shown in Figure 3.11, whereby B is the branch, σ is the branch load deficit, and $\bar{X}$ is the branch zero point. The only parameter required is the capacities of the proposed DG system. The branch load deficit is the amount by which the DG undersupplies the branch. The zero point is the node on the branch where the DG generation is equal to the cumulative load from the end of the branch.

The first step in the optimization procedure is to determine whether or not the branch is already occupied by DG(s). If the branch is unoccupied, the branch with the highest α and β in the network will be selected for the DG placement, considering the proposed DG's capacity. If the planned DG's capacity exceeds the branch load, the DG is placed on the highest HC node. Otherwise, the DG is placed at the branch's zero point. However, if the branch already has DG, the size of the proposed DG is compared with the branch's deficit load. If the proposed DG's capacity is greater than the branch's deficit load, the DG is placed on the node with the highest HC. Otherwise, the DG is placed at the branch's zero point. The decision tree classification was implemented on the WEKA

machine learning tool. WEKA software provides a collection of machine learning classification algorithms, including decision tree classification for data mining tasks.

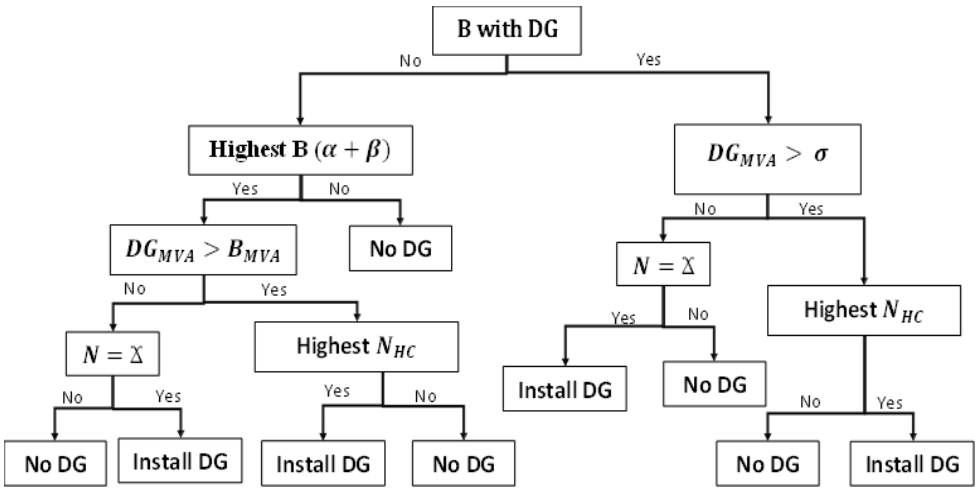

Figure 3.11: Implementation of the DT model

The proposed DT consists of nine leaf nodes from which nine rules may be created. The first five rules are applied to branches with only one DG allowed, while the last four rules are applied in scenarios where more than one DG may occupy a branch. Table 3.1 shows the rule table from which the DT model is developed. The DG considered in this paper is the photovoltaic (PV) system under three local voltage control techniques. This paper investigates two study instances (Study 1 and 2) representing the dispatchable power from the DGs. The branch status is used to inquire whether occupied branches are considered or not. The status is labeled "No" if only empty branches are considered and designated as "NC". If occupied branches are considered, the status is labeled "Yes" and designated as "OC". The first study instance considered when the total power from PVDG units is lesser than the total distribution network demand, while the second study instance considered when the total power from PVDG units is equal to the total distribution network demand.

The peak power generation from all installed PVDG units in operation under study 1 in this paper is 65% of the total load. The capacities of the proposed PVDG units for study 1 are approximated to be 32%, 21%, and 11% of the total network load, while the capacities of the proposed PVDG units for study 2 are approximated to be 50%, 33%, and 17% of the total network load. The composition of the simulation scenarios considered in this paper is shown in Table 3.2. Through the proposed DT model, considering a maximum of three PVDG units in the distribution network with the stated capacities, the optimal nodes for the PVDG units placement for scenarios 1 to 4 are shown in Tables 3.3 to 3.5. The optimal nodes for scenarios 3 and 4 are the same, as shown in Table 3.5. Except for case 3, the optimal nodes obtained for scenario 1 are the same as those for scenario 2.

Table 3.1: Proposed decision table

Conditions	***Rules***								
	R1	R2	R3	R4	R5	R6	R7	R8	R9
Branch (B) status	No	No	No	No	No	Yes	Yes	Yes	Yes
α and β	No	Yes	Yes	Yes	Yes	-	-	-	-
DG Capacity $\geq$ B_{MVA}	-	Yes	Yes	No	No	-	-	-	-
Node position	-	-	-	Yes	No	-	-	Yes	No
Nodal HC	-	Yes	No	-	-	Yes	No	-	-
DG Capacity $\geq$deficit	-	-	-	-	-	Yes	Yes	No	No
Action									
Install DG	No	Yes	No	Yes	No	Yes	No	Yes	No

Table 3.2: Simulation scenarios

Scenario 1	Study 1 + NC
Scenario 2	Study 1 + OC
Scenario 3	Study 2 + NC
Scenario 4	Study 2 + OC

Table 3.3: Optimal nodes for PVDG(s) placement for scenario 1

Cases	No of DG	DG capacity (MVA)	Node		
Case 1	1 DG	1.5	26		
Case 2	2 DGs	15, 1	26	9	
Case 3	3 DGs	1.5, 1, 0.5	26	9	24

Table 3.4: Optimal nodes for PVDG(s) placement for scenario 2

Cases	No of DG	DG capacity (MVA)	Node		
Case 1	1 DG	1.5	26		
Case 2	2 DGs	15, 1	26	9	
Case 3	3 DGs	1.5, 1, 0.5	26	9	16

Table 3.5: Optimal nodes for PVDG(s) placement for scenarios 3 and 4

Cases	No of DG	DG capacity (MVA)	Node		
Case 1	1 DG	2.25	26		
Case 2	2 DGs	2.25, 1.5	26	16	
Case 3	3 DGs	2.25, 1.5, 0.75	26	16	25

3.4.1.2 Optimal PVDG placement results

The impact of optimal DG placement on the network's voltage profile considering different PVDG local voltage control techniques is shown in the results presented in Figures 3.12 to 3.14. Figure 3.12 shows the normal state distribution network voltage profile for cases 1 to 3 under scenario 1, for the constant voltage control mode. Case 3 presents the best average normal and probabilistic voltage of 0.99 p.u. and 0.979 p.u. at the lowest standard deviations of 0.029. The highest active power loss reduction of 21.75% was obtained for branch 2 under case 2. The highest reactive power loss reduction of 71.9% was recorded for cases 2 and 3 under scenario 1 as well as case 2 under scenario 2. Also, the average RI was reduced by 83.9% for all the cases. The HC enhancement of 16.97% was obtained under case 1 and increased to 41% under case 3.

Figure 3.13 shows the network voltage profile for case 3 under the study 1 and 2 considering the constant voltage control mode. The minimum voltage of 0.97 p.u. was recorded for nodes 31 – 33 for all the scenarios. The average network voltage for study 1 and 2 is 0.99 p.u. For both studies, the probabilistic mean voltage and standard deviation are 0.98 p.u. and 0.002, respectively. The risk of overvoltage within the distribution network increases in scenarios 3 and 4. The lowest and highest HC enhancement of 39.9% and 41.8% were obtained under scenarios 1 and 3.

The impacts of the three common PVDG voltage control techniques on the network's performance under scenario 1 for case 3 are shown in Figure 3.14. Although the average voltage obtained under the Q-PF control is above 1 p.u., with overvoltages occurring around the PVDG connected nodes, the QV controlled network shows the highest risk of 4.1. The CV-controlled network shows the best probabilistic voltage, standard deviation, RI, and HC enhancements. Although the QV-controlled network has the worst probabilistic voltage, it offers a significant HC enhancement of 15% on the base network HC, whereas the Q-PF controlled network shows a reduction of 21.13%.

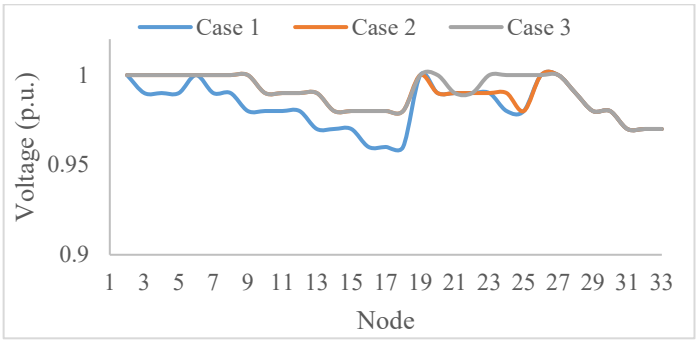

Figure 3.12: Network voltage profile under CV-control mode

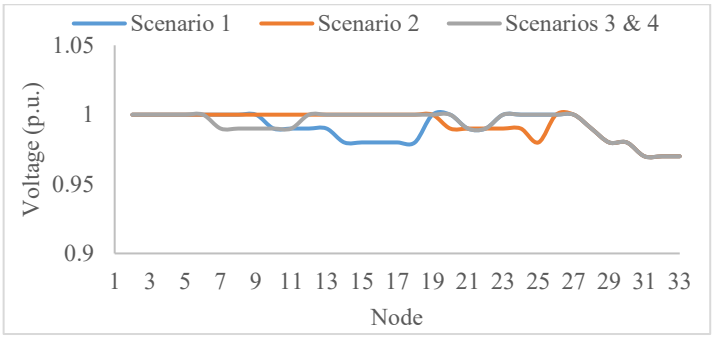

Figure 3.13: Network voltage profiles under different scenarios

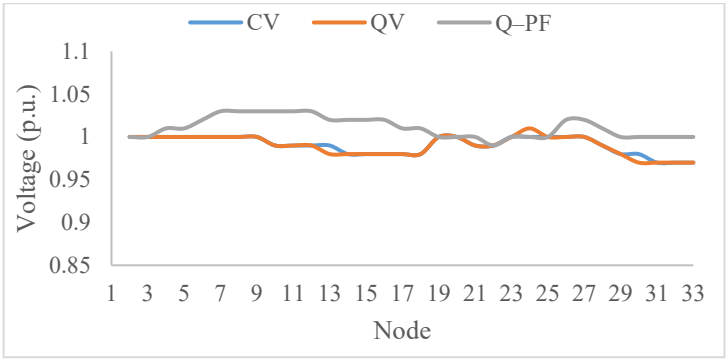

Figure 3.14: Network voltage profile for different control modes

Figures 3.15 to 3.17 show the performance of the proposed technique in terms of active power loss reduction. Figure 3.15 shows no strong correlation between the numbers of PVDG units and the total active power loss of the network. The active power loss may increase if more PVDG is added to the network beyond the optimal generation. The difference in active power loss under case 2 and case 3 for all the branches are insignificant. Branch 2 under Case 3 had the highest active power loss reduction of 22.65%.

The impacts of the PVDG unit voltage control techniques on the network's power loss under scenario 1 case 3 are shown in Figure 3.16. The active power loss for the Q-PF-controlled PVDG is consistently lesser than the CV and QV-controlled PVDG in a network except for branch 3. Although the Q-PF-controlled PVDG shows the best active power loss reduction for case 1, the total active power loss increases as the number of installed PVDG increases. In contrast, the total active power loss of the CV and QV-controlled PVDG reduces as the numbers of PVDG increases. The active power loss reduction for scenario 1 increases as the installed PVDG increases, as shown in Figure

3.17. The active power loss reduction of branch 4 is the same for all the cases at 1.7%. As the number of PVDG units increased from one to three, the percentage reductions of 350% and 384% were recorded for branches 1 and 3. For the QV-controlled PVDG instances, case 3 under scenario 1 presents the highest reactive power reduction of 57.8%. Like the CV-controlled PVDG units, the Q-PF-controlled units present a significant reactive power reduction of 72% for case 2 under scenarios 1 and 2.

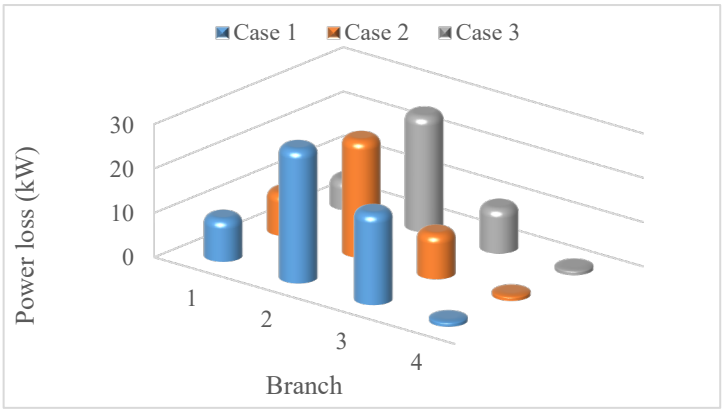

Figure 3.15: Network power loss under CV control mode

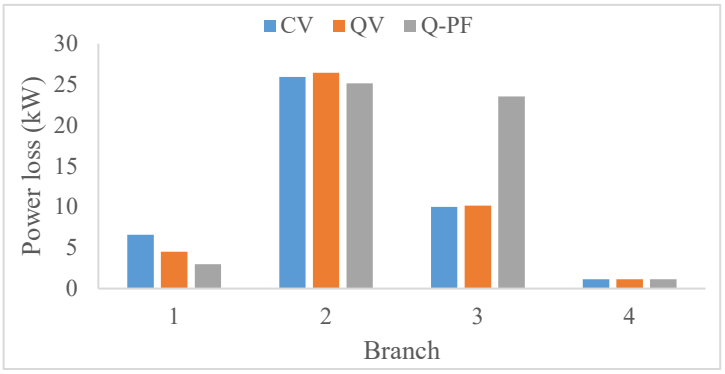

Figure 3.16: Normal power loss for different voltage control modes

Figure 3.17: Percentage power loss reduction for CV mode

The risk indices of the networks after placements of PVDG units for case 3 are shown in Figures 3.18 and 3.19. Figure 3.18 shows the RI of the network for scenario 1 with a CV-controlled PVDG unit. The installation of more PVDG units, as shown in cases 2 and 3, yields lower risk indices across the network's nodes. The highest RI reduction of 93.5% from the base case RI is obtained from case 2. The highest RI reduction on the network was observed for branch 3 (nodes 2 to18) from

13.57 to 0.15 under case 2. Since the voltages at the CV-controlled PVDG connected node are kept at 1 p.u., the risks of overvoltages are significantly reduced, as shown in Figure 3.19. However, the RI increases as the capacities of the PVDG units increase, as shown in scenario 3. In addition to the high RI shown by the QV-controlled PVDG, the maximum distribution network capacity is lesser than the CV and Q-PF-controlled PVDG units.

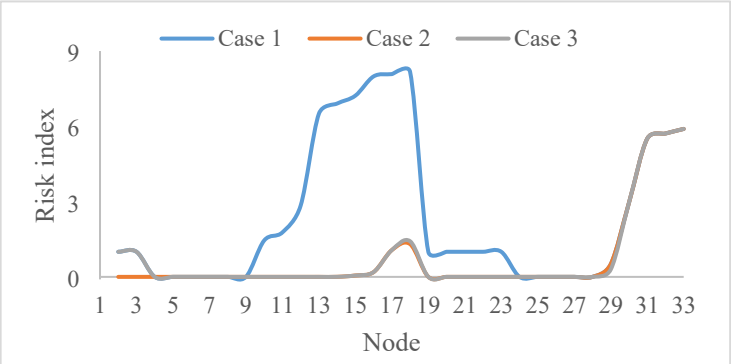

Figure 3.18: Network risk index under CV-control mode

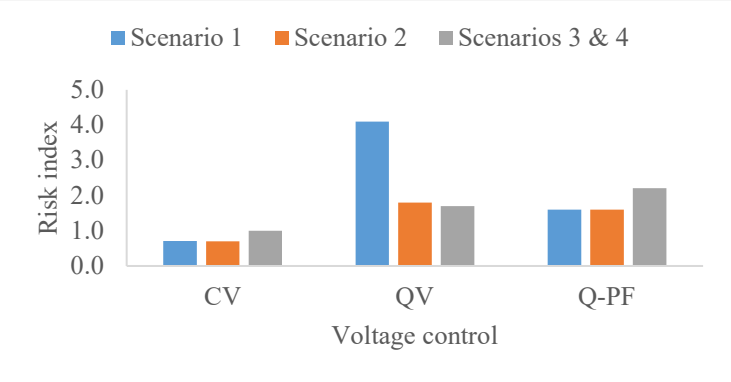

Figure 3.19: Network risk index under different control modes

3.4.2 IEEE 69 Nodes test case result

The results and discussions of testing the proposed approach on the IEEE 69 node distribution network shown in Figure 3.20 and data obtained from [202] are presented in this section. The network has eight branches, and the total apparent load is 4600 kVA, with 44% of the total load connected to branch 8. The total active power loss, reactive power loss and average voltage of the network are 210.8 kW, 140 kvar and 0.97 p.u., respectively. The voltage standard deviation and the average network risk index are 0.022 and 0.7. An average HC capacity of 8.3 MVA with the lowest value of 1.6 MVA for node 27 was recorded for the base network. Through the proposed DT model and considering a maximum of three PVDG units in the distribution network with the stated capacities for the IEEE 33 node distribution network, the optimal nodes for the PVDG units placement for scenarios 1 and 2 are the same, as shown in Tables 3.6. The optimal nodes for the PVDG units placement for scenarios 3 and 4 are also the same, as shown in Table 3.7.

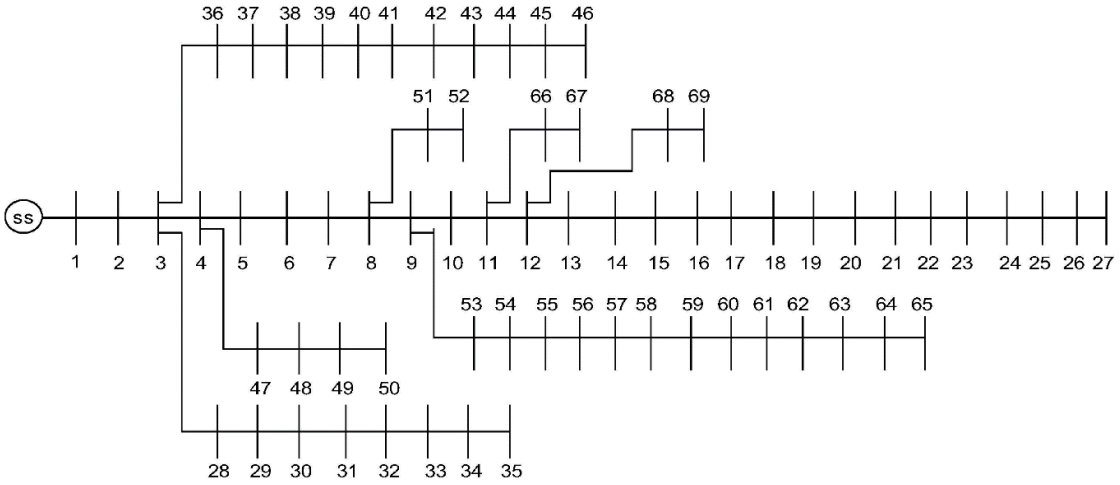

Figure 3.20: IEEE 69 Node distribution network

Table 3.6: Optimal nodes for PVDG(s) placement for scenarios 1 and 2

Cases	No of DG	DG capacity (MVA)	Node		
Case 1	1 DG	1.5	4		
Case 2	2 DGs	1.5, 1	4	61	48
Case 3	3 DGs	1.5, 1, 0.5	4	61	48

Table 3.7: Optimal nodes for PVDG(s) placement for scenarios 3 and 4

Cases	No of DG	DG capacity (MVA)	Node		
Case 1	1 DG	2.25	6		
Case 2	2 DGs	2.25, 1.5	6	58	
Case 3	3 DGs	2.25, 1.5, 0.75	6	58	50

Figures 3.21 to 3.23 show the PVDG unit placement results for the optimal node(s) in scenario 1. Cases 2 and 3 have the same network voltage profile, with a minimum value of 0.97 p.u. As shown in Figure 3.21, cases 2 and 3 have the best average voltage profile improvement from 0.977 p.u. to 0.99 p.u. There are no changes in the results of cases 2 and 3 due to the distribution network's size, the network load distribution, and the proximity of the optimal nodes. Figure 3.22 shows the probabilistic voltage and standard deviation for the base case network and PVDG case 3. The average probabilistic voltage was improved from 0.965 p.u. to 0.99 p.u. with a standard deviation of 0.019. The worst node probabilistic voltage was also improved from 0.941 p.u. to 0.975 p.u. The network risk index was reduced by 87.8%, while case 2 shows the best HC retainment of 6.85 MVA. The power loss for the base network case and the PVDG cases for branches 2, 4, and 8 are shown in Figure 3.23. The losses on the remaining five branches are negligible. Cases 2 and 3 show an overall power loss reduction of 29.6% and 37.5%, respectively. The average critical voltage was enhanced

from 0.81 p.u. to 0.96 p.u. The percentage loading of the highest loaded branch (branch 5) was reduced from 124.% to 82.9%.

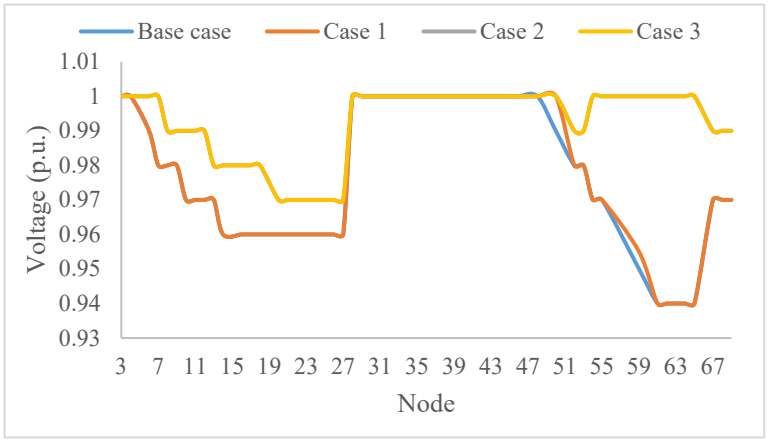

Figure 3.21: Network voltage profile for the considered cases

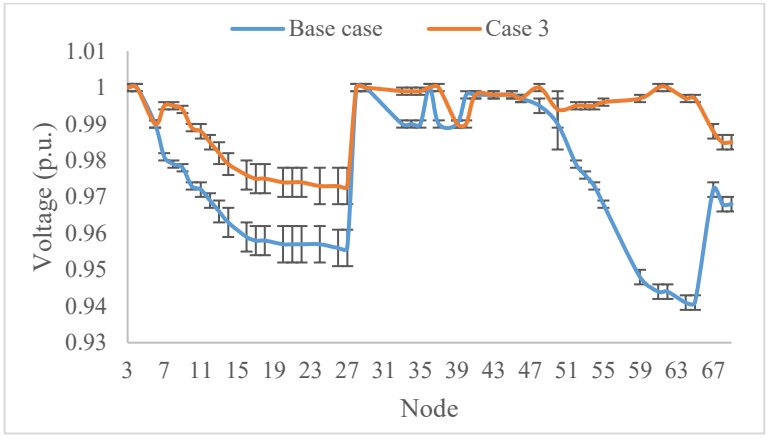

Figure 3.22: Network probabilistic voltage and standard deviation

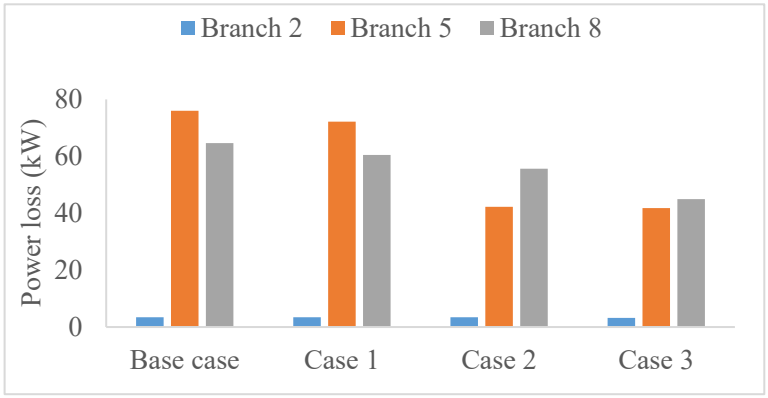

Figure 3.23: Average probabilistic power loss for considered cases

3.4.3 Comparison with existing techniques

A comparative study of various methods in literature in the last five years for voltage profile enhancement and loss minimization for both IEEE 33 and 69 nodes distribution network for 1 PVDG and 3 PVDG units scenarios is presented in Table 3.8 and Table 3.9, respectively. The tables compare the DG location, DG size, power loss, and the minimum voltage magnitude obtained. All the existing

methods have improved the performance of the base networks in terms of power loss reduction and minimum voltage enhancement. However, the highest power loss reduction of 46.72% is obtained by the technique proposed in [99] for the IEEE 33 node distribution network, although the same technique shows the least minimum voltage improvement. The techniques in [93] present good improvements for power loss reduction and minimum voltage improvement with almost the same PVDG capacity as the other compared techniques. For the IEEE 69 node distribution network, the method in [203] presents the lowest power loss with the highest total DG capacity. The difference in power loss reduction and minimum voltage values despite having the same PVDG capacity is due to the PVDG voltage control or the power factor.

The proposed technique in this paper shows the best minimum voltage improvement of 0.96 p.u. and performs well for power loss reduction with least PVDG capacity. The performance of the existing and proposed method regarding minimum voltage is the same for three PVDG units scenarios except for [204], which gives a low value of minimum voltage. Although the proposed technique's total PVDG unit capacity is 0.5 MVA lower than the compared techniques, it has the highest power loss reduction of 78%.

Table 3.8: Comparative results of optimal PVDG placement for IEEE 33 node network

1 PVDG				
Reference	**DG location**	**DG size (MVA)**	**Power loss (kW)**	**Minimum voltage (p.u.)**
[99]	30	1.94	98.11	0.938
[93]	6	2.57	103.9	0.951
[205]	6	2.59	111.02	0.952
[204]	6	2.6	111.03	0.942
[185]	6	2.6	107.4	0.952
Proposed Method	26	1.5	102.5	0.96
3 PVDGs				
[93]	14, 24, 30	0.761, 1.094, 1.068	71.4	0.968
[177]	14, 24, 30	0.755, 1.1, 1.07	71.3	0.965
[204]	6, 3, 28	1.34, 0.79, 0.82	99.8	0.93
[206]	14, 24, 30	0.75, 1.099, 1.072	71.3	0.97
Proposed Method	26, 9, 24	1.5, 1, 0.5	46.2	0.97

Table 3.9: Comparative results of optimal PVDG placement for IEEE 69 node network

1 PVDG				
Reference	**DG location**	**DG size (MVA)**	**Power loss (kW)**	**Minimum voltage (p.u.)**
[93]	61	1.87	83.2	0.96
[207]	61	1.87	83.2	0.96
[99]	30	1.54	125.1	0.92
[203]	61	1.86	81.6	0.96
Proposed Method	4	1.5	108.2	0.94
3 PVDGs				
[206]	17, 61, 64	0.5, 1.2. 0.54	131	0.92
[93]	11, 18, 61	0.57, 1.7, 0.37	70	0.97
[207]	12, 21, 61	0.45, 0.32,1.78	70	0.97
[203]	15, 61, 49	0.55, 1.77, 1.01	69.2	0.97
Proposed Method	4, 61, 48	1.5, 1, 0.5	73	0.97

3.5 CONCLUSIONS

Optimal allocation of distributed generation (DG) units has become an important task in modern distribution network planning. This paper presented an optimal PVDG placement technique to facilitate the increased penetration of DG security into the distribution network using specific security indices. The proposed approach includes a decision tree classification model to minimize the branches' risk index (RI) and power loss (PL) under the DG capacity and hosting capacity (HC) constraints. From the identified nodes for three PVDG installations under the constant voltage control mode, the branch PL and RI were reduced by 35.8% and 92%, respectively, for the IEEE 33 node distribution network. Also, the average branches' critical voltage and HC were improved by 29.3% and 41%, respectively. For the IEEE 69 node distribution network, the branch PL and RI were reduced by 32.72% and 85.7% for three PVDG installations under constant voltage control mode. Also, the average branches' critical voltage was improved from 0.81 p.u. to 0.97 p.u.

The results conclude that optimal multiple DG placement can effectively reduce the distribution network losses and the RI. Also, as shown in some cases and scenarios, high penetration

of PVDG may cause overvoltage near the nodes with DG units, especially under the Q-PF voltage control mode. The results show that the approach can determine the optimal node within a distribution network for DG placement under the specified security indices. Considering the capacities of the DG units, the proposed technique performs better than the compared techniques in terms of power loss reduction and voltage enhancement. The proposed method is effective for DG penetration planning for large distribution networks and the expansion of smaller networks.

4 Manuscript 3: Offline Security Prediction

Preamble

Another highlight of the review in Chapter 2 is the need for an effective security state prediction model for grids with a high penetration level of RES-DG. The time-changing reduced effective inertia caused by varying penetration level of RES-DG increases the grid's frequency change, leading to significant security risk considering potential contingencies in the grid. Prior knowledge of the system security state for proposed grid operating scenarios will assist grid operators in determining appropriate security control techniques for insecure states and possible increment in the penetration level of RES-DG for secure state predictions. Therefore, Chapter 4 presents a method for offline grid security state prediction. The chapter opens with a method for the critical clearing time prediction considering varying grid inertia and load. The effectiveness of security prediction models depends on the quality of the training dataset. The proposed method consists of a novel approach for comprehensive training dataset development considering both synchronous and non-synchronous DG types, several penetration levels, faulted elements, and fault types as attributes. The approach continues by using a density-based clustering technique to identify patterns between the attributes, grid frequency, and voltage responses and determine the security state. The dataset instances with the security states are afterward applied to train a probabilistic classifier from which future security state predictions can be obtained.

Density-based clustering and probabilistic classification for integrated transmission-distribution network security state prediction

Ifedayo oladeji*, Peter Makolo, Ramon Zamora, and Tek-Tjing Lie

Department of Electrical and Electronic Engineering, Auckland University of Technology – AUT, 55 Wellesley, Auckland, New Zealand

Abstract: The proliferation of renewable energy sources (RESs) into the distribution network necessitates the need for the capability to predict the security state of the grid. This paper proposes a density-based clustering and probabilistic classification approach to predict the security state of the modern grid. Firstly, an approach to predict the critical clearing time using the changes in inertia constant and system load is proposed. Secondly, an algorithm for training dataset development from the transient stability responses of the grid considering different operation scenarios is proposed. An expectation-maximization (EM) algorithm using the density-based clustering technique was applied to the dataset to obtain clusters representing the network's security states. Finally, a predictive model was obtained from the labeled dataset using a Naïve-Bayes (NB) probabilistic classifier. The feasibility of this approach is demonstrated using the IEEE 14 bus system. Respectively, an APA and RMSE of 98% and 3.6% were obtained. Also, an MAE of less than 1% was obtained when the proposed model was tested with seven different datasets having a different number of instances. The results show that the proposed technique can predict the security of the integrated transmission-distribution networks considering different DG types, penetration levels, and network disturbances with a high degree of accuracy.

Keywords: Density-based clustering; probabilistic classification; security state; distributed generation; renewable energy.

Nomenclature

E_{qi}	Voltage behind the transient reactance (V).
E'_{qi}	Terminal voltage (V).
X_{eq}	Equivalent reactance (Ω).
H_{eq}	Equivalent inertia (s).
Y_{ij}	Admittance between the buses (℧).
G_{ii}	Bus conductance (G).
δ	Machine rotor angle (rad).
P_m	Mechanical power (MW).
P_e	Electrical power (MW).
H_i	Inertia constant of *i*-th synchronous generator (s).
c	Security class.
L_f	Loss function.
R_f	Risk function.
DT	DG type.
PL	Penetration level (%).

CT	Contingency type.
ω	Angular velocity (s^{-1}).
k_p	Active power droop gain.
t_{cr}	Clearing time (s).
D	Damping coefficient (N.m.s).
V_{max}^{T}	Maximum transient voltage (pu).
ΔP	Acceleration power (MW).
W	Parameter of machine learning.
d	Unlabelled data sample.
N	Number of sample instances.
R_i	i-th adaptive neural FIS inference.
V_o	Initial voltage (pu).
V_{max}^{T}	Maximum transient voltage (pu).
Y_R	Equivalent network admittance matrix (℧).
$\underline{u_s}$	Stator voltage (V).
$\underline{u_r}$	Rotor voltage (V).
$\underline{\varphi}$	Flux linkage (Wb).
$\underline{i}$	Current (A).
ω_{ref}	Speed of rotation (pu).
ω_g	Electrical generator speed (pu).
ω_n	Rated speed (pu).
t_m	Mechanical torque (N.m).
t_e	Electrical torque (N.m).

*Corresponding Author: Tel.: +64225331241
E-mail address: ifedayo.oladeji@aut.ac.nz

4.1 Introduction

The increase in the demand for electricity and the proliferation of renewable energy sources (RESs) into the distribution networks have increased the complexities in the planning and operation of the grid. The high penetration of distributed renewable energy sources may reduce the predictability and controllability of the grid due to its output intermittency and variability if no mitigating schemes are put in place. Also, the response of the grid with modern control systems to large and sudden disturbances may not be sufficient to keep the system in the normal and alert states due to the absence of inertia support from distributed renewable sources [125]. Most security prediction techniques have been focused on small changes in system load (dynamic stability) and implemented on grids with only synchronous generators. However, recent reports on grid blackouts point to failures of the distributed RESs [26, 208-210]. Hence, future security prediction techniques should prevent insecure conditions caused by renewable energy sources distributed by generators. The ability to prevent future system failures is possible through predictive models where the predictions are adaptively tracked using the true outcomes as a reference.

The security of a power system is defined as its ability to remain in continuous operation within allowable boundaries in normal conditions (pre-fault) and after any disturbance (post-fault). Grid security is a grid's property that guarantees continuous operation in normal and transient

situations after any contingency. An increase in load demand, penetration of RES-DG units, and market-driven policy implementation often propel the grid operations towards their security limits[211]. Therefore, the assessment of modern grid security is more complicated than conventional grids. Grid security assessment techniques may be broadly categorized into deterministic and probabilistic approaches [13]. The deterministic approaches consider the operational limitations of grid elements after contingencies. The probabilistic evaluation methods consider the probability of the contingency scenarios and assess the grid's security to a tolerable level of confidence. The power flow and transient stability analyses are commonly used in deterministic security evaluation approaches [212].

Deterministic security assessment approaches can be divided into two main categories: the analytical and machine learning-based approaches. Implementation of analytical approaches requires high-speed processing tools and computationally efficient software. Analytical methods which involve system modeling for several credible contingencies are common for security assessment. The analytical evaluation method consists of comprehensive mathematical models that are reliable and adaptable to large power systems. The time for implementation of analytical techniques is significantly large for large power grids due to the several iterative steps involved. Also, the computation burden of solving differential-algebraic equations (DAE) from the full-time-domain simulation is overwhelming due to too many scenarios to consider [213]. Several network reduction techniques have been proposed and implemented to reduce the security assessment time. However, the assumption and simplifications involved with network reduction techniques may compromise the results obtained, especially for transient stability responses. Another deficiency of time-domain simulation includes its unsuitability for real-time grid security assessment and inaccessibility of the degree of system security. The overwhelming computational burden on simulation tools coupled with the deficiencies of time-domain simulations may undermine the ability of system operators to achieve the desired speed and reliability needed for the emerging grid. Cloud access and distributed computing have mitigated the limitations of analytical methods' computation and speed requirements. However, machine learning approaches do not require time-domain simulations; they can be implemented on common computers. Other advantages of machine learning approaches include fast decision-making, identifying hidden patterns, high accuracy, flexibility, and generalization capabilities [214].

Renewable energy sources distributed generation (DG) is characterized by varying and intermittent output, which might cause an imbalance between system generation and demand. Therefore, it is essential to emphasize that accurate and fast security prediction is required in grid operations with high penetration of RES-DG. Also, reliable models for security state prediction may best be developed by using real-life historical and real-time data with artificial intelligence (AI) tools [215]. Therefore, this paper proposes a machine learning-based grid security state prediction considering the increased penetration of RESs into the distribution networks.

4.1.1 Literature survey

In recent decades, machine learning methods have been employed for security assessment. With machine learning, it is practicable to circumvent the rigor of time-domain simulations to assess the grid's security. Machine learning algorithms and approaches rely on offline data extracted from past events and system responses and simulations representing possible operating conditions and contingency scenarios [216]. The challenge, however, is the suitability of the training data to predict the security of the network when the operating state lies in between two instances considered in the dataset. Several machine learning algorithms have been applied to classify power system states. Few of the algorithms include support vector machine, extreme learning machine, random forest classification techniques, and regression trees, to mention a few [217]. A lot of literature considers machine learning methods effective in providing critical security information regarding modern power systems. For example, [14-16] approaches provide simple yet reliable and unique security evaluation dimensions.

Artificial Neural Network (ANN) is a standard pattern recognition algorithm developed using specific neurons and weights to learn complex non-linear instances of input data [15, 18, 218]. In [219, 220], steady-state variables predicted frequency stability using the ANN approach. The application of ANN models extends beyond security prediction from learned data but can also provide a satisfactory result for the unlearned data. Extending ANN algorithms, an extreme learning machine (ELM) was also introduced to reduce learning time and training errors [221, 222]. Ref. [223] applied the extreme learning machine (ELM) and NN to predict the critical clearing time. In Refs. [20], static security assessment was carried out using the support vector machine and decision tree. Methods based on ELM, NN, and support vector machine (SVM) for dynamic security studies were presented in [16, 216]. Refs. [224, 225] applied the support vector machine-based classification algorithms for transient stability assessment and prediction.

Although time-domain simulation is widely regarded as the best tool for assessing transient stability, it has two main drawbacks: high computational complexity and incapability of providing degrees of stability. Due to the drawbacks of traditional stability assessments based on time-domain computations when applied to real-time situations, stability, and security assessment focus has been shifted to fast security classification. The voltage stability index is commonly used to classify the security state of a network. In [200, 226], techniques for security state classification into the stable, alert/alarm, and unstable states were proposed. In [200], the alert state is classified into out-of-grid limit states and marginally stable states while extending the method with oscillatory stability margins to develop a classification model. The methods in the above-reviewed reference consist of offline time-domain dynamic stability simulation for dataset development; the networks model did not include renewable energy sources distributed generations which will certainly impact the result of the security state classifications. Also, since dynamic stability only responds to small disturbances

such as gradual changes in load, the methods may not be applicable to classify the stability state of the network under transient conditions.

The decision tree-based security assessment model proposed in [17] was able to classify the security state into the secure, insecure, and uncertain regions under several contingencies. However, the result only shows the effects of load change, while the critical clearing times for the contingencies are not discussed. The approaches in the literature related to this paper and the review of techniques presented in [227] are direct classification techniques where the small datasets generated have been labeled. The applicability of these approaches to real power systems is highly doubtful, given that a large amount of data is required to develop a reliable classification model for security prediction. The direct security state classification approach is also liable to overfitting since the classes are already known. Therefore, the models may be unreliable. A similar approach for probabilistic machine learning-based security state prediction in [228] did not consider the impact of RES-DGs. The inclusion of RES-DGs will certainly impact the training dataset structure, choice of learning methods (batch or incremental), and learning algorithms due to constraints in the data type (attributes) representation. Also, only one grid steady-state or dynamic response variable has been applied as an attribute in the security prediction in the reviewed literature.

Clustering analysis using density-based clustering techniques has been successfully applied in power system analysis, including stability clustering. In principle, density-based clustering seeks to discover high-density clusters in which low-density cluster areas may split within a dataset [229, 230]. A DBSCAN technique was proposed in [231] to obtain clusters for the oscillatory modes of the grid. The technique involves frequency domain decomposition of the data obtained from PMUs for three days. The technique detected the grid operations in the normal and forced oscillation states. The determination of appropriate density-based clusters is an inherent problem that may be solved by carefully selecting and tuning the suitable clustering algorithm. The minor drawback of density-based clustering is the need for dimensionality reduction of high-dimension data. The reviewed machine learning-based approaches for grid security assessment and classification are summarized in Table 4.1 to compare the analysis type, methodologies, and major drawbacks. The reviewed approaches employ some prior knowledge of the grid's operating state to classify the grid's security state. Most research focuses on the steady-state/static security assessment using grid nodes' voltage deviations and their derivatives for the security classification. Although the proposed algorithms are suitable for online security assessment and classification, the impact of renewable energy source distributed generation on the behaviors of the input features was not considered.

Table 4.1: Literature review summary

Reference(s)	Theme/ Focus Area		Input feature(s)	Specific method	Major drawback
[217, 218]	Grid security state assessment		Line performance index and voltage performance index	Multiple machine learning algorithms [217]. Enhanced Artificial neural network [218].	Tedious calculation of inputs
[18, 216]	Dynamic security assessment		Energy functions, Voltage magnitude and angle [216]. Time domain trajectories [18]	Support vector machine [216]. Convolutional neural network [18].	Computational complexities of the kinetic and potential energy. Cumbersome due to need for time domain simulation.
[200, 224, 232, 233]	Voltage security assessment		Voltage stability index	Decision tree [200, 232]. Kohonen ANN-based clusterer [233]. Ball vector machine [224].	Large dataset reliance, low accuracy [224, 232]. Insufficient input data. limited model performance information [233], Steady-state operation centred [200]
[15-17]	Grid static security assessment.		Voltage magnitude, line flows, generations, and load	Artificial neural network [15]. Extreme learning machine [16]. Decision tree [17].	Small instance of dataset [15]. Large dataset reliance, likelihood of overfitting [16, 17],
[220]	Dynamic security assessment: Success rate, false alarm and missed alarm.		Power, voltage, wind penetration and spinning reserve	Multiple machine learning algorithms	Contingencies on generators only
[19-21]	Static security assessment: Secure, alarm or insecure		Composite security index	Support vector machine [20]. Least absolute shrinkage and selection operator[19]. Decision tree [21].	Tedious calculation of the inputs

4.1.2 Contributions and paper organization

The above reviews conclude that the models obtained from these data-driven techniques are capable of learning and identifying potential security boundaries in offline deployment. However, seeing that the penetration of distributed renewable sources will impact the security boundaries and introduce some variabilities into the system, there is a need to include renewable energy sources in the simulations and develop probabilistic security prediction models accordingly. An advantage of the proposed technique in this paper lies in considering the impact of the penetration of renewable energy source distributed generation systems on the grid's security. Another advantage of the proposed technique is the wide range of contingencies considered.

In conclusion, this paper proposes a novel approach for probabilistic security state prediction considering increased DG penetration, credible contingencies, and DG types (synchronous and wind turbine) for the integrated transmission-distribution network. A clustering via classification approach is proposed to overcome the challenge of evaluating the generated clusters' performance. In summary, the major contributions of this paper include:

- Development of critical clearing time (CCT) prediction technique under varying inertia constant and load conditions.
- Development of a novel algorithm for dataset development that considers the penetration levels of different types of DGs and contingencies on the elements in the network.
- Demonstration of grid security state clustering and classification using density-based clustering and probabilistic classification algorithms.

The rest of this paper is organized as follows. The network security state assessment, wind turbine modeling, and machine learning-based power system security problem formulation are presented in section 4.2. The proposed density-based clustering and probabilistic classification framework are presented in section 4.3. The IEEE 14 bus test network and its control elements are discussed in section 4.4. The results of implementing the proposed framework on the test network are presented and discussed in section 4.5. Finally, section 4.6 consists of conclusions from the results obtained.

4.2 Network security modeling and problem formulation

4.2.1 Network modeling and security assessment

For the modern grid's planning, operation, and control, accurate representation of both steady-state and dynamic characteristics of network elements is crucial [234]. Detailed modeling of each element irrespective of the grid size in the network is important to obtain an accurate grid response under transient disturbances. Also, utilities and system operators' network elements and control devices should be explicitly represented during transient stability studies. Sometimes, reasonable assumptions and simplifications are needed for networks where grid element models and parameters are not accessible. Although the assumptions and simplifications made create some level of disparity and inaccuracy in the results published in the literature, the results are useful in understanding the behavior of the grid in real life. It was common to reduce large power systems for transient stability analysis due to the computational burden on simulation tools. Network reduction results in approximations which considerably impacts the final results. Although grid reduction is no longer necessary due to modern computers' increased computation capabilities, network partitioning remains applicable for transient security assessment of large networks. Network partitioning is functional in focusing the assessments on particular areas linked together within the grid. The partitioned network technique may be applied to single and multi-voltage level grids. The integrated transmission-distribution (T-D) network with penetrations of renewable and non-renewable energy sources DGs considered in this paper may be regarded as a multi-voltage level grid. Therefore, the goal is to assess the transient stability responses at the T-D interfaces across the links within the grid.

4.2.1.1 Security assessment

Power system security generally refers to the ability of a power system to remain in a normal state after being subjected to a disturbance. According to [21], considering the impact of numerous possible contingencies on the system operations, the system is termed secure when the operation is normal, the system variable variations are within an acceptable range, and the contingencies optimization is possible. The system is considered insecure when a tradeoff between preventive and corrective control is necessary for one or two system variables outside the acceptable limit(s). Lastly, the system's state is considered asecure when every system variable is outside operational limits.

Transient stability studies the response of the grid when subjected to large disturbances. These disturbances may include faults, as well as a sudden and large change in system load. The occurrence of a large disturbance always results in significant perturbation of the rotor angle of machines within the system [19]. Transient stability evaluates the system's ability to attain a stable post-fault condition by assessing the characteristics of the pre-fault and during fault states. The consequences of prolonged perturbation include loss of machine synchronism, leading to partial or total grid failure. Preventive and emergency controls must be put in place to avoid these consequences. Typically, disturbance initialization and loss of synchronism happen in fractions of a second, making transient stability problems critical for system operators. The swing equation obtained from a single machine infinite bus network model is used to analyze the transient stability of the synchronous generator in the grid as expressed by (1), where H is the inertia constant of the generator, δ is the rotor angle, f is the network operating frequency, P_m and P_e are the mechanical and electrical power of the generator, respectively. For a multimachine system, the equivalent inertia constant (H_i) is expressed by (2), where S_{G-i} is the rated power of the *i*-th generator, S_B is the base power in MVA, H_i is the inertia constant of the *i*-th generator [235]. The two numerical attributes in the dataset are the maximum frequency and voltage deviations. The maximum frequency deviation (Δf) of the network can be derived from (3) to (5) where t is the time between the time of fault (t_f) and the clearing time (t_{cr}) [236], while the maximum voltage deviation (ΔV_T) is obtained from (6) [237, 238], where $\Delta P$is the power imbalance, V_o is the initial voltage and V_{max}^T is the maximum voltage dip after transient disturbance where ω is the angular speed of the rotor .

$$\frac{H}{\pi f}.\frac{d^2\delta}{dt^2} = \Delta P \text{ (on system base)} \tag{1}$$

$$H_{eq} = \frac{\sum S_{G-i}.H_i}{\sum S_B} \tag{2}$$

$$\frac{d\delta}{dt} = \Delta\omega \tag{3}$$

$$\frac{d\Delta\omega}{dt} = \frac{\pi f}{H_{eq}}\Delta P \tag{4}$$

$$\Delta f = \frac{\Delta P \times f}{2H_{eq}} t \quad (5)$$

$$\Delta V_T = \frac{V_0 \times V_{max}^T}{100} \quad (6)$$

4.2.1.2 Wind turbine modelling for renewable energy source DG

The type-3 wind turbine generators (WTGs) are currently the dominant technology for wind energy-based distributed generation systems. Type 3 WTG is also known as doubly-fed induction generators (DFIGs) or doubly-fed asynchronous generators. As shown in Figure 4.1, the DFIG is connected to the grid through a back-to-back inverter. The inverter excites the rotor of the induction machine with a variable AC source. This provides control of the rotor flux frequency, enabling the rotor shaft frequency to track wind speed optimally. The complete WTG model is divided into four functional blocks, as indicated in Figure 4.2. The converter control model is composed of separate active and reactive power control functions. Reactive power control is very fast, due to the power electronic converter. The dynamic behavior of a type-3 WTG, as seen from the grid, is therefore dominated by active and reactive power controller response rather than physical characteristics. The wind turbine rotor (along with the blades) and the electrical generator are modeled by their inertia parameters. The pitch control model is mainly formed by the addition of two PI controllers, usually depending on the WT rotor rotational speed and the active power reference provided by the active power control model. The proportional integrator (PI) is a standard controller for the wind turbine rotor system. The PI controller minimizes the error between a measured process variable and a desired reference value by calculating and outputting a control action that can adjust the process quickly. This process takes the form of a feedback loop control system as shown in Figure 4.3. The controller action is based on two measured quantities; output real power (primary) and rotor currents (secondary). The controller employs two loops; the outer loop is used to control the real power (p), while the inner loop is used to achieve rotor current control. The measured power signal is compared to the desired power, and the error drives a PI controller. The output of the PI controller is the reference rotor current. This reference current is compared with the measured rotor current, and the error is fed to another PI controller. The output of this PI controller is the rotor resistance value for achieving desired rotor current (and thus output power). Optimal speed overshoot magnitude can be achieved by tuning the proportional (Kpp, Kcp) and integral (Kcp, Kci) gains.

The model equation for the wind turbine system can be derived from the equivalent circuit diagram of the doubly-fed induction generator (DFIG). If $\underline{u}$ is the voltage, $\underline{\varphi}$ is the flux linkage, $\underline{i}$ is the current, ω_{ref} is the speed of rotation, ω_g is the electrical generator speed, ω_n is the rated speed, then the fifth-order model for the induction machine stator (s) and rotor (r) are derived in (7) and (8). The mechanical equation and the electrical torque of the induction machine can be modeled as (9) and (10), where t_m and t_e are the mechanical and electrical torques, respectively.

$$\underline{u_s} = \underline{r_s}\underline{i_s} + \frac{1}{\omega_n}\frac{d\underline{\varphi_s}}{dt} + j\underline{\varphi_s}\frac{\omega_{ref}}{\omega_n} \tag{7}$$

$$\underline{u_r} = \underline{r_r}\underline{i_r} + \frac{1}{\omega_n}\frac{d\underline{\varphi_r}}{dt} + j\underline{\varphi_r}\frac{\omega_{ref-}\omega_g}{\omega_n} \tag{8}$$

$$J\frac{d\omega_g}{dt} = t_m + t_e \tag{9}$$

$$t_e = I_m(\varphi_s + i_s) \tag{10}$$

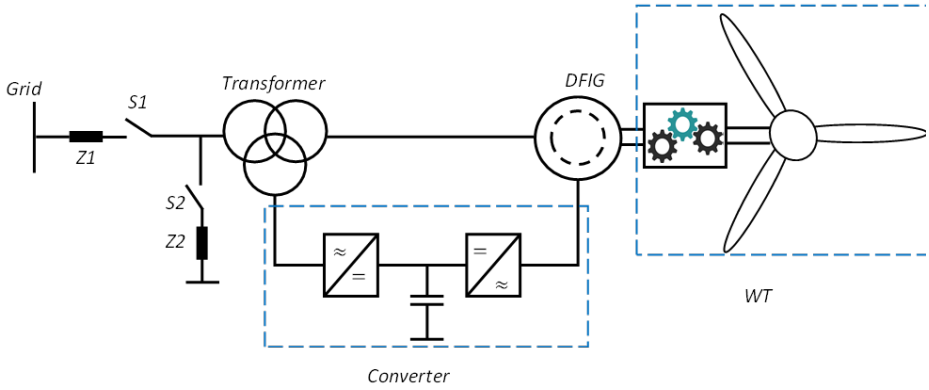

Figure 4.1: Type 3 wind turbine generator

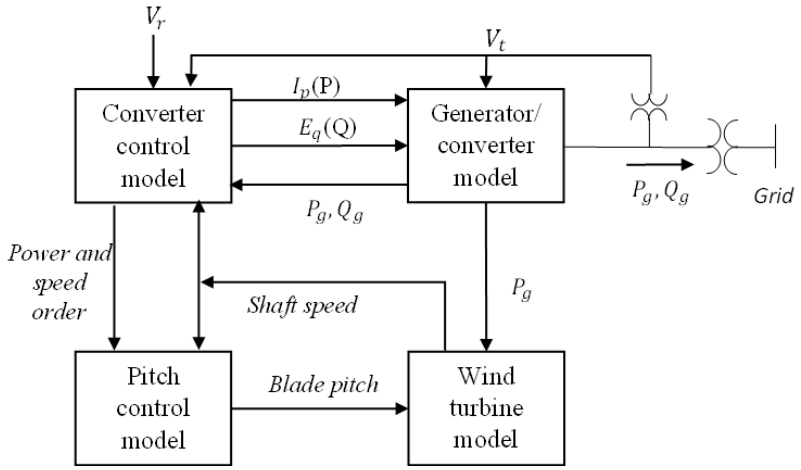

Figure 4.2: Dynamic model connection of Type-3 WTG

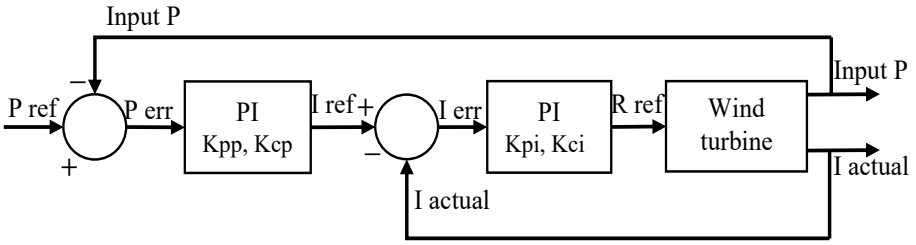

Figure 4.3: Controller for wind turbine rotor current and active power

4.2.2 Machine learning for power system security problem formulation

Emerging grid operation demands the prediction of the security state in the least time frame with the highest possible accuracy level. To overcome the speed, information, and real-time assessment capability limitations of conventional assessment methods, machine learning techniques

have been used recently for security prediction. Machine learning algorithms effectively handle large data consisting of different data types obtained from system security simulations and real-life operations. Machine learning (ML) models can be developed through batch (offline) and incremental (online) learning algorithms depending on dataset volume, preferences, and application. Generally, machine learning algorithms are grouped into supervised (classification), unsupervised (clustering), and reinforcement learning algorithms [239] as shown in Figure 4.4.

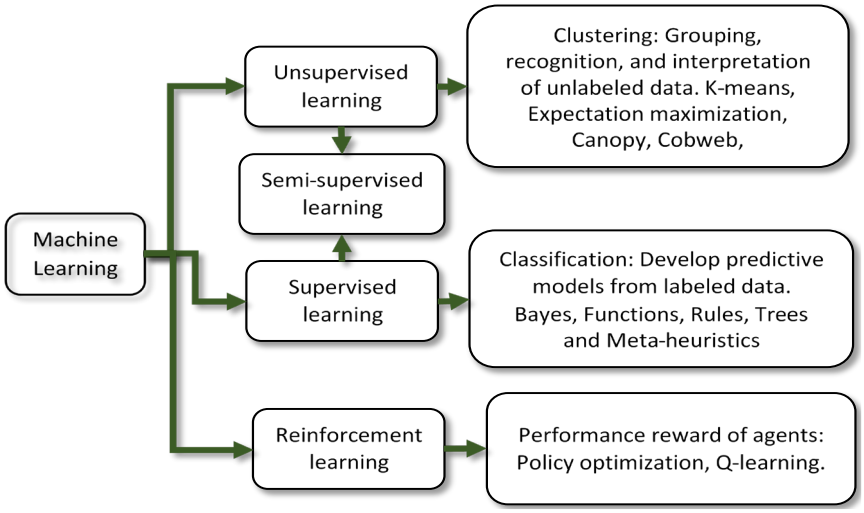

Figure 4.4: Machine learning classification and algorithms

In semi-supervised learning, a model is developed from a part labeled and unlabelled dataset. The model training begins with labeled data, after which the final model can identify patterns from the unlabelled data from the same dataset. After dataset generation, the major steps involved in ML model development are data preparation, model training, model testing, and lasting improvement. In the data preparation step, the data is cleaned from associated noise; also attributes are filtered to obtain the best results. If the performance of the trained model is satisfactory after testing, then the model is validated and deployed. Otherwise, the model will be improved by refining the data, reconsidering the choice of algorithm, and adjusting key algorithm parameters. The training datasets should include all possible scenarios extracted from security simulations for reliable network security state predictions. This paper adopts an offline learning model since the developed dataset can be processed in a single data batch. Also, the data is time-invariant, and its distribution does not drift over time.

Machine learning methods provide statistical tools to explore historical data and predict outcomes using live data. Unsupervised learning provides an option for pattern recognition with an unlabelled dataset and limited training sample size. The attributes considered in this paper are the post fault frequency and voltage deviations. The goal is to model a quasi-class c, which represents the security state of the network based on an identified pattern in the dataset. If u is the dataset and q is the center point of u, then c_i can be obtained for an instance u_i using (11), where $\rho(u_i)$ is the properties of u_i obtained through the learning model. Equation (11) is also used to minimize the intraclass variance of the derived quasi-classes c. The major optimization problem is given in (12),

where d is the unlabelled data sample, n is the number of sample instances obtained through simulations, W is the parameters of the machine learning model, and η is a positive constant [214, 240]. The unsupervised learning process is achieved through the iterative process of (11) and (12). Alternating the center point q and increasing the distance between the alternated points enhances the quasi-class differentiation, which in turn improves the performance of the unsupervised learning models.

$$c_i = \min_{i \in (1,2,..,P)} \|q_i - \rho(u_i)\| \qquad i = 1, 2, .., n \tag{11}$$

$$A = \max_{W, q_i} F(W|d, c_i) \qquad d = \{u_1, u_2, \dots u_n\} \tag{12}$$

s.t. $\eta g(W) \geq 0$

Supervised learning applications are prevalent in machine learning tasks since many real-life data are labeled. After the security state under certain conditions has been derived in the previous section through clustering, a model to predict the state of the grid for future conditions is therefore needed. Supervised learning aims to train a model that predicts the outcome of future events with a high degree of accuracy from an outcome measurement, which is available for each attribute occurrence [241]. A supervised machine learning problem may be developed as an optimization problem to minimize the loss function L_f of the dataset u as shown in (13) [242], where $\emptyset$ is the training parameter. The loss function evaluates the relationship metric using a distance function between the predicted output and actual outputs. To further improve the performance of supervised machine learning models, another optimization problem to minimize the risk R_f based on the loss function is introduced as shown in (14), where $p(u, c)$ is the probability of the observing data point (u, c) which is always unknown. However, since the data points (u_n, c_n) are obtained from the dataset, a predictive function (F_p) which reduces the empirical risks between two points can be obtained from (15) [243, 244], where N is the number of training samples.

$$L_f = L(c_i, f(u_i, \emptyset) \tag{13}$$

$$R_f|L(f(u), c)| = \iint p(u, c) L(f(u), c) du dc \tag{14}$$

$$F_p = \min_{\emptyset} \frac{1}{N} \sum_{i=1}^{N} L(c_i,\ f(u_i,\ \emptyset)) \tag{15}$$

4.2.3 Data clustering

Clustering is an unsupervised learning technique that groups similar data points into clusters within the dataset. Clustering is an essential and very useful technique used in data mining for pattern recognition based on characteristics. It involves an iterative process that divides clusters into sub-clusters. Clustering plays a vital role in text mining, web data analysis, spatial database application,

marketing, medical diagnostics, etc. The three most common clustering methods are density-based, hierarchical, and partitioning methods [245].

In density-based clustering methods, objects with similar densities are identified and grouped. The objective of this method is to partition a data set into regions based on its data point densities. The low-density data points as separated into one cluster, and high-density data points are also divided into another cluster in a region. The expectation-maximization (EM) algorithm is one of the high-performing density-based clustering algorithms [246].

Hierarchical clustering methods focus on the distance between data objects, where data objects nearer to each other are grouped to form a cluster. Data point connectivity technique is used to implement the hierarchical clustering methods where clusters in the form of a tree known as a dendrogram containing a root node, which has a sub-node, and the leaf node is established [247]. The hierarchical clusterer (HC) is a common algorithm for implementing the hierarchical method in top-down or bottom-up approaches.

In partitioning-based methods, a cluster is formed such that an object in the cluster is closer to its center than to the center of any other cluster. The center of a cluster is commonly referred to as the centroid. Partitioning-based methods aim to minimize the distance between data points and centroids by iteratively relocating data points between clusters until a local optimal partition is found. Because the number of data points in any dataset can be finite, the desired number of clusters may be specified at the start of the clustering algorithm [248]. In recent research, k-Mean (KM) and canopy clustering (CC) algorithms are among the commonly used partitioning-based clustering algorithms. The hierarchical and partitioning-based clustering methods can be referred to as non-density-based clustering methods. Table 4.2 show the comparisons between the density-based clustering methods and the other cluster methods (non-density based) using common criterion as obtained from [249]. Density-based clustering algorithms are better in general performance and require very little time to train, build, and deploy developed models. They are also simpler in complexity and preferred for datasets with non-correlated attributes.

Table 4.2: comparison between density-based clustering and non-density-based clustering

Categories	**Density-based Clustering**	**Non-density-based clustering**
Performance	Better (preferred)	Good
Time requirement	Insignificant	Significant (due to several iterations required)
Complexity level	Simple	Complex
Computational efficiency	Slow	Fast
General accuracy	High	High
Non-linear dataset	Preferred	Less preferred

4.2.4 Data classification

Classification is a method of predicting a target or class from categorical and/or non-categorical data. It is a useful machine learning technique for any type of statistical data and non-statistical data. Classification algorithms have found application in various power system schemes, including but not limited to renewable energy source generation prediction, voltage stability prediction, frequency stability classification, and dynamic stability classification [183]. The goal of classification is to generate a satisfactory and robust model that predicts the class label of a dataset from a given set of predictor features using an appropriate classification algorithm known as the classifier. The choice of the specific classifier is critical and depends on several factors, including the type of data, the size of data, time requirement, accuracy requirement, etc. Several classifier evaluation techniques, such as cross-validation, data splitting, and leave-one-out validation, can be used to perform preliminary testing of classifier performance.

Figure 4.5 shows the different groups of classification algorithms with examples considered in the paper. The tree classifiers are developed from sets of independent instances using the "divide-and-conquer" approach to the machine learning problems. The tree classifiers consist of nodes that are further reduced into leaf nodes based on the specific criteria. Rule classifiers, like tree classifiers, are algorithms with lines of conditions for tests. The precondition rules are a series of tests performed at the nodes, and the class of a dataset instance is determined by the inferences derived from such preconditions. A set of classification rules can be derived directly from a tree structure, with one rule generated from each leaf node [250]. Meta-learning is concerned with identifying patterns in a dataset and understanding their impacts on the algorithm's characteristics. The meta-learning method often involves combining several predictions from various predictive models from a single dataset to maximize accuracy [251]. A major drawback of meta-learning is the limitation in the amount of information that can be captured. The meta-learning algorithm can only detect patterns between two attributes or one attribute and the target [252]. Function classifiers are groups of machine learning algorithms that be explicitly and naturally mathematically modeled. Common function classifiers are simple linear regression, minimal sequential optimization (SMO), simple logistic, and the Gaussian process. The simple function classifier can only generate a predictive model from a single attribute data. Apart from being limited by the number of attributes, missing data and non-numeric features are not allowed in function classifiers [253].

The Bayes classifiers are probabilistic classifiers that attribute conditional density estimations to the multi-dimensional dataset. The Naïve-Baiyes algorithm, a common Bayes classifier, is easy to implement and performs well with both large and small training datasets. It is also ideal for numeric and nominal features as well as binary and non-binary class classification problems. Another major advantage of the Naïve-Bayes classifier is the short computational time [254]. The attributes considered for the grid's security prediction in this paper are probabilistic. Ttherefore, a probabilistic classifier is more suitable to obtain the required predictive model. The

comparison of the performance of the proposed probabilistic classifier (Naïve-Bayes) with the other classifiers (SMO, simple logistics, bagging, decision tree and logistic model tree) is shown in the results section 5.1. The detailed discussion on the development and implementation of the Naïve-Bayes classifier is presented in section 3.3.

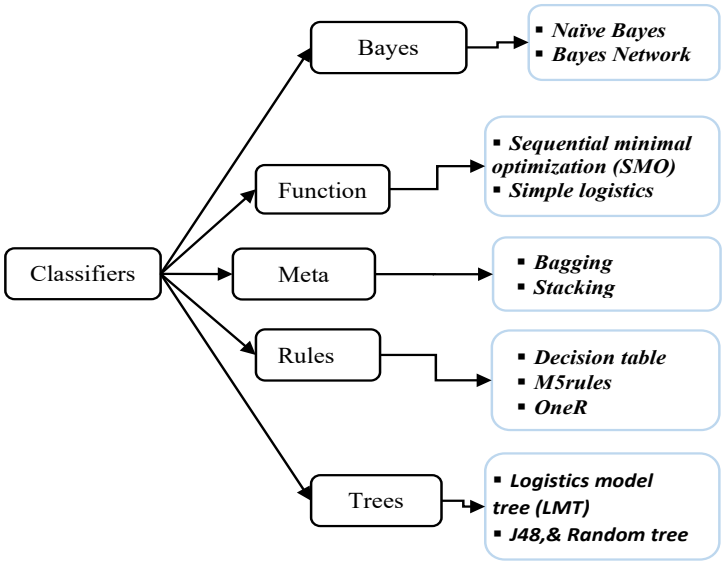

Figure 4.5: Classification algorithms techniques

4.3 Methodology

This section discusses the proposed network security state clustering, classification, and prediction technique. The goal is to predict the state of the grid under any disturbance, as shown in Figure 4.6. The proposed technique considers power generation from both the bulk and distributed generations as well as the maximum power transferrable by the grid and represented by P_{max}. The bulk generation is obtained from the transmission network synchronous generators represented by P_{g-syn}, while the power generation from the renewable energy source (P_{g-ren}) and non-renewable energy sources P_{g-nren} are considered for the distribution network power generation. The grid model is simplified and represented by a first-order transfer function with only the inertia (H) and damping (D) elements. The set of disturbances from which the frequency and voltage responses are obtained in this paper is represented by S. The elements of S include a sudden change in load and three-phase short circuit for several nodes within the grid as well as a fault in the transformers. The voltage and frequency responses of the grid to several disturbances are used to classify the security state of the grid. The grid is secured if all post fault system variables exist within the security limit, and the equality and inequality constraints are met under the N and N-1 security assessments. The state of the grid under only the N security assessment is insecure when at most two of the post fault system variables exist outside the limits, and both equality and inequality constraints are satisfied, and asecure when only the inequality constraints are satisfied and all the system variables outside the security limits. The frequency and voltage responses are obtained from transient stability assessments under several impulses, where t_f and t_c are the fault initiation time and clearing times, respectively.

A real-time feedback system is expected to aid corrective measures in the grid as a precautionary measure in case of insecure state prediction or failure in the prediction outcome. In case of insecure state prediction or failure in the prediction outcome, the feedback security control system is expected to activate the necessary corrective measures in the grid. The corrective measures applicable in this research are the intelligent load shedding scheme and the RES-DG penetration level reduction.

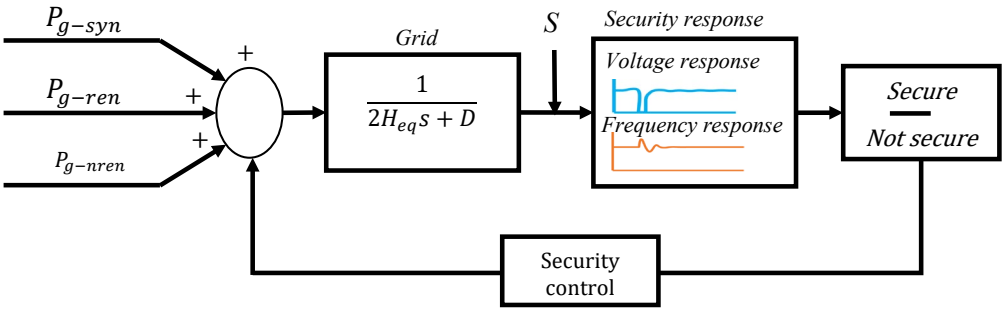

Figure 4.6: Grid security state classifier

The methodology proposed in this paper is divided into two major stages. The first stage involves dataset development using the determined impulses and grid responses. The attributes are prepared for training to develop the required security prediction model in this stage. The critical clearing time was predicted using the described process in section 3.1. Key attributes with a high correlation to the security of the network were extracted from possible operation scenarios of DG types, penetration level, and contingencies. The attributes are the maximum post-fault voltage and frequency deviations. These attributes are obtained from transient stability responses of the networks to different disturbances. The second stage involves identifying and training a suitable machine learning algorithm using the dataset with instances extracted using the proposed algorithm. Given the stochastic characteristics of RESs and potential contingencies occurrence within the network, probabilistic machine learning algorithms are proposed for the security state classification and prediction. The expectation-maximization (EM) and Naïve-Bayes (NB) algorithms are selected for the density-based clustering and classification, respectively, due to their capabilities in handling numerical and nominal attributes.

4.3.1 Critical clearing time prediction

When a fault occurs on any of the transmission lines in the grid, the equivalent reactance $X_{eq,0}$ increases, and the corresponding power transfer P_e decreases. Considering a multimachine system, if DT is the DG type, PL is the penetration level, and CT is the contingency type, then the power transfers $P_{n,\,max}$ and the initial stable rotor angle δ_0 is represented in (16) to (18), where A is the ratio of the mechanical power P_m to $P_{n,max}$, and $\delta_{0\,max}$ is the maximum rotor angle, where $n = 0, 1$ and 2 representing the pre-fault, during-fault, and post-fault conditions, respectively. Figure 4.7 shows the $P_e - \delta$ plots for a single machine infinite bus system (SMIB) model showing the P_e for the pre-fault, during faults, and post-fault conditions for a three-phase fault away from the sending

end. After the fault is cleared, X_{eq2} for the grid is established with value depending on the characteristics of the other transmission lines and the configuration of the grid. Usually, after fault clearing, the value of X_{eq2} is larger than $X_{eq,0}$ but smaller than the $X_{eq,1}$ of the grid during fault condition. Consequently, $P_{e,2}$ is lesser than $P_{e,1}$. If the grid's stability is to be maintained after the occurrence of a fault on any transmission line, then the $P_{e,2}$ must be greater than P_m. For a stable grid before a fault, the rate of change of the rotor's angle $d\delta/dt$ is zero, therefore, the equilibrium point is δ_0. The change in the rotor angle in the time domain is given by (19), where k_p is the active droop gain. At the occurrence of a fault at time t_f, P_m exceeds the $P_{e,1}$ as shown in Figure 4.7. Consequently, the rate of change of the rotor angle $d\delta/dt$ is greater than zero, thereby resulting in gradual angular accelerating speed from δ_0 until the fault is cleared. At the clearing of the fault at critical clearing time t_{cr} corresponding to the critical rotor angle δ_{cr}, the P_m is again less than $P_{e,2}$, thereby generating a gradual angular decelerating speed until it gets to the maximum rotor angle δ_{max}. The decelerating speed will cause the rotor to oscillate periodically until a new rotor angle is achieved. If the fault is cleared in time δ_{cr}, the maximum rotor angle δ_{max} will be less than the new decelerating rotor angle, hence the grid is considered transiently stable. When the time to clear the fault is longer, the decelerating rotor angle increases beyond δ_{max}. Hence the grid is considered transiently unstable. The critical clearing time t_{cr} corresponds to the time the rotor angle reaches the critical angle δ_{cr} during a fault. Equation 20 for evaluating δ_{cr} is derived from the equal area criterion from the shaded areas A and B in Figure 4.7. The clearing time which represents the maximum fault duration that guarantees the security of the system derived by integrating (20), is given by (21).

$$P_{\mathrm{n},max}(DT, PL, CT) = \frac{E_{qi}E'_{qi}}{X_{eq.n}} \tag{16}$$

$$\delta_0(DT, PL, CT) = \sin^{-1} A_0 \tag{17}$$

$$\delta_{0\,max} = \pi - \sin^{-1} A_0 \tag{18}$$

$$\delta(t) = k_p \omega_0 P_m(t) + \delta_0 \tag{19}$$

$$\delta_{cr} = \cos^{-1}\left(\frac{P_m(\delta_{max}-\delta_0) - P_1 cos\delta_0 + P_2 cos\delta_{max}}{P_2 - P_1}\right) \tag{20}$$

$$t_{cr} = \sqrt{\frac{2H_{eq}(\delta_{cr}-\delta_0)}{\pi f P_m}} \tag{21}$$

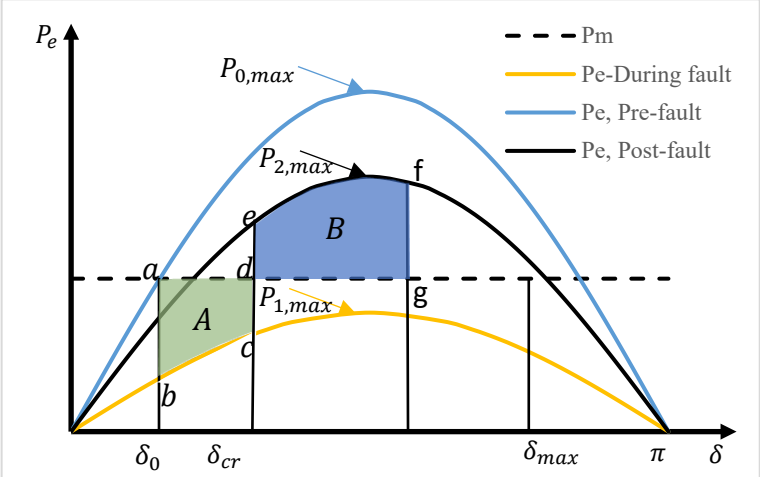

Figure 4.7: Power-angle plot under 3 phase fault

In this paper, the critical clearing time for each considered scenario for the considered multi-machine test system is obtained using the time domain simulation technique. The techniques involve increasing the fault clearing time for the most severe type of fault until one of the synchronous generators in the system is about to go out of step. Further increase in the clearing time will take the generator out of synchronism then the network is regarded as transiently unstable. In a multi-machine system, different critical clearing times are obtained for each synchronous generator in the system. The least critical clearing time is assumed to be the critical clearing time for the entire system.

For a specific transmission capacity, the critical clearing time is affected by several factors, including the equivalent grid inertia, generators' parameters, fault type, fault location, network transfer capability, network loading, and generators distribution within the grid. The variability of the output power from the renewable energy source DG leads to a change in the equivalent inertia of the grid. Likewise, the load level of the grid varies throughout the day and seasons. Therefore, this paper proposes time-varying grid features: the equivalent inertia constant and the system loading for the critical clearing time prediction. The proposed model for the critical clearing time (t_{cr}) prediction for each observation of DT - PL in this paper is given in the following steps and represented in the flowchart in Figure 4.8, where ε is the error tolerance:

1. Model the integrated network for transient stability assessment.
2. Track the change in clearing time with the inertia constant change and large load change. In this paper, the magnitudes of load changes considered are estimated from the three-phase short circuit fault currents at the nodes and applied through a step increase on the loads.
3. Develop an input-output model to predict the changing clearing time. This paper adopts an adaptive neuro-fuzzy inference system (ANFIS) due to its suitability for real-time applications, as shown in Figure 4.9. If R represents the rules developed from step 2, the ANFIS inference for R_i is given in (22), where x_i corresponds to the variables been tracked, b is a constant and P is the total number of variables. The clearing time y from the inference process is estimated by (23) where α_i is the firing strength of the rule R_i.

$$R_i = q_{i0} + q_{i1}x_1 + .. + q_{ir}x_i + b \text{ for } i = 1, 2, \dots, P \quad (22)$$

$$y = \frac{\sum_{i=1}^{P} \alpha_i (q_{i0} + q_{i1}x_1 + \cdots + q_{ir}x_i)}{\sum_{i=1}^{P} \alpha_i} \quad (23)$$

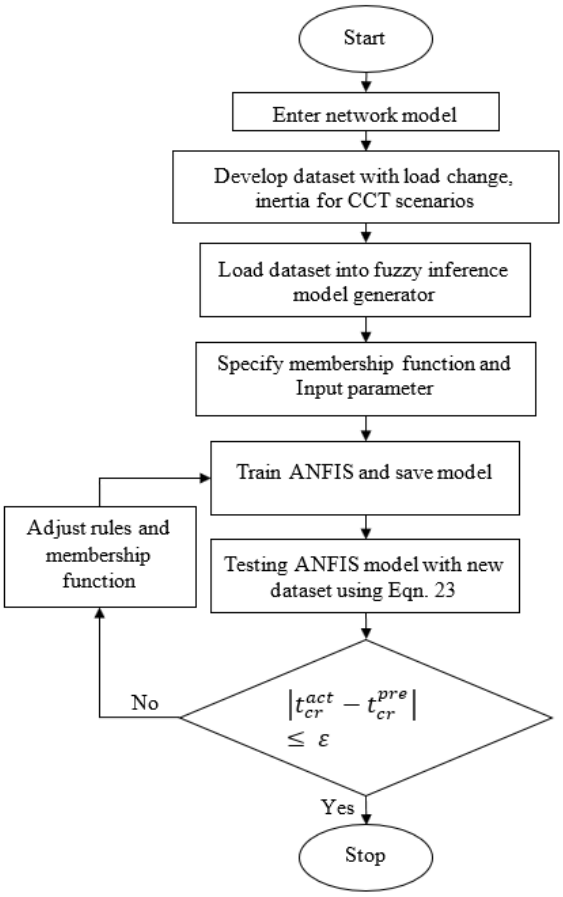

Figure 4.8: ANFIS-based critical clearing time prediction flowchart

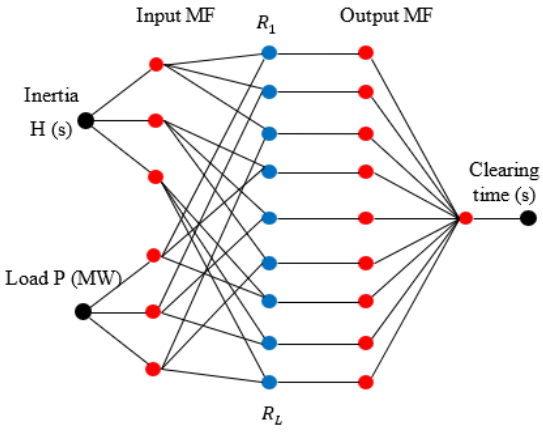

Figure 4.9: ANFIS-based varying clearing time prediction

4.3.2 Training dataset from transient stability assessment

Figure 4.10 shows the flowchart for the proposed continuous transient stability assessment algorithm to obtain the training attributes for the predictive model development where $M, N,$ and L are the total numbers of contingency, penetration levels, and DG types, respectively. The proposed

algorithm for the continual transient stability assessment in this paper is terminated when the responses of the grid to all seven contingency types (CT) considered for the five different penetration levels (PL) under the two DG types (DT) have been obtained. Table 4.3 describes the DG type (DT) and penetration levels (PL), while the considered elements and contingency types (CT) are shown in Table 4.4, where $M, N,$ and L are 7, 5, and 2, respectively. The performance of the machine learning-based model depends intrinsically on the training dataset size. A common way to assess the sufficiency of a training dataset is to apply the ten times rule. The rule implied that the number of dataset instances should be at least ten times the number of attributes. Although the impact of training dataset size cannot be ignored, the results of applying the proposed CCT prediction model in this research to other networks will differ due to differences in architecture and elements. The size of the training dataset for the machine learning-based security state prediction in this research can be increased by reducing the step increments of DG penetration level, considering more elements, and including contingency types in the transient stability simulations.

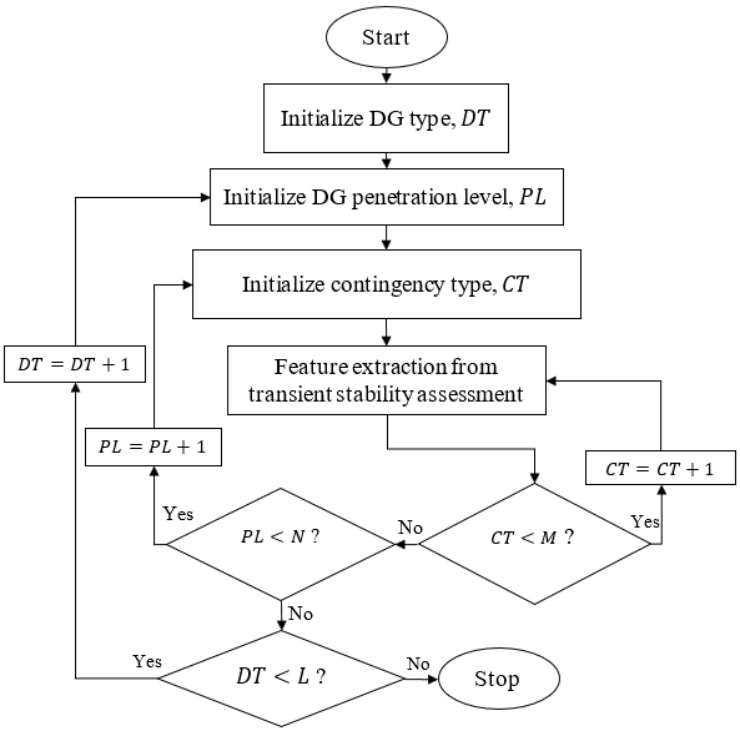

Figure 4.10: Continuous transient stability assessment for dataset development

Table 4.3: DG types and penetration levels

DG Type	Code (DT)
Synchronous	1
Renewable	2
DG Penetration Level	Code (PL)
0 %	1
25 %	2
50 %	3
75 %	4
100 %	5

Table 4.4: Elements and contingency types

Faulted element	Contingency	Code (CT)
Transmission node	Three-phase short circuit	1
Distribution node	Three-phase short circuit	2
Transformer	Tap changer fault	3
Transmission line	Three-phase short circuit	4
Distribution line	Three-phase short circuit	5
Transmission load	Sudden load increase	6
Distribution load	Sudden load increase	7

4.3.3 Density-based clustering and probabilistic classification

Clustering is the task of identifying a set of groups of related entities within a data set while keeping dissimilar entities segregated into other groups or the noise group. Clustering is considered an unsupervised machine learning task. The goal is to discover meaningful categories given a set of instances from a specific data set and a dissimilarity function. The dataset is typically a set of multi-dimensional real-valued points, which is considered a sample from an unknown probability density. The dissimilarity functions can be estimated using the Euclidean distance model or any statistical distance model. Density-based clustering is a form of machine learning clustering approach for extracting previously unknown patterns from data sets. The density-based clustering technique has been useful in identifying non-linear-shaped structures based on density. The advantages of density-based clustering include identifying noisy data and clusters of any distribution. Also, with density-based clustering, it is not necessary to specify the number of clusters in a-priori. Using the technique in this paper, the clusters will represent the security states (class) of the network, namely secure and insecure states based on the post contingencies values of the frequency and voltage for individual power system standards.

Expectation maximization (EM) is a density-based algorithm for estimating the maximum likelihood of an outcome using a series of cluster conditions for a dataset having an incomplete data problem (security state in this case). The major steps involved in the application of this algorithm in the clustering model development in this paper are the expectation (E-step) and maximization (M-

step) functions. In the E-step function, class probabilities are attached to the unlabelled security dataset. In the M-step function, a new classifier is trained using the probabilistic labels for all the data obtained from the E-step. The EM algorithm is guaranteed to obtain model parameters that have equal or greater likelihood at each iteration until convergence [247, 255]. Figure 4.11 presents the flowchart of the proposed approach where the major functions within the EM algorithm are highlighted.

Let u_i be a random vector in the desired secured training dataset u, with a probability density function g(u:$\hat{\mathbf{w}}$), where $\hat{\mathrm{w}} = (\hat{\mathrm{w}}_1, \ldots., \hat{\mathrm{w}}_d)^T$ is a vector of unknown parameters with parameter space ϖ. Also, assuming a complete dataset, if $d_c(u{:}\,\hat{\mathrm{w}})$ represent the probability density function of the random u that corresponds to the vector u_i, then the log-likelihood function for $\hat{\mathrm{w}}$ considering u is given by (24). Since the algorithm applies an indirect iterative approach, to proceed with the fuzzy data nature, a conditional expectation step (E-step) of c considering $\hat{\mathbf{w}}$ is introduced. The missing data (required forecast point) is estimated given the observed data and current estimate of the model parameter in the E-step. If $\hat{\mathrm{w}}_0$ is an initial value of $\hat{\mathbf{w}}$, then for the first iteration, the E-step is estimated as (25).

$$\log L(\hat{\mathrm{w}}) = \log d_c(u{:}\,\hat{\mathrm{w}}) \tag{24}$$

$$Q(\hat{\mathrm{w}}{:}\,\hat{\mathrm{w}}_0) = E_{\hat{\mathrm{w}}_0}\langle \log L(\hat{\mathrm{w}}) \,|c\rangle \tag{25}$$

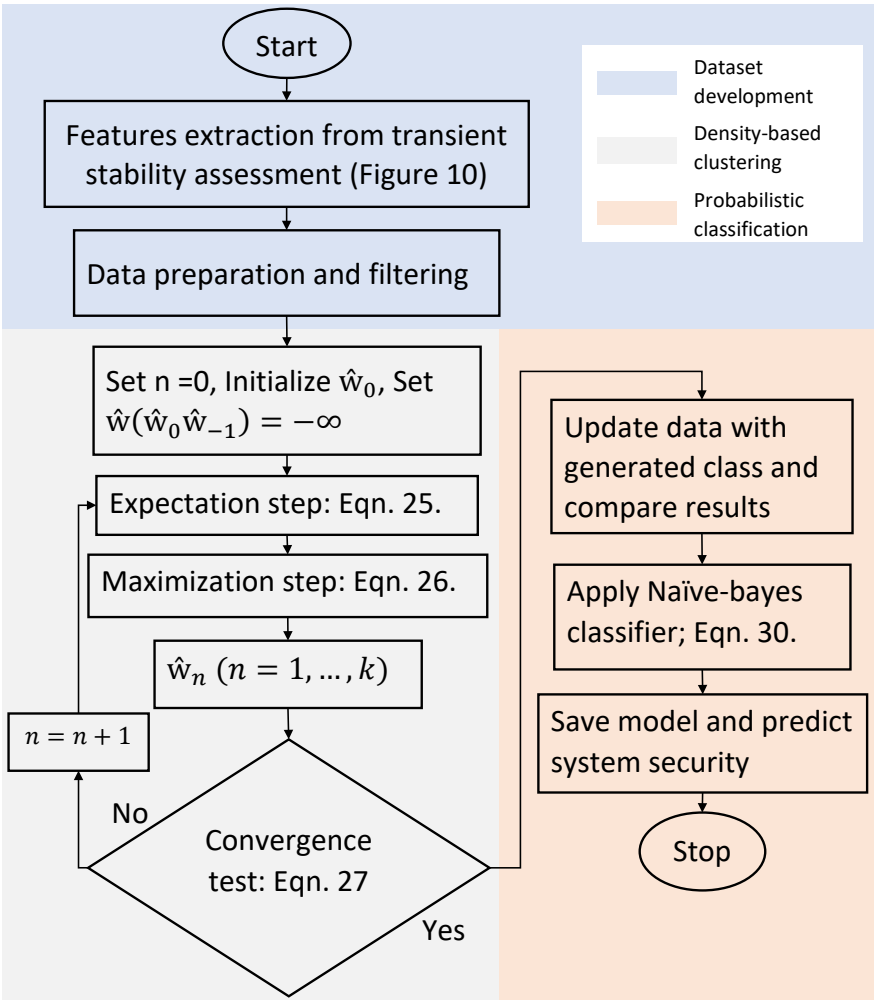

Figure 4.11: Flowchart for the security state prediction

In the M-step, the likelihood function is maximized under the assumption that the missing data is known. The M-step is formulated as (26). The likelihood increases after every iteration based on the likelihood function given in convergence criteria in (27), where ε is a specified constant. In this paper, probabilistic classification is proposed to classify and predict the network's future security states. The probabilistic approach is expected to accommodate the network's uncertainties and inconsistencies, which will impact the future data and consequences security states. The Naïve Bayes (NB) algorithm, which is a generative probabilistic classification model, is proposed. The NB classifier is a simple yet effective probabilistic classifier that predicts the outcome from some given data attributes. It requires a small amount of training data to estimate the parameters needed for classification. From the training dataset u of k classified classes, the unconditional probability $P(z|c)$ for a new attribute $u_i^* = [u_1^*, \ldots., u_n^*]$ associated with the class c can be predicted using (26) where u_i^* is the value of the attribute u_i^* and $z \in [1, \ldots. d]$ is a value of class variable Z. Given that $P(Z)$ which is the ratio of the number of instances to the total number of training samples is constant for all classes, then, only the numerator $P(u|z)$ needs to be maximized. Consequently, the conditional properties are independent, as shown in (29) [256]. Therefore, the final class chosen by the NB classifier is given by (30).

$$\hat{w}_0 = arg \max_{\hat{w}} E\,(w|L\hat{w}_0) Log\langle \log L(\hat{w})\,|c\rangle \tag{26}$$

$$\frac{|L(\hat{w}_{n+1}) - L(\hat{w}_n)|}{|L(\hat{w}_n)|} < \xi \tag{27}$$

$$P(z|u) = \frac{P(u|Z)P(z)}{P(u)} \tag{28}$$

$$P(z|u) \propto P(z) \prod_{c \in C} P(u|z) \tag{29}$$

$$NB_u = \underset{u \in U}{\operatorname{argmax}} P(U) \prod_{c \in C} P(u|z) \tag{30}$$

4.4 Test systems

The IEEE-14 bus test network represents an integrated medium voltage transmission-distribution network which is ideal for testing the proposed model. The IEEE-14 bus network comprises 14 buses, 5 generators, 11 loads, and 16 lines as modeled in Figure 4.12. The test network consists of two voltage levels of 220kV and 132kV representing the transmission and distribution networks, respectively. Generators 1, 2, and 3 are considered coherent generators, while the synchronous DGs 6 and 8 are replaced afterward with doubly fed induction generator wind turbine (WT) DG for the simulation scenarios. The responses of the integrated network to transient disturbances are monitored at the two transmission-distribution (T-D) network interfaces (buses 06 - 07 and buses 04 - 07) through links 1 to 4 representing the simulation scenarios I – IV. The considered DG types (DT) and penetration level (PL) with their respective associated codes are shown in Table 4.3. The DG penetration level (PL) in MW is initialized from 0% and terminated at 100% with an increment value of 25% of the total distribution network load. This paper considers multiple contingencies on both the transmission and distribution sides of the integrated network. The faulted element and contingency type (CT) selection for a particular dynamic stability simulation session follows the order presented in Table 4.4.

Table 4.5 shows the dynamic parameters of the IEEE 14 bus network synchronous generators. The control system diagrams for the automatic voltage regulator (AVR), and the power system stabilizers (PSS) are shown in Figure 4.13, with parameters as given in Table 6. The function of the AVR system is to ensure that the generator's terminal voltage (V_t) is equal to the reference value ($VRef$) through the VPSS, which is the sum of the signal from the PSS and the excitation limiters. The IEEET1 exciter is developed based on a DC generator model. The first-order lag block delays the voltage compensator (Vc) by the time constant (TR). The lead-lag block is used to model the exciter's inherent time constants. The derivative of the resultant of the delayed compensator, the signal from the system stabilizer ($VPSS$), and the reference voltage signal ($VRef$) are then obtained with a scaling factor KA and delay constant TA. The output of the derivation is zero in the steady-state grid operation. The last blocks of the exciter include the exciter constant KE, exciter time

constant TE, the exciter saturation functions SE, the feedback gain KF, and the feedback time constant TF functions as the protective circuits and limiters. After a disturbance, the PSS is intended to minimize the power system oscillations which are represented by the speed deviations ($\Delta\omega$) of the grid machines. The first block $KPSS$ is the PSS gain, while the second block is a first-order filter with washing time constants TW. The last two blocks are lead-lag compensators, where $T1\ to\ T4$ are time constants.

The steam turbine-governor model with fast valving (TGOV2) used in the test system is shown in Figure 4.14. The TGOV2 model ensures machine frequency regulation in grid-connected and island modes. Fast turbine valving is used to improve the grid's transient stability. The constant speed/frequency of the grid is achieved using the various possible steam timing combinations from the control valves. During contingencies, the steam volume is insufficient to maintain the individual generator's speed. Consequently, the automatic governor control receives the signal using the reference power level (Pref) and the speed change (Δω) to determine the necessary adjustment to the steam valve to achieve a mechanical power output (Pm) which maintains the frequency of the grid. Generally, the grid operators vary each generator's contribution based on its power drop (PD). The range of values of the time constants (T1, T2, and T3), the damping coefficient (D), the governor gain (K) as well as the maximum and minimum valve positions are given in Table 4.6. The mechanical torque is derived through a Proportional-Integral-Derivative (PID) controller. The tuning and configuration of the control blocks according to the regulation performances determine the system's response. The configuration is also essential to achieve the desired mechanical power of the machines. The grid operator can request a different contribution from each power plant according to its capability of regulating the grid frequency by adjusting its power production.

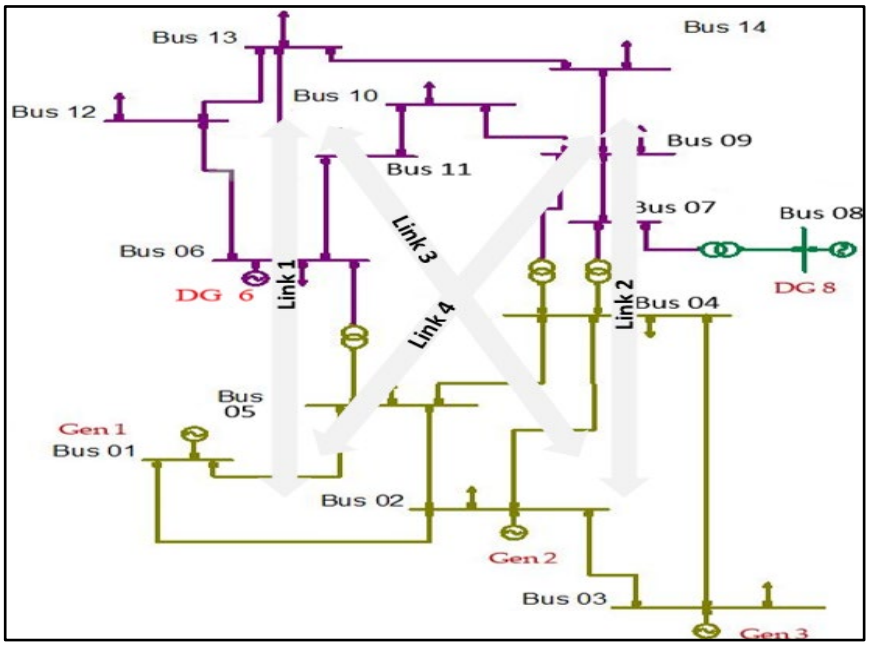

Figure 4.12: IEEE 14-bus test case

Table 4.5: IEEE 14 bus dynamic and short circuit data

Machine data					
Parameters	Gen 1	Gen 2	Gen 3	DG 6	DG 8
H (s)	6.3	10.7	3.37	2.66	2.66
X_d (%)	89.8	105	105	125	125
X'_d (%)	60	18.5	18.5	23.2	23.2
X_q (%)	64.6	98	98	122	122
X'_q (%)	64.6	36	36	71.5	71.5
T'_{d0} (s)	7.4	6.1	6.1	4.75	4.75
T'_{q0} (s)	0	0.3	0.3	1.5	1.5

Table 4.6: Synchronous generator and wind turbine parameter

SYNCHRONOUS GENERATOR					
Exciter		**PSS**		Governor	
Para meter	Value	Para meter	Value	Para meter	Range
TR (s)	0.001	KPSS	10	PD	0 - 0.1
KA	20	TW	10	T1	0.04 - 0.5
TA (s)	0.02	T1	0.29	VMax	0.5 - 1.2
KF	0.063	T2	0.02	VMin	0 ≤ 1
TF (s)	1	T3	0.5	T2	1 - 10
TE (s)	0.7	T4	0.05	D	0 - 0.5
AE	0.0006	VPSS	0.2	T3	0.04 - 0.5
TC	15	Max	-0.2	K	0.1 – 0.5
TB	10	VPSS			
KE	0.1	Min			
TE	0.5				

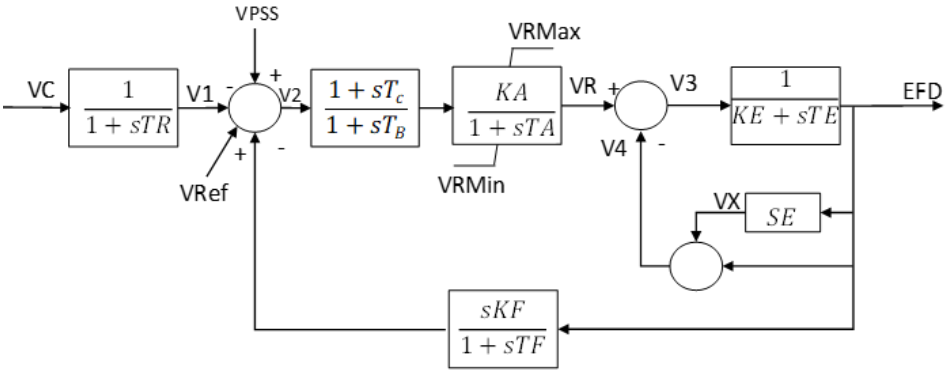

(a)

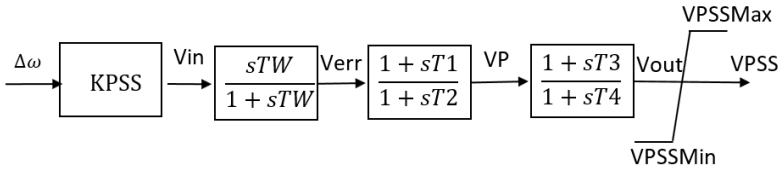

(b)

Figure 4.13: (a) Exciter IEEET1 control system; (b) Conventional PSS

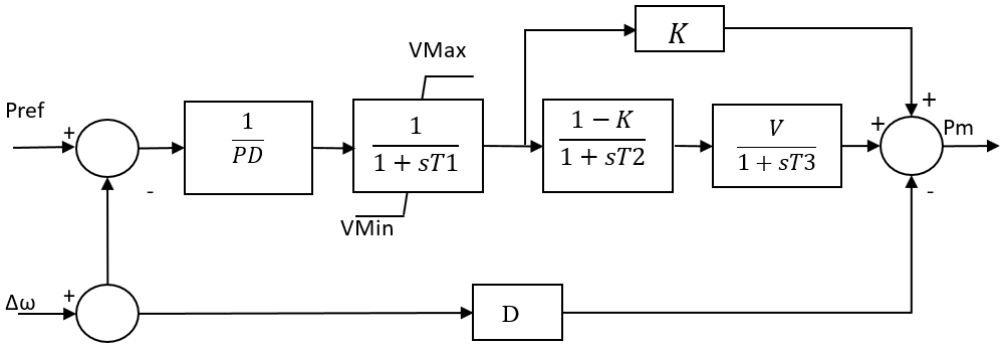

Figure 4.14: Steam turbine-Governor with fast valving- TGOV2

4.5 Results and discussion

4.5.1 Simulation scenarios and results

The transient responses of the network with two (2) DG types and five (5) different penetration levels under seven (7) different possible disturbances as described in Section 3 are discussed in this section. Figure 4.15 shows the pre-fault and post-fault conditions on the network under a three-phase short circuit fault on the highest loaded transmission line. The network with type 2 DG generates the least loadabilities, with the highest attained at 25% penetration. Types 1 DG generates post-fault loadability increments of 88.2%, while type 2 DG records a decrement of 29.5 %. The result of the network with type 2 DG also shows that the network pre-fault loadability may not always be proportional to the DG penetration level, as implied in the result of networks with types 1 DG. The average collapse voltage for the types 1 and 2 DGs are 0.66 pu and 0.70 pu, respectively, under 0%, 25%, and 75% penetration levels. Similar to the pre-fault loadability, the post-fault loadabilities for the network with type 2 DG produce the least values with a sharp decline at 100% penetration. With these pre-fault and post-fault conditions, the critical clearing angles corresponding to each DG type and penetration level are estimated as shown in Figure 4.16. The highest and least critical clearing times were obtained for the network with type 2 DG and the values remain constant between 25% - 100% of the type 2 DG penetration. The resulting critical clearing time is hereafter employed for the dynamic stability simulation of the networks. The frequency and voltage responses of the network at 0% penetration level are shown in Figures 4.17 and 4.18. A simulation scenario includes a combination of faults, types of DGs, and DG penetration levels, generating a total of 70 data instances for each scenario. The types of contingencies are shown in Table 4.4, with all faults set at 1s and cleared at 1.3s. The during-fault voltage is between 0.2 pu and 0.65 pu for all the simulation scenarios. The post-fault voltage and frequency deviations, which are strong indicators of the network's security states, are extracted to develop a classification model for security prediction. A significant proportion of the instances in all the scenarios have voltage deviations between 0.01-0.05, as shown in Figure 4.19. The highest mean voltage deviation of 0.09 was recorded for scenario 1. Scenario 4 has the least average frequency deviation with a peak of 0.011, as shown in the distributions in Figure 4.20.

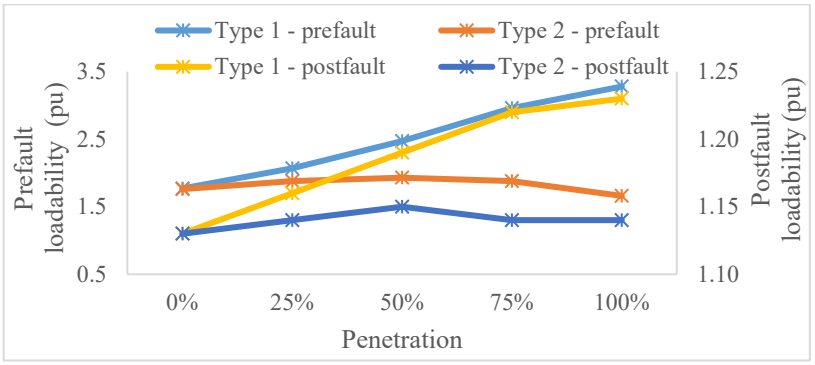

Figure 4.15: Pre-fault and post-fault loadability

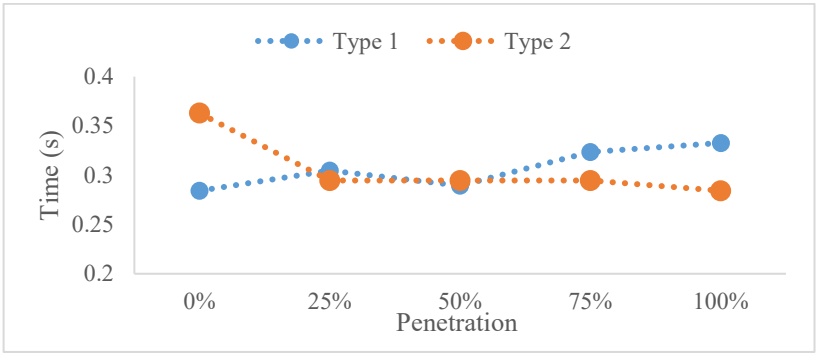

Figure 4.16: Predicted critical clearing times vs penetration levels

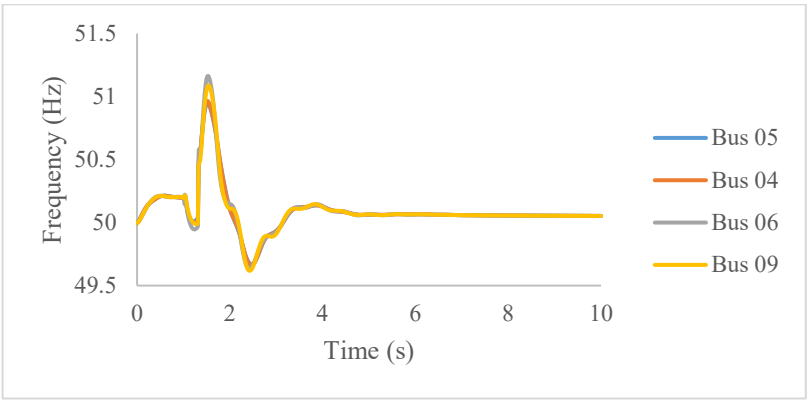

Figure 4.17: Network initial frequency response

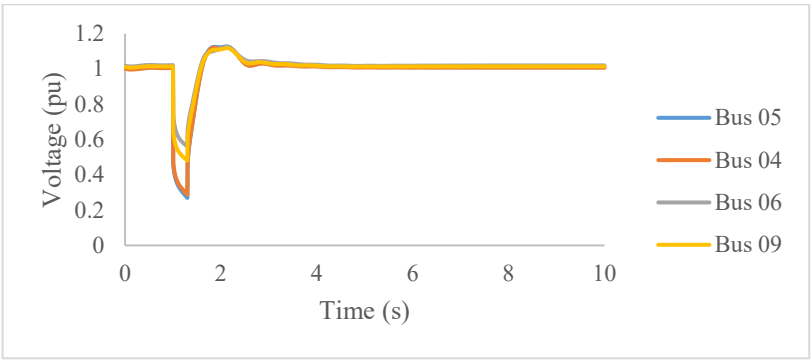

Figure 4.18: Network initial voltage response

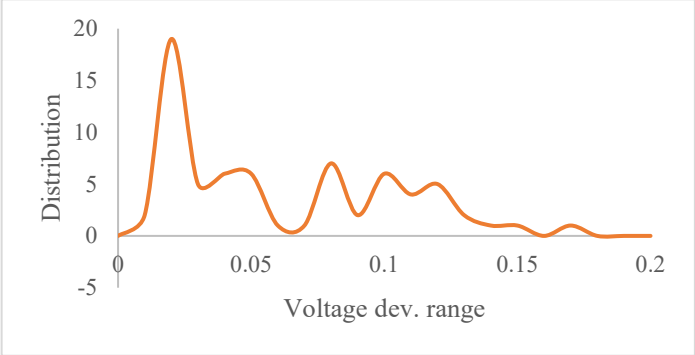

Figure 4.19: Voltage deviation distribution

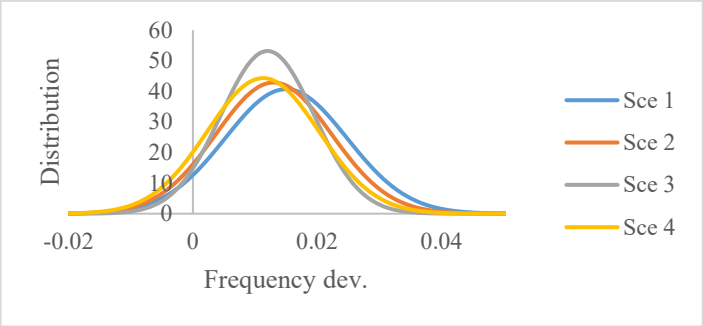

Figure 4.20: Frequency deviation distribution

4.5.2 Model training and security class prediction

From the obtained responses, 6 attributes and 70 instances for four simulation scenarios were extracted and prepared for clustering. The types of contingencies, DG types, penetration levels, and the security states are assigned nominal data types; and the voltage and frequency deviations are assigned numeric data types. The clustering model is based on pattern recognition of the post-fault voltage and frequency ranges described by IEEE standards 1346-1998 and 1547-2005, respectively. The filtering and distribution estimation of the attributes was implemented during data pre-processing. The highest and lowest ratios of secure to insecure states extracted from the networks' dynamic simulation are 1.72 and 1.12 representing scenarios 2 and 1, respectively. A three-phase short circuit fault on the transmission nodes leads to insecurity for both DG types for simulation scenarios 1 and 4. While implementing the density-based clustering, the results of the proposed EM clusterer are compared with similar clusterers: namely the K-means (KM), canopy clusterer (CC), and the hierarchical clusterer (HC). The clusterers are trained on 70% of each scenario dataset, while the remaining 30% is used for testing. The EM and CC clusterers are set up with 10 seeds, while the Euclidean distance function is adopted for the KM and HC clusterers. Figure 4.21 shows the clusters' voltage range distributions for scenario 1. The cluster formations obtained from the EM and CC clusterer are well defined compared with the KM and HC clusterers. The clusterers are consistent in terms of the mean voltage and frequency deviations for all scenarios except scenario 2. Figure 4.22 shows the prior probabilities which represent the distribution of the clusters obtained from the density-based clustering technique. The generated clusters average distribution of 57% and 43%

corresponding to clusters 1 and 2 for all the scenarios was obtained from the EM clusterer under the build time.

A classification via clustering technique is applied to evaluate the performance of the proposed density-based clusterers. Through this technique, the performance of the clustering model can be evaluated using classifier parameters. The accuracies of the proposed clusterer for the considered simulation scenarios with the other compared clusterers are shown in Figure 4.23. The accuracies of all the clusterers increase consistently from scenario 1 to scenario 2 except for the KM clusterer. The highest and lowest accuracies are obtained from the EM and KM clusterers under scenarios 4 and 1, respectively. Table 4.7 shows the average accuracy, kappa statistics, log-likelihood, and root mean square errors (RMSE) of the proposed density-based EM and the compared models. The EM model has the best accuracy as well the likelihood values for all the scenarios followed by the K-Means model when compared with the other density-based models. The number of incorrectly clustered instances extracted from the confusion matrix correlates with the accuracy of the EM model for the scenarios as shown in Figure 4.24.

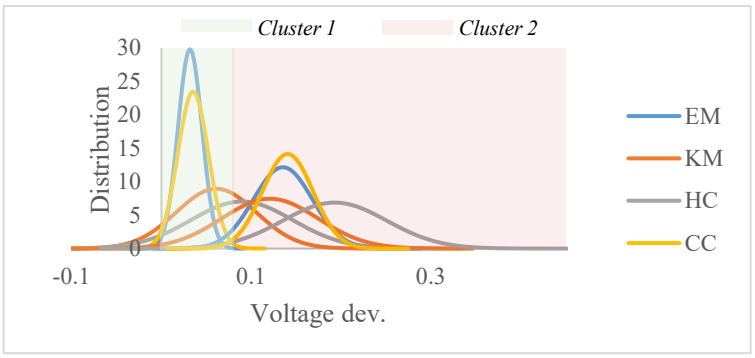

Figure 4.21: Voltage range distribution for clusters 1 and 2

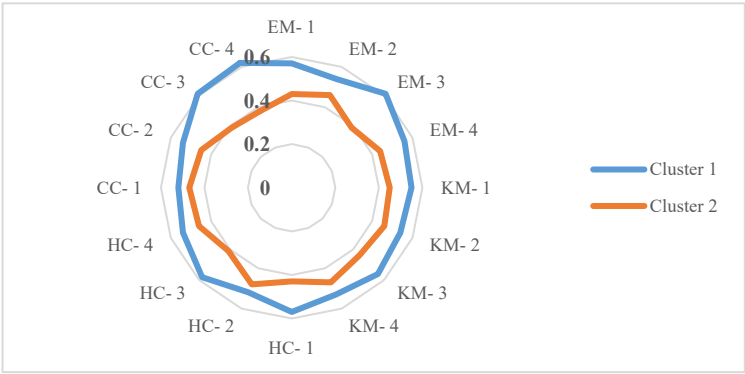

Figure 4.22: Cluster prior probabilities

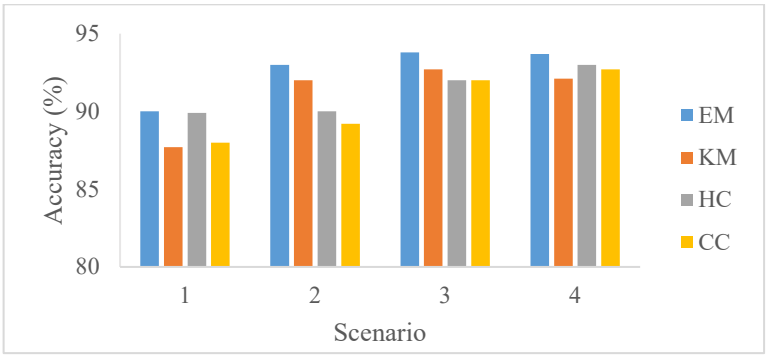

Figure 4.23: Model accuracy for network scenarios

Table 4.7: Clusterers' average performance evaluation

Models	Accuracy (%)	Kappa	Log likelihood	RMSE
EM	**92.7**	**0.93**	**-2.7**	**0.21**
KM	91.8	0.92	-2.5	0.21
HC	91.3	0.92	-2.5	0.22
CC	90	0.9	-2.18	0.22

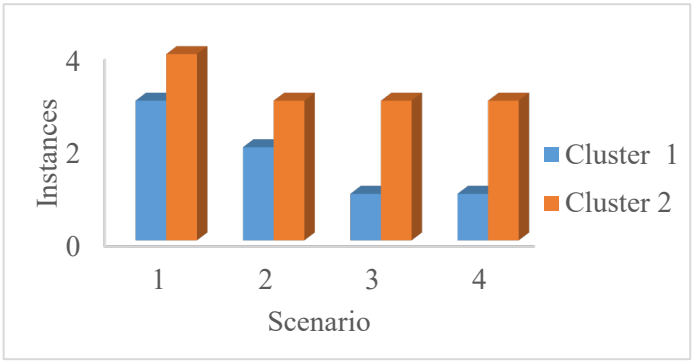

Figure 4.24: Incorrectly clustered instances

The trained Naïve Bayes classification model with the class label from the density-based EM clustering model for scenario 1 gives a mean absolute error (MAE) of 0.0078 with no incorrectly classified instance. The average prediction accuracy (APA) is 98% and the Kappa statistics is approximately 1. Figure 4.25 shows the model's average prediction accuracy (APA) when tested with seven (7) separate datasets of different instance sizes. The first test dataset (sample 1) consists of 70 instances, then the number of instances was reduced by 10 after reshuffling until the last test dataset (sample 7). Except for sample number 6 where the error is uncharacteristically small compared to the test sample size, the error margin increases with every decrease in test sample size. The comparison of the Naïve-Bayes classifier with other common classifiers showing the APA, MAE, RMSE, RAE, and the building time is presented in Table 4.8. The APAs and estimated errors of the proposed approach as well as the compared models, are shown in Figure 4.26.

The proposed Naïve-Bayes classifier performs better than the compared classifiers in terms of accuracy and errors. While the LMT model has the lowest RMSE, its average prediction accuracy of 93% is significantly lower. The proposed technique is also computationally efficient, with a build time of 0.01s. Table 4.9 compares the proposed technique with existing techniques for security

assessment of the grid, considering the accuracy, model training time and average error values. The proposed technique performs better with the highest average prediction accuracy of 98% and the least model building time of 0.01s. However, the technique proposed in [23] has the least RMSE value with a significantly high model building time. The notable advantage of the proposed approach in this paper is the capability of the classifier to adapt to the probabilistic characteristic of the power grid parameters. The attributes considered for the grid's security prediction in this paper are probabilistic. Therefore, a probabilistic classifier is more suitable for developing a predictive model. The proposed Naïve-Bayes classifier can be trained in an incremental configuration with the dataset divided into several smaller batches for online security state classification.

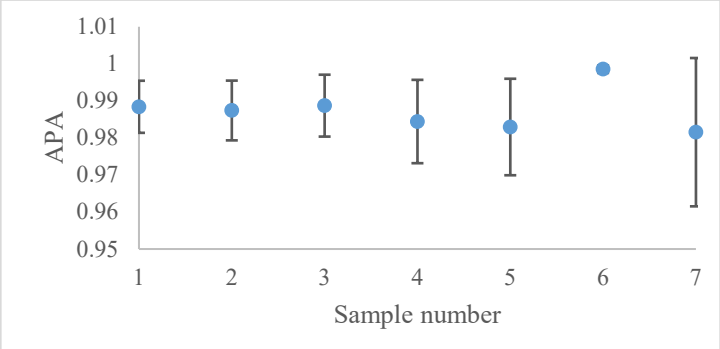

Figure 4.25: Prediction accuracy

Table 4.8: Classification model comparison

Models	APA (%)	MAE	RMSE	Build time
Naïve-Bayes	**98**	**0.0078**	**0.036**	**0.01**
Simple logistics	94	0.0104	0.106	0.084
Sequential minimal Optimization (SMO)	94.5	0.0223	0.075	0.06
Logistic model tree (LMT)	93	0.05	0.0106	0.05
Decision table	95	0.06	0.0978	0.03
Bagging	96	0.03	0.082	0.03

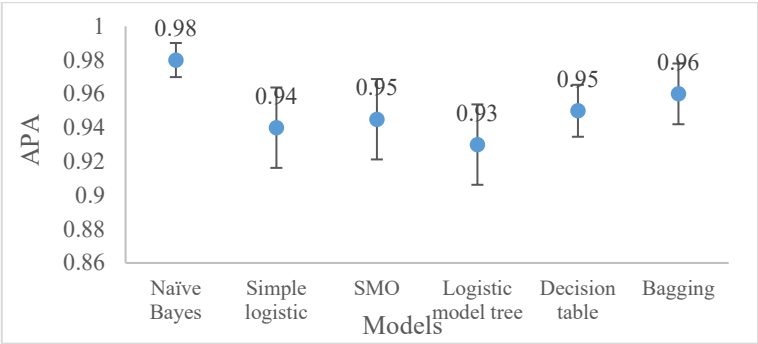

Figure 4.26: Model prediction accuracy comparison

Table 4.9: Comparison of proposed technique compared with existing techniques

Reference	Classifier	APA (%)	Time (s)	RMSE
Propose approach	Expectation maximization and Naïve-Bayes	98	0.01	0.036
[216]	Support vector machine	96.5	0.63	-
[232]	Decision tree	97.7	-	-
[220]	Decision tree and Artificial neural network	95.3	-	0.053
[15]	Neural network	95.6	1.32	0.043
[20]	Support vector machine	94.2	-	-
[224]	Ball vector machine	97.1	5.6	0.0315

4.6 Conclusions

To ensure the security of the modern grid, it is necessary to be able to predict its security considering increased RESs penetration. This paper presents an efficient machine learning-based technique for grid security state prediction. The proposed methodology involves attribute extraction from numerous transient state responses considering different DG types, penetration levels, and contingency locations. The extracted attributes (voltage deviation and frequency deviations) with the network operation and contingency scenario form the historical training dataset of four simulation scenarios with 70 instances each. Two clusters representing the network's security states were generated from this dataset using the density-based clustering technique. Afterward, a predictive model was trained from the labeled dataset using a Naïve-Bayes probabilistic classifier. The model produced a high APA and low MAE of 98% and 0.78%, respectively, with a very short model training and building time of 0.01 seconds. The model testing results with seven different datasets with varying instance sizes present an average MAE of less than 1%. The results show that the proposed EM and Naïve-Bayes models perform well compared to similar machine learning models. Finally, this paper has demonstrated the feasibility of employing the attributes extracted from the transient response for the security prediction of the modern grid, considering varying DG penetration levels.

While the proposed approach in this paper can predict the grid's critical clearing time and security state through dataset clustering and classification techniques, few limitations have been identified. For easier data clustering and due to the capability of the Naïve-Bayes algorithm, the DG penetration level is designated as nominal. The nominal data structure of the DG penetration level enhances the difficulty of identifying the grid security state between two distinct RES-DG penetration levels. Also, the proposed technique relies on data clustering, therefore, it is heavily dependent on a large dataset which in turn may increase the total model build and deployment time. Future research from this paper may focus on estimating the load shed value and RES-DG penetration level during insecure prediction or prediction algorithm failure. It is also important to assess how the incremental alternative of the clustering and classification algorithms impacts the security prediction while reducing the training time as the dataset increases. The result in this paper is based on the type III wind turbine system. The impact of the other wind farm types (asynchronous, full converter, etc.) on the grid's security

response may be investigated for future research. The deployment of the proposed model as an executable software for system operator utilization after being evaluated for robustness and scalability is also a good consideration for future research.

5 Manuscript 4: Online Security Prediction

Preamble

Prior knowledge of the grid's security state for the proposed operation scenario is crucial for modern grid operation. Offline prediction models require significant data storage and models need to be trained again each time a new set of data is available. This chapter presents a framework for online security state prediction using an incremental machine learning algorithm. With an incremental training technique, the performance of the previous model is improved by the new data set, thereby improving the model's accuracy. The model may be deployed for prediction at any stage of training, making it suitable for real-time security state predictions. As demonstrated in this chapter, prior information on the grid's security state is essential for planning and security control of low inertia grids. Therefore, Chapter 5 proposes a Gaussian process-based load shedding technique for the intelligent security control system. The proposed intelligent security control helps estimate the required load shed to ensure the security of predicted, planned operating scenarios. Furthermore, the method introduces a prequential model training technique that improves the accuracy of the incremental Naïve-Bayes models. Compared to other security prediction methods in the literature, the presented method can predict the security state of the grid with varying grid attributes and determine the optimal node for load shedding to ensure the grid's security ahead of time.

An online security prediction and control framework for modern power grids

ifedayo Oladeji*, Ramon Zamora and Tek-Tjing Lie

Department of Electrical and Electronic Engineering, Auckland University of Technology, Auckland 1010, New Zealand

Abstract: The proliferation of renewable energy sources distributed generation (RES-DG) into the grid results in time-varying inertia constant. To ensure the security of the grid under varying inertia, techniques for fast security assessment are required. In addition, considering the high penetration of RES-DG units into the modern grids, security prediction using varying grid features is crucial. The computation burden concerns of conventional time-domain security assessment techniques make it unsuitable for real-time security prediction. This paper, therefore, proposes a fast security monitoring model which includes security prediction and load shedding for security control. The attributes considered in this paper include the load level, inertia constant, fault location, and power dispatched from the renewable energy sources generator. An incremental Naïve Bayes algorithm is applied on the training dataset developed from the responses of the grid to transient stability simulations. An additive Gaussian process regression (GPR) model is proposed to estimate the load shedding required for the predicted insecure states. Finally, an algorithm based on the nodes' security margin is proposed to determine the optimal node(s) for the load shedding. The average security prediction and load shedding estimation model training times are 1.2s and 3s, respectively. The result shows that the proposed model can predict the security of the grid, estimate the amount of load shed required, and determine the specific node for load shedding operation.

Keywords: Security, Incremental machine learning, Renewable energy sources, Distributed generation.

*Corresponding Author: Tel.: +64225331241
E-mail address: ifedayo.oladeji@aut.ac.nz

5.1 Introduction

The emerging grid is used to describe the future power system with a clean, affordable, sustainable energy generation and delivery system. The emerging grid is also characterized by high efficiency and reliability achievable through the accompanying components such as renewable energy sources distributed generation systems (RES-DGs). There has been a concerted effort to enhance the emerging grid to accommodate high penetration levels of RES-DGs as the power grid moves to a carbon-less grid. To deliver a reliable resilient and secure grid, the power grid requires intelligence to sense, assess and predict the security state of the grid [257]. The rapid transition

towards a more active and intelligent grid will help to achieve high RES-DG penetration, improved security, and reliability. As the emerging grid evolves to accommodate the increasing integration of RES-DGs and energy storage systems (ESS), it is essential to ensure its security through security analysis and prediction.

Figure 5.1 shows the emerging power grid with several components related to the generation, control and utilization of energy. These components may be categorized into smart generation, smart transmission, smart distribution, and smart communication systems [258]. The smart generation is strongly linked to decarbonization and digitalization since the grid will contain a mix of large and small RES-based generation units. The smart generation also considers the microgrid model where active customer (prosumers) generates power through the distributed generation together with storage systems and transfers the surplus power generated to the grid [48]. The smart distribution system is based on the adoption of advanced distribution management technologies that will help optimize distribution network operations and increase network resiliency. The use of smart meters is also critical for energy usage monitoring and management. Smart distribution is the most recent notion, and it entails putting in place managerial measures. Smart distribution's most recent concept is the use of managerial strategies to develop resources on the demand side by influencing load demand. The goal of smart communication systems is to eliminate information asymmetry and hence improve supply reliability. Power line communication technology, which allows bi-directional communication over existing power lines, is a key technology to achieve this goal [150].

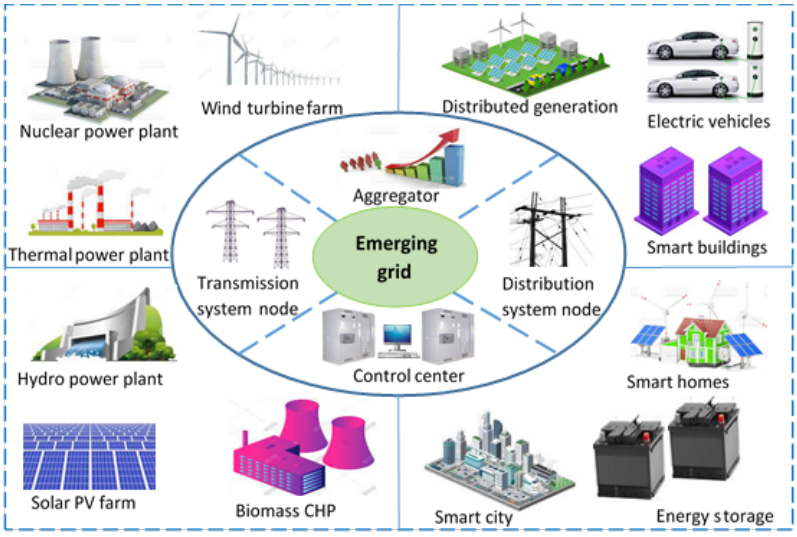

Figure 5.1: Emerging power grid with RES-DG units

System security has been defined by system regulators and operators for decades as the ability of the grid to withstand sudden and disturbances such as short circuits or unexpected network elements losses due to natural causes. Under this definition, the grid's security can be evaluated under static security through voltage and thermal limits and under dynamic/transient security through voltage, angular, frequency stability studies [259]. The assessment of grids' security under the impact of disturbances and unexpected network elements losses using these limits and stability studies may be regarded as a conventional security assessment. However, in modern grids with several Internet

of Things (IoT) devices and wide area network controls, the focus of security assessments has been expanded to include cybersecurity assessment of the cyber-physical grid. The assessment of the cyber-physical grid security includes estimating the impacts of feasible cyber-physical attacks, evaluating the grid's dependency on its cyberinfrastructure, and assessing the ability of the grid to tolerate potential failures due to the cyberinfrastructure [260]. Comprehensive security assessment for the modern grid will be performed under the conventional security and cybersecurity assessments. However, the security state of the grid due to the impact of either the traditional disturbances or cyberattacks remains classifiable into the secure, insecure, and asecure states as given by Liacco [21].

As more renewable energy sources distributed generations (RES-DGs) are added to the grid, the existing synchronous generators are disconnected and decommissioned. Since the RES-DGs do not support the grid with any significant mechanical inertial energy, the grid's resultant inertia constant is therefore notably reduced under high penetration of RES-DGs [6]. At reduced inertia, the steady-state operation of the grid may be secure since the disturbance is usually small and gradual. However, during fault conditions and large changes in load, the security of the grid may not be guaranteed. The insecure state is consequential to the grid not having sufficient inertial energy to withstand the perturbation during the period of the fault or large change in load. In addition to the inertia constant challenge of RES-DGs, variability, and intermittency of the power generation from RES-DGs, may be compromised the reliability of the grid at high penetration levels [261].

The deployment of data acquisition devices within the grid enables the generation of enormous data related to the state of the grid. Recent research has been focused on the application of machine learning techniques to identify patterns within the generated data to predict the security of the grid. Machine learning techniques are basically of two types, batch, and incremental learning techniques. In real life application environment, machine learning is implemented as a repetitive process. A trained model is obtained using an appropriate algorithm on a preprocessed training dataset. If model performance is satisfactory, predictions of the class of new instances from the test dataset can then be obtained using the trained model [262]. The old (training) and the new (testing) datasets may then be combined to generate a new and larger dataset. Under the batch machine learning process, the predictive model needs to be retrained using the new and larger dataset. The performance of the latest model does not depend on the former model [263].

With the rapid deployment of data acquisition devices, the modern power grid will continue to generate a large amount of data in short time intervals. The models developed from the batch training modes are often discarded when a new model is obtained. There are several challenges associated with developing a batch machine learning model from a large dataset considering the continual increase in the dataset volume. To begin with, the time required in retraining a model from the combination of the old and new datasets is a significant challenge. The training time is proportional to the volume of the data. Consequently, the time lost between model retraining and deployment impacts the model user experience. In addition, the challenge of large memory requirements for the storage of the data for future applications will also be considered. The

incremental learning process provides a solution to these challenges [264]. With batch training algorithms, the obtained classification model is seamlessly updated with new instances. The capability to effortlessly update the incremental machine learning models make them more suitable for real life and online applications [265].

Many security predictions and control strategies have been proposed for the grid with and without considerations of the penetration of RES-DGs. One of the recent strategies is the application of a suitable machine learning algorithm to the existing dataset containing the historical security information of the grid. These machine learning-based prediction techniques have been implemented in [14, 213, 266, 267]. These techniques have shown their effectiveness to predict the security of the grid in case of transient security [14], frequency deviation [213], and distance to insecurity [268] without considering the penetration of any type of distributed generation into the grid. The techniques were based on only one system variable (voltage [14, 266-268], frequency [213]). Considering the grid with high penetration of RES-DG, the proposed techniques may not be applicable under changing inertia and system loading. Batch machine learning-based techniques were proposed in [217, 225]. Batch models may not be effective for real-time security prediction considering the time required to retrain the model when new data is available. For real-time security prediction capability, an incremental model which requires less amount of data for initial training is more effective.

Many existing techniques for security control in recent literature are based on restorative actions aimed to restore the system from the unstable to the normal state. Refs. [269, 270] present cases with primary responses while [239, 271] proposed techniques for secondary responses for frequency control. Models based on virtual power plant (VPP) application were proposed in [272, 273], synthetic inertia techniques were developed in [274, 275] and fast frequency response (FFR) control methods using backup generators were proposed in [276, 277]. The VPP and FFR controls require complex algorithms, which are made more difficult by the significant penetration of RES-DG in the grid.

Considering the existing methods for under-frequency control due to the substantial variance in generation and load, demand-side contribution with load shed have been effective to ensure quick system recovery grids frequency [24, 278]. To estimate the load shed required for frequency recovery, conventional analytical and optimization techniques [8, 279, 280], adaptive techniques [281, 282] and meta-heuristic techniques [283, 284] have been proposed. Although the existing methods can estimate and predict to a reasonable degree of accuracy the load shed required to ensure the security of the grid through frequency control, the determination of the optimal load shed nodes were not discussed. Also, most of the existing techniques are developed based on the relation of the grid's power imbalance, the rate of change of frequency (ROCOF), and the frequency nadir, therefore the applicability of the techniques to a grid under varying attributes is highly doubtful. Furthermore, as synthetic inertia techniques for supporting conventional inertia in low inertia grids become more popular [285], it is necessary to anticipate the security of the grid for a specific level of inertia. Table

5.1 shows a summary of existing techniques in recent literature for the security assessment and prediction of a power grid.

Table 5.1 Literature review summary

References	Main objective	Approach	Main predictor(s)
[267]	Short-term voltage stability online prediction	Online	Voltage magnitude
[14]	Transient stability prediction	Offline	Rotor angle
[225]	Framework for transient stability prediction	Offline	Rotor angle
[286]	Prediction of the transient Stability Boundary	Offline	Voltage magnitude and rotor angle
[20]	Static security assessment	Offline	Voltage magnitude
[17]	Security assessment for multiple contingencies	Offline	Voltage magnitude
[21]	Power systems security assessment	Offline	Voltage magnitude
[266]	voltage stability prediction	Online	Voltage magnitude
[19]	Online static security Assessment	Online	Voltage magnitude and angle
[18]	Online transient stability prediction	Online	Voltage magnitude and rotor angle

Security predictors in existing frameworks and techniques have largely been determined by changes in system load and generation. These determinants are effective for conventional grids with insignificant penetration of non-synchronous generators. However, to achieve effective security prediction for the modern and emerging grid, there is a need to extend the predictor determinants to include varying parameters critical to the grids with high penetration of non-synchronous generators. Consequently, it is important to develop a method to achieve fast security prediction and control that takes into consideration changes in inertia, generation levels from renewable energy systems, and network contingencies. Hence, the contributions of this paper include:

- demonstrating the feasibility of security prediction using a time-varying system's deterministic and probabilistic attributes,
- developing a model using an incremental Naïve-Bayes algorithm for online security prediction for the emerging grid,
- proposing a gaussian process regression load shed estimation method to ensure the security of the predicted insecure network operation instances and,
- proposing a voltage security index ranking technique for optimal load shed node(s) selection.

This paper is focused on the emerging grid with variable penetration levels of RES-DG units which will result in varying inertia constants of the grid. The proposed model is based on an incremental Naïve Bayes classification algorithm for security prediction based on the rotor angle

response obtained from the transient stability assessment of the network to a three-phase short circuit fault. The attributes considered for the classification are inertia constants, the system loadings, the RES-DG power generation, and the fault location within the grid. An additive Gaussian process regression (GPR) model using the Pearson Universal kernel (PUK) is developed to estimate the amount of load shed required to ensure the security of the insecure predicted network instances. In conclusion, the suitable node (s) for the load shedding is determined using a ranking algorithm based on the node loads and voltage security margins.

The rest of this paper is organized as follows. Section 5.2 discusses the impact of high penetration of RES-DG units on the power grid as well as the security modeling and assessment of the integrated transmission and distribution network considering time-changing inertia. Online machine learning with the proposed incremental classification algorithm and intelligent security control are presented in section 5.3. Section 5.4 contains the results and discussions obtained from testing the proposed techniques on the IEEE 39 bus network, while the conclusions are presented in section 5.5.

5.2 System Security and Inertia Constant Modelling

5.2.1 RES-DG units and time changing inertia

More fossil fuel-based synchronous generators will be made redundant as the penetration of RES-DG units increases. The RES-DG units are connected to the grid through electronic converters, therefore they do not supply mechanical inertia to the grid. The frequency of the power grid is controlled by the inertia supplied by synchronous generators within the grid. At low penetration of RES-DG into the grid, the frequency response may not be significantly impacted. However, as the RES penetration level increases, frequency stability and power oscillations within the grid under disturbances becomes a challenge. Attempts have been made to estimate the instantaneous RES-DG penetration level beyond which the grid frequency may fall below the security range after a disturbance.

Traditionally, the inertial response from the synchronous generator is an inherent characteristic, and it is not treated as an ancillary service. However, with the increase in penetration of RES-DG, the grid operators in several power systems have identified inertia as an ancillary service [287]. From the grid operator's perspective, the grid can be categorized as a high and low inertia grid depending on the penetration level of RES-DG. A grid with low penetration of RES-DG is referred to as a high inertia grid and a grid with a high penetration of RES-DG is described as a low inertia grid. Figure 5.2 shows the frequency responses of the grid under high and low inertia values. Under low inertia values, the frequency Nadir and the rate of change of frequency (ROCOF) are both increased. Also, more oscillations are experienced by grids with low inertia values before attaining stability.

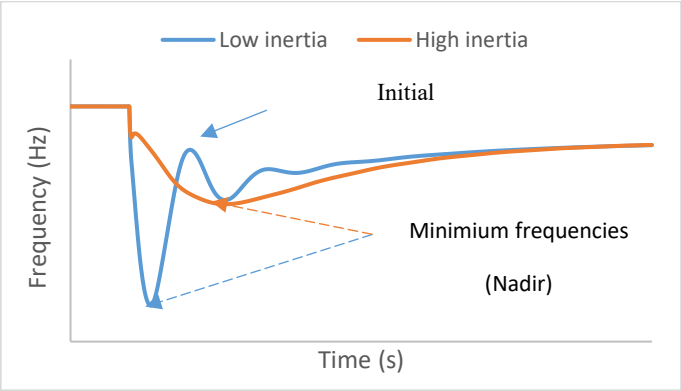

Figure 5.2: Frequency response under varying inertia

Considering the rapid proliferation of RES-DG units into the grid, it is therefore important to be able to predict the security of the grid under changing inertia values. The equivalent inertia constant (H_{eq}) for a grid at a particular time can be derived as shown in (1) and (2).

$$H_i = \frac{E_k}{S_{r,i}} \tag{1}$$

$$H_{eq} = \frac{\sum_{i=1}^{N} H_i \times S_{r,i}}{S_B} \tag{2}$$

where H_i is the inertia of the $i-th$ synchronous generator, $S_{r,i}$ is the rated apparent power of the $i-th$ synchronous generator, E_k is the total rotational kinetic energy stored in the grid, S_B is the base power of the grid, and N is the total number of synchronous generators connected to the grid.

5.2.2 Power system security modeling and assessment

System security is defined as the ability of the system operating point to remain within the secured zone in which any of the constraints are not violated under dynamic and transient conditions [288]. According to IEEE standard 1547.1-2015 [289], the operation of RES-DGs within a grid should not result in the insecurity of the grid. Consequently, at high penetrations of RES-DGs, the grid should be able to remain in a secure state during and after the occurrence of contingencies. Any constraints violations leading to insecurity during and after the occurrence of a contingency should be confined to an area within the grid. The constraints under which the security can be assessed are developed based on the system variables of concern. As shown in Figure 5.3, a, b, c, and d may represent the node voltage, rotor angle, frequency, and current limits for the $i-th$ operating point for the system under contingencies. The $i-th$ operating point is represented by the dots along the trajectory of each variable at a specific time. The operating points represented by the different coloured dots move from the secure state (green colour) to the insecure state (red colour). Depending on several factors, including the type of contingency, a network may have operational points in different security states at the same time. However, it is common to have the system variable operating points existing in the same security state.

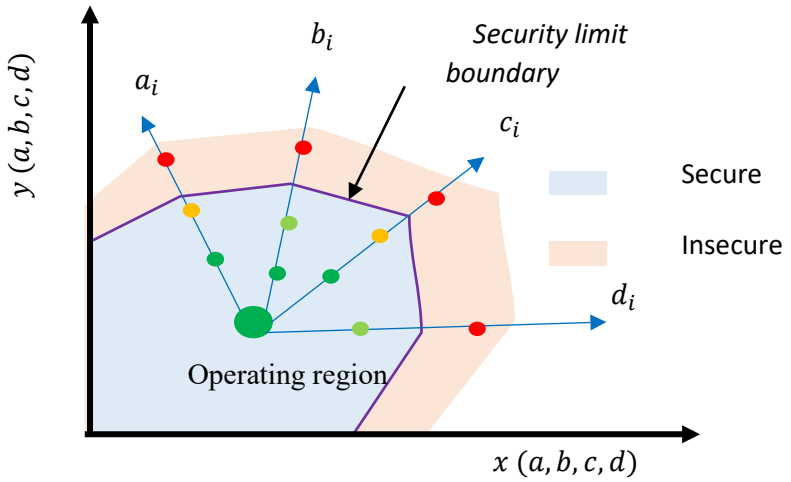

Figure 5.3: System security region modeling

As stated earlier, the security state of a network may be assessed using several network variables including the post contingency voltage and frequency values as well as the rotor angle response of the synchronous machines. During contingencies, the values of network variables are allowed to deviate over a specified security limit. However, to achieve a new security state, the grid's frequency and voltage must return to the initial values while the rotor angle settles at a new stability point. The security of the grid largely depends on the dynamic parameters of the generators, transmission system, and load. The general steps to security assessment include contingency screening, contingency ranking, and security assessment using appropriate indices.

5.2.3 System modeling for transient stability assessment

A disturbance within a grid caused by a fault or sudden change in load leads to the exchange of stored kinetic energy between the system's synchronous generators. The result is a change in the speed of each generator. Since the change is different for each generator, the generators swing relative to each other and relative to the reference generator in the grid causing the flow of synchronizing power among the generators. Faults within a section of the grid create large disturbances within the boundaries of such grid section. The fault may be due to but not limited to equipment malfunction, human errors, natural disasters, and attacks. The effects of the disturbances may spread across the whole grid if quick action is not taken. It is, therefore, the responsibility of the grid operators to ensure the reliability of the power supply considering the possibility of disturbances.

The general model used to ensure reliability is to anticipate and assess the fault conditions through transient security studies, and implement appropriate methods to limit the impact of the disturbances. The model of the power grid is based on the synchronized operation of several generators connected in parallel within the grid. If the synchronization criteria are met, generators can be readily added and removed, depending on the situation of the grid. To elaborate, the degree of security of the grid depends on the size of the generators, the locations of the generators within

the grid, the transfer capacity of the transmission network, the load distribution, and the type of disturbance.

The relative swinging of the synchronous generators to each other and the reference generator is due to the non-uniformity in sizes and other dynamic parameters such as the inertia constant. Synchronism is lost when the swing of one or more synchronous generator(s) is beyond control; hence, the generator is said to be out of step. To avoid grid collapse, the out-of-step generator must be swiftly disconnected from the grid through the protection devices. The ability of the system to remain in synchronism after the occurrence of a fault is assessed under transient security studies. Considering the dynamic model of the synchronous machines, the grid can be represented by differential-algebraic equations models using the $d-q\ axis$ model [290].

$$T'_{doi}\frac{dE'_{qi}}{dt} = -E'_{qi} - (X_{di} - X'_{di})I_{di} + E_{fdi} \tag{3}$$

$$T'_{qoi}\frac{dE'_{di}}{dt} = -E'_{di} + \left(X_{qi} - X'_{qi}\right)I_{qi} \tag{4}$$

$$T_{avi}\frac{dE_{fdi}}{dt} = -E_{fdi} + K_A(V_{ref} - V) \tag{5}$$

where T'_{di} and T'_{qi} are the open-circuit time constants in the d and q axis, respectively; E'_{di} and E'_{qi} are the d-axis and q-axis transient voltages; X_{di} and X_{qi} are the d and q synchronous reactances; X'_{di} and X'_{qi} are the d and q transient reactances; E_{fdi} is the excitation system voltage; I_{di} and I_{qi} are the d and q armature current, respectively; T_{avi} is the voltage regulator time constant, K_A is the voltage regulator gain, V_{ref} is the reference voltage and V is the generator terminal voltage. If ω_i is the $i-th$ synchronous generator rotor angular speed, ω_s is the synchronous angular speed of the grid, P_m is the synchronous generator mechanical power, P_e is the synchronous generator electrical power, then the rotational dynamics of the synchronous generators' rotor is given by (7) and (8).

$$\frac{d\delta_i}{dt} = \omega_i - \omega_s \tag{6}$$

$$\frac{2H_i}{\omega_s}\frac{d\omega_i}{dt} = P_m - P_e - D_i(\omega_i - \omega_s) \tag{7}$$

where δ_i is the rotor angle of the $i-th$ synchronous generator. If R_{ai} is the armature resistance, then the synchronous generator stator can be modeled using the algebraic equations given by (9) and (10).

$$E'_{qi} - V_i cos(\delta_i - \theta_i) - R_{si}I_{qi} - X'_{di}I_{di} = 0 \tag{8}$$

$$E'_{di} - V_i sin(\delta_i - \theta_i) - R_{si}I_{di} - X'_{qi}I_{qi} = 0 \tag{9}$$

5.3 Online Security Prediction

This section describes the steps involved in the development and deployment of an online machine learning model. As shown in Figure 5.4, historical training data is obtained through recorded

real-life operations and responses to significant events such as three-phase short circuit fault. Historical training data can also be represented by the responses of the network to several transient stability simulation scenarios using an appropriate simulation tool. The training dataset is then preprocessed to determine attribute suitability and impact on security (class of dataset) through filtering and/or correlation. A suitable machine learning algorithm is selected and then applied to the training dataset. The suitability of an algorithm for a classification model depends on several factors which include the data types, storage availability, type of training (batch or incremental). The step-by-step operation of an online prediction model is shown in Figure 5.4. Since the model in the paper is intended for online security prediction, this paper focuses on the incremental Naïve Bayes classification algorithm.

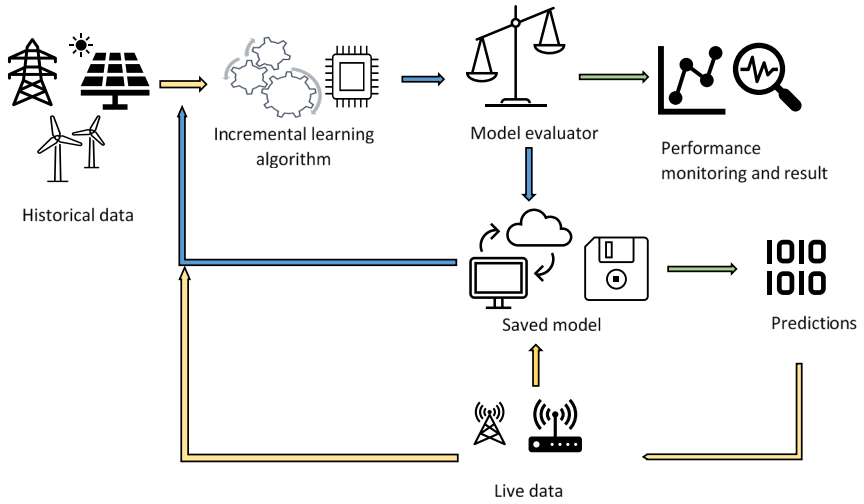

Figure 5.4: Online system security modeling

The performance of the incremental model is evaluated at each training step. In a classification problem, a model with high accuracy (α) and low misclassification rate (β) is desirable. If N_c is the total correctly classified instances in the stream of the dataset, N is the total instances in the stream of the dataset, N_m is the number of misclassification in the $k-th$ and Nk is the total number of instances in the $k-th$ class [20], then the accuracy and misclassification of a model can be evaluated using (11) and (12).

$$\% \, \alpha = \frac{N_c}{N} \times 100 \tag{10}$$

$$\% \, \beta = \frac{N_m}{Nk} \times 100 \tag{11}$$

The approach proposed in this paper involves transient security assessment under varying system parameters and grid operation points. The methodology proposed in the section above is focused on the prediction of the security of the grid for a given grid operating point. The knowledge of the security state of the grid using past and present data is required to determine techniques to ensure the security of the grid. The steps for the online security prediction and control technique proposed in this paper are described in the flowchart in Figure 5.5. The integrated transmission and

distribution network is modeled with a suitable automatic voltage regulator, power system stabilizer, and governor control for transient stability assessment with the necessary controllers for the RES-DG units. Transient stability assessment is performed on the grid to determine its response to three-phase bolted fault. The transient security assessment is performed several times using varying network parameters and grid operation points to obtain instances for the training dataset. The variable network parameters and grid operation points are regarded as the attributes of the training dataset and include the equivalent inertia constant, the load level, the aggregated RES-DG units output, and the fault distance. To optimize the model's accuracy and performance, the incremental Naïve-Bayes based-model training is carried out using the continual learning approach. With continual learning, the model can autonomously relearn from a stream of data and adapt automatically as new data is available to improve accuracy and performance.

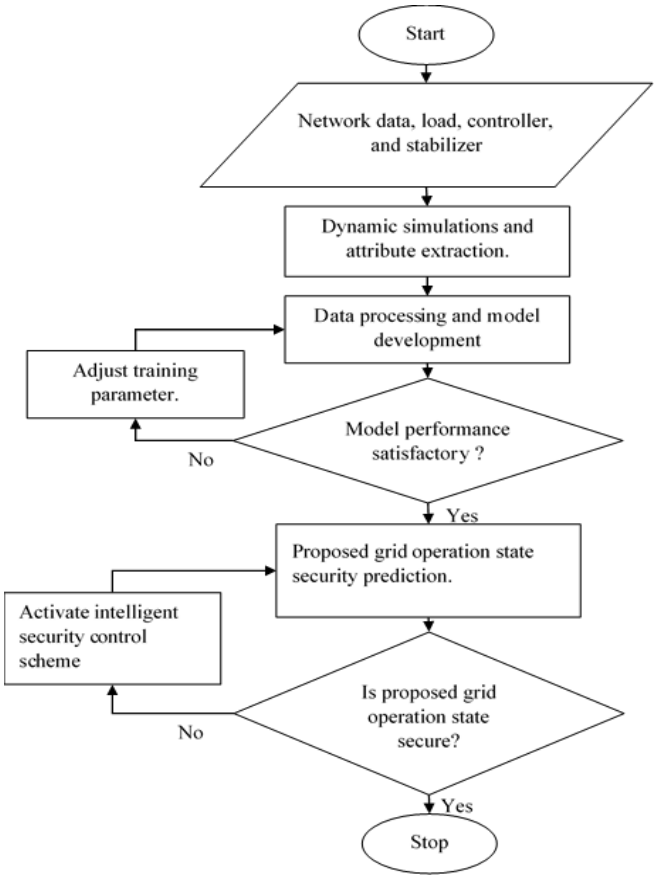

Figure 5.5: Proposed security control flowchart

The continually trained model is saved after the best obtainable accuracy is obtained. The obtained Naïve- Bayes security prediction model is ready for deployment at any stage of the training between each data streams. If the security state prediction of the model to a proposed system operating state (live data) is correct, the predicted security state with the system operating state is afterward considered as historical data and used to improve the performance of the model. For the predicted insecure states, a regression-based model is proposed to estimate the amount of load shed required to ensure the security of the grid. Also, an algorithm to determine the optimal node for load shedding is proposed.

5.3.1 Online machine learning model development

Online security prediction is the response to system operation state given the knowledge of the true security state of previous operation states and, possibly, the availability of additional information. Online prediction models imitate the ability of humans to give responses and make rational decisions in an intelligent and programmed manner using basic everyday attributes. An online prediction model is used to predict the outcome of successive instances. In this paper, a binary classification model to predict whether the grid is secured or not using specific grid attributes is proposed. After the proposed grid event (instance), the true security response is received as feedback from the grid. Using this feedback, the difference in the precision of the prediction and the true security state can be measured. Based on the precision difference, the model is updated to improve predictive performance for future predictions. If w is the classification model and N is the number of training rounds for the model, then the steps for the development of an online binary classification model can be summarized as below [291]:

1. Initialize the prediction function, F_1,
2. Receive new instance: $x_t \in R$; where $t = 1, 2, 3 \ldots T$,
3. Predict class $y_t = F_t X_t$, for x_t,
4. Obtain true class label: $y_t{}^* \in \{secure\ , not\ secure\}$,
5. Measure the loss suffered: $l_t(F_t)$,
6. Update model from w_t to w_{t+1}.

The number of classification mistakes made by online learning algorithm can be measured using (15). The performance of an online algorithm is measured by the cumulative loss it suffers during the run of the T sequences. The objective of the online learning task is to minimize the regret function of the model's predictions against the best-saved model before the present prediction task as defined in (16). Assuming that the true responses are generated by an unknown but fixed hypothetical factor g, such that $y_t = g(x_f)$ for all $t \in T$, the cumulative loss of g over an entire sequence is zero and is independent of T. The loss function in this paper is formulated as an online convex optimization (OCO) problem with respect to w and is defined as (17).

$$M_T = \sum_{t=1}^{T} (y_t{}^* \neq y_t) \tag{12}$$

$$R_T = \sum_{t=1}^{T} l_t(w_t) - \min_{F} \sum_{t=1}^{T} l_t(w) \tag{13}$$

$$f_{c-t} = l\big(g_w, (x_t, y_t)\big) \tag{14}$$

where w is the classification model, l_t is the loss suffered by the optimal model. It is important to note that w_t can only be known after the examination of all the instances and their class labels.

5.3.1.1 Incremental Naïve-Bayes model

The incremental Naïve-Bayes algorithm is used to realize the online classification model in this paper. The basic idea of the incremental Naive Bayes algorithm is to calculate a posterior probability based on the prior probability and new data [292]. The ability of the incremental Naive Bayes classification algorithm to support online learning is due to its leverage on and exploitation of prior information of the datasets. The structure for the incremental Naïve- Bayes algorithm is shown in Figure 5.6. The posterior probability is estimated from the prior probability and existing data. The predicted posterior probability will then become the new prior probability for the next learning batch [293, 294]. Subsequently, the incremental learning algorithm saves the updated prior probability as knowledge. To achieve unification of knowledge when new data is received, incremental learning algorithms estimate a new knowledge for the new data based on the old knowledge. The classification accuracy and precision are improved by adjusting the prior probability.

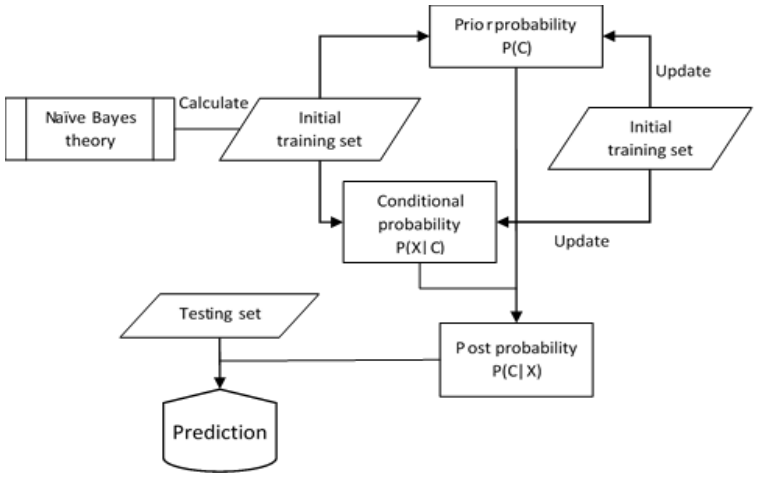

Figure 5.6: Incremental Naïve Bayes learning model

The post probability $P(C|X)$ is the probability of an instance belonging to class C. The conditional probability $P(X|C)$ is the likelihood of a specific class occurring, based on the occurrence of a previous instance. The class prior probability $P(C)$ is the estimate of the probability that a randomly sampled instance from a dataset will yield a given class notwithstanding the attributes of the instance. If $X = [A_1, A_2, .., A_n]$ is a sample dataset with n attributes, then, the post probability from the traditional Naïve Bayes principle can be evaluated from (19).

$$P(C|X) = \frac{P(X|C)P(C)}{P(X)} \tag{15}$$

If $C_1, C_2, \dots, C_m$ denotes the m different possible classes, then for each dataset X, the post probability $P(C_j|X)$ is evaluated using the prior probability $P(C = C_j)$ and conditional probability $P(X|C_j)$ as given in (20).

$$\frac{P(X|C_i)P(C_i)}{P(X)} > \frac{P(X|C_j)P(C_j)}{P(X)} \tag{16}$$

where $P(C_i|X) > P(C_j|X) \dots \dots 1 \leq i \neq j \leq m$.

From Figure 5.6, it is shown that the process of updating the incremental learning of the Naïve Bayes classifier is a recursive Bayesian estimation of parameters. Its advantage is that information in initial training data is preserved in the form of parameters. During the incremental learning process the initial training data can be discarded to conserve memory since the information contained in the initial training set has been stored in the form of two key statistic parameters; the class prior probability and the conditional probability. Suppose X^* is the new testing dataset and $X^* = [A_1, A_2, .., A_n]^* \in M$ are the new instances for updating the prior and conditional probabilities, then the model for updating the class prior probability is given in (21).

$$\varphi_j = \begin{cases} \frac{\tau}{\tau+1}\varphi_j + \frac{1}{1+\tau} & when\ C_d = C_j \\ \frac{\tau}{\tau+1}\varphi_j & when\ C_d \neq C_j \end{cases} \tag{17}$$

where ${C_d}^*$ is the class label, $\varphi_j = P(C = C_j)$ is the class prior probability of class label C_j, $\tau = n + m$, n is the number of instances in the initial training set N, m is the number of instances in the new training dataset M.

The performance of incremental Nave-Bayes models is assessed using specified metrics, similar to the traditional Nave-Bayes models. Generality, accuracy, learning rate, classification costs, and storage requirements are some of the common metrics. This paper, however, focuses on the accuracy evaluation metrics which can be expressed using the precision (Pre), recall (Rec), and F measure (Fm) as shown in (22) to (24). The precision of the model is the proportion of the predicted security state from the dataset that is correct, the recall is the proportion of the dataset that is correctly classified. Occasionally, the precision or recall may not truly represent the properties of a model. Consequently, the F-Measure is employed to combine the recall and precision into a single metric that effectively captures the performance of the model as given in as given in (21) [295].

$$ACC\ (\%) = \frac{TN+TP}{(TN+FN+FP+TP)} \tag{18}$$

$$Pre\ (\%) = \frac{TP}{(FP+TP)} \tag{19}$$

$$Rec\ (\%) = \frac{TP}{(FN+TP)} \tag{20}$$

$$Fm\ (\%) = \frac{2Pre\ \mathrm{x}\ Rec}{Pre + Rec} \tag{21}$$

where TP (true positive) is the number of correct predictions that an instance is relevant, TN is the number of correct predictions that an instance is irrelevant, FP (false positive) is the number of incorrect predictions that an instance is relevant, FN (false negative) is the number of incorrect predictions that an instance is irrelevant.

5.3.1.2 Implementation for real-time security prediction

The dimensionality and types of attributes of the dataset determine the feasibility of real-time applicability. Using the incremental learning technique, highly dimensional large training

datasets are reduced into small dataset batches. In this case for power system real network application, security predictions are made for a single instance as obtained from field devices such as PMU, therefore, the prediction time is diminutive. The situation that may be regarded as a challenge is the speed at which the saved incremental classifier can be retrieved from the different storage means.

There are several artificial intelligence application development tools for implementing incremental learning approaches. However, only a few tools support online applications. Weka software is one of the few tools that provides an online machine learning application development environment [292]. In particularly demanding real-world applications like security state prediction for the grid operators, the Weka environment can be used to produce real-time predictions. On Weka, many classifiers can be trained and implemented using the incremental mode. However, training classifiers on large datasetscan be challenging even after reduction into smaller batches, particularly using the Weka explorer interface.

In the Weka explorer interface, due to the visualization and other functionalities, the computer's memory may be overloaded, which may significantly impact the training and prediction times. An alternative to the graphical user interface is the Knowledge Flow interface. The knowledge flow layout showing the important steps and elements for the proposed set-up is shown in Figure 5.7. The knowledge flow interface makes it possible to process large datasets that would have significantly impacted the computer's processing speed. By loading and processing each instance in a dataset separately, updateable classifiers may be trained incrementally. After each successful training, the serialized model saver saves the most recent model, which is then retrieved by the model retriever to make future security state predictions using live data.

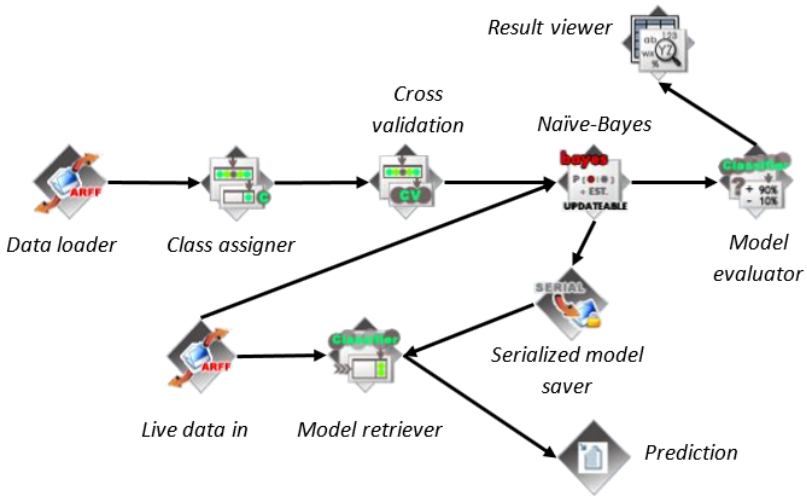

Figure 5.7: Knowledge flow layout for proposed security state prediction

5.3.2 Intelligent security control system

An intelligent security control ((ISC) system based on load shedding is proposed to ensure the security of the grid for predicted insecure states. The ISC system determines the secured load level for an insecure state, estimates the required load shed value and determines the best node within

the network for load shedding action. The ISC system model is developed from a dataset of proposed grid operating points with a new load and simulated response from the offline transient security studies. A load shed value for an insecure proposed grid operation point is estimated to ensure grid security by constantly monitoring the output of the security prediction model. The proposed ISC system is implemented on the physical distribution network through the distributed controls enabled by communication devices as shown in the modern grid structure in Figure 5.8. The proposed security prediction and ISC model exists on the first layer of the integrated grid structure. Layer 2 comprises distributed control systems for different zones of the distribution network. Commands from the ISC are implemented to activate the necessary switches in sections of the distribution network on layer 3 of the integrated transmission and distribution network structure.

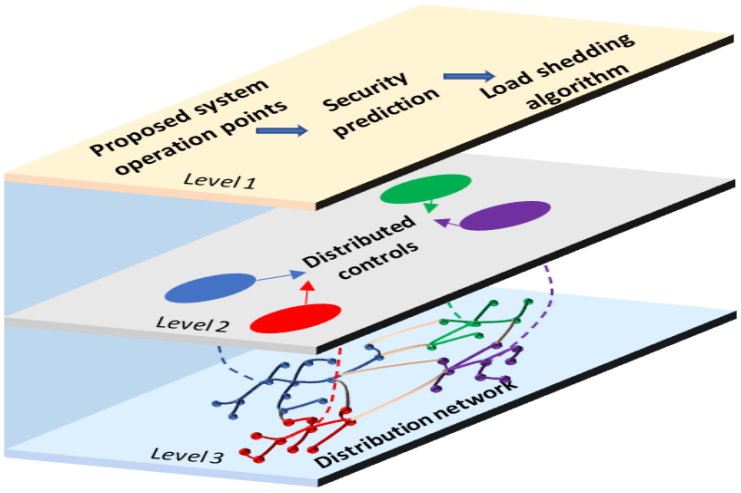

Figure 5.8: Structure of the modern integrated power grid

The development of the model for the ISC is achieved in two stages. In the first stage, the estimation of the amount of load shed to ensure the security for the predicted insecure state of the network is carried out. To estimate the load shed amount, an additive Gaussian process regression algorithm is applied to train the developed dataset. In the second stage, the optimal node for load shedding action is determined using a ranking algorithm based on the network node's security margin.

5.3.2.1 Gaussian process-based load shed value estimation

This section describes the proposed algorithm to estimate the amount of load shed required to ensure the security of the grid for all predicted insecure states. A new dataset containing the new loads' values for every insecure instance from the initial dataset is developed. An additive Gaussian process regression (GPR) prediction algorithm is proposed to predict the secured load level for insecure predictions from section 3.1. GPR is a nonparametric Bayesian approach with several benefits. A few of the benefits include the capability to work well on small datasets and the ability to provide uncertainty measurements on the predictions. A GPR is a generalization of the Gaussian probability distribution. It is a stochastic process in which a multivariate normal distribution exists

for every finite collection of random variables. In other words, a normal distribution is assumed for any finite combination of variables.

Since the proposed load shedding model is described by more than one attribute $(x_1, x_2, \dots, x_N)$ with high correlation to each other, the distribution of the attribute can be represented by a multivariate Gaussian distribution model defined in (26).

$$\aleph(x|\mu, \sum) = \frac{1}{2\pi^{N/2}\sum^{1/2}} exp\left[-\frac{1}{2}(x-\mu)^T\sum^{-1}(x-\mu)\right] \tag{22}$$

where N is the dimension of the dataset, x is the variable, μ is the mean vector, and $\sum$ is the $N \times N$ covariance matrix. Since it is possible to have a probability distribution function for all possible predictions in GPR, the means of the predictions, as well as the prediction variances, can be calculated. The multivariate regression prediction can be modeled as given in (27).

$$P(f|X) = \aleph\,(f|\mu, K) \tag{23}$$

where X is the vector of attributes denoted by $X = [x_1, x_2, \dots, x_N]$, $f = [f(x_1), f(x_2), .., f(x_N)]$, $\mu = [\tau(x_1),\ \tau(x_2), .., \tau(x_N)]$ and $K_{ij} = k(x_i, x_j)$, τ represents the mean function and K represents a positive kernel function. A kernel function is commonly used in GPR to represent the behavior of the dataset. The Pearson Universal Kernel (PUK) function expressed in (28) is chosen due to its ability to adapt to various other functions [296]. The conditional densities and posterior for prediction are given by (29) and (30), respectively. The GPR performance indices α and β are given in (31) and (32).

$$K(a, a_0) = \frac{1}{\left[1+\left(\frac{\sqrt[2]{|a-a_0|^2\sqrt{2^{(1/\omega)}-1}}}{\sigma}\right)^2\right]^{\omega}} \tag{24}$$

$$\begin{bmatrix} p(x_1) = \aleph(x_1|\mu_1, \sum_{11}) \\ p(x_2) = \aleph(x_2|\mu_2, \sum_{22}) \\ p(x_3) = \aleph(x_3|\mu_3, \sum_{33}) \end{bmatrix} \tag{25}$$

$$p(x_1|x_2) = \aleph(x_1|\mu_{1|2}, \sum_{1|2}) \tag{26}$$

$$\alpha = ICM_{lv} \times \overrightarrow{TV} \tag{27}$$

$$\beta = ICM_{hv} \times \overrightarrow{TV} \tag{28}$$

where $\mu_{1|2} = \mu_1 + \sum\sum_{12}^{-1}(x_2 - \mu_2)$, a_0 is the center of the peak of the kernel function, a represents an independent variable, ω is used to control the Pearson width, σ is the tailing factor of the function peak, $\overrightarrow{TV}$ is the vector of the target values, ICM_{lv} and ICM_{hv} are the lowest and highest values of the inverted covariance matrix, respectively. To optimize the performance of the GPR model, the model is implemented using the additive function. An additive GPR is a function that decomposes into a sum of low-dimensional functions, each depending on only a subset of the input attributes. If the

attribute-class pair is $(x_i, y_i) \in$ Rd x R, where $i = 1, 2, \ldots, N$, then the additive non-parametric GPR is defined as (33) and (34) [297].

$$y_i = F(\mathrm{x}_i) + \epsilon_i, \quad \epsilon_i \sim N(0, \sigma^2) \tag{29}$$

$$F(\mathrm{x}_i) = \varphi_1 f_1(\mathrm{x}_i) + \varphi_2 f_2(\mathrm{x}_i) + \ldots + \varphi_z f_z(\mathrm{x}_i) \tag{30}$$

where N is the sample dimension, d is the dimensions of x_i, F is the sum of the z regression function and φ is the parameter that prevents F from sample overfitting.

5.3.2.2 Optimal node selection

After estimating the load shed value required to ensure the security of the grid, the next step is to determine the appropriate node within the grid to apply the intelligent load shedding scheme. The proposed optimal node selection algorithm is based on the security margin of individual nodes within the network. Security margin is defined as the closeness of a node to insecurity, and is obtained from the critical voltage (V_{cr}) and the initial voltage (V_{in}). The V_{cr} is the voltage at the point of collapse obtained from the voltage stability assessment for each node while V_{in} is the initial voltage at the node. If N is the total nodes in the network, the proposed algorithm for load shedding node identification is given below. The critical voltage is adopted in the optimal node selection process due to its relationship with the load (P). With an increase in P, the voltage at the load nodes decreases and reaches a critical value corresponding to the security limit. Since the impact of the load has been considered in the voltage security estimation, there is no need to include P as a separate entity in the optimization process.

Model 1: Load shedding node(s) selection

1. System initialization $i = 1, 2, 3 \ldots N$.
2. Read the node load $P(i)$ and required load shed value P_{ls}.
3. Evaluate the node's security margin $\alpha(i)$,
4. $\alpha(i) = \left(\frac{V_{in}\,(i) - V_{cr}(i)}{V_{cr}(i)}\right) \times 100$.
5. Sort $\alpha(\nabla) == \alpha(i)$(largest → smallest).
6. Initialize $i = 1$.
7. if $P(i)[\alpha(\nabla)] \geq P_{ls}$ then.
8. i is a load shedding node.
9. else $i = i + 1$.
10. until $\sum_i^n P(i) \geq P_{ls}$.
11. end
12. return node(s), i.

5.4 Results and Discussion

5.4.1 Test Network

The proposed technique was tested on the IEEE 39 bus test network with ten (10) generators and nineteen (19) load buses as shown in Figure 5.9. The synchronous generators are modeled with the constant gain exciters and conventional power system stabilizers. Generator G3 is chosen as the center of inertia due to its lateral position with the grid. The network is reduced to a single machine infinite bus model and modified to include a non-synchronous generator at the lower voltage side. The wind turbine system is used to represent the aggregated power generation from renewable sources. The network operation parameters considered for the transient security assessment are given in Table 5.2. These parameters are also considered as the attributes in the training dataset to obtain the security prediction model. A three-phase short circuit fault is applied on one of the lines at different distances from the synchronous generation as an impulse to obtain the rotor angle response from the transient security assessment. The fault was activated at 1s and cleared at the estimated critical clearing time of 0.1s.

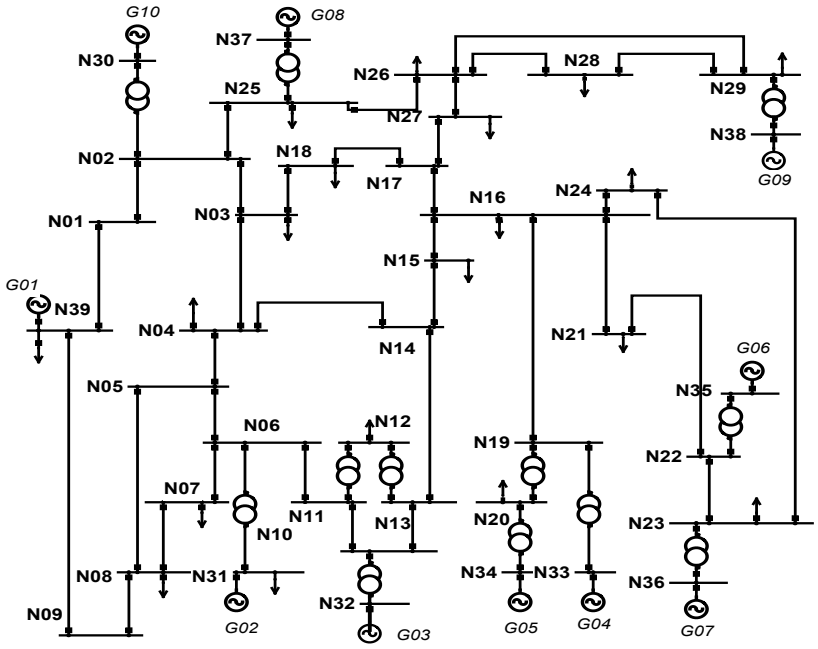

Figure 5.9: One-line diagram of the IEEE 39-bus system

Table 5.2: Parameter for security assessment

Attributes	Value range
Load (MW)	500 – 2500
Inertia Constant (s)	0.1 - 3.5
RES-DG output (MW)	100 - 1000
Fault distance (%)	10 - 100

5.4.2 Attribute extraction and processing

The transient security studies with 3 phase short circuit fault were performed to obtain 700 instances of possible system operating points (attributes). The attributes were obtained through random number generators considering the minimum and maximum values for each attribute. The numbers of secured and insecure instances concerning the output of the renewable energy source distributed generation (RES-DG) and load level are shown in Figures 5.10 and 5.11. The penetration of RES-DG alone does not contribute to the insecurity of the grid since the grid can be secure under high penetration of RES-DG if the system inertia can be maintained at the required level as shown in Figure 5.10. Significant insecure conditions are recorded during very low RES-DG penetration even at relatively high/maintained inertia. For example, about 60% of instances with inertia constants greater than 1.75s which is half of the equivalent inertia of the network are unstable. Also, only 64.7% of the total instances for the most secure RES-DG output range are above the inertia constant of 1.75s.

The average inertia constants for the secure and insecure states considering the varying RES-DG output are 2.23s and 1.33s, respectively. Figure 5.11 shows the secure and insecure scenarios of the grid focusing on the load level. The result aligns with common knowledge showing a significant number of insecure instances as the load is increased. The average inertia constants of the two highest insecure loading bands are respectively 42.7% and 56.6% more than the average inertia constants of the secure instances of the same loading bands. Figure 5.12 shows the inertia distribution against the network's stability state. The highest and least stability to instability ratios were recorded for inertia bands 2.7 – 2.9 and 0.3 – 0.5, respectively. The resulting ratios show that with high inertia levels, the network will be more stable than at low inertia values. As shown in Figure 5.13, the system is more likely to be secure under scenarios with high inertia constant. Average inertia constant of 2.02s and 1s is recorded for the secure and insecure states, respectively, considering the possible system loading bands.

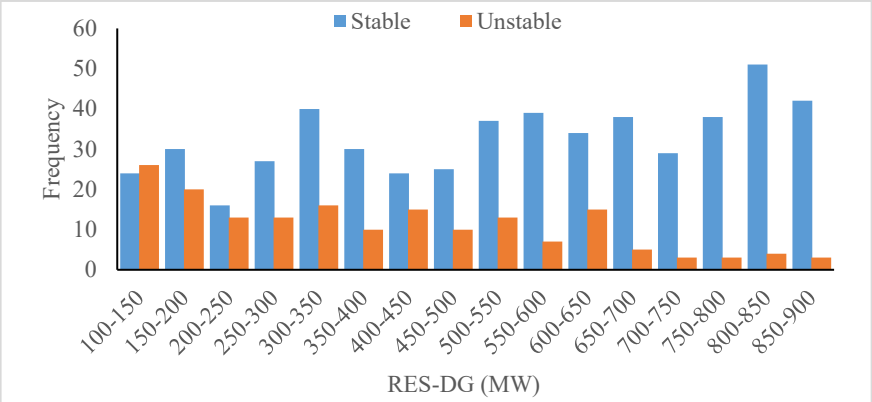

Figure 5.10: Security scenarios with RES-DG dispatch

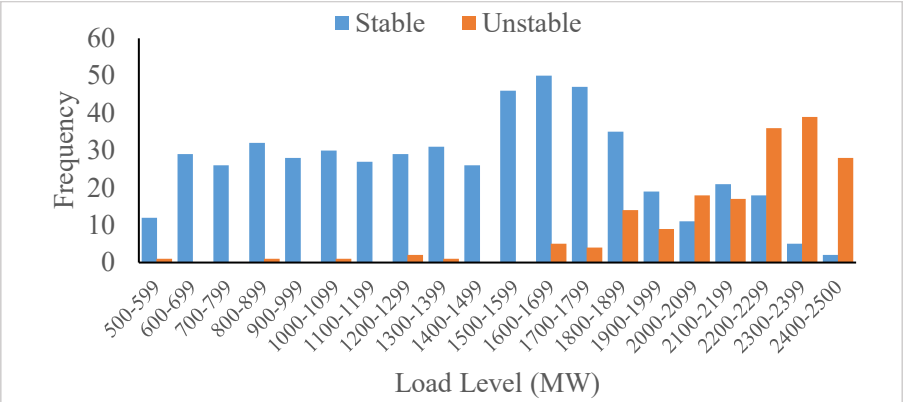

Figure 5.11: Security scenarios with Load Level

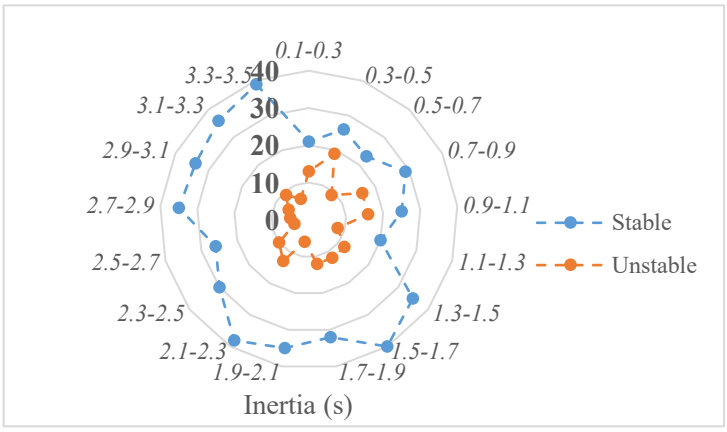

Figure 5.12: Stability state inertia distribution

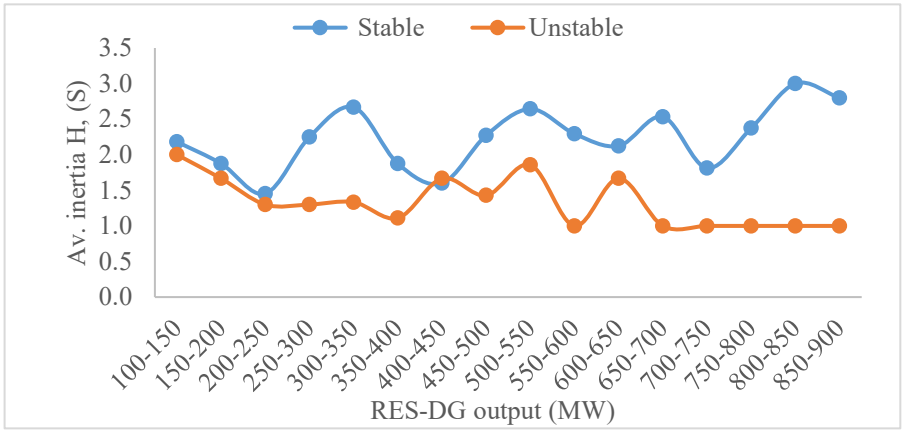

Figure 5.13: Average inertia constant for RES-DG output.

5.4.3 Security prediction

This section presents the results of training a Naïve-Bayes classification model after preprocessing data obtained from randomizing each attribute to obtain instances that represent possible operation scenarios for the grid. Each generated scenario is classified as secure or insecure from the response obtained from the time domain transient security simulations. The Naïve-Bayes updateable classifier is utilized to implement the proposed incremental Naïve-Bayes algorithm using the continuous training approach. The obtained model after each batch is saved using a serialized model saver which is included in the classifier algorithm. To train each batch in a continual mode,

the classifier is programmed to load and update the initial model for each training batch until the best performance is obtained.

Figures 5.14 and 5.15 show the performance indices obtained from normal and continual training modes with six batches of 100 instances with a batch size of 5 instances. The NB model is trained and tested using 85.7% and 14.3% of the training dataset, respectively. Compared with the normally trained model where the changes in the Kappa and RMSE values improve smoothly across the batches, the continually trained model experiences an impulsive improvement at the beginning of each training batch. Since there is more data for the normally trained model, the accuracy may be slightly higher than that of the continually trained mode for the first few batches. However, the eventual accuracy of the continuously trained model is usually higher than that of the normally trained models. The final model results from the continual and normal training modes are shown in Table 5.3. The confusion matrix which gives the total correctly and incorrectly classified instances is shown in Table 5.4. The best performance of the model obtained with the continual mode is improved after the first few next training batches until the maximum accuracy is reached. Figure 5.16 shows the accuracy and k-coefficient of the normal and continual models after each data batch. Compared with the normally trained batch modes, the mean accuracy of the models obtained from the continual training method is approximately 3.5% improved. Since the continual training methods seeks to produce the best results for the new data batch based on the previous model, the consistent improvement in the accuracy of the model may be impacted as seen in batch 3 and batch 4. The comparison of the proposed Naïve-Bayes incremental algorithm with other available incremental algorithms on the knowledge flow interface for real-time training and testing imitation is shown in Table 5.5. The selection of the Naïve-Bayes model is based on the evaluated performance indices as well as the overall time required for model training and testing.

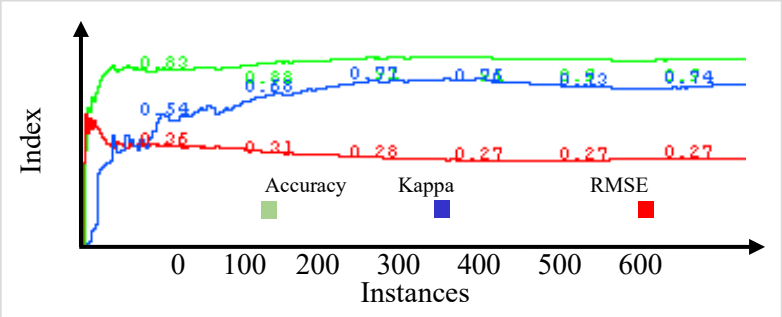

Figure 5.14: Performance in normal training mode

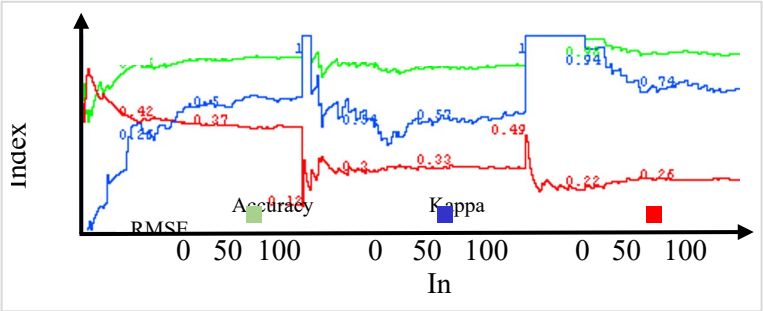

Figure 5.15: Performance in continual training mode

Table 5.3: Models performance indices

Training method	Precision	K-Coefficient	π-Coefficient	Precision recall curve	Root means squared error
Normal	90.7	0.752	0.752	0.942	0.267
Continual	94.5	0.824	0.826	0.96	0.25

Table 5.4: Model confusion matrix

Normal training			Continual training		
Class	Yes	No	Class	Yes	No
Yes	493 (TP)	31 (FP)	Yes	508 TP)	16 (FP)
No	34 (FN)	142 (TN)	No	29 (FN)	147 TN)

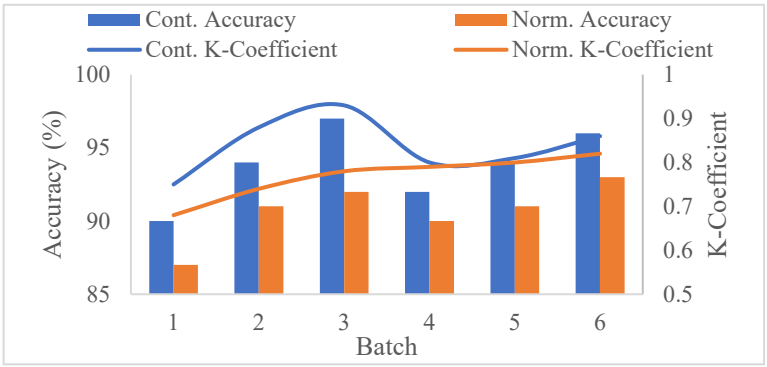

Figure 5.16: Model batch performance indices

Table 5.5: Incremental model comparison

Models	Acc (%)	Pre (%)	Rec (%)	Fm (%)	Build time (s)	Test time (s)	
NB-Updateable	94.5	94.8	96.6	95.7	0	0.01	
Hoeffding tree	92.7	93.8	93.9	93.8	0.01	0	
Locally weighted learning (LWL)	90.4	92	90	93	0	0.68	
Stochastic gradient descent (SGD)	94.1	94.7	94	94.7	0.02	0	

The prediction results from the model obtained with the proposed technique using different test datasets are shown in Figures 5.17 to 5.20. Considering that the accuracy of the models improves as more training batches are introduced, the prediction confidence is also expected to progressively increase with the addition of more training datasets. The dip in the confidence of the fifth model in Figure 5.17 coincides with the decrease in k-coefficients from 0.76 to 0.73. By grouping the test dataset into 10 batches with 10 instances each, Figure 5.18 shows the composition of the 88% confidence level obtained for the final model (6th model). The prediction confidence for the secure and insecure states lies between 53%-93% and 51%-100%, respectively. The accuracy of the final continual model for 10 data samples with different instance sizes using the 95% confidence level is presented in Figure5. 19. The obtained mean and standard deviations of 0.96 and 0.006, respectively indicate a high prediction accuracy range for future predictions. To emulate an online security prediction, Figure 5.20 shows the prediction outcomes and associated precisions for 10 sequential grid proposed operating points. A 90% true prediction was obtained with the lowest precision of 0.61 for a true prediction.

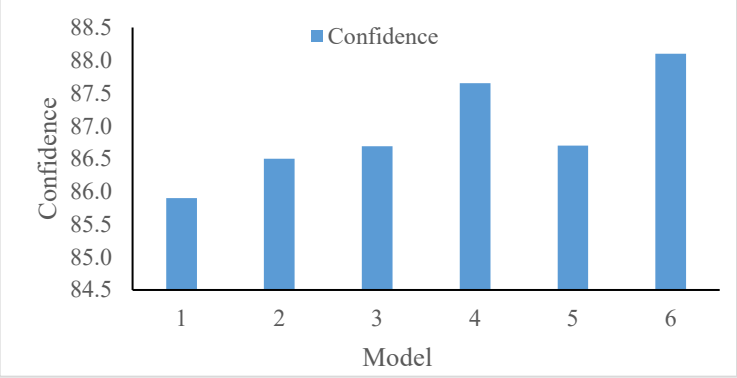

Figure 5.17: Incremental model prediction confidence

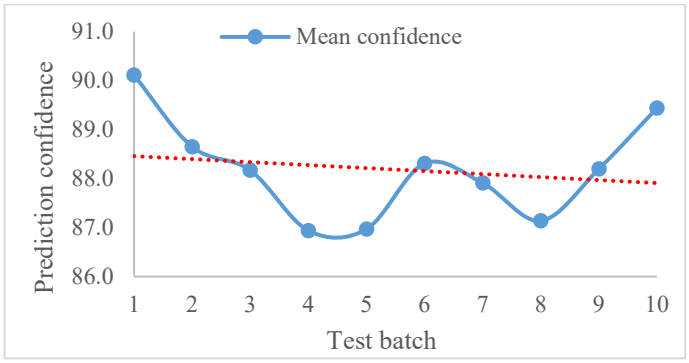

Figure 5.18: Mean prediction confidence

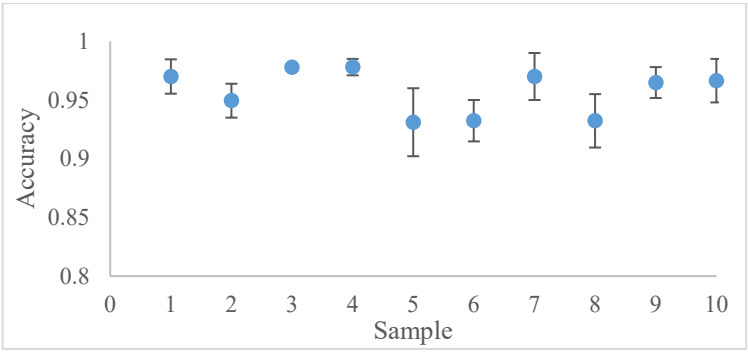

Figure 5.19: Model mean accuracy

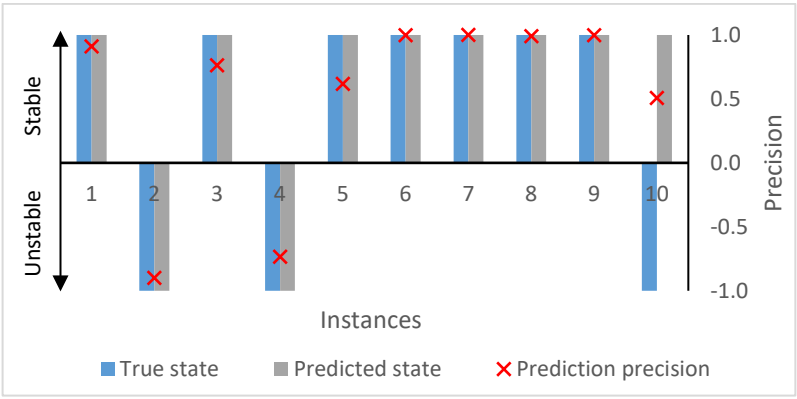

Figure 5.20: True security and predicted security

5.4.4 Load shedding for security control

This section presents the results from the proposed model using the intelligent load shedding for security control. For every insecure state prediction with high precision obtained from the classification model, the quantity of load to be shed is estimated alongside the optimal node for load shedding action. To justify the recommendation of load shedding for the security control, an attribute evaluation technique using ranking algorithms was employed to assess the degree of correlation of the attributes employed for the security prediction. As shown in Table 5.6, the system load level has the highest impact consistent with the three ranking algorithms. The frequency distribution of the load shed quantities obtained for 170 instances is shown in Figure 5.21. The probability that the required amount of load shed for any predicted insecure state would be between 300 MW - 550 MW is about 0.46. Figures 5.22 and 5.23 show the density distributions of the load shedding required for different levels of system inertia and RES-DG, respectively. The equivalent inertia constant is

classified as follows: low (0.1s-1.1s), medium (1.1s-2.2s) and high (2.3s-3.5s). Likewise, the RES-DG dispatch is classified as follows: low (100-330 MW), medium (331-660 MW), and high (661-1000 MW). For the mean load level of 2198 MW, a mean of 480 MW of load shedding is estimated to ensure the security of the system under the proposed medium inertia constant and RES-DG dispatch. The required average amount of load shed is highest for instances with low inertia constant and RES-DG generation.

Table 5.6: Attribute impact evaluation

Ranking algorithm	**Inertia (s)**	**Load level (MW)**	**RES-DG (MW)**	**Fault Distance (%)**
Gain Ratio	0.0246	0.2208	0.0641	0.031
Information Gain	0.223	0.3865	0.0567	0.01
Correlation	0.4861	0.6004	0.2857	0.0278

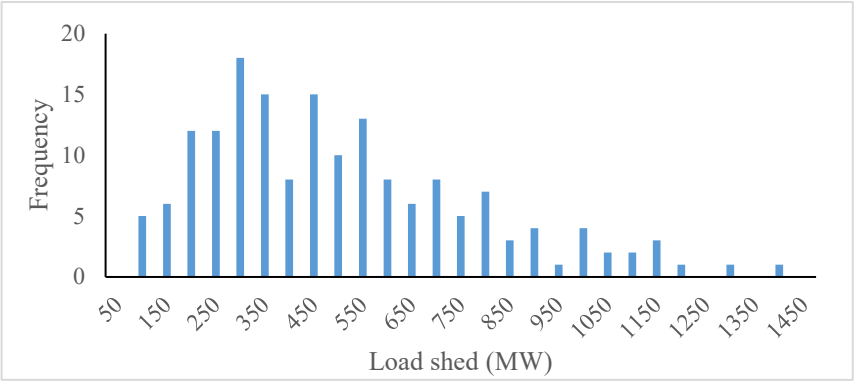

Figure 5.21: Load shedding distribution

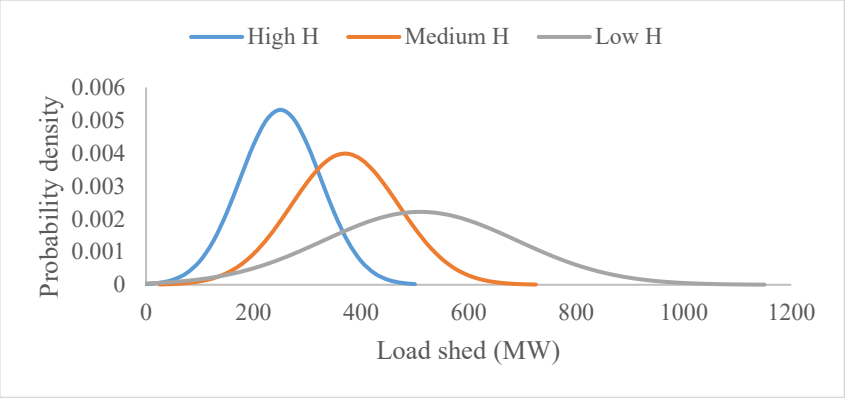

Figure 5.22: Load shedding density considering system inertia

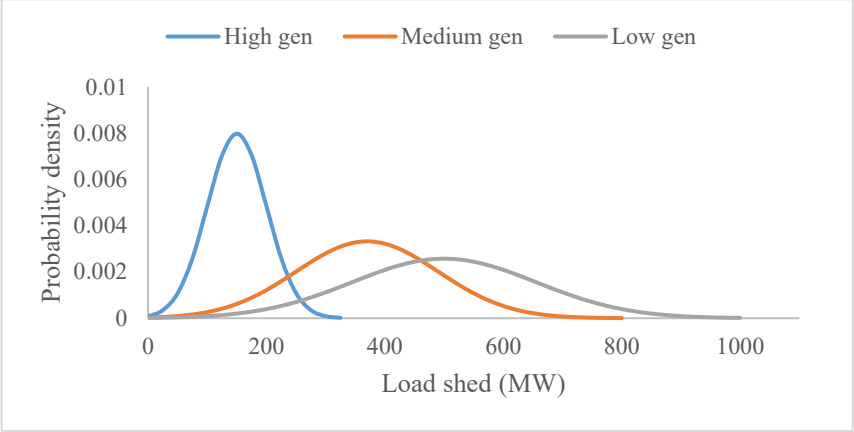

Figure 5.23: Load shedding density considering RES-DG output

This section presents the results from the proposed model for the intelligent load shedding (ILS) for security control. The attribute was normalized. Since the required load shed values are not linear with the predictors, a kernel is applied to obtain a quasi-linear class. The Pearson Universal Kernel (PUK) kernel was adopted due to its adaptability to various functions including the Gaussian. The performance of the additive GPR depends not only on the data preparation and choice of the kernel but also on the number of models. The number of models required is proportional to the average training time. Unlike the incremental classification models, the additive GRP cannot be deployed until the final model is obtained. Therefore, the optimal number of models to reduce the average training time is selected. The performance of the proposed additive GPR with 10 models compared with the normal Gaussian regression process is shown in Table 5.7. The proposed algorithm is compared with similar regression-based algorithms with numerical class capability for as shown in Table 5.8. Since the time it takes to generate all the models is negligible, priority is given to models with the highest correlation coefficients for high prediction accuracies. Figure 5.24 shows the variance between the actual and predicted load shed values using a new test dataset with 15 instances. Since the predicted load shed values and the variance are uncorrelated, the prediction must be made for each unstable instance. Also, there is a variance of 15.16 kW for every 1 MW load shed required. Instances with low inertia constant (0.1s - 1.1s) contribute about 93% of the predicted values with variance greater than 10 MW. The grid achieved 90% security when the new proposed load values were tested on previous insecure instances.

To implement the load shedding, the optimal node(s) is determined using the proposed ranking model. The voltage security index and the nodal power used to determine the optimal node are shown in Figure 5.25. For example, considering instance 14 in Figure 5.25 where a load shed of 327.9 MW is required, the optimal nodes for load shedding are nodes N04 and N15 considering high load level and RES generation. The voltage security index for each node changes based on the node loads and proposed quantity of generation from RES. Consequently, the ranking algorithm is continuously implemented for each scenario with insecure prediction. The matrix in Table 5.9 shows the feasible nodes for the mean low, medium, and high load shed values under different load levels

and RES generations. The proposed security prediction and load shedding models are suitable for real-time applications since their average model training times are 1.2s and 3s, respectively.

Table 5.7: Trained GRP model

Model	Correlation coefficient	RAE (%)	α	β	Av. Target Value
Addictive GRP	0.99	6.5	-0.52	0.41	5.34E-01
Normal GRP	0.96	22.8	-0.1	0.2	3.19E-01

Table 5.8: Regression-based model comparison

Models	Correlation coefficient	RMSE	RAE (%)	Build time (s)
Normal GRP	0.96	69	22.8	0.01
Linear regression	0.92	107.1	36.9	0
Sequential minimal optimization for regression (SMO-Reg)	0.9	123.8	32.9	0.02
Reduced error pruning tree (REPTree)	0.95	90.3	28.6	0

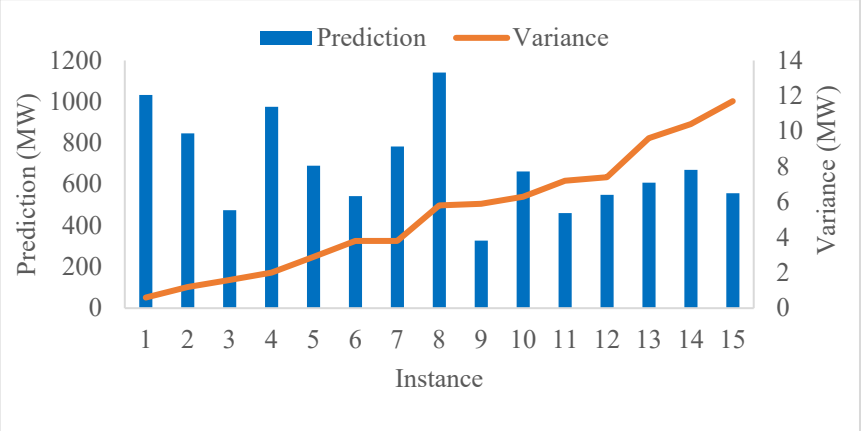

Figure 5.24: True load shed values vs predicted load shed values

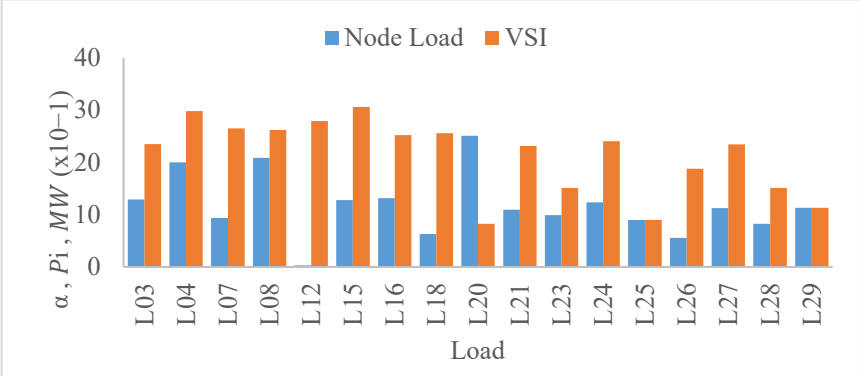

Figure 5.25: Optimal node selection indices

Table 5.9: Optimal nodes for load shedding

RES Generation (MW)	Load Level (MW)			
	Low	Medium	High	
Low	N15, N04	N07, N08, N12, N04	N15, N03, N04, N07	
Medium	N08, N07	N04, N07, N08, N03	N20, N12, N08, N07	
High	N28, N07, N04	N07, N04, N08, N03	N04, N16, N15	

5.5 Conclusions

The replacement of synchronous generators with renewable energy sources distributed generation (RES-DG) reduces the resultant inertia constant of the grid, thereby undermining the ability of the grid to remain secure after the occurrence of disturbances. The proliferation of RES-DG units into the grid results in a time-varying inertia constant which necessitates the prediction of the security state for every proposed grid operation. This paper proposed a suitable model for real-time security prediction and control using machine learning algorithms. The proposed model includes an incremental Naïve-Bayes algorithm for dataset classification and future security state prediction. The dataset comprised of 700 instances of inertia constant, load level, generation from the renewable energy sources, fault distance, and security label as the attributes. The proposed intelligent security control technique involves an additive Gaussian process regression to estimate the load shed required to ensure the security of predicted insecure outcomes, and a node ranking model to determine the optimal node for load shedding. The optimal node selection model is based on the cumulative sum of the node loads ranked by the voltage security index.

The security prediction models are obtained at the end of each batch training. The mean accuracy and standard deviation of 0.94 and 0.025, respectively, were obtained from six dataset batches of 100 instances per batch. A 90% accurate prediction of the security state of a testing dataset with 10 instances was obtained when compared to the true security state. The obtained AGRP model for security control was able to predict the load shed values within 50 MW variance for 30 test instances. A 100% secure state was achieved using the proposed optimal load shedding node

identification. In conclusion, the proposed models can predict and control the security state of the emerging power grid under the described varying grid attributes.

Future research of this paper will focus on considering parallel computation techniques to improve the efficiency of the proposed online security prediction model, especially for very large power systems. It is also important to see how the Gaussian regression process model can be optimized to avoid unnecessary interruption of supply through appropriate hyperparameter selection. Although this paper has presented and discussed the possibility of implementing the proposed technique in a real power system, the deployment of the proposed model as an executable software for system operator utilization after being evaluated for robustness and scalability is a good consideration. Lastly, considering that synthetic inertia is a tradable but costly commodity, the estimation of the optimal amount of synthetic inertia needed to ensure the stability of every unstable grid operation instance is also a significant and relevant future research area.

Author Contributions: Conceptualization, I.O; methodology, I.O; validation, I.O; writing—original draft preparation, I.O; writing—review and editing, I.O, R.Z, and T.L; Supervision, R.Z, and T.L.

Conflicts of Interest: The authors declare no conflict of interest.

6 Manuscript 5: Optimal flexibility operation

Preamble

The growing demand for flexibility support using resources connected to the distribution network necessitates ensuring optimal flexibility operations. Optimal flexibility operation would be cost-effective and provide the required support to minimize voltage deviations during disturbances. Therefore, the operation cost will be according to the flexibility resources required from the distribution network. Consequently, Chapter 6 examines the impacts of voltage support units connected to the distribution networks using a probabilistic voltage risk index and proposes a bi-level security-constrained model for the optimal flexibility operation. The first and second optimization levels consider economic and technical objectives, respectively. The economic objective is to minimize the power loss through network reconfiguration, while the technical objective is to maximize the voltage support through flexibility quantity estimation. The reconfiguration optimization problem is solved using a fmincon solver, while the flexibility quantity estimation is achieved through an improved decision-tree classification model. The proposed method reduces the operation cost by reducing the power loss as well as the risk index during flexibility operations and optimizing the flexibility quantity needed during disturbances.

A bi-level security constrained model for optimal flexibility operation

Ifedayo Oladeji*, Ramon Zamora and Tek-Tjing Lie

Department of Electrical and Electronic Engineering, Auckland University of Technology, Auckland 1010, New Zealand

Abstract: Aggregated distributed energy resources (DER) units in the distribution networks are utilized to support flexibility services in modern grids. To ensure modern grid security, active and reactive flexibility operation must not increase the risk index at the transmission-distribution (T-D) network boundary and the distribution network nodes. This paper assesses the impact of aggregated DER units on the distribution networks and proposes a bilevel optimization approach to mitigate the impact on the grid's security. The bilevel optimization approach involves distribution network reconfiguration and flexibility quantity estimation. Many existing flexibility operation models in recent literature are developed based on economic objectives and constraints rather than security constraints. Also, the existing flexibility operating models do not account for probabilistic scenarios, leading to security issues during flexibility operations. The probabilistic risk index and hosting capacity are included as security objectives in the reconfiguration problem formulation to minimize the total distribution network power loss. A decision tree classification approach is proposed to estimate the minimum flexibility MVA to achieve a desired voltage deviation reduction. The proposed approach was tested on IEEE 33- and 69-node distribution networks. Under a 100% increase in load at specific nodes, the proposed technique achieved a significant improvement of 16.67% in the voltage deviation of the worst nodes in both the IEEE 33- and 69-node test networks. The results show that the proposed bilevel technique optimally reconfigures the network and effectively estimates the flexibility support required to ensure the grid's security during disturbances. The proposed model will enhance the interaction between the transmission and distribution network operators.

Keywords: Distributed energy resources, Flexibility, Integrated grid, Network reconfiguration, System operators.

*Corresponding Author: Tel.: +64225331241
E-mail address: ifedayo.oladeji@aut.ac.nz

6.1 Introduction

6.1.1 Background and motivation

High penetration of variable energy generation source units into the modern power grid will provide technical merits when optimally planned and efficiently operated. A major requirement of modern transmission system operators (TSO) is to mitigate security challenges associated with the

modern power grid. The grid's security can be ensured through enhanced interaction between the TSOs and the distribution system operators (DSO) [298]. The existing interaction includes congestion management and flexibility services. The process of achieving enhanced interaction involves the ability to perform quasi-real-time network assessments using varying grid measurements. The process also ensures the grid's security when several ancillary services are simultaneously involved under dynamic conditions and constraints. Since the modern grid's security depends on the level of interaction between the TSO and DSO, it is essential to develop approaches that integrate local solutions at the transmission-distribution (T-D) network boundaries [299]. Flexibility refers to a grid's ability to manage the unpredictability of demand and supply reliably and cost-effectively across all relevant timescales. The operational flexibilities estimate the rate, duration, and capacity of the services required to absorb steady and transient disturbances to secure the grid operation [300]. Demand-side services, including real-time balance of frequency and voltage management previously provided by centralized generators, have been replaced by new market structures supported by aggregators. Therefore, the distribution networks hosting the variable energy generation source units will have an active role in controlling and managing every market participant connected to them. The flexibility operation may include a change in network topology, deployment of reserves, and demand-side participation. Flexibility planning and operation problems for modern grids are multi-objective problems that require all-inclusive formulation, which may best be solved using new computational methods and artificial intelligence techniques [301].

For enhanced interaction between the transmission and distribution network operators, specifically during flexibility services for disturbances, the combinations of considered parameters under the prevailing constraints will increase the complexity of the flexibility operation and the computational requirements for the employed tools [302]. The operational flexibility estimation techniques must be extended beyond the planning horizon to include estimations for operations in the short-term ahead under both steady and transient state constraints. Existing flexibility operation models are focused on economic considerations to minimize the cost and duration of flexibility operations without considering the impact of flexibility operation on the distribution networks. Consequently, new flexibility operation techniques should consider approaches combining economic and technical considerations with probabilistic security constraints.

Flexibility services involve properly shaping injected active and reactive power from controlled and aggregated power sources connected to the distribution networks. The increasing penetration of variable energy generation sources into the grid requires new regulations concerning power reserve and flexibility services. With the new regulations, aggregated DER units may participate in the voltage support of the grid during disturbances. Aggregated DER units and their interactions have to be well coordinated. The aggregated DER units with well-coordinated control can significantly improve the grid's local and area-wide voltage stability [303, 304]. Using dispatchable power from aggregated DER units for voltage support services presents a new challenge. The challenge is associated with controlling a large, distributed load, the configuration of

the distribution network, and the impact of the aggregated DER units' operations on the distribution network. Control of large, distributed loads includes the charging pattern of electric vehicles and other power electronics-based loads. The constraints associated with the configuration are due to the load distribution, size, and network configuration type. Consequently, the methods for optimal operations of the aggregated DER units for optimal voltage support should consider some of these constraints [130].

6.1.2 Network Configuration and flexibility services

The configuration of the distribution network influences the voltage response of the network. Therefore, developing a specific numerical measure for any configuration is crucial to evaluate it against other configurations. In recent research, the number of node connections, total branch impedance, and the electrical distance between the node where the disturbance occurs and other nodes has been considered to distinguish each configuration [305]. Using the system impedance matrix, the impedance as viewed from the disturbance node is given by (1), where k is the network node, Z is the total impedance, Z_{ii} is the self-impedance in the node where the disturbance occurs and Z_{ij} refers to the connection impedance between the node where the disturbance occurs and the node where the aggregated DER unit is connected. The summation of the impedances creates the overall topology measure ($\boldsymbol{\lambda}$) given in (2), which indicates the electrical distance between the areas. A high value of $\boldsymbol{\lambda}$ implies high impedance. The network configuration largely impacts the system voltage angles and magnitudes, which define the subsequent generator pick up and post disturbance power flow. A node with a high electrical distance from the rest of the system will experience a larger voltage angle than the rest of the network. When subjected to a large and sudden load increase, such nodes experience voltage deviations beyond the security limits [306]**.** A high electrical distance can result in a highly localized voltage response. As the magnitude of the voltage deviation continues to increase, it is imperative to activate nearby flexibility services to prevent the grid from progressing into an insecure state during the disturbance window.

$$Z = \sum_{j=1}^{N-1}(Z_{ii} + Z_{jj} + 2Z_{ij}) \quad (1)$$

$$\lambda = \frac{Z}{k} \quad (2)$$

The location and magnitude of the generation and load determine the power flow, voltage magnitudes, and angles in a network. The voltage stability and response of different networks with different penetration levels of variable energy generation source units will differ depending on the network generation and load points. The power flow into the area of the disturbance can be used as a quantity to indicate the voltage angle differences with respect to the location of the disturbance. It is anticipated that the voltage angle differences will increase as the power flow into the disturbance area increases. This resultant larger angle difference due to a greater power transfer into the disturbance area is expected to have a detrimental impact on voltage stability and lead to larger voltage deviations [307].

6.1.3 Distribution Network Voltage Support

Reconfiguration is an important technique for improving distribution networks' performance under normal and recovery conditions. The increasing penetration of variable energy generation source units and variable loads introduce significant variation in the distribution networks' operation, rendering the common reconfiguration objectives inadequate. Improper distribution network configuration may lead to increased power losses, bad voltage profile, low power factor, high reverse current, and high short circuit current contribution considering the high penetration of variable energy generation sources into the distribution network [11]. The hosting capacity and risk index are terms associated with the security condition of the modern distribution network with variable energy generation sources penetration. The hosting capacity represents the amount of variable energy generation sources that can penetrate the distribution network securely. Adequate hosting capacity is important for aggregated DER units and energy storage systems in the distribution network to ensure the network's security under varying generation conditions [308]. The risk associated with undervoltages and overvoltages at the network nodes due to the impact of the variabilities in the power generation from variable energy generation sources units is modeled by the risk index. The utilization of the distribution network flexibilities during grid contingencies necessitates the modern reconfiguration techniques to be adaptive to achieve effective voltage support. The common reconfiguration objectives in the literature are minimizing power loss and enhancing voltage profile [309]. However, there is a need to include more security objectives in the reconfiguration problem formulation due to the increased penetration of variable energy generation sources into the distribution network. Therefore, this paper proposes a network reconfiguration technique that maximizes the hosting capacity and minimizes the risk index to achieve an effective voltage response support from aggregated DER units during network disturbances.

6.2 Review of Relevant Literature

The functioning of the grid at different levels becomes more challenging when the responsibilities of managing grid contingencies are transferred to the DSO [299]. Therefore, developing new structures and models that enhance the interaction between the TSO and DSO is important to ensure secure and reliable grid operation. Many literature on active distribution network planning and optimal operations focused on interaction between transmission and distribution network operations related to dynamic distribution network reconfiguration have been published. The combination of distribution network reconfiguration and optimal placement of DG unit schemes as a single problem is discussed in [310]. The literature already contains many methods for reconfiguring distribution networks to meet various objectives. The majority of the prior research on network reconfiguration may be broken down into three main classifications: heuristics [311-313], mixed approaches [314, 315], and evolutionary and knowledge-based strategies [316, 317]. Although techniques based on evolution and knowledge may handle more complex goals, they have relatively

large computing runtimes and are consequently less suited for online distribution automation. To reduce computing runtime without compromising solution quality, hybrid reconfiguration approaches are mixed solutions that incorporate evolutionary and heuristic methodologies. They nonetheless require more processing power than heuristics, although having runtimes that are often shorter than those of evolutionary approaches. It has been demonstrated that heuristic algorithms provide great outcomes with noticeably shorter runtimes. Considering loss minimization objectives, heuristic algorithms are among the most acceptable algorithms for real-time distribution system reconfiguration [311, 318].

Optimizing a single objective can no longer satisfy the techno-economic requirements of the distribution network as operation becomes more complex. Ref. [309] reviews recent literature's common network reconfiguration objectives and optimization techniques. Multi-objective optimization techniques are more common compared to single-objective techniques. In numerous studies, the objective of minimizing power loss appears alongside other objectives. In addition to the reduction of power loss, voltage profile improvement [201], reliability improvement [319],[112], service restoration [320], resiliency improvement [321],[322], and operation cost reduction [323] are some of the objectives that have been proposed in multi-objective studies. The optimization methods used to solve distribution network reconfiguration problems can be broadly categorized into classical/conventional and artificial intelligence-based optimization methods. Classical optimization methods include linear and non-linear programming and optimal power flow [324]. The artificial intelligence method mainly includes fuzzy system, artificial neural network algorithm, genetic algorithm, tabu search algorithm, ant colony algorithm, cuckoo search algorithm, and other population search-based algorithms [325]. The choice of the algorithm used to solve the generated multi-objective problems determines the global and/or local optima and the convergence time, both of which are critical in achieving a good reconfiguration scheme. The reconfiguration problem is a complex multi-constraint problem. Therefore, metaheuristic optimization approaches are widely used due to their ability to achieve convergence with complex and non-linear problems. Although literature concludes that metaheuristic approaches perform better for complex problems, conventional optimization methods can be used for problems with small networks and problems with fewer constraints as shown in [326]. Compared to evolutionary algorithms, swarm intelligence-based algorithms are more extensively used under the metaheuristic approaches [309]. The extensive use of swarm intelligence-based algorithms is due to the emergence of collective swarm behaviour to achieve a global optimal despite the environmental constraints of the individual swarm entities [327]. Metaheuristic and machine learning optimization methods have demonstrated promising results with single and multiobjective problems. However, traditional analytical optimization techniques are still effective for distribution network reconfiguration problems with a single objective.

Another important factor determining the performance of reconfiguration algorithms is the constraints that bind the solutions. The radiality constraint is an essential constraint since it ensures

no mesh exists within the network after reconfiguration. It also ensures no isolated area/zones within the network; consequently, no node is left unserved after network reconfiguration [328]. Several other constraints have been used to bind the solution of the formulated optimization problems. The most common constraints include the node voltage, line thermal capacity, and power imbalance constraints which may also be considered under the powerflow constraint. When formulating the reconfiguration problem with DG units, the units' capacities, and power injection constraints must be taken into account [309]. Other constraints found in the literature include protection constraints [310, 329], switching [320], and reliability constraints [330, 331]. It is worth noting that besides the voltage and thermal constraints, which are the common constraints used together, no literature applies the voltage, thermal, power quality, and protection constraints in a distribution network reconfiguration problem.

Many literature on active distribution network planning and optimal operations focused on interaction between transmission and distribution network operations related to flexibility modeling and operations in a distribution network have been published. A linearized model was proposed in [332] for the aggregation of active and reactive power at TSO-DSO connection points. The interaction between the TSO and DSO regarding optimal flexibility operation has been studied under a game theory approach [333]. A method for estimating the quantity of time-varying ancillary services of a distribution network to the transmission grid is proposed in [334]. Many papers have discussed and proposed methods for estimating the flexibility operating regions under various components like market parameters, generation types, and energy storage systems. Ref. [335] presents reviews on issues ranging from quantifying flexibilities and modeling flexibility boundaries to procurement and management services from the energy components in the distribution network. Techniques based on optimal power flow [336, 337] and economical generation dispatch [338, 339] are commonly used in literature to estimate the flexibility operating region for different generation scenarios. The optimal power flow techniques are straightforward, and their results are reliable under stated conditions and operational constraints. The economic dispatch-based models are typically used to manage the flexibilities based on demands from the transmission system. A multi-objective genetic algorithm optimization approach to minimize the cost and power losses during flexibility operation was proposed in [336]. In [59, 340], analytical models based on the active power injection technique optimization at the transmission-distribution network boundary were proposed to estimate the flexibility ramping for generation, loading, and contingencies scenarios.

Considering that variable energy generation sources and energy storage systems are becoming more widely implemented, recent literature has presented approaches for maximizing distribution system flexibility. The common flexibility supports in literature are the voltage and frequency support from the DG [123], [341]. Ref. [44] proposed a weighted analytical hierarchy process for the operation of vehicle to grid (V2G) systems to achieve optimal flexibility services. A non-linear optimization technique for power loss and hosting capacity optimization is proposed in [111] to achieve effective load shifting within the distribution network. A network reduction

technique for microgrids was also proposed in [342] to enhance the frequency response of the grid. A technique based on adapted optimal power flow (AOPF) was proposed in [343] to achieve flexible interaction at the transmission and distribution network interface. With the AOPF technique, the operating area at the interface can be roughly modeled in real time, considering the system operator's constraints.

The review shows that the impact of voltage support units connected to the distribution networks has not been investigated. Furthermore, many of the techniques focus only on economic considerations to minimize the cost of flexibility operation. Likewise, there are no security constraints in the optimization problem formulation to mitigate the negative impact on the grid's security during flexibility activation. The existing models focus on the distribution networks and do not consider interaction between the transmission and distribution network operators.

6.3 Contribution and Organisation

This research aims to study the impact of voltage support unit operation on the distribution network during flexibility operation and to propose a method to mitigate such impact to achieve optimal voltage support. A voltage risk index is proposed to assess the impact of aggregated DER unit operation of the network. The probabilistic risk index is the probability that the voltage at the aggregated DER units' connection points as well as the neighbouring nodes, will exist outside the security limits. A bi-level model consisting of network reconfiguration and flexibility value estimation is proposed to achieve optimal voltage support. The probabilistic risk index is included as a constraint alongside the hosting capacity for the distribution network reconfiguration problem formulation. The hosting capacity encapsulates four security constraints: voltage, thermal, power quality, and protection. An improved decision tree classification technique is developed to estimate the active power from aggregated DER units to minimize voltage deviations during disturbances. The proposed classification technique consists of attributes obtained from the interaction between the transmission and distribution system operators (TSOs and DSOs). Therefore, the proposed bi-level optimal flexibility operation technique will be suitable for enhanced interaction between the transmission and distribution network operators. The review shows the need for more research to include probabilistic and security constraints in the reconfiguration problem formulation for optimal flexibility support from the distribution network. Also, there is a need to enhance the interaction between the transmission and distribution network operators for effective voltage support from aggregated DER units. Based on the above explanations, the contributions of this paper can be summarized as follows:

1. developing a bi-level analytical and machine learning-based approach for optimal time-ahead flexibility operation
2. proposing a probabilistic risk index to examining the impact of aggregated DER units operation on the distribution network,

3. including the probabilistic risk index and the hosting capacity as variables for optimal network reconfiguration and
4. proposing an improved decision tree classification-based model to estimate optimal flexibility value from aggregated DER units for optimal voltage support.

The rest of this paper is organized as follows. Section 6.2 discusses modern distribution network operations, focusing on the interaction between the transmission and distribution networks and flexibility for voltage management. The proposed approach for optimal flexibility operation is presented in Section 6.3. The results of testing the proposed approach on IEEE 33 and 69 node networks are presented and discussed in Section 6.4. Lastly, the conclusions of this research are presented in Section 6.5.

6.4 Modern Distribution Network Operation

6.4.1 Power system flexibility

The interaction between the transmission and distribution networks for optimal flexibility operation is critical to ensuring the security of the modern grid. Several control techniques have been proposed to achieve optimal interaction considering available technologies and emerging markets [344]. The distributed control technique is feasible and most applicable for systems with high penetration of distributed generation (DG) and electric vehicles (EVs). Aggregated DER units for demand-side participation in real-time active and reactive power balancing corresponding to frequency and voltage control from distributed systems have been explored as a solution to local and grid-wide voltage control during disturbances. The solution will involve real-time voltage trackers at the TSO/DSO boundary. In addition, DER units can be employed to provide frequency and voltage support for load peak shaving, valley filling, and shifting.

The concern, however, is how to ensure the grid's security during flexibility exchange from the DER units in the distressed transmission network regions. The flexibility operating region for the active and reactive power transfer from the distribution network under security constraints is one of the proposed approaches to ensure the grid's security during flexibility operations [11]. Figure 6.1 illustrates the interaction between the TSO and DSO for optimal flexibility operation in the modern grid. The interaction is established through coordinated real-time data exchange at the phasor measurement unit (PMU) hub. The flexibility operating region is subsequently established using appropriate optimization techniques considering required constraints at the T-D network boundary. The DER units within the distribution network are aggregated and dispatched following successful negotiations. The aggregator uses real-time synchronized data to achieve flexibility activation from the VPPs at the optimal cost.

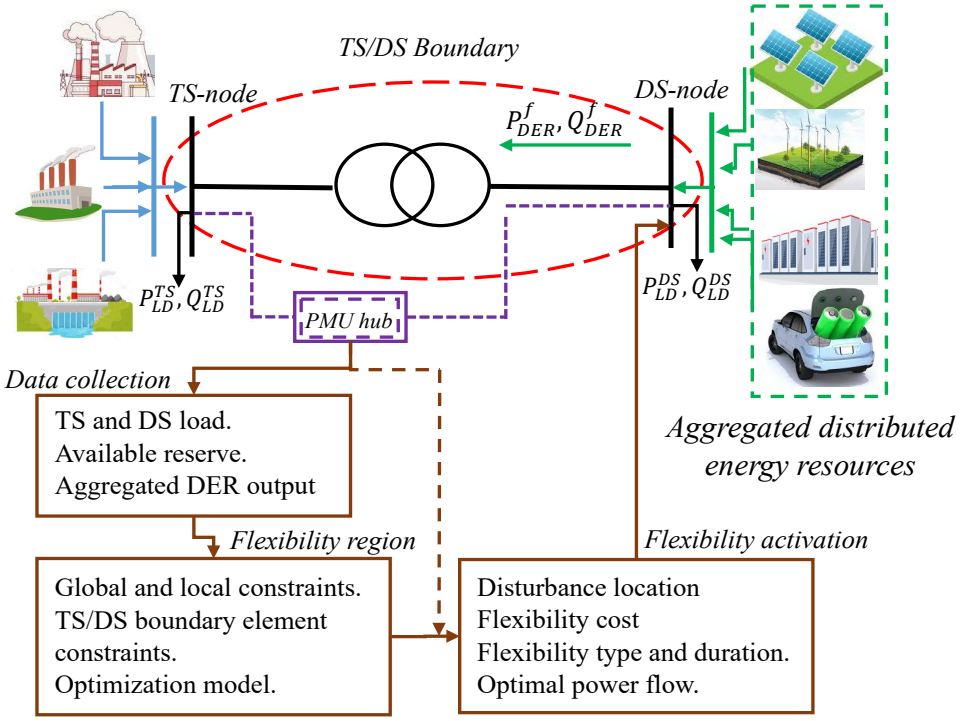

Figure 6.1: Interaction illustration between the TSO and DSO

Aggregated distributed energy resources (DERs) units operate similarly to conventional power plants when participating in the energy market as a unit [272]. A major component of the aggregated DER units is an efficient energy management system that can schedule and control the individual power generation sources in the aggregated units. Depending on the need of the grid for voltage regulation, DER unit proprietors may act as load or generators accordingly. Efficient operation of the aggregated DER units can minimize reliance on fossil fuels generation units, reduce the cost of voltage control and significantly reduce carbon emissions caused by power generation. Aggregating DER units also reduces the impact of unstable output from individual DER units on the grid. A major drawback of aggregated DER units is that the units are installed at different locations within the distribution network. Also, the interaction between the transmission and distribution network operator for efficient control of aggregated DER units during flexibility operation requires complex algorithms [345].

Assuming a balanced distribution network, the operational constraints of aggregated DER units are formulated as shown in (3) to (5). The active and reactive power injection into the network branches is given in (3) and (4), where B is the vector of possible active and reactive dispatch from the aggregated DER units. The security with respect to the distribution network branch (i, j) where the aggregated DER units are connected is constrained by (5). The active and reactive power balance at each node is constrained by (6). The voltage magnitude limit at each network node during DER unit operation is enforced by the inequality constraint in (7). The aggregated DER units operating limits are represented by (8), where R is the set of active and reactive power that can be activated securely by the distribution network operators.

$$P_{DER}^{f(i,j)} = F_{i,j}(v,\theta) \qquad \forall_{ij} \in B \tag{3}$$

$$Q_{VPP}^{f(i,j)} = F_{i,j}(v,\theta) \qquad \forall_{ij} \in B \tag{4}$$

$$P_{VPP}^{f\,(i,j)} + Q_{VPP}^{f(i,j)} \leq S_{VPP}^{i,j}\ \forall_{ij} \in B \tag{5}$$

$$P_g^i - P_d^i = \sum P_t^{i,j}\ ,\ Q_g^i - Q_d^i = \sum Q_t^{i,j} \qquad \forall \in N \tag{6}$$

$$V_{min}^i \leq V^i \leq V_{max}^i \qquad \forall \in N \tag{7}$$

$$(P_{DER}, Q_{DER}) \in R \qquad \forall \in N \tag{8}$$

6.4.2 Flexibility categories and implementation

The increased penetration of variable energy generation source units into the distribution network will increase the responsibilities of the network operators, from ensuring the secured network operation to managing flexibility services. Excess power generation, overvoltage, and reverse power flow are some challenges to consider during network planning and operation. Energy storage systems and power flow redirection effectively mitigate the challenges. While energy storage systems can only store a limited amount of power, power flow redirection achieved by network reconfiguration can transfer the excess power to areas at lesser losses and without violating security constraints. One of the objectives of the grid operators is to maximize the flexibilities of the modern distribution network to enhance the performance of the grid. Integrating tie-lines for possible network reconfiguration in responding to changes in generation and load within the distribution network is one way to achieve this objective. Also, in the event of planned or unplanned outages, tie-lines are employed to ensure network reliability and resilience [346]. Conclusively, the use of network reconfiguration in the modern distribution network is associated with the distribution network's flexibility services. Figure 6.2 shows examples of flexibilities categories and implementation technologies. The flexibility categories and technologies can be implemented at all levels of the network, from local to system-wide implementation. However, due to specific device characteristics, some technologies are more suitable for specific categories and implementation levels. As flexibility is measured in quantity and time, optimization is thereby necessary to achieve the best flexibility operation. The optimal flexibility operation is not completed without considering the electrical distance from the implementation technologies to the area/zone of interest. Since the implementation technologies are pre-installed within the distribution networks, dynamic distribution network reconfiguration can be used to minimize the electrical distance between the flexibility source and the disturbed area/zone within the network.

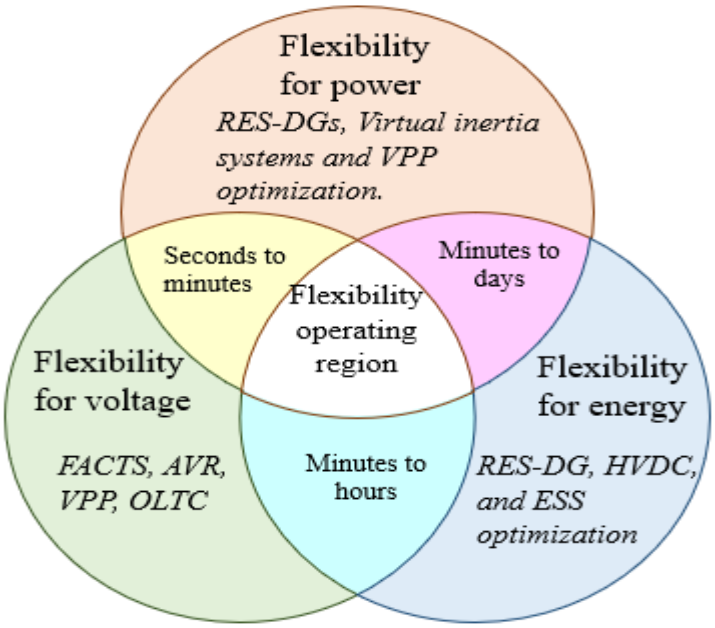

Figure 6.2: Flexibility categories and implementation

Utilizing the substantial potential of variable energy generation sources to provide regulation power and voltage control supports is essential for a secured and reliable power grid with high penetration of variable energy generation sources. Recent studies have demonstrated the capability of these variable energy generation sources of modern grids to contribute to the grid's localized and area-wide voltage control. Modern operators are revising their grid codes to create more effective voltage controllers for control support from variable energy generation sources [127]. Modern power grid management and control face major challenges, including planning the necessary power reserve in light of the rapidly increasing variable energy generation sources and their effects on power grid performance. A suitable approach can be seen in the contribution of variable energy generation sources to the provision of a regulated power reserve. Currently, in some cases, the design and functionalities of variable energy generation sources are comparable to conventional SGs [127]. For example, the time required for a conventional generating unit to ramp up power generation to the desired level is significantly larger than the time required by the variable energy generation sources. The variable generation resources can therefore be configured to perform grid regulation tasks as traditional generators. The variable generation resources can receive the desired voltage set-points and other required operation/control commands from the distribution network operators to produce the required voltage regulation support. These commands are distributed between the aggregator to determine the contribution amount for each participant aggregated DER units in the grid voltage regulation. The required amount of active and reactive power from the aggregated DER units will be determined through the hosting capacity of the distribution network.

Power system flexibility planning and operation is a complex optimization problem that involves various components for implementation through embedded algorithms [302]. The planning and operation process of flexibility in modern distribution networks can be modeled in three steps, as

depicted in Figure 6.3. The evaluation of the impact of flexibility operation in the individual network is important in the flexibility planning stage in step one. An estimation of the level of flexibility reserve and security constraints is necessary to plan the flexibility operation of the power system appropriately and to identify both immediate and probabilistic future demands. Step two emphasizes the need to invest in sources of different types of flexibility that may be required if the flexibility security requirements of the grid in step one are not met. The flexibility sources are preferred based on factors such as cost-effectiveness, gestation period, and location. The modeling and estimation of the safe flexibility operating region with respect to the flexibility exchange between area/zones and the transmission/distribution boundary in the network is also important for secured grid operation. The final step involves optimizing the flexibility generation considering parameters like location, generation mix, and generation capacities. The final step in the optimal flexibility operation model is flexibility quantity estimation and prediction. The ability to predict the exact quantity needed to support the grid for anticipated disturbances will reduce the cost of flexibility operations.

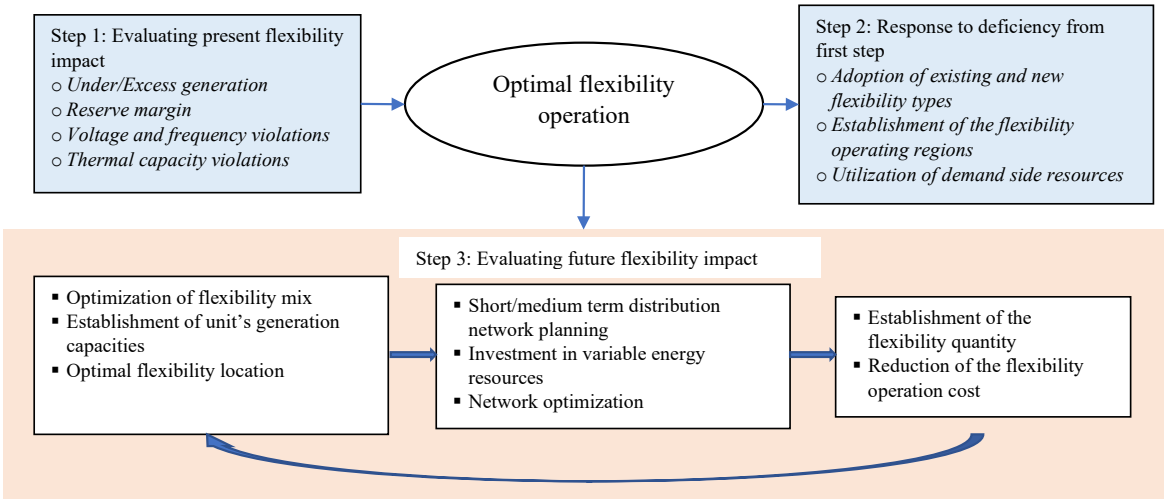

Figure 6.3: Operation model for optimal power and voltage flexibility

6.5 Proposed Approach

The reconfiguration of the distribution network considering the operations of variable energy generation sources is a probabilistic planning and operation problem that must account for uncertainties. Possible contingencies and variations in the output of the variable energy generation sources units and node loads are among the uncertainties that must be considered for modern distribution network reconfiguration. The variations in the node load are modeled using probability distribution functions. However, given that the distribution network's topology remains constant before and after implementing reconfiguration schemes, both deterministic and stochastic variables can be considered in the reconfiguration problem formulation. This paper, therefore, seeks to propose a technique to mitigate the impact of voltage support unit operations such as aggregated DER units on the distribution network through network reconfiguration and flexibility quantity estimation.

The bilevel process of the proposed technique in this paper is shown in Figure 6.4. The first stage involves economic consideration, achieved through reconfiguration problem modeling. The objective is to minimize the cost of flexibility operations through reduced net power loss after network reconfiguration. The variables and the constraints considered are the probabilistic risk index and the network hosting capacity. The developed multi-variable optimization problem is solved using the constrained fmincon optimizer. The fmincon optimizer starts from an initial estimate and finds a constrained minimum of a scalar function of several variables. The fmincon optimizer supports linear and non-linear constraints while performing non-linear constrained optimization. The solver configuration includes settings for convergence criteria, maximum iterations, and the calculation of gradients. The second stage involves technical considerations, estimating the flexibility required to achieve specific voltage support during disturbances. The machine learning classification technique is applied to the developed dataset from several Quasi-dynamic state simulations with specific attributes.

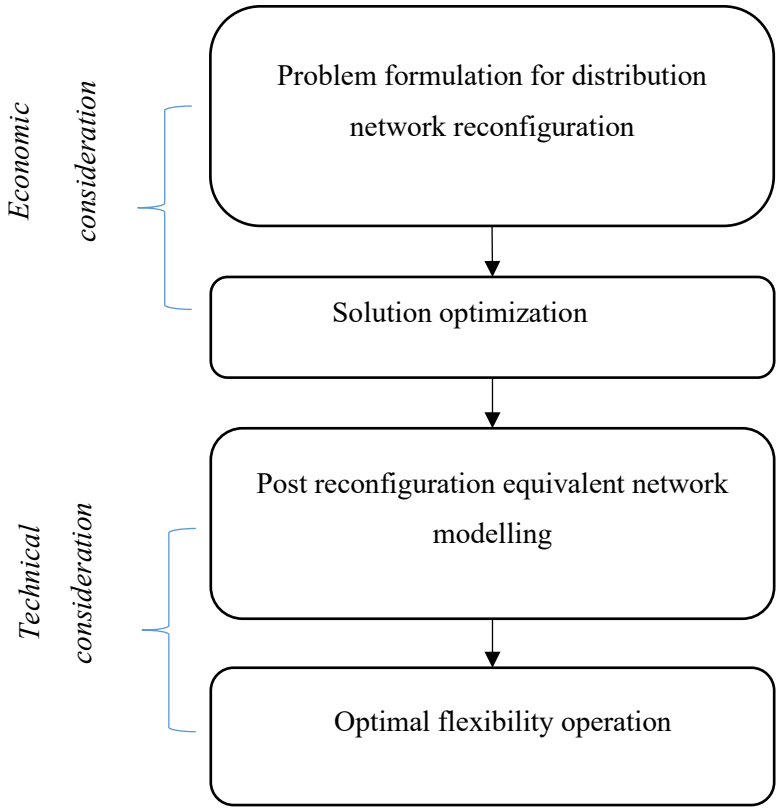

Figure 6.4: Overall framework of the proposed bilevel optimization approach

6.5.1 Network reconfiguration problem formulation

Radial distribution network reconfiguration is a practical method for enhancing distribution network performance. Changes in configurations can be made to ensure load supply, power loss reduction, system security improvement, and power quality enhancement. Additionally, the reconfiguration lessens the network components' overload. Switching operations for reconfiguration action can be either manual or automatic. The reconfiguration also relieves the overloading of the

network components [318]. The goal of distribution network reconfiguration is to reduce net power loss (PL) while considering the distribution network's suggested deterministic and probabilistic factors. To achieve this goal, the network's switches' states must be changed while adhering to equality and inequality requirements. The distribution network reconfiguration problem is formulated as (9) subject to the power flow (PF), probabilistic risk index (x),hosting capacity (y), and radiality constraints in (10) to (14).

$$\min PL = f(x, y) \tag{9}$$

$$PF\left(P_j, Q_j, V_i, \theta_i\right) = 0 \tag{10}$$

Subject to:

$$x_1 \leq x \geq x_2 \tag{11}$$

$$y \geq y_1 \tag{12}$$

$$PL = \sum_{j=1}^{m}. I^2(j)R(j) \tag{13}$$

$$m = n - 1 \tag{14}$$

where n is the number of nodes, m is the number of branches, I is the current, R is the resistance of the line, and Q_j are the active and reactive power flow on the branch j, respectively.

6.5.1.1 Hosting Capacity

IEEE 1547.1 standard must be followed in designing and managing a distribution network using variable generation resources. This standard provides crucial variable generation resource penetration conditions for safe network operations. The hosting capacity (HC) is an index that determines how much power generated by variable generation resource units can reach the distribution network while maintaining the grid's security within acceptable parameters, given the limits and limitations of the current network setup. After a change in network configuration via reconfiguration, enlargement, and reinforcement, the network's new hosting capacity must be established. With the ability to estimate hosting capacity, distribution operators now have a new security-based index to measure how variable generation resources have affected the functioning of the distribution network and the grid as a whole. Hosting capacity values may be assigned to network nodes while considering nodal restrictions. It is possible to obtain the hosting capacity values for each node and for the entire distribution network. The nodal hosting capacity is preferable and common in the literature because it is a function of the distance between the network substation and each distribution network node. The nodal hosting capacity is expressed as the ratio of the total power generation from the variable generation resources units (S_{vr}) to the total load (S_{ld}) connected to the node. Constraints selection, definition, hosting capacity estimation, and verification of security limit violations are the major steps in establishing a network's hosting capacity. If i and j represent the node and branches, respectively, then the current (I) which represents thermal, voltage (V), voltage

harmonics (V_{thd}) and fault current (I_f) constraints used to evaluate the distribution network nodal hosting capacities in this paper are defined in (15) to (18).

$$I_i \leq I_{i,max} \tag{15}$$

$$V_{j,min} \leq V_j \leq V_{j,max} \tag{16}$$

$$V_{thd,i} \leq V_{thd,i,max} \tag{17}$$

$$I_{f,i} \leq I_{f,i,max}, \tag{18}$$

6.5.1.2 Distribution Network Probabilistic Risk Assessment

This study models the network nodes' probabilistic risk index before and after changes in the network configuration using the risk related to node voltage. The probabilistic risk index measures the likelihood that the voltage at the distribution network nodes will exceed predetermined security thresholds. The nodal probabilistic risk index (PRI) can be estimated using (19), where the voltage probability (P_v) and the severity (A) can be derived using (20) and (21), respectively. Using the Monte-Carlo simulation-based probabilistic load flow (MCSPLF) approach, the overvoltage or undervoltage probabilities are determined. The probability distribution function used to simulate changes in the loads and power generation under the assumption of a constant power factor is shown in (22).

$$RI(i) = P_v(i) * A(i) \tag{19}$$

$$P_v(i) = \lim_{N\to\infty} \frac{(n_1)}{N} + \lim_{N\to\infty} \frac{(n_2)}{N} \tag{20}$$

$$A(i) = \left|1 - \overline{V}(i)\right| \tag{21}$$

$$f(P_s, Q_s: P_l, Q_l) = \frac{1}{\sqrt{2\pi\sigma(P,Q)}} exp\left(-\frac{((P,Q)-\mu(P,Q))^2}{2\sigma^2_{P,Q}}\right) \tag{22}$$

where N is the number of simulations, $\overline{V}$ is the average voltage for N sample of instances, n_1 is the total number of $\overline{V}$ lesser than 0.95 pu, n_2 is the total number of $\overline{V}$ greater than 1.05 pu, P_s is the active power supply, Q_s is the reactive power supply, P_l is the active load, Q_l is the reactive load, while μ and σ are the expected mean value and standard deviations, respectively.

6.5.2 A Random tree classification algorithm

A random tree is constructed randomly from a set of possible trees with K random features at each node. Each tree is assigned an equal sampling probability in the set of trees. Random trees (RT) provide simple human-readable rules and are effective for classification optimization problems. The model of the RT is from the physical tree structure consisting of roots, nodes, and branches. An RT is constructed from nodes and edges that are arranged in a hierarchical pattern [347]. The RT node represents specific characteristics and attributes of the dataset, while the branches represent the

values of the attributes. The attribute's range of values impacts the attributes' partitioning points. To create the RT structure, a data instance is classified based on predefined conditions and characteristics that best divide the dataset. The classification progresses from top to bottom, and the dataset instances are split according to the values of the attributes until a terminal node representing the objective is obtained. The classification process is applied to each split subset of the dataset recursively. The process terminates when all the dataset instances in a current subset belong to the same class. The RT algorithm was adopted in this paper because of its flexibility, capability to handle numerical and categorical data, and excellent performance with small and large datasets. Random trees can be generated efficiently, and combining large sets of random trees generally leads to accurate models [348]. The generic structure of an RT is shown in Figure 6.5. The three major steps to developing an RT classification model are attribute selection for the root node, splitting instances into subsets, and recursive repetition for each RT node.

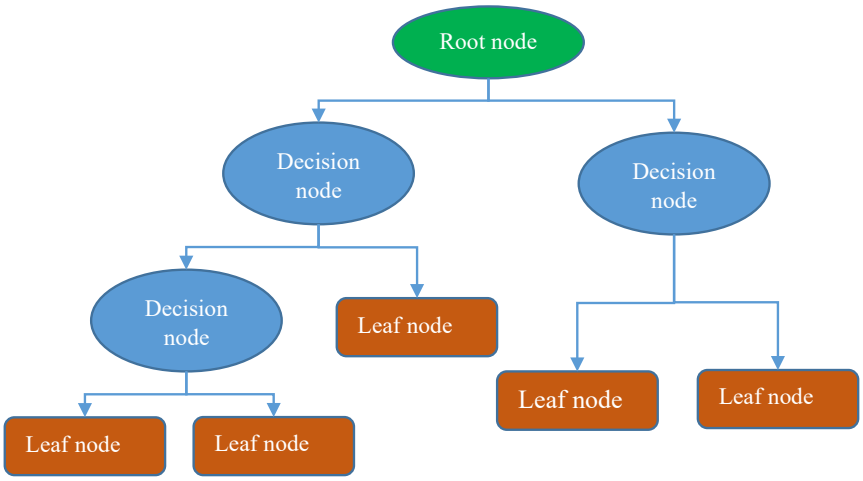

Figure 6.5: Decision tree model

The Gini index measures the integrity of the attributes on which the splitting action is performed. Since the Gini index measures the impurity of the dataset, the dataset attributes with the highest Gini index are chosen as the best split for that node [301]. The Gini index can be calculated using (23).

$$Gini(n) = \frac{1}{2} - [1 - \sum_i p(\omega_i)^2] \quad (23)$$

where $p(\omega_i)$ is the relative frequency of class ω_i at node n. The impurity in the attribute is zero if the samples are in the same group; otherwise, (23) returns a positive value. The classification outcome is impacted by the predictive power of the developed dataset. The predictive power can be estimated using the entropy-based information gain model. The entropy-based information gain is a feature selection method used to calculate the loss in entropy, representing the impurity level in a given dataset [313]. The information of the attributes with an information gain value higher than the average represents the predictive power of the dataset. For example, given a dataset N containing instances with each of k outcomes, the entropy of N is given in (24), where $p(I)$ is a portion of N

belonging to class I. If the value of the entropy is k, then all instances of N belong to the same class. For an attribute x of sample set N, the information gain $G\ (N,x)$ is defined as (25).

$$E(N) = -\sum_{I \in k} p(I) \log_2 p(I) \tag{24}$$

$$G((N,x) = E(N) - \sum_{j \in x} \left(\frac{|N_j|}{N} \right) \tag{25}$$

6.6 Results and Discussion

6.6.1 IEEE 33 node Distribution network

6.6.1.1 Base network result

This section presents the results of testing the proposed technique on the IEEE 33-nodes distribution network. The test distribution network with the identified loops generated from the tie lines (T) and section line switches (S) is shown in Figure 6.6. The loops are obtained by closing the normally open switch T. The substation represents the interface between the transmission and the distribution networks. The normal load flow result shows that 18 nodes out of 33 nodes are outside the security limit. Also, under probabilistic load flow analysis, 72% of the node exist out of the security limit with the mean voltage and standard deviation of 0.89 and 0.009, respectively. The total normal state power loss is 212.4 kW, with nodes 1 to 6 accounting for about 68.6% of the total loss. Figure 6.7 shows the probabilistic risk index (PRI) of the IEEE 33-node network when the aggregated DER unit is connected to branch 1. The PRI is proportional to the total branch load and the distance of the connecting node from the substation. The values of the PRI for the base network are considerably high due to constant variations of loads on the branches. The connection and operation of aggregated DER units will understandably increase the PRI value due to variations in the output levels of the generations. At certain periods of the day, undervoltages and overvoltages may be experienced around the nodes with connected DER units due to undergeneration and overgeneration of power, respectively. Branch 4 has the highest branch contribution to the network average risk index, at 9.24%, accounting for 42% of the network's PRI.

The technique proposed in this paper will enable distribution network operators and aggregators to securely operate aggregated DER units, thereby promoting more penetration of DER units in the distribution network. Branches 4 and 2 have the highest and lowest average hosting capacities of 5.56 MVA and 0.57 MVA, respectively. Figure 6.8 shows the probabilistic line loading of the network with and without the operation of aggregated DER unit on the first node of the network branches. In consistency with the advantage of the DER's optimal operation, the network's line loading under probabilistic loading is considerably reduced for each branch. The branch loading and the distance of the branch from the substation impact the percentage line loading reduction obtainable under constant network parameters. The highest reduction of 55.1% was obtained from branch 4. The probabilistic power loss reduction obtained for branch one is inconsiderable due to the number

of load points connected and the size of the load connected. The power loss reduction of 140 MVA was obtained after connecting the aggregated DER unit on the first nodes on branches 2 and 3, shown in Figure 6.9. The best hosting capacity conservation of 90.7% was obtained when the aggregated DER unit was connected to branch 4. An average percentage reduction of 39.42% in the hosting capacity was recorded after connecting the DER unit to the distribution network.

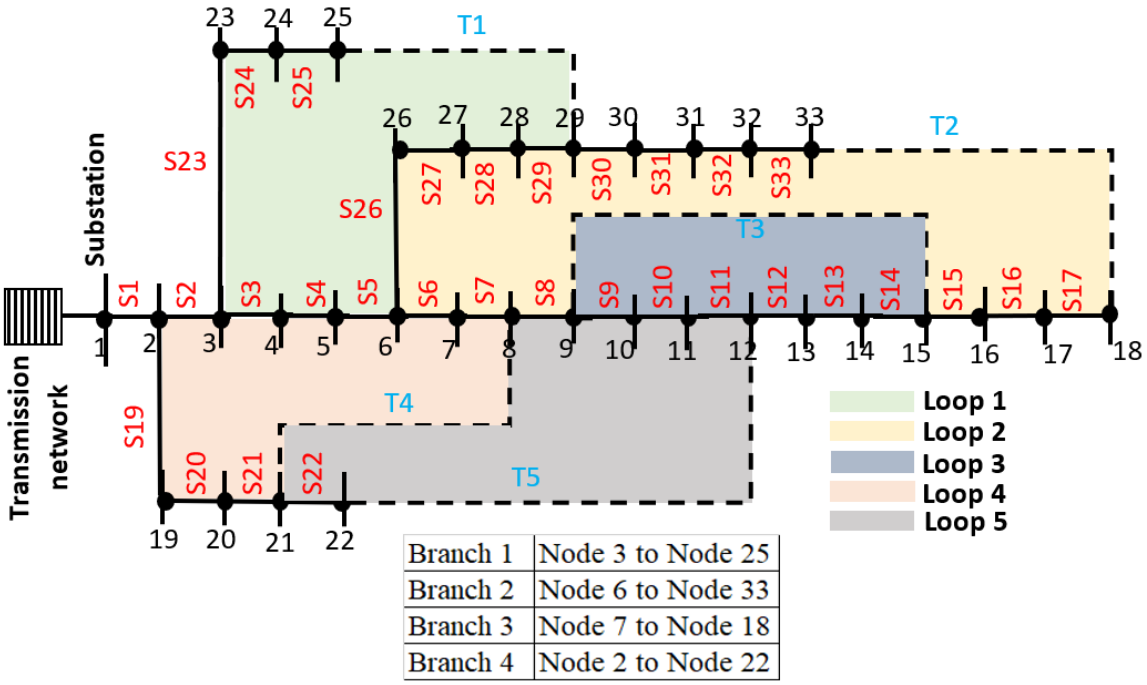

Figure 6.6: Initial networks showing the loops

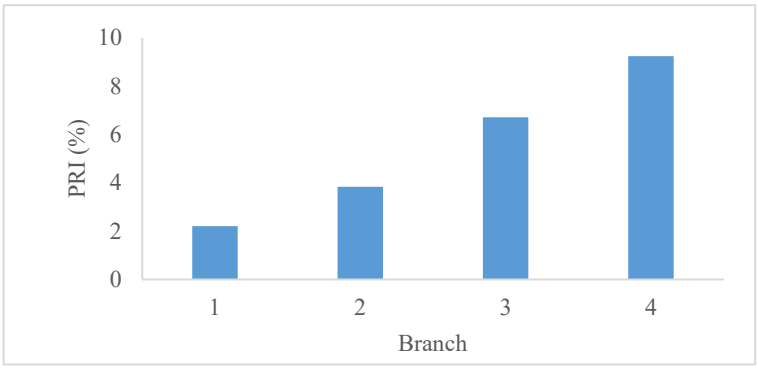

Figure 6.7: Network hosting capacity and risk index

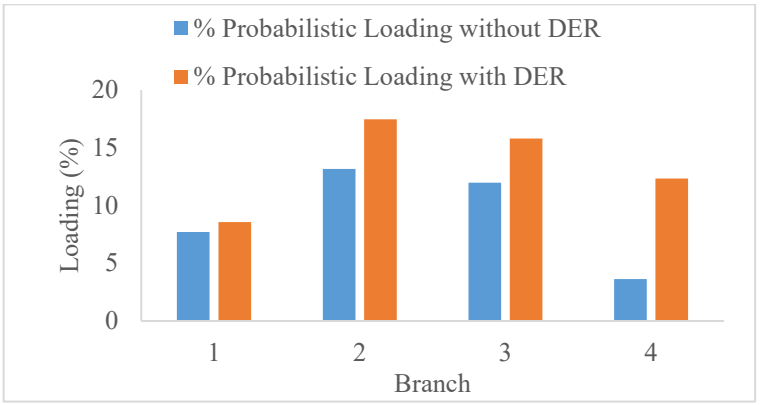

Figure 6.8: Probabilistic line loading with and without aggregated DERs

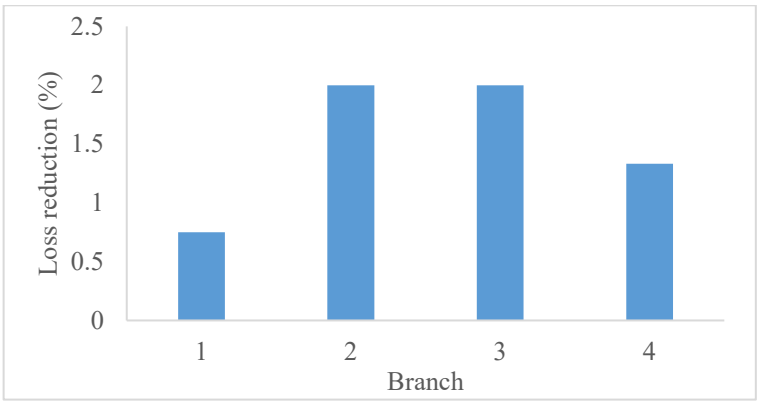

Figure 6.9: Percentage power loss reduction with DER units operations

6.6.1.2 Optimization results

This section presents the solution to the distribution network reconfiguration optimization problem. The fitness functions in this paper are developed to achieve a configuration that minimizes the network power loss considering the risk index and hosting capacity variables presented in section III. The opening operations of the section (S) and the tie (T) switches for the loop under consideration achieve the desired configuration. Also, the fitness functions are derived such that there is no mesh network within the distribution network, thereby ensuring the radiality constraint of distribution network reconfiguration. The radiality constraint ensures that no node is left unserved after network reconfiguration. The fitness functions are developed for each loop within the distribution network. Figure 6.10 shows the global optimal values after 20 iterations for the loops obtained using the fmincon optimization algorithm. The lowest and highest standard deviations of 0.032 and 0.0779 from the optimal values were obtained from loop 1 after 20 iterations. The x and y values corresponding to the PRI and the hosting capacity values for the optimal power loss values for each loop are shown in Table 6.1. The section line switch to achieve the required reconfiguration is indicated in Table 6.1.

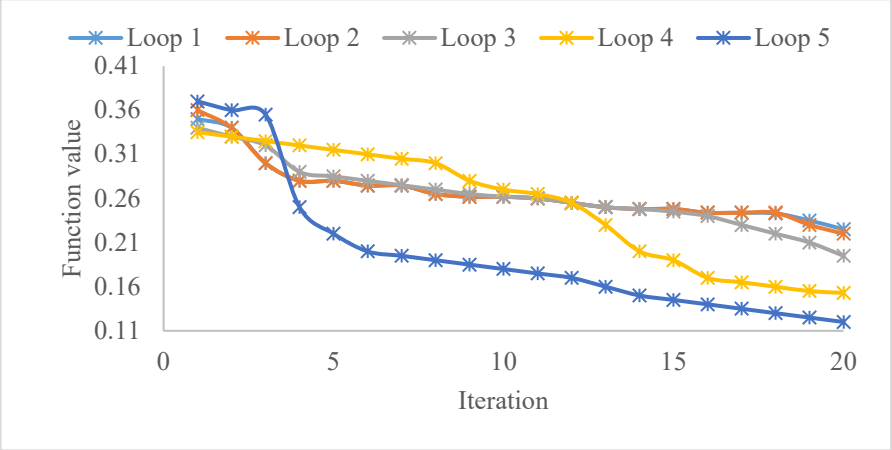

Figure 6.10: Loop optimization objective values

Table 6.1: Optimal solutions for reconfiguration

Loop	*PLI*	*HC*	Section line switch (S)
1	8.95	2.32	S29
2	8.56	2.16	S11
3	10.76	2.3	S12
4	7.22	2.28	S6
5	6.64	2.32	S8

6.6.1.3 Reconfigured network results

The reconfigured network models and the optimization variables' results are presented in this section. Figure 6.11 shows the reconfigured networks for each loop. The highest probabilistic risk index reduction is obtained from the reconfigured network for loop 1, as shown in Figure 6.12. The average network PRI was reduced by 41.8%, with the highest reduction of 94.6% from loop 4. The maximum and average hosting capacity was increased by 62.5% and 13.36% for loop 1 network reconfiguration. Figures 6.13 and 6.14 show the power loss and line loading reduction of the network with aggregated DER unit operation before and after network reconfiguration. Considerable reductions of 25% and 22% were achieved for the power loss and line loading, respectively, by connecting the aggregated DER units to branch 1 on node 23 of the reconfigured network considering loop 1.

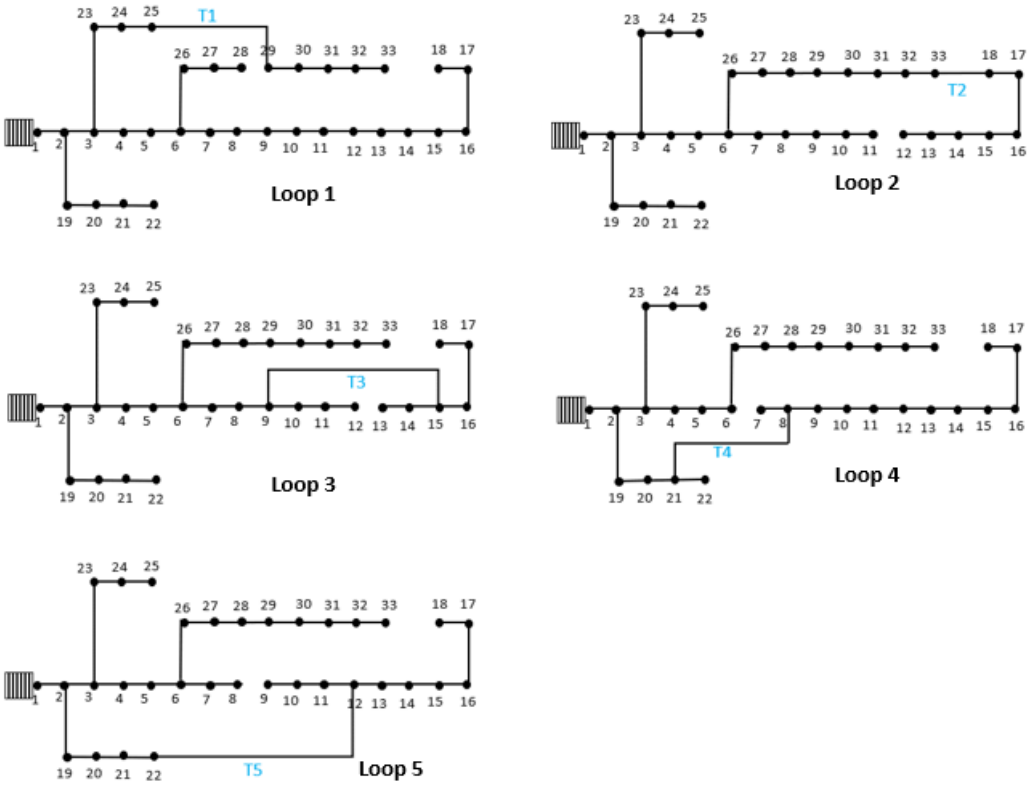

Figure 6.11: Reconfigured network for each loop

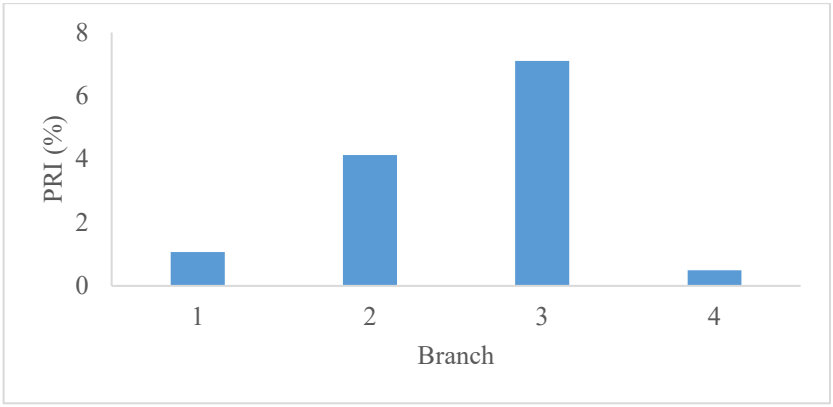

Figure 6.12: Probabilistic risk index of branch with aggregated DERs

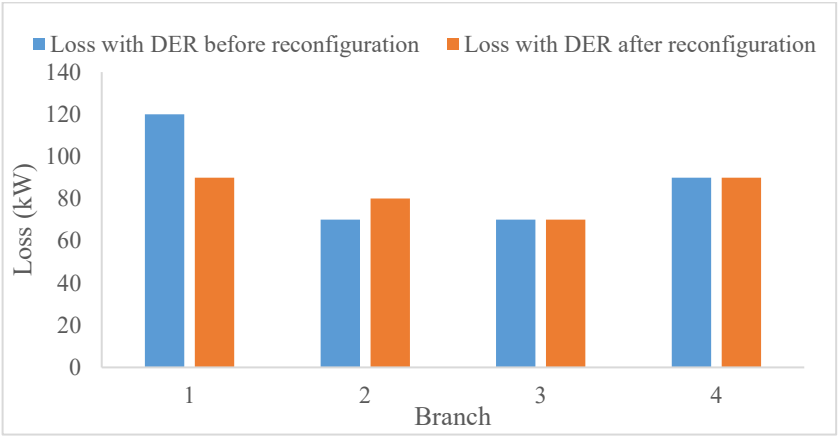

Figure 6.13: Power loss change with DER units' operations

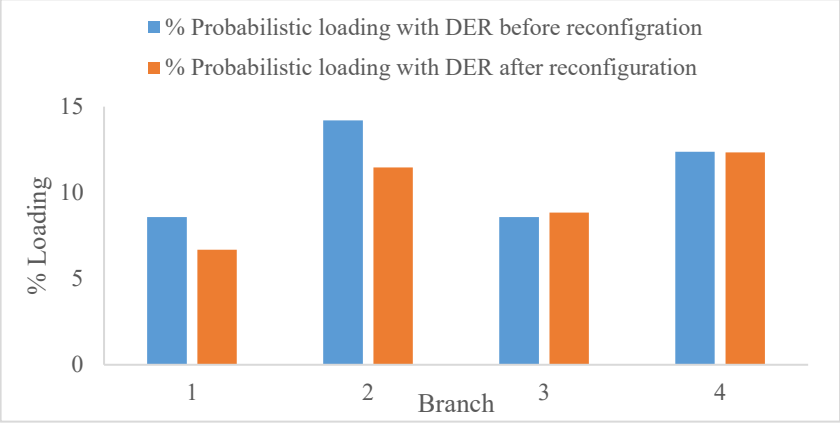

Figure 6.14: Probabilistic line loading with DER units

Figure 6.16 shows the voltage response of the reconfigured networks under the step load changes in the load profile shown in Figure 6.15 with and without the operation of the aggregated DER units. The operation of the aggregated DER unit is implemented through the dispatch and switch events. The sudden increase in load is activated on the node with the highest load on the branch at 4.00 pm. The flexibility from the aggregated DER unit is also activated on the first node on the branch and activated at 4.00 pm and deactivated through the switch event at 6.00 pm. The minimum voltage obtained from branch 3 due to the 100% load increase from the average network load was improved by 5.05%. More voltage deviation reductions are obtained through the minimum generation of 3 MW and power factor of 0.85 from the aggregated DER units.

Figure 6.17 shows the improvement in the voltage deviations obtained in loop 1 for branches 2, 3, and 4. The highest improvements of 8.99% and 5.87% were obtained when the aggregated DER unit was connected to branches 4 and 3, respectively. The minimum voltage is greater for low impedance branches and large load change events. Figure 6.18 shows the voltage deviation improvements for the loops and branches of the network load changes. The voltage deviation improvements are greater for branches with lower impedance values. Branch 1 presents a uniform average improvement of 3.8% in the minimum voltage during the load change event across the network loops. Reconfigured network with loop 3 generates the highest minimum voltage improvement with DER unit operation.

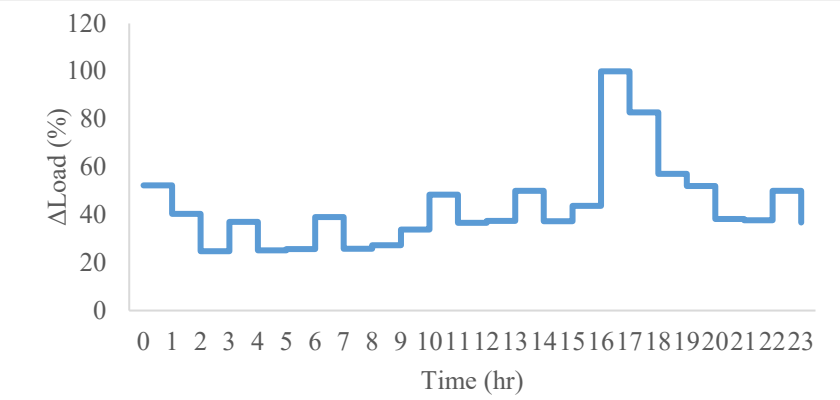

Figure 6.15: Load change event profile

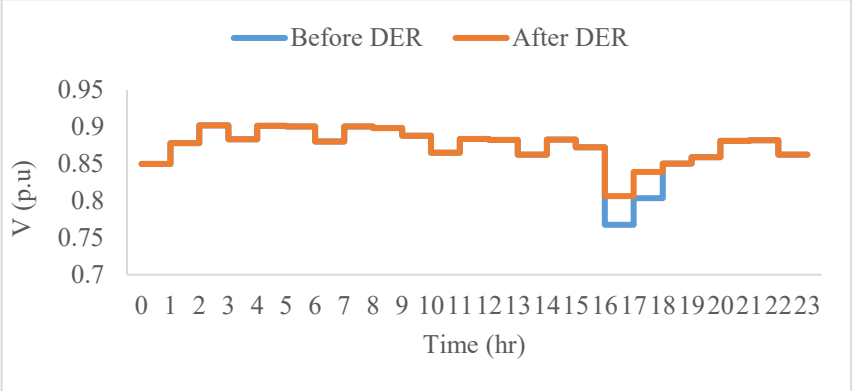

Figure 6.16: Voltage support from the DER units on Branch 1 from loop 1

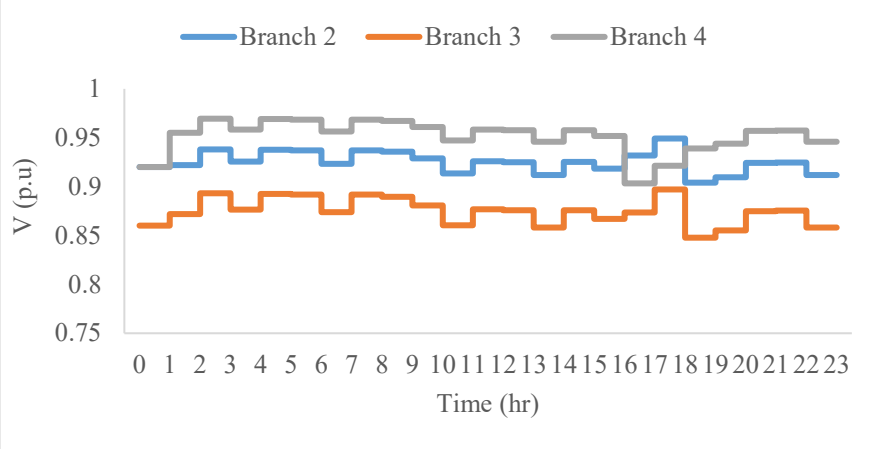

Figure 6.17: Voltage support from DER units for branches 2, 3 and 4

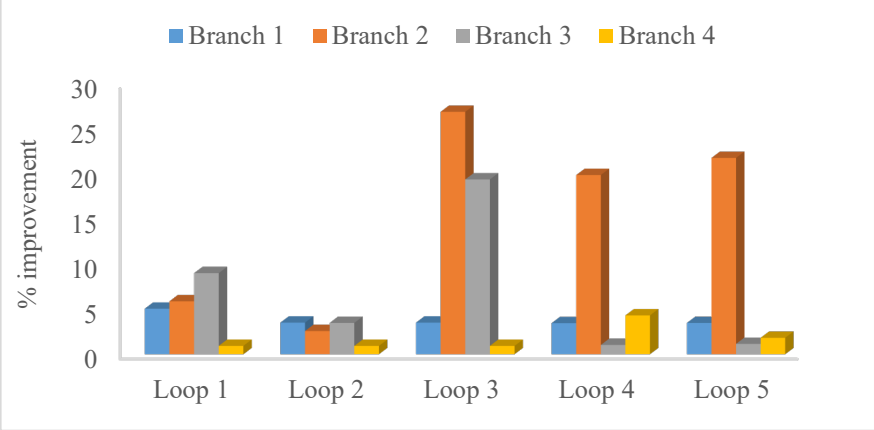

Figure 6.18: Percentage improvement from DER units for each loop and branch

6.6.2 IEEE 69 node distribution network

6.6.2.1 Base network results

This section presents the results of testing the proposed technique on the IEEE 69 nodes distribution network. The test distribution network with the identified loops generated from the tie lines (T) and section line switches (S) is shown in Figure 6.19. The normal load flow result shows 47 out of 69 nodes are outside the security limit. Also, under probabilistic load flow analysis, 80% of the node exist out of the security limit with the mean voltage and standard deviation of 0.88 and 0.0163, respectively. The normal state power loss is 210.8 kW, with branch 6 accounting for about

56.17%. Figure 6.20 shows the probabilistic risk index of the IEEE 69 node network. The values of the PRI for the base network are considerably high due to constant variations of loads on the branches. Like the IEEE 33-node test network, the connection and operation of aggregated DER units predictably increase the PRI value due to variations in the output levels of the generations. Branches 7 and 8 have the highest and lowest average hosting capacities of 3.01 MVA and 2.24 MVA, respectively. The average hosting capacity conservation of 93.3% was obtained when the aggregated DER unit was connected to branch 1 of the distribution network. Branch 4 has the highest branch contribution to the network average risk index at 22.76 %. The risk index contribution of branches 1 and 7 are insignificant since the least probabilistic voltage of its nodes is within the voltage security limit.

Figure 6.21 shows the probabilistic line loading of the network with and without the operation of aggregated DER unit on the first node of the network branches. In consistency with the advantage of the DER's unit optimal operation, the network's line loading under probabilistic loading is reduced for each branch. The branch loading and the distance of the branch from the substation impact the percentage line loading reduction obtainable under constant network parameters. The highest line loading reduction of 99.83% was obtained from branch 2. The probabilistic line loading reduction obtained for branch 6 is inconsiderable due to the number of load points connected and the size of the load connected. The percentage power loss reduction obtained after the connection of the aggregated DER unit is shown in Figure 6.22. An average power loss reduction of 77.4 MVA was obtained after connecting the aggregated DER unit to the distribution network. The voltage responses of the reconfigured network for several scenarios are afterward determined.

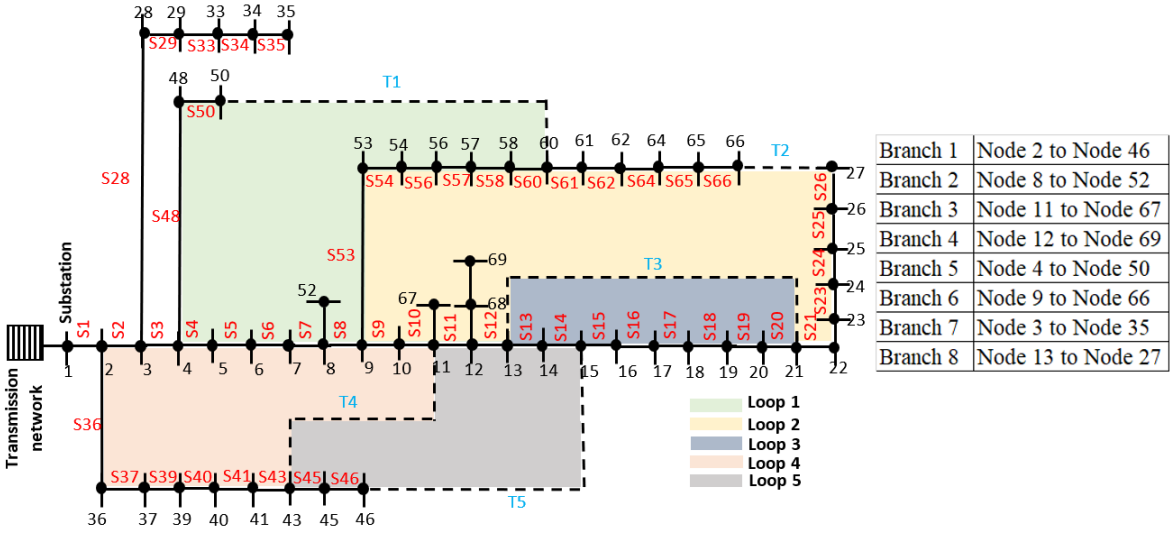

Figure 6.19: Initial networks showing the loops

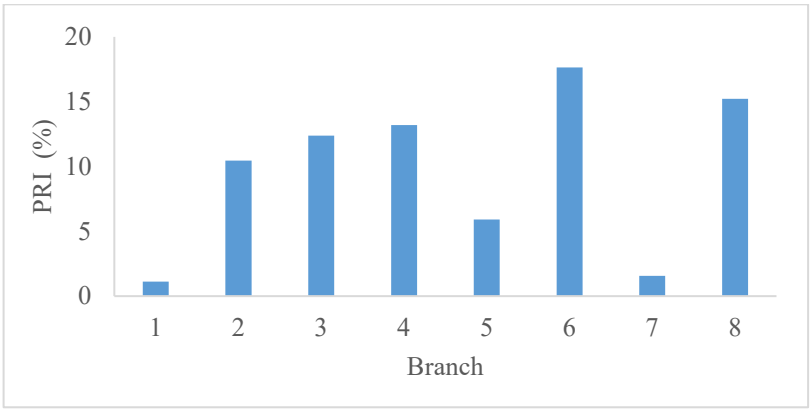

Figure 6.20: Probabilistic risk index of branches with aggregated DER units

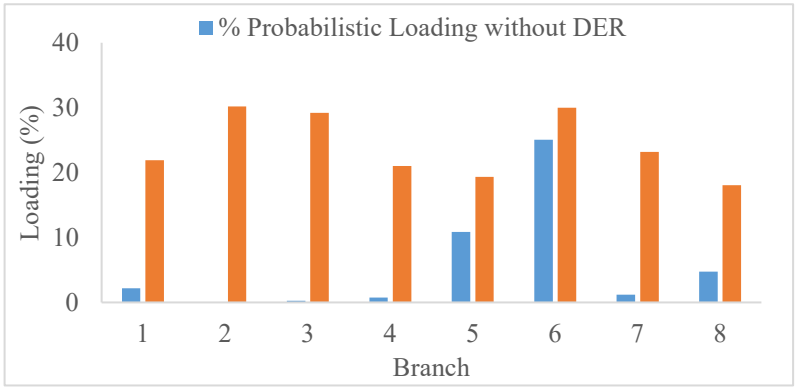

Figure 6.21: Probabilistic line loading with and without aggregated DER units

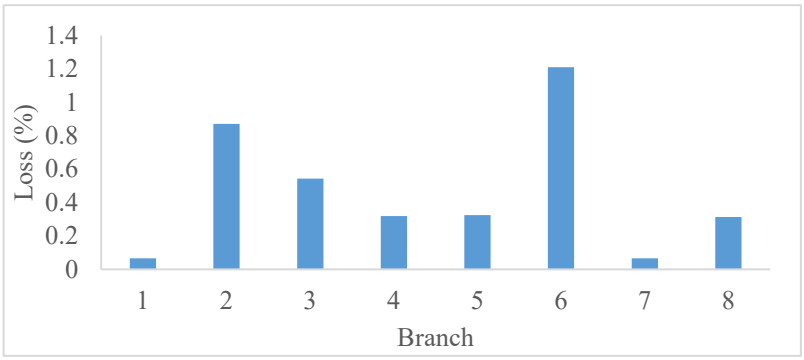

Figure 6.22: Percentage power loss change with DER unit operations

6.6.2.2 Optimization results

The fitness functions for the IEEE 69-node test network are also developed for each loop within the distribution network. The fitness functions are developed to achieve a network configuration that minimizes the network power loss considering the risk index and hosting capacity variables through operations of the section switches (S) and the tie switches (T). Figure 6.23 shows the global optimal values after 20 iterations for the loops. The lowest and highest standard deviations of 0.018 and 0.032 from the optimal values were obtained from loop 1 after 20 iterations. The x and y values corresponding to the PRI and hosting capacity values for the optimal power loss values and the section line switch (S) to achieve the required reconfiguration for each loop are shown in Table 6.2. The fitness function is also derived such that there is no mesh network within the

distribution network, thereby ensuring the radiality constraint of distribution network reconfiguration.

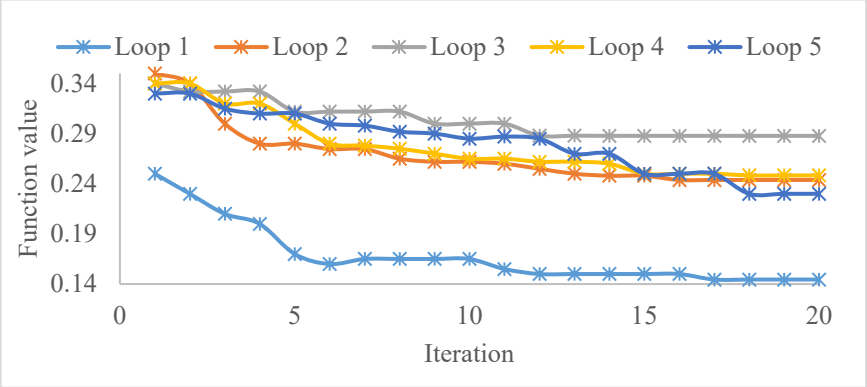

Figure 6.23: Loop optimization objective values

Table 6.2: Optimal solutions for reconfiguration

Loop	*PLI*	*HC*	Section line
1	8.012	3.1	S56
2	12	3.01	S64
3	11.05	3.05	S20
4	9.5	2.95	S41
5	8.68	2.98	S12

6.6.2.3 Reconfigured network results

The reconfigured network models and the optimization variables' results are presented in this section. Figures 6.24 shows the reconfigured networks for each loop. The highest probabilistic risk index reduction is obtained from the reconfigured network for loop 2, as shown in Figure 6.25. The average network *PRI* was reduced by 92.7%, with the highest reduction of 99.2% from loop 2. The minimum and maximum hosting capacity were increased by 16.7% and 2% for loop 1 network reconfiguration. Figures 6.26 and 6.27 show the power loss and line loading reduction of the network with aggregated DER unit operation before and after network reconfiguration. Considerable reductions of 31.7% and 17.58% were achieved for the power loss and line loading, respectively, by connecting the DER unit to branch 1 of the reconfigured networks considering loop 1.

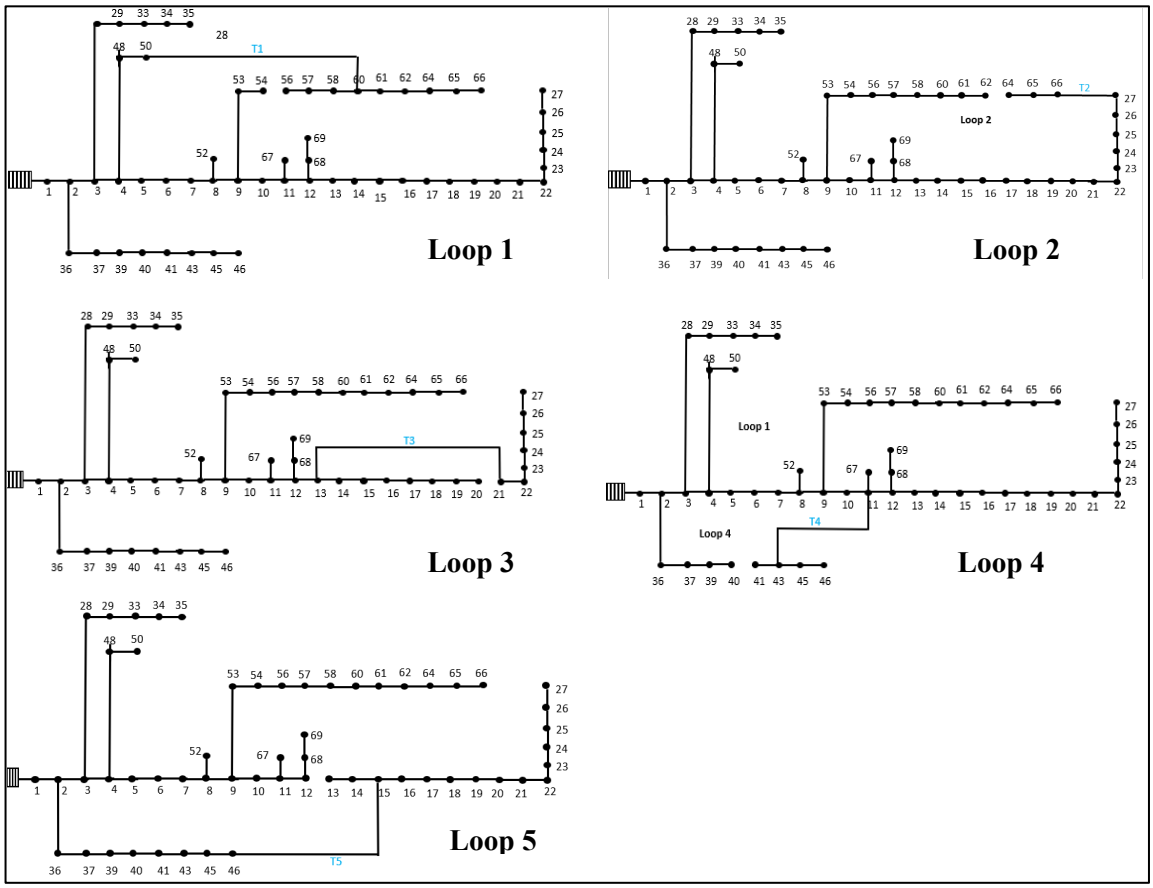

Figure 6.24: Reconfigured network for each loop

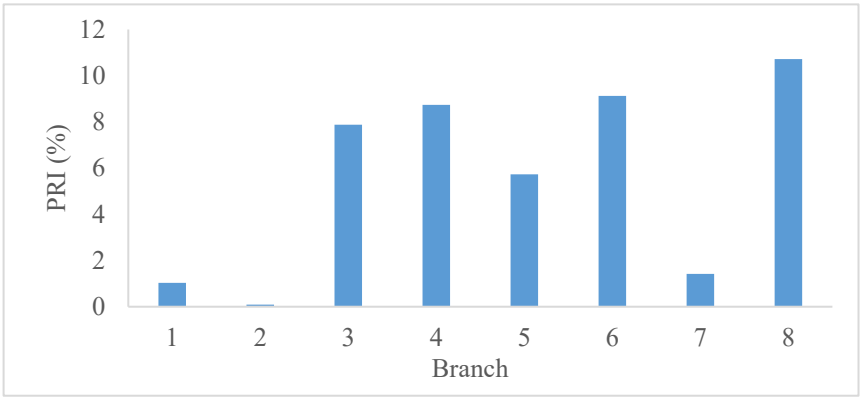

Figure 6.25: Probabilistic risk index of branches with aggregated DERs

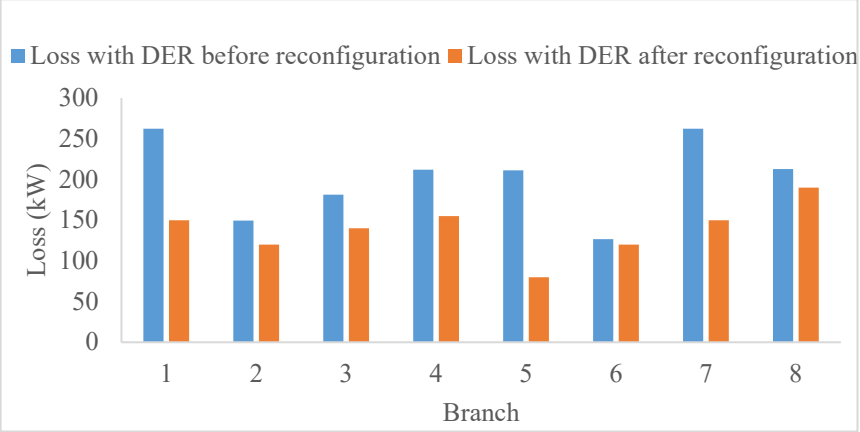

Figure 6.26: Power loss change with DER unit operations

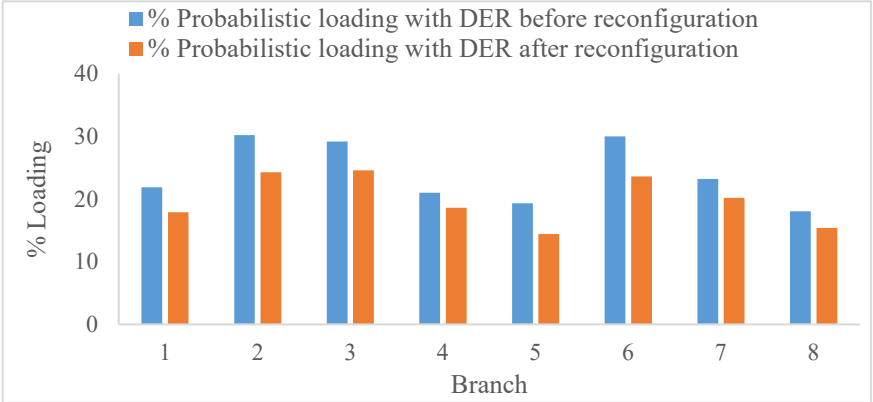

Figure 6.27: Probabilistic line loading with DER units

Figure 6.28 shows the voltage response of reconfigured networks under the step load changes in the load profile shown in Figure 6.15 with and without the operation of the aggregated DER unit. The operations of the aggregated DER unit and the activation of the load and switch events are the same as in section 4.1. The highest minimum voltage improvement of 2.3% was obtained from branch 8. More voltage deviation improvements are obtained through the minimum generation of 3 MW and power factor of 0.85 from the aggregated DER unit. Figure 6.29 shows the improvement in the voltage deviations obtained in loop 1 for branches 5, 7, and 8. The highest improvements of 0.32% and 0.58% were obtained when the aggregated DER unit was connected to branches 5 and 8, respectively. The minimum voltage is greater for low impedance branches and large load change events. Figure 6.30 shows the voltage deviation improvements for the loops and branches of the network load changes. The voltage deviation improvements are greater for branches with lower impedance values. Branch 2 presents the highest average improvement of 15.4% in the minimum voltage during the load change event across the network loops. The reconfigured network with loop 3 for branch 2 generates the highest minimum voltage improvement of 26.8% with aggregated DER unit operation.

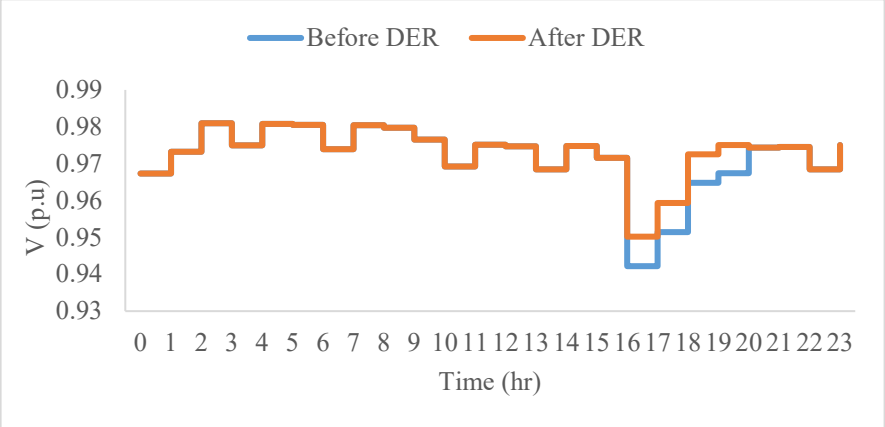

Figure 6.28: Voltage support from the DER unit on Branch 1 from loop 1

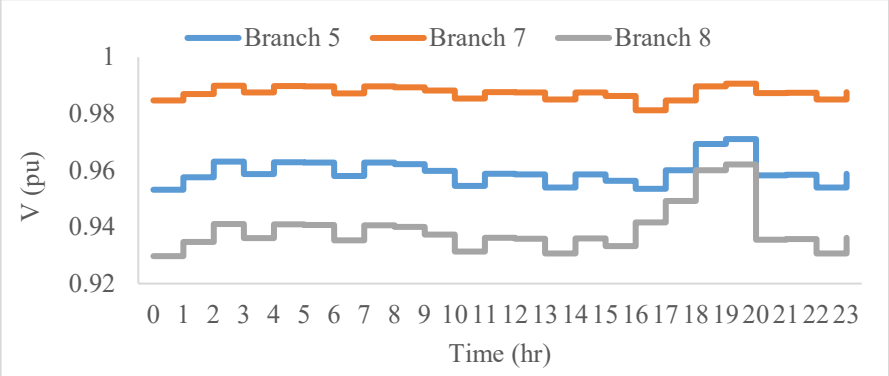

Figure 6.29: Voltage support from DER unit for branches 5, 7 and 8

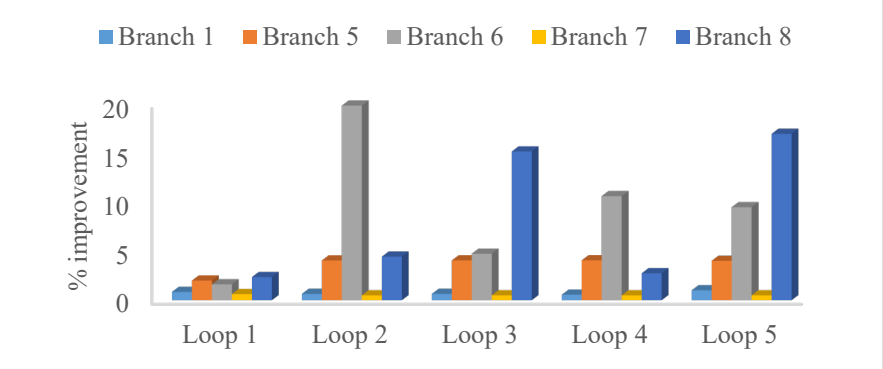

Figure 6.30: Percentage improvement from DER unit for each loop and branches

Table 6.3 compares the proposed methods with other methods described in the literature from the optimization objective(s) perspective. The considered objectives and scenarios in existing literature include but are not limited to power loss, voltage index, economic index, reliability index, probabilistic voltage risk index, and the consideration of renewable energy sources and energy storage systems. Conventional/analytical metaheuristic optimization techniques have proved effective in solving network reconfiguration optimization problems, as shown in Table 6.3. Metaheuristic and machine learning techniques have also shown great potential in network reconfiguration schemes, as shown in the proposed methods. While optimizing the power losses and voltage indices remains the primary objective for most literature, the probabilistic assessments and the consideration for RES-DG units remain scarce. As can be seen, the proposed method in this research addresses the problem of the probabilistic assessment compared with recent papers.

Table 6.3: Comparison with recent literature

Ref	Power loss	Voltage index	Reliability index	Probabilistic assessment	Economic index	RES-DG consideration	Optimization method
[319]	✓		✓				Analytical
[349]					✓	✓	Analytical
[326]	✓				✓		Analytical
[350]	✓	✓					Metaheuristic
[351]	✓	✓				✓	Metaheuristic
[331]		✓	✓		✓		Heuristic
[352]	✓	✓	✓				Metaheuristic
[353]	✓	✓			✓		Metaheuristic
[325, 354]	✓	✓				✓	Metaheuristic
[355]	✓	✓	✓				Machine learning
[356]	✓	✓			✓		Metaheuristic
[357]	✓	✓				✓	Machine learning
[310]		✓			✓	✓	Analytical
[358]	✓	✓				✓	Metaheuristic
[359]	✓	✓				✓	Metaheuristic
[321]		✓			✓	✓	Heuristic
[360]	✓	✓					Metaheuristic
Proposed	✓	✓		✓		✓	Analytical

6.6.3 Flexibility quantity estimation

This section presents the results of simulations and machine learning model training to estimate the required flexibility quantity to achieve a desired voltage deviation improvement considering the reconfigured distribution network for loop 1. The approach proposed in this paper considers the impedance (Z) between the node where the aggregated DER unit is connected and the node where the load change disturbance occurs. The voltage deviation is monitored at the last node of the branch. The impedance between the node where the aggregated DER unit is connected is clustered into low, medium, and high impedances. Figure 6.31 shows the estimated flexibility dispatch from the aggregated DER unit considering the step load change and the branch impedance clusters. The required aggregated DER unit dispatch to obtain the maximum voltage deviation improvement (21.95% to 24.32%) is 3MW for the medium and high impedance connections and 2.5MW for the low impedance connection. With the highest average load change of 3390 MW and the medium impedance connection, the average voltage deviation is improved by 13.46%. Figure 6.32 shows the estimated flexibility dispatch from the aggregated DER units considering the step load change and the expected voltage deviation improvement during the disturbance. Notwithstanding the level of load change disturbance on the network, the highest voltage deviation improvement is generally recorded with DER units' dispatch values between 2.25 MW to 3 MW. The average voltage deviation improvement of 13.58% with a deviation of 3.46% was obtained with 2.15 MW average dispatch from the aggregated DER units during the 100 load change events

simulated in the grid. The medium connection impedance generates the highest voltage deviation improvement of 36.46 % greater than the mean of 13.5%.

A dataset with four attributes and 100 instances was developed with quasi-dynamic simulations with several possible operation states. The results of training the decision tree model to estimate the quantity of flexibility needed to achieve the desired outcome voltage deviation support are shown in Figure 6.33. The developed dataset is divided into five data batches of 20 instances each. The average model build time for all five models is 4s. The average correlation coefficient and RMSE from all the batches are 0.957 and 0.187, respectively. The minimum model build time of 3s and RMSE of 0.161 was achieved with Batch 5. The constructed tree model obtained during the model's classification process with batch 5 is shown in Figure 6.34. The root node represents the voltage deviation improvement attributes, while the load change and connection impedance are considered at the decision nodes. The decision rules are generated from the leaf nodes on a root node's path in the decision tree. The classification obtained from each leaf node from the path of a root node forms the rule, while the leaf nodes represent the estimated flexibility quantity. Thirty-one classification rules were extracted from the RT model. The rules serve as a condition for the considered attributes that, when met, return an estimated flexibility quantity predicted grade. Figure 6.35 shows the actual and estimated flexibility quantities obtained from the developed random tree model using a different dataset with twenty instances. The estimation model is effective as only 35% of the estimations exceed the average estimation error of 0.1725. The estimated flexibility quantity will ensure the anticipated voltage support is obtained during load change disturbances within the distribution network.

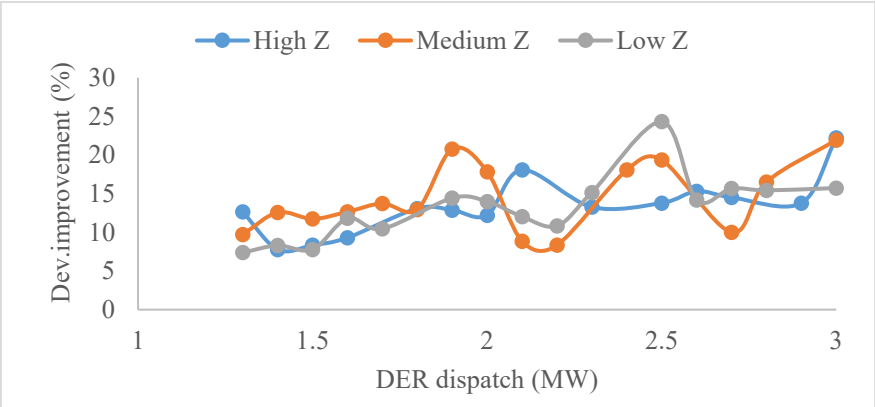

Figure 6.31: DER units dispatch level, connection impedance and voltage deviation improvement

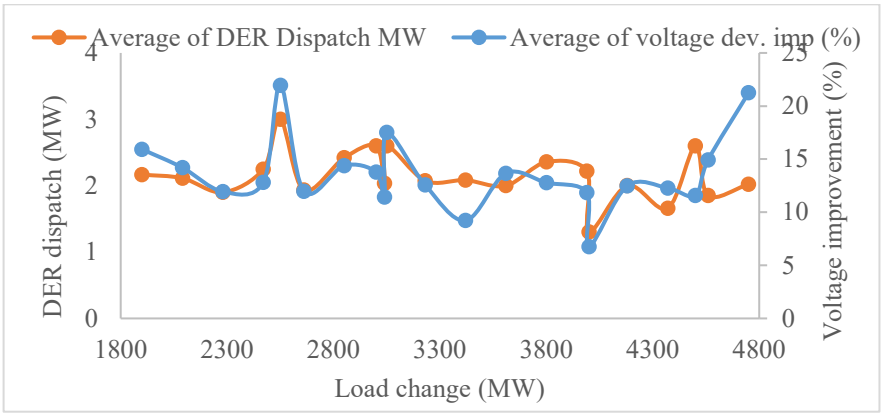

Figure 6.32: DER unit dispatch level, load change and voltage deviation improvement

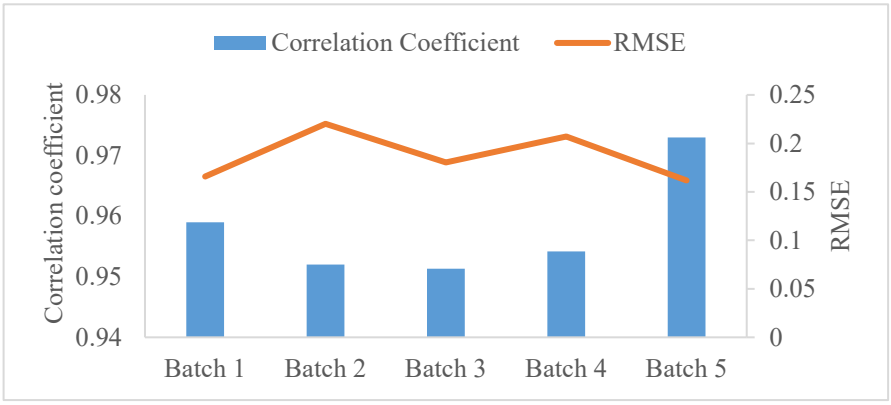

Figure 6.33: Flexibility quantity classification performance

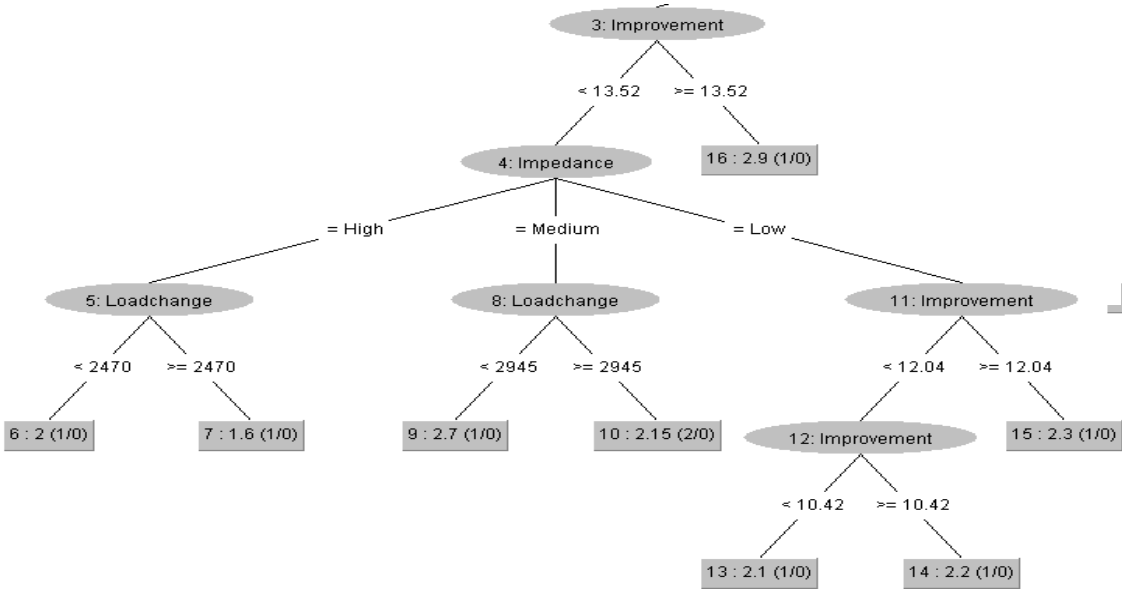

Figure 6.34: Random tree flexibility estimation model

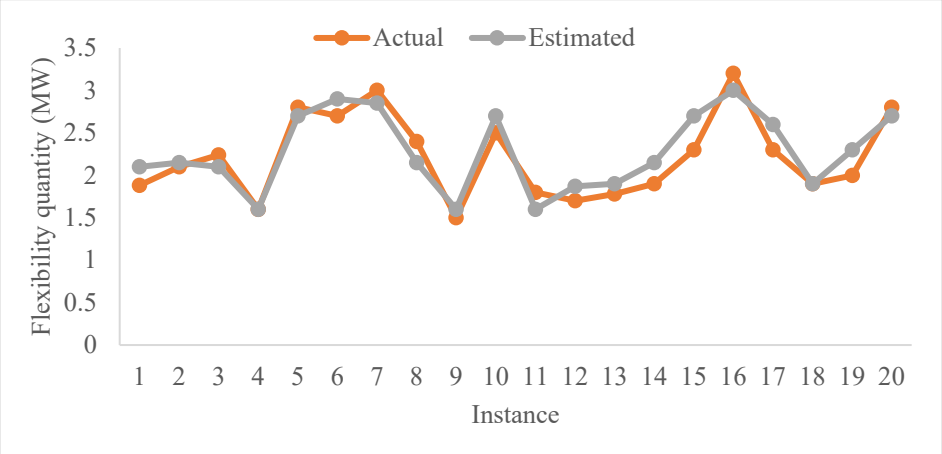

Figure 6.35: Flexibility quantity actual and estimated

7 Discussion, Conclusion and Future Work

7.1 Discussion

Intermittency, availability, and security issues are the main problems associated with substantial penetrations of RES-DG devices into the grid. Power generation is intermittent as a result of the sources' unpredictability, which could lead to fluctuations in the generation level. The RES-DG units cannot provide support during large disturbances due to the absence of mechanical inertia. Recent blackouts prove that low inertia grids quickly transition from secure to insecure state during disturbances that would not have been significant to high inertia grids. Optimal placement of RES-DG units within the distribution system remains an important part of maintaining the grid's security. The variability in the power output from RES-DG units results in probabilistic scenarios that can only be accommodated with probabilistic security indices and constraints. Optimal placement ensures that the risk of overvoltage and overgeneration is reduced if probabilistic security variables are included in the optimization problem formulation. Optimal placement also reduces the impact of unintended bidirectional power flow on the grid components and the protection systems. It is also important to evaluate the impact of the different inverter voltage control modes on the performances of RES-DG units in the grid. The interactive decision tree classification algorithm adopted provides options for future distribution network expansion with RES-DG unit.

In addition to limiting the impact of RES-DG unit penetration on the grid' security through optimal RES-DG units placement, monitoring and predicting the grid's security is also important. The time-changing, reduced effective inertia caused by varying penetration levels of RES-DG increases the grid's frequency change, leading to significant security risk considering potential contingencies in the grid. Prior knowledge of the system security state for proposed grid operating scenarios will assist grid operators in determining appropriate security control techniques. The effectiveness of the proposed machine learning-based prediction model is ensured by first developing an algorithm for the training dataset development. The algorithm considers several parameters, including generator type, penetration levels, elements, and contingency type. The training dataset patterns are identified and grouped using a density-based clustering algorithm. A probabilistic classifier is afterward applied to obtain security state predictions for the future. There are several challenges with an offline model, including large storage space requirements, the time required to retrain a model, and its unsuitability for real-time security prediction. To overcome these challenges, an online training technique is also applied to predict the grid's security using varying grid attributes. The performance of the online model is improved by performing the training in a prequential mode. For predicted insecure states, an intelligent load-shedding technique is used to ensure grid-secured operations

Interaction between the distribution and transmission networks regarding flexibility exchange is essential to ensure the security of the modern grid. Voltage instabilities during disturbances can be minimized by applying flexibility from the distribution networks. To achieve optimal flexibility operations, the probabilistic voltage risk due to voltage support unit operations must be investigated. The proposed bi-level optimization levels considered economic and technical objectives. The objective is to achieve maximum voltage support with the estimated MW dispatch from the RES-DG units with the minimum power loss network reconfiguration. The combination of classical and machine learning-based optimization techniques ensures the optimized cost during flexibility operations

7.2 Conclusion

This thesis assesses the impact of high penetration of RES-DG units on the security of the modern grid. Alongside the security assessment, this thesis proposes methods to ensure, predict and enhance the grid's security using machine learning approaches. The methods proposed in this thesis focused on the transmission network, the distribution network, and the boundary between the transmission and distribution networks. Integrating these methods, emerging grids may achieve 100% renewable energy generation with a high share of generation from the RES-DG units. The results obtained from testing the models on appropriate IEEE test networks suggest that the proposed methods help assess, predict, and ensure the grid's security with varying penetration levels of RES-DGs and other grid attributes.

A comprehensive literature review of the role of power generation units in the distribution networks and their related challenges was presented. The literature review discusses the positive and negative technical impacts of the penetration of RES-DG units. It also examines various proposed recommendations to limit the negative impacts on the grid’s security. Furthermore, it discusses the directions on the possible research areas to ensure and enhance the grid’s security under high penetration levels of RES-DG, considering components, models, and interaction between the transmission and distribution network operators. Research areas with challenges suggested in future trends of this chapter need to be researched more to get valuable solutions for implementation. The discussion in the literature review shows the importance of the RES-DG unit in the transition process from a traditionally passive high-carbon emission grid to an active zero-carbon emission future grid. More flexible, efficient, dynamic, real-time, and probabilistic planning and operation models would replace the conventional, static, deterministic, and offline models in the future grid. Techniques to maximize the benefits of high RES-DG unit penetration into the grid while limiting the negative impact on the grid’s security should be further explored. Proper active distribution network planning and operation, grid-wide security assessment and prediction, and coordinated flexibility interaction between the transmission and distribution networks support the achievement of high penetration of RES-DG units into the modern grid.

A novel approach to allocating multi-type RES-DG units in an unbalanced distribution network to achieve high penetration of RES was developed in this thesis. The proposed approach introduced a voltage risk index to estimate the nodes' voltage insecurity probability under different scenarios. It also demonstrates the possibility of determining the optimal branches and nodes for RES-DG placement using a decision tree classification technique. Additionally, the impact of inverter voltage control modes on the performance of the distribution network was investigated.

A method for offline grid security state clustering and classification using post-contingencies network state parameters considering time-varying inertia and critical clearing time of the grid was afterward developed. The method introduces a comprehensive data development technique considering penetration levels of different types of RES-DG units, faulted elements, and contingency types within the grid. This chapter also includes an approach to predicting the critical clearing time for the grid under varying grid attributes. The proposed security prediction and critical clearing time methods demonstrate the possibility of identifying the patterns and connections between the post-contingency frequency and voltage responses and the changing parameters of the grid. Due to the limitations of offline prediction methods, this thesis also includes a model for online prediction of the grid's security with varying grid attributes and penetration levels of RES-DG. The online prediction model uses the prequential incremental model training technique to achieve an effective model for online security prediction. The online proposed security prediction and control technique does not require large data storage as the previous training dataset does not need to be stored after each training process. Also, since time-domain simulations have been eliminated, the associated computation burden on the tool is significantly reduced.

To conclude the thesis, a novel bi-level security-constrained optimization technique for effective flexibility operation by the distribution network operators was developed. The technique initiates by investigating the impact of flexibility operations of the distribution network using the voltage risk index, then proceeds to develop a dynamic distribution network reconfiguration for economic and technical considerations. The technical consideration proposes a decision tree classification technique for optimal voltage flexibility operation from the reconfigured distribution network. The quantity of the disturbance estimated in MW, the connection impedance, and the expected voltage deviation improvement are the attributes considered to estimate the quantity of flexibility to be dispatchable from the aggregated distributed energy resources during disturbances for optimal voltage flexibility operation.

For application to real power system networks, the proposed models in this research can be developed into a deployable user-centred design (UFD)-based software for system operator utilization. The software will be interactive and particularly useful to the TSO and power aggregators to monitor the grid's security for varying levels of renewable energy generation in the energy pool. The software will also estimate the parameters required to maintain the grid in a secured state during emergencies. The predictions (security, maximum RES-DG penetration, load shed value, and critical

clearing time predictions) are made for every change of operation point as an online prediction model using real-time data instances. A major challenge that may inhibit the application of the online prediction model to real power system networks is the unavailability of sensors to extract the attributes at specific grid nodes. Another challenge is the required speed of execution of the model commencing from saved model retrieval, result prediction, model update, and model storage. The implementation cost of the proposed model will be high due to the requirement to develop new sensors and use high-speed processors.

The highlights and remarks of this thesis are summarized as follows:

1. The modern and emerging grids with high penetration levels of RES-DG necessitate comprehensive and integrated models across the grid levels for fast grid attributes extraction for security state prediction.
2. Grids operating under a high penetration level of RES-DG may quickly transition from the secure to insecure state without existing in the alert state.
3. Objectives and constraints for distribution network planning and expansions considering high penetration levels of RES-DG units should be extended from deterministic objectives to probabilistic security objectives and constraints.
4. Probabilistic techniques based on offline security state prediction can identify post-contingency response patterns, which are essential for grids with high and varying penetration level RES-DG.
5. Real-time security state monitoring and prediction for the modern grid with several varying attributes can be easily achieved using incremental prequential machine learning techniques.
6. Time ahead estimations of the load shed and critical clearing time values for proposed grid operation scenarios with high penetration levels of RES-DG are required to ensure the grid's security.
7. Considerations for techno-economic objectives and constraints are required for optimizing the tradeable flexibility from the active distribution networks for voltage support during contingency events.

7.3 Future work

Notwithstanding the valuable contributions and findings from this study, there are several possibilities for future research and potential study areas to provide more insights on the subjects addressed in this study. Some of the critical research areas needing further investigation are as follows:

- The present independent frequency and voltage control techniques at the transmission and distribution network levels may not be effective for the emerging grid. There is a need for research on integrated distributed frequency and voltage control techniques across the transmission and distribution networks.

- The frameworks for implementing the offline and online security state prediction on a real power system have been presented in this thesis. There is a need to investigate the predicted security state and control parameter communication between the transmission and distribution network operators. Improve communication, and enhanced interaction between the operators reduce decision-making times for the different protection components within the grid.
- Synthetic inertia, a costly flexible commodity, is one of the practicable techniques for enhancing the security of low inertia grids. Estimating the optimal amount of synthetic inertia needed to ensure the security of every predicted insecure grid operation scenario is a significant future research area.
- There is a need to extend the objectives and constraints for flexibility operating regions modeling at the transmission and distribution network boundaries beyond the deterministic steady-state objectives to include probabilistic transient state objectives and constraints to ensure the grid's security during flexibility operations.

References

1. M. Obi and R. Bass, *Trends and challenges of grid-connected photovoltaic systems – A review.* Renewable and Sustainable Energy Reviews, 2016. 58: p. 1082-1094.
2. K. Sun, et al., *A Review of Clean Electricity Policies—From Countries to Utilities.* Sustainability, 2020. 12(19).
3. R. Cossent, T. Gómez, and P. Frías, *Towards a future with large penetration of distributed generation: Is the current regulation of electricity distribution ready? Regulatory recommendations under a European perspective.* Energy Policy, 2009. 37(3): p. 1145-1155.
4. B.P. Heard, et al., *Burden of proof: A comprehensive review of the feasibility of 100% renewable-electricity systems.* Renewable and Sustainable Energy Reviews, 2017. 76: p. 1122-1133.
5. B.K. Poolla, D. Groß, and F. Dörfler, *Placement and implementation of grid-forming and grid-following virtual inertia and fast frequency response.* IEEE Transactions on Power Systems, 2019. 34(4): p. 3035-3046.
6. M. Rezkalla, M. Pertl, and M. Marinelli, *Electric power system inertia: requirements, challenges and solutions.* Electrical Engineering, 2018. 100(4): p. 2677-2693.
7. P. Mancarella and F. Billimoria, *The Fragile Grid: The Physics and Economics of Security Services in Low-Carbon Power Systems.* IEEE Power and Energy Magazine, 2021. 19(2): p. 79-88.
8. H. Haes Alhelou, M.E. Hamedani Golshan, and N.D. Hatziargyriou, *Deterministic Dynamic State Estimation-Based Optimal LFC for Interconnected Power Systems Using Unknown Input Observer.* IEEE Transactions on Smart Grid, 2020. 11(2): p. 1582-1592.
9. Y.K. Wu, S.M. Chang and Y.L. Hu, *Literaturte Review of Power System Blackouts*, in *4th International Conference on Power and Energy Systems Engineering, CPESE 2017*, Elsevier, Editor. 2017, Elsevier: Berlin, Germany. p. 25-29.
10. O.P. Veloza, and F. Santamaria, *Analysis of major blackouts from 2003 to 2015: Classification of incidents and review of main causes.* The Electricity Journal, 2016. 29(7): p. 42-49.
11. I. Oladeji, et al., *Security Impacts Assessment of Active Distribution Network on the Modern Grid Operation—A Review.* Electronics, 2021. 10(16).
12. I. Oladeji, R. Zamora, and T.T. Lie, *An Online Security Prediction and Control Framework for Modern Power Grids.* Energies, 2021. 14(20).
13. M. Gholami, et al., *Static security assessment of power systems: A review.* International Transactions on Electrical Energy Systems, 2020. 30(9).
14. S. Jafarzadeh, and V.M.I. Genc, *Real-time transient stability prediction of power systems based on the energy of signals obtained from PMUs.* Electric Power Systems Research, 2021. 192.
15. D. Seyed Javan, H. Rajabi Mashhadi, and M. Rouhani, *A fast static security assessment method based on radial basis function neural networks using enhanced clustering.* International Journal of Electrical Power & Energy Systems, 2013. 44(1): p. 988-996.
16. R. Liu, G. Verbič, and J. Ma, *A new dynamic security assessment framework based on semi-supervised learning and data editing.* Electric Power Systems Research, 2019. 172: p. 221-229.
17. W.D. Oliveira, et al., *Power system security assessment for multiple contingencies using multiway decision tree.* Electric Power Systems Research, 2017. 148: p. 264-272.
18. L. Zhu, D.J. Hill, and C. Lu, *Hierarchical Deep Learning Machine for Power System Online Transient Stability Prediction.* IEEE Transactions on Power Systems, 2020. 35(3): p. 2399-2411.
19. Y. Li, Y. Li, and Y. Sun, *Online Static Security Assessment of Power Systems Based on Lasso Algorithm.* Applied Sciences, 2018. 8(9): p. 1442.
20. A. Dhandhia, V. Pandya, and P. Bhatt, *Multi-class support vector machines for static security assessment of power system.* Ain Shams Engineering Journal, 2020. 11(1): p. 57-65.
21. A. Zhukov, et al., *Ensemble methods of classification for power systems security assessment.* Applied Computing and Informatics, 2019. 15(1): p. 45-53.

22. K. Tuttelberg, et al., *Estimation of Power System Inertia from Ambient Wide Area Measurements.* IEEE Transactions on Power Systems, 2018. 33(6): p. 7249 - 7257.
23. C. Spanias and I. Lestas, *A System Reference Frame Approach for Stability Analysis and Control of Power Grids.* IEEE transactions on power systems, 2019. Vol. 34(NO. 2): p. 1105-1115.
24. A. Delavari, and I. Kamwa, *Demand-Side Contribution to Power System Frequency Regulation : -A Critical Review on Decentralized Strategies.* International Journal of Emerging Electric Power Systems, 2017. 18(3).
25. P.E. Carvajal, et al., *Large hydropower, decarbonisation and climate change uncertainty: Modelling power sector pathways for Ecuador.* Energy Strategy Reviews, 2019. 23: p. 86-99.
26. H. Haes Alhelou, et al., *A Survey on Power System Blackout and Cascading Events: Research Motivations and Challenges.* Energies, 2019. 12(4): p. 682.
27. P. Moriarty, and D. Honnery, *What is the global potential for renewable energy?* Renewable and Sustainable Energy Reviews, 2012. 16(1): p. 244-252.
28. J.A. Momoh, S. Meliopoulos, R. Saint, *Centralized and Distributed Generated Power Systems - A Comparison Approach*, Future grid initiative white paper 2012, PSERC Publication: Howard University.
29. M. Sarwar, B. Asad. *A review on future powersystems; technologies and research for smart grids*. In International Conference on EmergingTechnologies (ICET), 2016, pp. 1-6, doi: 10.1109/ICET.2016.7813247.
30. M.M. Othman, Y.G. Hegazy, and AY. Abdelaziz, *Electrical energy management in unbalanced distribution networks using virtual power plant concept.* Electric Power Systems Research, 2017. 145: p. 157-165.
31. G. Allan, et al., *The economics of distributed energy generation: A literature review.* Renewable and Sustainable Energy Reviews, 2015. 42: p. 543-556.
32. International Renewable energy Agency (2018), Renewable capacity highlights. https://www.irena.org/-/media/Files/IRENA/Agency/Publication.
33. K. Sun, et al., *Operation Modes and Combination Control for Urban Multivoltage-Level DC Grid.* IEEE Transactions on Power Delivery, 2018. 33(1): p. 360-370.
34. A. Mohammad, R. Zamora, and T.T. Lie, *Integration of Electric Vehicles in the Distribution Network: A Review of PV Based Electric Vehicle Modelling.* Energies, 2020. 13(17).
35. F. F. Wu, K. Moslehi and A. Bose, *Power System Control Centers: Past, Present, and Future*, Proceedings of the IEEE, Vol. 93, no. 11, pp. 1890-1908, Nov. 2005, doi: 10.1109/JPROC.2005.857499.
36. A.Q. Huang, et al., *The future renewable electric energy delivery and management (FREEDM) system: the energy internet* . Proceedings of the IEEE, 2011. 99(1): p. 133-148.
37. A. Joseph and P. Balachandra, *Smart grid to energy internet: A systematic review of transitioning electricity systems.* IEEE Access, 2020. 8: p. 215787-215805.
38. A. Alassi, et al., *HVDC Transmission: Technology Review, Market Trends and Future Outlook.* Renewable and Sustainable Energy Reviews, 2019. 112: p. 530-554.
39. M.Z. Hossain, N.A. Rahim, and J.A.L. Selvaraj, *Recent progress and development on power DC-DC converter topology, control, design and applications: A review.* Renewable and Sustainable Energy Reviews, 2018. 81: p. 205-230.
40. O. Gomis-Bellmunt, et al., *Flexible Converters for Meshed HVDC Grids: From Flexible AC Transmission Systems (FACTS) to Flexible DC Grids.* IEEE Transactions on Power Delivery, 2020. 35(1): p. 2-15.
41. O. Ellabban, H. Abu-Rub, and F. Blaabjerg, *Renewable energy resources: Current status, future prospects and their enabling technology.* Renewable and Sustainable Energy Reviews, 2014. 39: p. 748-764.
42. S. Mekhilef, R. Saidur, and A. Safari, *A review on solar energy use in industries.* Renewable and Sustainable Energy Reviews, 2011. 15(4): p. 1777-1790.
43. International Renewable Energy Agency (2021), Renewable capacity statistics 2021, International Renewable Energy Agency (IRENA), Abu Dhabi.https://www.irena.org/-/media/Files/IRENA/Agency/Publications/2021/Apr/IRENA_RE_Capacity_statistics_2021.pdf?rev=a189d053a1844fafb918b6f3c735acc2.

44. E. Kabir, et al., *Solar energy: Potential and future prospects.* Renewable and Sustainable Energy Reviews, 2018. 82: p. 894-900.
45. M. Bajaj and A.K. Singh, *Grid integrated renewable DG systems: A review of power quality challenges and state-of-the-art mitigation techniques.* International Journal of Energy Research, 2019. 44(1): p. 26-69.
46. Mercon india (2020). Clean energy news and insights 03(02). https://mercomindia.com/product-category/india-reports/page/4/.
47. M. Resch, et al., *Impact of operation strategies of large scale battery systems on distribution grid planning in Germany.* Renewable and Sustainable Energy Reviews, 2017. 74: p. 1042-1063.
48. G.G. Dranka,. and P. Ferreira, *Towards a smart grid power system in Brazil: Challenges and opportunities.* Energy Policy, 2020. 136.
49. M. Simionescu, W. Strielkowski, and M. Tvaronavičienė, *Renewable Energy in Final Energy Consumption and Income in the EU-28 Countries.* Energies, 2020. 13(9).
50. O.M. Babatunde, J.L. Munda, and Y. Hamam, *Power system flexibility: A review.* Energy Reports, 2020. 6: p. 101-106.
51. A. Ehsan and Q. Yang, *Optimal integration and planning of renewable distributed generation in the power distribution networks: A review of analytical techniques.* Applied Energy, 2018. 210: p. 44-59.
52. P. Makolo, et al., *Data-driven inertia estimation based on frequency gradient for power systems with high penetration of renewable energy sources.* Electric Power Systems Research, 2021. 195.
53. A.K. Srivastava, R. Zamora, and D. Bowman. *Impact of distributed generation with storage on electric grid stability*. in *2011 IEEE Power and Energy Society General Meeting*. 2011.
54. J. Li, et al., *Research on penetration of distributed generation considering fluctuation and load frequency characteristics.* The Journal of Engineering, 2017. 2017(13): p. 2319-2323.
55. C.J. Dent, L.F. Ochoa, and G.P. Harrison, *Network Distributed Generation Capacity Analysis Using OPF With Voltage Step Constraints.* IEEE Transactions on Power Systems, 2010. 25(1): p. 296-304.
56. L.D.P. Ospina, and T.Van Cutsem, *Power factor improvement by active distribution networks during voltage emergency situations.* Electric Power Systems Research, 2020. 189.
57. *IEEE Standard for Interconnection and Interoperability of Distributed Energy Resources with Associated Electric Power Systems Interfaces.* IEEE Std 1547-2018 (Revision of IEEE Std 1547-2003), 2018: p. 1-138.
58. P. Chaudhary and M. Rizwan, *Voltage regulation mitigation techniques in distribution system with high PV penetration: A review.* Renewable and Sustainable Energy Reviews, 2018. 82: p. 3279-3287.
59. H. Nosair and F. Bouffard, *Flexibility Envelopes for Power System Operational Planning.* IEEE Transactions on Sustainable Energy, 2015. 6(3): p. 800-809.
60. I. Adebayo and Y. Sun, *New Performance Indices for Voltage Stability Analysis in a Power System.* Energies, 2017. 10(12): p. 2042.
61. K.Z. Heetun, S.H.E. Abdel Aleem, and A.F. Zobaa, *Voltage stability analysis of grid-connected wind farms with FACTS: Static and dynamic analysis.* Energy and Policy Research, 2015. 3(1): p. 1-12.
62. H. Su, *An Efficient Approach for Fast and Accurate Voltage Stability Margin Computation in Large Power Grids.* Applied Sciences, 2016. 6(11).
63. A.R. Nageswa Rao, P. Vijaya and M. Kowsalya, *Voltage stability indices for stability assessment: a review.* International Journal of Ambient Energy, 2018. 42(7): p. 829-845.
64. J. Modarresi, E. Gholipour and A. Khodabakhshian, *A comprehensive review of the voltage stability indices.* Renewable and Sustainable Energy Reviews, 2016. 63: p. 1-12.
65. U. Sultana, et al., *A review of optimum DG placement based on minimization of power losses and voltage stability enhancement of distribution system.* Renewable and Sustainable Energy Reviews, 2016. 63: p. 363-378.
66. S. Kalambe and G. Agnihotri, *Loss minimization techniques used in distribution network: bibliographical survey.* Renewable and Sustainable Energy Reviews, 2014. 29: p. 184-200.
67. P. Kayal and C.K. Chanda, *Placement of wind and solar based DGs in distribution system*

for power loss minimization and voltage stability improvement. International Journal of Electrical Power & Energy Systems, 2013. 53: p. 795-809.
68. B. Poornazaryan, et al., *Optimal allocation and sizing of DG units considering voltage stability, losses and load variations.* International Journal of Electrical Power & Energy Systems, 2016. 79: p. 42-52.
69. A. Ramamoorthy and R. Ramachandran, *Optimal Siting and Sizing of Multiple DG Units for the Enhancement of Voltage Profile and Loss Minimization in Transmission Systems Using Nature Inspired Algorithms.* Scientific World Journal, 2016. 2016: p. 1086579.
70. B. Banerjee and S.M. Islam, *Reliability based optimum location of distributed generation.* International Journal of Electrical Power & Energy Systems, 2011. 33(8): p. 1470-1478.
71. P. Zhou, R.Y. Jin and L.W. Fan, *Reliability and economic evaluation of power system with renewables: A review.* Renewable and Sustainable Energy Reviews, 2016. 58: p. 537-547.
72. R.S. Pinto, C. Unsihuay-Vila and T.S.P. Fernandes, *Multi-objective and multi-period distribution expansion planning considering reliability, distributed generation and self-healing.* IET Generation, Transmission & Distribution, 2019. 13(2): p. 219-228.
73. C. Novoa and T. Jin, *Reliability centered planning for distributed generation considering wind power volatility.* Electric Power Systems Research, 2011. 81(8): p. 1654-1661.
74. H. Yang, et al., *Reliability evaluation of power systems in the presence of energy storage system as demand management resource.* International Journal of Electrical Power & Energy Systems, 2019. 110: p. 1-10.
75. B. Wojszczyk and M. Brandao. *High penetration of distributed generation and its impact on electric grid performance - utility perspective*. in *2011 IEEE PES Innovative Smart Grid Technologies*. 2011.
76. A. Ehsan, and Q. Yang, *State-of-the-art techniques for modelling of uncertainties in active distribution network planning: A review.* Applied Energy, 2019. 239: p. 1509-1523.
77. D.L. Woodruff, et al., *Constructing probabilistic scenarios for wide-area solar power generation.* Solar Energy, 2018. 160: p. 153-167.
78. D.W. Van der Meer, J. Widén and J. Munkhammar *Review on probabilistic forecasting of photovoltaic power production and electricity consumption.* Renewable and Sustainable Energy Reviews, 2018. 81: p. 1484-1512.
79. A. Couto and A. Estanqueiro, *Exploring Wind and Solar PV Generation Complementarity to Meet Electricity Demand.* Energies, 2020. 13(16).
80. S. Bhattacharjee and S. Acharya, *PV–wind hybrid power option for a low wind topography.* Energy Conversion and Management, 2015. 89: p. 942-954.
81. S. Jerez, et al., *Future changes, or lack thereof, in the temporal variability of the combined wind-plus-solar power production in Europe.* Renewable Energy, 2019. 139: p. 251-260.
82. J.B. Fulzele and M.B. Daigavane, *Design and Optimization of Hybrid PV-Wind Renewable Energy System.* Materials Today: Proceedings, 2018. 5(1): p. 810-818.
83. S. Camal, et al., *Scenario generation of aggregated Wind, Photovoltaics and small Hydro production for power systems applications.* Applied Energy, 2019. 242: p. 1396-1406.
84. B. Singh, V. Mukherjee, and P. Tiwari, *Genetic algorithm for impact assessment of optimally placed distributed generations with different load models from minimum total MVA intake viewpoint of main substation.* Renewable and Sustainable Energy Reviews, 2016. 57: p. 1611-1636.
85. M. Ebad and W.M. Grady, *An approach for assessing high-penetration PV impact on distribution feeders.* Electric Power Systems Research, 2016. 133: p. 347-354.
86. T.M. Masaud, G. Nannapaneni, and R. Challoo, *Optimal placement and sizing of distributed generation-based wind energy considering optimal self VAR control.* IET Renewable Power Generation, 2017. 11(3): p. 281-288.
87. M.M. Aman, et al., *A new approach for optimum DG placement and sizing based on voltage stability maximization and minimization of power losses.* Energy Conversion and Management, 2013. 70: p. 202-210.
88. B. Singh and J. Sharma, *A review on distributed generation planning.* Renewable and Sustainable Energy Reviews, 2017. 76: p. 529-544.
89. Z. Abdmouleh, et al., *Review of optimization techniques applied for the integration of distributed generation from renewable energy sources.* Renewable Energy, 2017. 113: p.

266-280.
90. H. HassanzadehFard and A. Jalilian, *Optimal sizing and siting of renewable energy resources in distribution systems considering time varying electrical/heating/cooling loads using PSO algorithm.* International Journal of Green Energy, 2018. 15(2): p. 113-128.
91. S. M. Dawoud, X. Lin, and M. I. Okba, *Optimal placement of different types of RDGs based on maximization of microgrid loadability.* Journal of Cleaner Production, 2017. 168: p. 63-73.
92. S. Kansal, V. Kumar and B. Tyagi, *Optimal placement of different type of DG sources in distribution networks.* International Journal of Electrical Power & Energy Systems, 2013. 53: p. 752-760.
93. M. R. Elkadeem, et al., *Optimal Planning of Renewable Energy-Integrated Distribution System Considering Uncertainties.* IEEE Access, 2019. 7: p. 164887-164907.
94. S. Kansal, V. Kumar and B. Tyagi, *Hybrid approach for optimal placement of multiple DGs of multiple types in distribution networks.* International Journal of Electrical Power & Energy Systems, 2016. 75: p. 226-235.
95. F. Abbasi and S.M. Hosseini, *Optimal DG allocation and sizing in presence of storage systems considering network configuration effects in distribution systems.* IET Generation, Transmission & Distribution, 2016. 10(3): p. 617-624.
96. S.R. Gampa, and D. Das, *Optimum placement and sizing of DGs considering average hourly variations of load.* International Journal of Electrical Power & Energy Systems, 2015. 66: p. 25-40.
97. A.A. Hassan et al., *Hybrid genetic multi objective/fuzzy algorithm for optimal sizing and allocation of renewable DG systems.* International Transactions on Electrical Energy Systems, 2016. 26(12): p. 2588-2617.
98. E.S. Ali, S.M. Abd Elazim and A.Y. Abdelaziz, *Ant Lion Optimization Algorithm for optimal location and sizing of renewable distributed generations.* Renewable Energy, 2017. 101: p. 1311-1324.
99. P, Dinakara Prasasd Reddy, V. C. Veera Reddy and T. Gowri Manohar, *Ant Lion optimization algorithm for optimal sizing of renewable energy resources for loss reduction in distribution systems.* Journal of Electrical Systems and Information Technology, 2018. 5(3): p. 663-680.
100. M. Naghdi, M. A. Shafiyi and M. R. Haghifam, *A combined probabilistic modeling of renewable generation and system load types to determine allowable DG penetration level in distribution networks.* International Transactions on Electrical Energy Systems, 2019. 29(1): p. e2696.
101. M. Natarajan, B. Ramadoss and L. Lakshmanarao, *Optimal location and sizing of MW and MVAR based DG units to improve voltage stability margin in distribution system using a chaotic artificial bee colony algorithm.* International Transactions on Electrical Energy Systems, 2017. 27(4): p. e2287.
102. T. Niknam, et al., *A modified honey bee mating optimization algorithm for multiobjective placement of renewable energy resources.* Applied Energy, 2011. 88(12): p. 4817-4830.
103. L.D. Arya, A. Koshti, and S.C. Choube, *Distributed generation planning using differential evolution accounting voltage stability consideration.* International Journal of Electrical Power & Energy Systems, 2012. 42(1): p. 196-207.
104. D.K. Khatod, V. Pant, and J. Sharma, *Evolutionary programming based optimal placement of renewable distributed generators.* IEEE Transactions on Power Systems, 2013. 28(2): p. 683-695.
105. M.H. Moradi, S.M. Reza Tousi and M. Abedini, *Multi-objective PFDE algorithm for solving the optimal siting and sizing problem of multiple DG sources.* International Journal of Electrical Power & Energy Systems, 2014. 56: p. 117-126.
106. P, Dinakara Prasasd Reddy, V.C. Veera Reddy and T. Gowri Manohar, *Optimal renewable resources placement in distribution networks by combined power loss index and whale optimization algorithms.* Journal of Electrical Systems and Information Technology, 2018. 5(2): p. 175-191.
107. M.C.V. Suresh and E. J. Belwin, *Optimal DG placement for benefit maximization in distribution networks by using Dragonfly algorithm.* Renewables: Wind, Water, and Solar,

2018. 5(1).
108. Photovoltaics, Distributed Generation, and Energy Storage. *IEEE Standard Conformance Test Procedures for Equipment Interconnecting Distributed Energy Resources with Electric Power Systems and Associated Interfaces.* IEEE Std 1547.1-2020, 2020: p. 1-282.
109. S.M. Ismael, et al., *State-of-the-art of hosting capacity in modern power systems with distributed generation.* Renewable Energy, 2019. 130: p. 1002-1020.
110. M.S.S. Abad, J. Ma and X. Han, *Distribution systems hosting capacity assessment: Relaxation and linearization*. Smart Power Distribution Systems. Academic Press, 2019. p. 555-586.
111. A. Soroudi, A. Rabiee and A. Keane, *Distribution networks' energy losses versus hosting capacity of wind power in the presence of demand flexibility.* Renewable Energy, 2017. 102: p. 316-325.
112. A. Azizivahed, et al., *Energy Management Strategy in Dynamic Distribution Network Reconfiguration Considering Renewable Energy Resources and Storage.* IEEE Transactions on Sustainable Energy, 2020. 11(2): p. 662-673.
113. I.G. Guimarães, et al., *A decomposition heuristic algorithm for dynamic reconfiguration after contingency situations in distribution systems considering island operations.* Electric Power Systems Research, 2021. 192.
114. F. Capitanescu, et al., *Assessing the Potential of Network Reconfiguration to Improve Distributed Generation Hosting Capacity in Active Distribution Systems.* IEEE Transactions on Power Systems, 2015. 30(1): p. 346-356.
115. P. Zhang, K. Meng and Z. Dong, *Probabilistic vs Deterministic Power System Stability and Reliability Assessment* in *Emerging Techniques in Power System Analysis*, Springer, Editor. 2010, Springer: Berlin, Heidelberg.
116. Z. Li, *A Distributed Transmission-Distribution-Coupled Static Voltage Stability Assessment Method Considering Distributed Generation.* IEEE Transactions on Power Systems, 2018. 33(3): p. 2621-2632.
117. M. Vukobratović, et al., *Distributed Generation Harmonic Interaction in the Active Distribution Network.* Tehnicki vjesnik - Technical Gazette, 2018. 25(6).
118. P.M. Triveni Ambre, *Power System Analysis based on Dynamic Security Assessment Using Fuzzy Logic.* International Journal of Advanced Research in Computer Engineering & Technology (IJARCET), 2016. 5(7): p. 2152-2156.
119. A. Kargarian, et al., *Toward Distributed/Decentralized DC Optimal Power Flow Implementation in Future Electric Power Systems.* IEEE Transactions on Smart Grid, 2018. 9(4): p. 2574-2594.
120. X. Liu and Y. Liu, *Optimal planning of AC-DC hybrid transmission and distributed energy resource system: Review and prospects.* CSEE Journal of Power and Energy Systems, 2019.
121. E. Heylen, G. Deconinck and D. Van Hertem, *Review and classification of reliability indicators for power systems with a high share of renewable energy sources.* Renewable and Sustainable Energy Reviews, 2018. 97: p. 554-568.
122. G. Mokryani, et al., *Active distribution networks planning with high penetration of wind power.* Renewable Energy, 2017. 104: p. 40-49.
123. I. B. Sperstad, M.Z. Degefa, and G. Kjølle, *The impact of flexible resources in distribution systems on the security of electricity supply: A literature review.* Electric Power Systems Research, 2020. 188.
124. P. Gopakumar, M.J.B. Reddy, and D.K. Mohanta, *Letter to the Editor: Stability Concerns in Smart Grid with Emerging Renewable Energy Technologies.* Electric Power Components and Systems, 2014. 42(3-4): p. 418-425.
125. F. Sanchez Gorostiza and F. Gonzalez-Longatt, *Optimised TSO–DSO interaction in unbalanced networks through frequency-responsive EV clusters in virtual power plants.* IET Generation, Transmission & Distribution, 2020. 14(21): p. 4908-4917.
126. Z. Lu, et al., *A Security Level Classification Method for Power Systems under N-1 Contingency.* Energies, 2017. 10(12): p. 2055.
127. H. Bevrani, et al., *Power system frequency control: An updated review of current solutions and new challenges.* Electric Power Systems Research, 2021. 194.
128. K.E. Antoniadou-Plytaria, et al., *Distributed and Decentralized Voltage Control of Smart*

Distribution Networks: Models, Methods, and Future Research. IEEE Transactions on Smart Grid, 2017. 8(6): p. 2999-3008.
129. N. O'Connell, et al., *Benefits and challenges of electrical demand response: A critical review.* Renewable and Sustainable Energy Reviews, 2014. 39: p. 686-699.
130. Z.A. Obaid, et al., *Frequency control of future power systems: reviewing and evaluating challenges and new control methods.* Journal of Modern Power Systems and Clean Energy, 2018. 7(1): p. 9-25.
131. D.K. Molzahn et al., *A Survey of Distributed Optimization and Control Algorithms for Electric Power Systems.* IEEE Transactions On Smart Grid, 2017. Vol. 8(NO. 6): p. 2941-2962.
132. A. Mohammadi, et al., *A System of Systems Engineering Framework for Modern Power System Operation*, Sustainable interdependent networks II: from smart power grids to intelligent transportation networks. Cham: Springer International Publishing. 2019. p. 217-247.
133. R. Zamora and A.K. Srivastava, *Controls for microgrids with storage: Review, challenges, and research needs.* Renewable and Sustainable Energy Reviews, 2010. 14(7): p. 2009-2018.
134. V. Trovato, I.M. Sanz, B. Chaudhuri and G. Strbac, *Advanced Control of Thermostatic Loads for Rapid Frequency Response in Great Britain.* IEEE Transactions On Power Systems, 2017. Vol. 32(NO. 3): p. 2106-2117.
135. E. Devane, et al., *Primary Frequency Regulation With Load-Side Participation—Part II: Beyond Passivity Approaches.* IEEE Transactions On Power Systems, 2017. Vol. 32(NO. 5): p. 3519-3528.
136. C. Zhao, et al., *Design and Stability of Load-Side Primary Frequency Control in Power Systems.* IEEE Transactions on Automatic Control, 2013. p. 1177-1189
137. A. Delavari, *Novel Load-based Control Strategies for Power System Primary Frequency Regulation*, Doctoral dissertation 2018, Unversite Laval: Quebec Canada.
138. A Kasis, et al., *Primary Frequency Regulation With Load-Side Participation—Part I: Stability and Optimality.* IEEE Transactions On Power Systems, 2017. Vol. 32(NO. 5): p. 3505-3518.
139. A. Vicente-Pastor, et al., *Evaluation of Flexibility Markets for Retailer–DSO–TSO Coordination.* IEEE Transactions on Power Systems, 2019. 34(3): p. 2003-2012.
140. J. Silva, et al., *Estimating the Active and Reactive Power Flexibility Area at the TSO-DSO Interface.* IEEE Transactions on Power Systems, 2018. 33(5): p. 4741-4750.
141. R. T. Elliott, et al., *Sharing Energy Storage Between Transmission and Distribution.* IEEE Transactions on Power Systems, 2019. 34(1): p. 152-162.
142. A. Pappachen and A.P. Fathima, *Critical research areas on load frequency control issues in a deregulated power system: A state-of-the-art-of-review.* Renewable and Sustainable Energy Reviews, 2017. 72: p. 163-177.
143. D. Boroyevich, et al., *Intergrid: A Future Electronic Energy Network?* IEEE Journal of Emerging and Selected Topics in Power Electronics, 2013. 1(3): p. 127-138.
144. Z. Zhang, et al., *A review of technologies and applications on versatile energy storage systems.* Renewable and Sustainable Energy Reviews, 2021. 148.
145. P. Betancourt-Paulino, et al., *On the perspective of grid architecture model with high TSO-DSO interaction.* IET Energy Systems Integration, 2021. 3(1): p. 1-12.
146. S. Ruiz-Romero, et al., *Integration of distributed generation in the power distribution network: The need for smart grid control systems, communication and equipment for a smart city — Use cases.* Renewable and Sustainable Energy Reviews, 2014. 38: p. 223-234.
147. J. Li, X. Feng and C. Kang. *The WARMAP system closed-loop simulate validation based on RTDS.* In 2011 International Conference on Advanced Power System Automation and Protection. 2011.
148. S. Qian, et al. *Reliability Analysis of Communication Channels in Wide Area Monitoring Analysis Protection-control System*. In 2020 12th IEEE PES Asia-Pacific Power and Energy Engineering Conference (APPEEC). 2020.
149. H.M. Hussain, et al., *What is Energy Internet? Concepts, Technologies, and Future Directions.* IEEE Access, 2020. 8: p. 183127-183145.

150. S.M.S. Hussain, et al., *The Emerging Energy Internet: Architecture, Benefits, Challenges, and Future Prospects.* Electronics, 2019. 8(9).
151. K. Wang, et al., *A Survey on Energy Internet: Architecture, Approach, and Emerging Technologies.* IEEE Systems Journal, 2018. 12(3): p. 2403-2416.
152. R. Morello, et al., *A Smart Power Meter to Monitor Energy Flow in Smart Grids: The Role of Advanced Sensing and IoT in the Electric Grid of the Future.* IEEE Sensors Journal, 2017. 17(23): p. 7828-7837.
153. F. Meng, B. Chowdhury, and M. S. Hossan, *Optimal integration of DER and SST in active distribution networks.* International Journal of Electrical Power & Energy Systems, 2019. 104: p. 626-634.
154. K. Sharma, and L.M. Saini, *Power-line communications for smart grid: Progress, challenges, opportunities and status.* Renewable and Sustainable Energy Reviews, 2017. 67: p. 704-751.
155. N. Gaeini, et al., *Cooperative secondary frequency control of distributed generation: The role of data communication network topology.* International Journal of Electrical Power & Energy Systems, 2017. 92: p. 221-229.
156. H.E Farag, E.F. El-Saadany, and R. Seethapathy, *A Two Ways Communication-Based Distributed Control for Voltage Regulation in Smart Distribution Feeders.* IEEE Transactions on Smart Grid, 2012. 3(1): p. 271-281.
157. D. Zheng, A. Eseye and J. Zhang, *A Communication-Supported Comprehensive Protection Strategy for Converter-Interfaced Islanded Microgrids.* Sustainability, 2018. 10(5): p. 1335.
158. R. Huang, et al., *Design and implementation of communication architecture in a distributed energy resource system using IEC 61850 standard.* International Journal of Energy Research, 2016. 40(5): p. 692-701.
159. P.I. Radoglou-Grammatikis and P. G. Sarigiannidis, *Securing the Smart Grid: A Comprehensive Compilation of Intrusion Detection and Prevention Systems.* IEEE Access, 2019. 7: p. 46595-46620.
160. D. Pliatsios, et al., *A Survey on SCADA Systems: Secure Protocols, Incidents, Threats and Tactics.* IEEE Communications Surveys & Tutorials, 2020. 22(3): p. 1942-1976.
161. T. Aziz and N. Ketjoy, *PV Penetration Limits in Low Voltage Networks and Voltage Variations.* IEEE Access, 2017. 5: p. 16784-16792.
162. A. Hoke, et al., *Steady-State Analysis of Maximum Photovoltaic Penetration Levels on Typical Distribution Feeders.* IEEE Transactions on Sustainable Energy, 2013. 4(2): p. 350-357.
163. T.W. Brown, et al., *Response to 'Burden of proof: A comprehensive review of the feasibility of 100% renewable-electricity systems'.* Renewable and Sustainable Energy Reviews, 2018. 92: p. 834-847.
164. D. Saheb-Koussa, M. Koussa, and N. Said, *A technical, economic, and environmental performance of grid-connected hybrid (photovoltaic-wind) power system in Algeria.* Scientific World Journal, 2013: p. 123160.
165. Y.-Y. Fu, and H.-D. Chiang, *Toward Optimal Multiperiod Network Reconfiguration for Increasing the Hosting Capacity of Distribution Networks.* IEEE Transactions on Power Delivery, 2018. 33(5): p. 2294-2304.
166. R.W. Kenyon, et al., *Stability and control of power systems with high penetrations of inverter-based resources: An accessible review of current knowledge and open questions.* Solar Energy, 2020. 210: p. 149-168.
167. G. Li, et al., *Probabilistic assessment of oscillatory stability margin of power systems incorporating wind farms.* International Journal of Electrical Power & Energy Systems, 2014. 58: p. 47-56.
168. Y.-F. Huang, et al., *State Estimation in Electric Power Grids: Meeting New Challenges Presented by the Requirements of the Future Grid.* IEEE Signal Processing Magazine, 2012. 29(5): p. 33-43.
169. D.L. Hau Aik and G. Andersson, *Impact of renewable energy sources on steady-state stability of weak AC/DC systems.* CSEE Journal of Power and Energy Systems, 2017. 3(4): p. 419-430.
170. S. Zolfaghari Moghaddam, *Generation and transmission expansion planning with high*

penetration of wind farms considering spatial distribution of wind speed. International Journal of Electrical Power & Energy Systems, 2019. 106: p. 232-241.

171. A. Mohammadi, M. Mehrtash, and A. Kargarian, *Diagonal Quadratic Approximation for Decentralized Collaborative TSO+DSO Optimal Power Flow.* IEEE Transactions on Smart Grid, 2019. 10(3): p. 2358-2370.
172. L. Mehigan, et al., *A review of the role of distributed generation (DG) in future electricity systems.* Energy, 2018. 163: p. 822-836.
173. I. Capellán-Pérez, C. de Castro, and I. Arto, *Assessing vulnerabilities and limits in the transition to renewable energies: Land requirements under 100% solar energy scenarios.* Renewable and Sustainable Energy Reviews, 2017. 77: p. 760-782.
174. W.L. Theo, et al., *Review of distributed generation (DG) system planning and optimisation techniques: Comparison of numerical and mathematical modelling methods.* Renewable and Sustainable Energy Reviews, 2017. 67: p. 531-573.
175. H.A.M. Pesaran, P.D. Huy, and V.K. Ramachandaramurthy, *A review of the optimal allocation of distributed generation: Objectives, constraints, methods, and algorithms.* Renewable and Sustainable Energy Reviews, 2017. 75: p. 293-312.
176. A.K. Singh,. and S.K. Parida, *A review on distributed generation allocation and planning in deregulated electricity market.* Renewable and Sustainable Energy Reviews, 2018. 82: p. 4132-4141.
177. A. Rajendran, and K. Narayanan, *Optimal Installation of Different DG Types in Radial Distribution System Considering Load Growth.* Electric Power Components and Systems, 2017. 45(7): p. 739-751.
178. A. Maleki, M.G. Khajeh, and M. Ameri, *Optimal sizing of a grid independent hybrid renewable energy system incorporating resource uncertainty, and load uncertainty.* International Journal of Electrical Power & Energy Systems, 2016. 83: p. 514-524.
179. M. Sugimura, et al., *Optimal sizing and operation for microgrid with renewable energy considering two types demand response.* Journal of Renewable and Sustainable Energy, 2020. 12(6).
180. S. Mashayekh, et al., *A mixed integer linear programming approach for optimal DER portfolio, sizing, and placement in multi-energy microgrids.* Applied Energy, 2017. 187: p. 154-168.
181. Ž.N. Popović, V.D. Kerleta, and D.S. Popović, *Hybrid simulated annealing and mixed integer linear programming algorithm for optimal planning of radial distribution networks with distributed generation.* Electric Power Systems Research, 2014. 108: p. 211-222.
182. M. Nemati, M. Braun, and S. Tenbohlen, *Optimization of unit commitment and economic dispatch in microgrids based on genetic algorithm and mixed integer linear programming.* Applied Energy, 2018. 210: p. 944-963.
183. M.S. Ibrahim, W. Dong and Q. Yang, *Machine learning driven smart electric power systems: Current trends and new perspectives.* Applied Energy, 2020. 272.
184. N.M. Kumar, et al., *Distributed Energy Resources and the Application of AI, IoT, and Blockchain in Smart Grids.* Energies, 2020. 13(21).
185. K.N. Maya and E.A. Jasmin, *Optimal integration of distributed generation (DG) resources in unbalanced distribution system considering uncertainty modelling.* International Transactions on Electrical Energy Systems, 2017. 27(1): p. e2248.
186. A.F. Bastos, et al., 2020. Machine Learning-Based Prediction of Distribution Network Voltage and Sensors Allocation: Preprint. (No. NREL/CP-5D00-75247). National Renewable Energy Lab.(NREL), Golden, CO (United States)
187. M.U. Afzaal, et al., *Probabilistic Generation Model of Solar Irradiance for Grid Connected Photovoltaic Systems Using Weibull Distribution.* Sustainability, 2020. 12(6).
188. F. Sossan, et al., *Solar irradiance estimations for modeling the variability of photovoltaic generation and assessing violations of grid constraints: A comparison between satellite and pyranometers measurements with load flow simulations.* Journal of Renewable and Sustainable Energy, 2019. 11(5).
189. A. El-Fergany, *Optimal allocation of multi-type distributed generators using backtracking search optimization algorithm.* International Journal of Electrical Power & Energy Systems, 2015. 64: p. 1197-1205.

190. L. Lledó, et al., *Seasonal forecasts of wind power generation.* Renewable Energy, 2019. 143: p. 91-100.
191. A. Bagheri, H. Monsef, and H. Lesani, *Integrated distribution network expansion planning incorporating distributed generation considering uncertainties, reliability, and operational conditions.* International Journal of Electrical Power & Energy Systems, 2015. 73: p. 56-70.
192. Y. Liu, et al. *Study on control characteristic of grid-connected solar photovoltaic plant based on simulation*. in 2015 5th International Conference on Electric Utility Deregulation and Restructuring and Power Technologies (DRPT). 2015.
193. S. Alagammal, N.R. Prabha, and I. Aarthy, *Centralized Solar PV Systems for Static Loads Using Constant Voltage Control Method.* Circuits and Systems, 2016. 07(13): p. 4213-4226.
194. X. Huang, et al., *Research on local voltage control strategy based on high-penetration distributed PV systems.* The Journal of Engineering, 2019. 2019(18): p. 5044-5048.
195. M.S.S. Abad, et al., *Probabilistic Assessment of Hosting Capacity in Radial Distribution Systems.* IEEE Transactions on Sustainable Energy, 2018. 9(4): p. 1935-1947.
196. I. Oladeji, R. Zamora, and T.T. Lie. *Optimal Placement of Renewable Energy Sources Distributed Generation in an Unbalanced Network for Modern Grid Operations*. in International Conference on Smart Energy Systems and Technologies (SEST). 2021.
197. D. Keihan Asl, et al., *Optimal energy flow in integrated energy distribution systems considering unbalanced operation of power distribution systems.* International Journal of Electrical Power & Energy Systems, 2020. 121.
198. C.F. Sabillón, et al., *Mathematical Optimization of Unbalanced Networks with Smart Grid Devices*, in *Electric Distribution Network Planning*. 2018. p. 65-114.
199. J.R. Quinlan*, Decision trees and decision-making*. IEEE Transactions on Systems, Man, and Cybernetics 20.2 (1990): 339-346.
200. L. Vanfretti, and V.S.N. Arava, *Decision tree-based classification of multiple operating conditions for power system voltage stability assessment.* International Journal of Electrical Power & Energy Systems, 2020. 123.
201. A.O. Salau, Y.W. Gebru, and D. Bitew, *Optimal network reconfiguration for power loss minimization and voltage profile enhancement in distribution systems.* Heliyon, 2020. 6(6): p. e04233.
202. A.F. Abdul Kadir, et al., *Optimal placement and sizing of distributed generations in distribution systems for minimizing losses and THD using evolutionary programming.* Turkish Journal of Electrical Engineering & Computer Sciences, 2013. 21: p. 2269-2282.
203. S.A. ChithraDevi, L. Lakshminarasimman, and R. Balamurugan, *Stud Krill herd Algorithm for multiple DG placement and sizing in a radial distribution system.* Engineering Science and Technology, an International Journal, 2017. 20(2): p. 748-759.
204. K. Muthukumar and S. Jayalalitha, *Optimal placement and sizing of distributed generators and shunt capacitors for power loss minimization in radial distribution networks using hybrid heuristic search optimization technique.* International Journal of Electrical Power & Energy Systems, 2016. 78: p. 299-319.
205. K.B. Babu and S. Maheswarapu, *A solution to multi-objective optimal accommodation of distributed generation problem of power distribution networks: An analytical approach.* International Transactions on Electrical Energy Systems, 2019. 29(10).
206. S. Saha and V. Mukherjee, *Optimal placement and sizing of DGs in RDS using chaos embedded SOS algorithm.* IET Generation, Transmission & Distribution, 2016. 10(14): p. 3671-3680.
207. S. Kumar, K.K. Mandal, and N. Chakraborty, *Optimal DG placement by multi-objective opposition based chaotic differential evolution for techno-economic analysis.* Applied Soft Computing, 2019. 78: p. 70-83.
208. R. Yan, et al., *The Anatomy of the 2016 South Australia Blackout: A Catastrophic Event in a High Renewable Network.* IEEE Transactions on Power Systems, 2018. 33(5): p. 5374-5388.
209. D. Stenclik, et al., *Quantifying Risk in an Uncertain Future: The Evolution of Resource Adequacy.* IEEE Power and Energy Magazine, 2021. 19(6): p. 29-36.
210. M. Nagpal, et al., *Lessons Learned From a Regional System Blackout and Restoration in BC Hydro.* IEEE Transactions on Power Delivery, 2018. 33(4): p. 1954-1961.

211. D. Baluev, M. Ali and E. Gryazina, *State of the Art Approach for Comprehensive Power System Security Assessment - Real Case Study.* Available at SSRN, 4250751. 2022.
212. J. McCalley, et al. *Probabilistic security assessment for power system operations*. in IEEE Power Engineering Society General Meeting, IEEE 2004. p. 212-220.
213. H. Li, C. Li, and Y. Liu, *Maximum frequency deviation assessment with clustering based on metric learning.* International Journal of Electrical Power & Energy Systems, 2020. 120.
214. Z. Gong, P. Zhong, and W. Hu, *Diversity in Machine Learning.* IEEE Access, 2019. 7: p. 64323-64350.
215. M. Panteli, and D.S. Kirschen, *Situation awareness in power systems: Theory, challenges and applications.* Electric Power Systems Research, 2015. 122: p. 140-151.
216. J. Geeganage, et al., *Application of Energy-Based Power System Features for Dynamic Security Assessment.* IEEE Transactions on Power Systems, 2015. 30(4): p. 1957-1965.
217. N.V. Tomin, et al., *Machine Learning Techniques for Power System Security Assessment, Endeavour Scholarship and Fellowship program.* IFAC-PapersOnLine, 2016. 49(27): p. 445-450.
218. P. Sekhar and S. Mohanty, *An online power system static security assessment module using multi-layer perceptron and radial basis function network.* International Journal of Electrical Power & Energy Systems, 2016. 76: p. 165-173.
219. Y.-K. Wu, *Frequency Stability for an Island Power System: Developing an Intelligent Preventive-Corrective Control Mechanism for an Offshore Location.* IEEE Industry Applications Magazine, 2017. 23(2): p. 74-87.
220. E.S. Karapidakis, *Machine learning for frequency estimation of power systems.* Applied Soft Computing, 2007. 7(1): p. 105-114.
221. R. Zhang, et al., *Dynamic extreme learning machine and its approximation capability.* IEEE Transactions on Cybernetics, 2013. 43(6): p. 2054-65.
222. Y. Lei, et al., *A Hybrid Regularization Semi-Supervised Extreme Learning Machine Method and Its Application.* IEEE Access, 2019. 7: p. 30102-30111.
223. I.B. Sulistiawati, et al., *Critical Clearing Time prediction within various loads for transient stability assessment by means of the Extreme Learning Machine method.* International Journal of Electrical Power & Energy Systems, 2016. 77: p. 345-352.
224. M. Mohammadi and G.B. Gharehpetian, *On-line transient stability assessment of large-scale power systems by using ball vector machines.* Energy Conversion and Management, 2010. 51(4): p. 640-647.
225. A. Bashiri Mosavi, A. Amiri and H. Hosseini, , *A Learning Framework for Size and Type Independent Transient Stability Prediction of Power System Using Twin Convolutional Support Vector Machine.* IEEE Access, 2018. 6: p. 69937-69947.
226. C. Zheng, V. Malbasa, and M. Kezunovic. *A fast stability assessment scheme based on classification and regression tree*. in *2012 IEEE International Conference on Power System Technology (POWERCON)*. 2012.
227. A.R. Sobbouhi and A. Vahedi, *Transient stability prediction of power system; a review on methods, classification and considerations.* Electric Power Systems Research, 2021. 190.
228. J.L. Cremer and G. Strbac, *A machine-learning based probabilistic perspective on dynamic security assessment.* International Journal of Electrical Power & Energy Systems, 2021. 128.
229. R.J.G.B. Campello, et al., *Density-based clustering.* WIREs Data Mining and Knowledge Discovery, 2019. p. 231–240 10(2).
230. H. Huang, et al., *Robust Bad Data Detection Method for Microgrid Using Improved ELM and DBSCAN Algorithm.* Journal of Energy Engineering, 2018. 144(3).
231. M.M. Farrokhifard, et al., *Clustering of Power System Oscillatory Modes Using DBSCAN Technique*, in 2019 North American Power Symposium (NAPS). 2019. p. 1-6.
232. D. Ruisheng, et al., *Decision Tree-Based Online Voltage Security Assessment Using PMU Measurements.* IEEE Transactions on Power Systems, 2009. 24(2): p. 832-839.
233. M. Negnevitsky, et al. *Preventing large-scale blackouts in power systems under uncertainty*. in 2014 Power Systems Computation Conference. 2014.
234. N. Tong, et al., *Dynamic Model Reduction for Large-Scale Power Systems Using Wide-Area Measurements.* IEEE Access, 2020. 8: p. 97863-97872.
235. S. Wang, J. Yu, and W. Zhang, *Transient Stability Assessment Using Individual Machine*

Equal Area Criterion PART III: Reference Machine. IEEE Access, 2019. 7: p. 80174-80193.
236. I. Egido, et al., *Maximum Frequency Deviation Calculation in Small Isolated Power Systems.* IEEE Transactions on Power Systems, 2009. 24(4): p. 1731-1738.
237. D. J. Shoup, J. J. Paserba and C. W. Taylor, *A survey of current practices for transient voltage dip/sag criteria related to power system stability*, IEEE PES Power Systems Conference and Exposition, 2004., New York, NY, USA, 2004, pp. 1140-1147 vol.2, doi: 10.1109/PSCE.2004.1397688.
238. H. Liu, et al., *Optimal planning of static and dynamic reactive power resources.* IET Generation, Transmission & Distribution, 2014. 8(12): p. 1916-1927.
239. Y. Dai, et al., *Real-time prediction of event-driven load shedding for frequency stability enhancement of power systems.* IET Generation, Transmission & Distribution, 2012. 6(9).
240. P. Dangeti, *Statistics for machine learning*. 2017: Packt Publishing Ltd.
241. T. Jiang, J.L. Gradus, and A.J. Rosellini, *Supervised Machine Learning: A Brief Primer.* Behavior Therapy , 2020. 51(5): p. 675-687.
242. C. Gambella, B. Ghaddar, and J. Naoum-Sawaya, *Optimization problems for machine learning: A survey.* European Journal of Operational Research, 2020.
243. S. Sun, et al., *A Survey of Optimization Methods From a Machine Learning Perspective.* IEEE Transaction of Cybernetics, 2020. 50(8): p. 3668-3681.
244. V. Vapnik, *The nature of statistical learning theory*. 2013: Springer science & business media.
245. M. Kantardzic, *Data mining. Concepts, models, methods, and algorithms*. 2020: Wiley.
246. S. Chander and P. Vijaya, *3 - Unsupervised learning methods for data clustering*, in Artificial Intelligence in Data Mining, Academic Press. 2021, p. 41-64.
247. I.H. Witten, E. Frank, and M.A. Hall, *Data Mining: Practical Machine Learning Tools and Techniques*. 2011: Elsevier Science.
248. R. Garcia-Dias, et al., *Clustering analysis*, Machine learning. Academic Press . 2020. p. 227-247.
249. J. Gandhi, et al., *Comparative Study on Hierarchical and Density based Methods of Clustering using Data Analysis* in International Conference on IoT based Control Networks and Intelligent Systems (ICICNIS 2020). 2020, SSRN.
250. S.B. Kotsiantis, I.D. Zaharakis, and P.E. Pintelas, *Machine learning: a review of classification and combining techniques.* Artificial Intelligence Review, 2007. 26(3): p. 159-190.
251. R. Vilalta, C. Giraud-Carrier, and P. Brazdil, *Meta-Learning - Concepts and Techniques*, in *Data Mining and Knowledge Discovery Handbook*. 2009. p. 717-731.
252. J.P. Monteiro, et al., *Meta-learning and the new challenges of machine learning.* International Journal of Intelligent Systems, 2021. 36(11): p. 6240-6272.
253. S. Aized Amin, and A. Arshad, *Classification Techniques in Machine Learning: Applications and Issues.* Journal of Basic & Applied Sciences, 2017. 13: p. 459-465.
254. S.B. Kotsiantis, I.D. Zaharakis, and P.E. Pintelas, *Machine learning: a review of classification and combining techniques.* Artificial Intelligence Review, 2006. 26(3): p. 159-190.
255. N. Sammaknejad, Y. Zhao, and B. Huang, *A review of the Expectation Maximization algorithm in data-driven process identification.* Journal of Process Control, 2019. 73: p. 123-136.
256. X. Yang, et al., *A Naive Bayesian Wind Power Interval Prediction Approach Based on Rough Set Attribute Reduction and Weight Optimization.* Energies, 2017. 10(11).
257. G. Arcia-Garibaldi, P. Cruz-Romero, and A. Gómez-Expósito, *Future power transmission: Visions, technologies and challenges.* Renewable and Sustainable Energy Reviews, 2018. 94: p. 285-301.
258. M.E. El-hawary, *The Smart Grid—State-of-the-art and Future Trends.* Electric Power Components and Systems, 2014. 42(3-4): p. 239-250.
259. B. Shakerighadi, et al., *A New Guideline for Security Assessment of Power Systems with a High Penetration of Wind Turbines.* Applied Sciences, 2020. 10(9).
260. S. Sridhar, A. Hahn, and M. Govindarasu, *Cyber–Physical System Security for the Electric Power Grid.* Proceedings of the IEEE, 2012. 100(1): p. 210-224.

261. U. Agarwal and N. Jain, *Distributed Energy Resources and Supportive Methodologies for their Optimal Planning under Modern Distribution Network: a Review.* Technology and Economics of Smart Grids and Sustainable Energy, 2019. 4(1).
262. S. Vieira, W.H. L. Pinaya and A. Mechelli, *Main concepts in machine learning*, Machine Learning. Academic Press. 2020. p. 21-44.
263. W. Cai, M. Zhang, and Y. Zhang, *Batch Mode Active Learning for Regression With Expected Model Change.* IEEE Trans Neural Networks and Learning Systems, 2017. 28(7): p. 1668-1681.
264. Q. Yang, Y. Gu, and D. Wu. *Survey of incremental learning*. in 2019 Chinese Control And Decision Conference (CCDC). 2019.
265. M. Sharifzadeh, A. Sikinioti-Lock, and N. Shah, *Machine-learning methods for integrated renewable power generation: A comparative study of artificial neural networks, support vector regression, and Gaussian Process Regression.* Renewable and Sustainable Energy Reviews, 2019. 108: p. 513-538.
266. H. Yang, et al., *PMU-based voltage stability prediction using least square support vector machine with online learning.* Electric Power Systems Research, 2018. 160: p. 234-242.
267. G. Wang, et al., *A short-term voltage stability online prediction method based on graph convolutional networks and long short-term memory networks.* International Journal of Electrical Power & Energy Systems, 2021. 127.
268. W.M. Villa-Acevedo, J.M. López-Lezama, and D.G. Colomé, *Voltage Stability Margin Index Estimation Using a Hybrid Kernel Extreme Learning Machine Approach.* Energies, 2020. 13(4).
269. J. Huang, et al., *Interconnection-level primary frequency control by MBPSS with wind generation and evaluation of economic impacts.* International Journal of Electrical Power & Energy Systems, 2020. 119.
270. M. Dreidy, H. Mokhlis, and S. Mekhilef, *Inertia response and frequency control techniques for renewable energy sources: A review.* Renewable and Sustainable Energy Reviews, 2017. 69: p. 144-155.
271. N.L. Mo, et al., *Data-driven based optimal distributed frequency control for islanded AC microgrids.* International Journal of Electrical Power & Energy Systems, 2020. 119.
272. C. Liu, et al., *Virtual power plants for a sustainable urban future.* Sustainable Cities and Society, 2021. 65.
273. W. Zhong, et al., *Impact of Virtual Power Plants on Power System Short-Term Transient Response.* Electric Power Systems Research, 2020. 189.
274. A. Bolzoni, and R. Perini, *Feedback Couplings Evaluation on Synthetic Inertia Provision for Grid Frequency Support.* IEEE Transactions on Energy Conversion, 2021. 36(2): p. 863-873.
275. S.S. Guggilam, et al., *Optimizing DER Participation in Inertial and Primary-Frequency Response.* IEEE Transactions on Power Systems, 2018. 33(5): p. 5194-5205.
276. K. Singh and Zaheeruddin, *Enhancement of frequency regulation in tidal turbine power plant using virtual inertia from capacitive energy storage system.* Journal of Energy Storage, 2021. 35.
277. D. Feldmann, and R.V. de Oliveira, *Operational and control approach for PV power plants to provide inertial response and primary frequency control support to power system black-start.* International Journal of Electrical Power & Energy Systems, 2021. 127.
278. A. Kasis, E. Devane, I. Lestas, *Primary frequency regulation in power networks with ancillary service from load-side participation*, IFAC-PapersOnLine, 50(1), 4394-4399.
279. Q. Walger, et al., *OPF-based under frequency load shedding predicting the dynamic frequency trajectory.* Electric Power Systems Research, 2020. 189.
280. S. Sarwar, et al., *Application of polynomial regression and MILP for under-frequency load shedding scheme in islanded distribution system.* Alexandria Engineering Journal, 2021.
281. S.S. Silva Jr, and T.M.L. Assis, *Adaptive underfrequency load shedding in systems with renewable energy sources and storage capability.* Electric Power Systems Research, 2020. 189.
282. A. Ketabi, and M. Hajiakbari Fini, *Adaptive underfrequency load shedding using particle swarm optimization algorithm.* Journal of Applied Research and Technology, 2017. 15(1):

p. 54-60.
283. N.M. Sapari, et al., *Application of load shedding schemes for distribution network connected with distributed generation: A review.* Renewable and Sustainable Energy Reviews, 2018. 82: p. 858-867.
284. J. Jallad, et al., *Application of Hybrid Meta-Heuristic Techniques for Optimal Load Shedding Planning and Operation in an Islanded Distribution Network Integrated with Distributed Generation.* Energies, 2018. 11(5).
285. J. Marchgraber, et al., *Comparison of Control Strategies to Realize Synthetic Inertia in Converters.* Energies, 2020. 13(13).
286. J. Lv, M. Pawlak, and U.D. Annakkage, *Prediction of the Transient Stability Boundary Based on Nonparametric Additive Modeling.* IEEE Transactions on Power Systems, 2017. 32(6): p. 4362-4369.
287. L. Su, et al., *Fast frequency response of inverter-based resources and its impact on system frequency characteristics.* Global Energy Interconnection, 2020. 3(5): p. 475-485.
288. Y. Yu, et al., *Theory and Method of Power System Integrated Security Region Irrelevant to Operation States: An Introduction.* Engineering, 2020. 6(7): p. 754-777.
289. Photovoltaics, Distributed Generation, and Energy Storage. *IEEE standard for interconnection and interoperability of distributed energy resources with associated electric power systems interfaces*. IEEE Std 1547 (2018): 1547-2018..
290. I. Muzaffer and M. ud din Mufti, *Modeling of a multi-machine system aided with power system stabilizers and shunt compensator for transient stability enhancement*. in 2017 International Conference on Energy, Communication, Data Analytics and Soft Computing (ICECDS). 2017.
291. S.C. Hoi, et al., *Online learning: A comprehensive survey.* Neurocomputing 459 (2021): p. 249-289.
292. Y. Luo, et al., *An Appraisal of Incremental Learning Methods.* Entropy, 2020. 22(11), 1190.
293. J. Zhong, et al. *A Survey on Incremental Learning.* in 5th International Conference on Computer, Automation and Power Electronics (CAPE 2017).
294. S. Ren, Y. Lian, and X. Zou, *Incremental Naïve Bayesian Learning Algorithm based on Classification Contribution Degree.* Journal of Computers, 2014. 9(8).
295. A. Cervantes, et al., *Evaluating and Characterizing Incremental Learning from Non-Stationary Data.* arXiv preprint arXiv:1806.06610.
296. S. Chapaneri, R. Lopes, and D. Jayaswal, *Evaluation of Music Features for PUK Kernel Based Genre Classification.* Procedia Computer Science, 2015. 45: p. 186-196.
297. G. Vo and D. Pati, *Sparse Additive Gaussian Process with Soft Interactions.* Open Journal of Statistics, 2017. 07(04): p. 567-588.
298. F. Capitanescu, *TSO–DSO interaction: Active distribution network power chart for TSO ancillary services provision.* Electric Power Systems Research, 2018. 163: p. 226-230.
299. A. Saint-Pierre and P. Mancarella, *Active Distribution System Management: A Dual-Horizon Scheduling Framework for DSO/TSO Interface Under Uncertainty.* IEEE Transactions on Smart Grid, 2017. 8(5): p. 2186-2197.
300. S. Impram, S.V Nese, and B. Oral, *Challenges of renewable energy penetration on power system flexibility: A survey.* Energy Strategy Reviews, 2020. 31.
301. H. Sæle, et al. *Utilization of distributed energy resources' flexibility in power system operation – Evaluation of today's status and description of a future concept*. in *2018 53rd International Universities Power Engineering Conference (UPEC)*. 2018.
302. A. Ulbig, S. Koch, and G. Andersson, *The Power Nodes Modeling Framework –Modeling and Assessing the Operational Flexibility of Hydro Power Units*, in *Symposium Of Specialists In Electric Operational And Expansion Planning*. 2012: Brazil.
303. D. Wu, et al., *Distributed Optimal Coordination for Distributed Energy Resources in Power Systems.* IEEE Transactions on Automation Science and Engineering, 2017. 14(2): p. 414-424.
304. A. Ghafouri, J. Milimonfared, and G.B. Gharehpetian, *Coordinated Control of Distributed Energy Resources and Conventional Power Plants for Frequency Control of Power Systems.* IEEE Transactions on Smart Grid, 2015. 6(1): p. 104-114.
305. J. Fradley, R. Preece, and M. Barnes, *The Influence of Network Factors on Frequency*

Stability. IEEE Transactions on Power Systems, 2020. 35(4): p. 2826-2834.
306. V.V.S.N. Murty Vallem and A. Kumar. *Impact of Reconfiguration and Network Topology on Voltage Stability Margin*. in *Advances in Smart Grid Automation and Industry 4.0*. 2021. Singapore: Springer Singapore.
307. Y. Song, D.J. Hill, and T. Liu, *Static Voltage Stability Analysis of Distribution Systems Based on Network-Load Admittance Ratio.* IEEE Transactions on Power Systems, 2019. 34(3): p. 2270-2280.
308. R. Gupta, F. Sossan, and M. Paolone, *Countrywide PV hosting capacity and energy storage requirements for distribution networks: The case of Switzerland.* Applied Energy, 2021. 281.
309. O. Badran, et al., *Optimal reconfiguration of distribution system connected with distributed generations: A review of different methodologies.* Renewable and Sustainable Energy Reviews, 2017. 73: p. 854-867.
310. L.H. Macedo, et al., *Short-circuit constrained distribution network reconfiguration considering closed-loop operation.* Sustainable Energy, Grids and Networks, 2022. 32.
311. O. Kahouli, et al., *Power System Reconfiguration in Distribution Network for Improving Reliability Using Genetic Algorithm and Particle Swarm Optimization.* Applied Sciences, 2021. 11(7).
312. R. Rajaram, K. Sathish Kumar, and N. Rajasekar, *Power system reconfiguration in a radial distribution network for reducing losses and to improve voltage profile using modified plant growth simulation algorithm with Distributed Generation (DG).* Energy Reports, 2015. 1: p. 116-122.
313. R. Chidanandappa, T. Ananthapadmanabha, and R. H.C, *Genetic Algorithm Based Network Reconfiguration in Distribution Systems with Multiple DGs for Time Varying Loads.* Procedia Technology, 2015. 21: p. 460-467.
314. S. Ching-Tzong and L. Chu-Sheng, *Network reconfiguration of distribution systems using improved mixed-integer hybrid differential evolution.* IEEE Transactions on Power Delivery, 2003. 18(3): p. 1022-1027.
315. M. Rahmani-Andebili, *Dynamic and adaptive reconfiguration of electrical distribution system including renewables applying stochastic model predictive control.* IET Generation, Transmission & Distribution, 2017. 11(16): p. 3912-3921.
316. H. Salimi, *Stochastic Fractal Search: A powerful metaheuristic algorithm.* Knowledge-Based Systems, 2015. 75: p. 1-18.
317. J. Zhu, et al., *A rule based comprehensive approach for reconfiguration of electrical distribution network.* Electric Power Systems Research, 2009. 79(2): p. 311-315.
318. S. Mishra, D. Das, and S. Paul, *A comprehensive review on power distribution network reconfiguration.* Energy Systems, 2016. 8(2): p. 227-284.
319. M.A.T.G Jahani, et al., *Multi-objective optimization model for optimal reconfiguration of distribution networks with demand response services.* Sustainable Cities and Society, 2019. 47: p. 101514.
320. A.E.B. Abu-Elanien, M.M.A. Salama, and K.B. Shaban, *Modern network reconfiguration techniques for service restoration in distribution systems: A step to a smarter grid.* Alexandria Engineering Journal, 2018. 57(4): p. 3959-3967.
321. Q. Shi, et al., *Network reconfiguration and distributed energy resource scheduling for improved distribution system resilience.* International Journal of Electrical Power & Energy Systems, 2021. 124.
322. K.M.C. Atendido and R. Zamora. *Reconfiguration and load shedding for resilient and reliable multiple microgrids*. in *2017 IEEE Innovative Smart Grid Technologies - Asia (ISGT-Asia)*. 2017.
323. F.N. Lima, et al., *Power Distribution Network Reconfiguration Considering the Transmission System Usage.* IEEE Latin America Transactions, 2021. 19(12): p. 2113-2121.
324. C. Lee, et al., *Robust Distribution Network Reconfiguration.* IEEE Transactions on Smart Grid, 2015. 6(2): p. 836-842.
325. Wang, H.-J., et al., *Distribution network reconfiguration with distributed generation based on parallel slime mould algorithm.* Energy, 2022. 244.
326. H.F. Zhai, et al., *Dynamic reconfiguration of three-phase unbalanced distribution networks.* International Journal of Electrical Power & Energy Systems, 2018. 99: p. 1-10.

327. Q.-V. Pham, et al., *Swarm intelligence for next-generation networks: Recent advances and applications.* Journal of Network and Computer Applications, 2021. 191.
328. X.-S Yang, and S. Deb, *Multiobjective cuckoo search for design optimization.* Computers & Operations Research, 2013. 40(6): p. 1616-1624.
329. V. Fathi, , H. Seyedi, and B.M. Ivatloo, *Reconfiguration of distribution systems in the presence of distributed generation considering protective constraints and uncertainties.* International Transactions on Electrical Energy Systems, 2020. 30(5).
330. J.C. López, et al., *Robust optimisation applied to the reconfiguration of distribution systems with reliability constraints.* IET Generation, Transmission & Distribution, 2016. 10(4): p. 917-927.
331. S. Ghasemi, *Balanced and unbalanced distribution networks reconfiguration considering reliability indices.* Ain Shams Engineering Journal, 2018. 9(4): p. 1567-1579.
332. M. Rossi, et al., *Fast estimation of equivalent capability for active distribution networks.* CIRED - Open Access Proceedings Journal, 2017. 2017(1): p. 1763-1767.
333. H. Le Cadre, I. Mezghani, and A. Papavasiliou, *A game-theoretic analysis of transmission-distribution system operator coordination.* European Journal of Operational Research, 2019. 274(1): p. 317-339.
334. D.A. Contreras and K. Rudion. *Improved Assessment of the Flexibility Range of Distribution Grids Using Linear Optimization*. in *2018 Power Systems Computation Conference (PSCC)*. 2018.
335. Z. Kaheh, R.B. Kazemzadeh, and M.K. Sheikh-El-Eslami, *Flexible Ramping Services in Power Systems: Background, Challenges, and Procurement Methods.* Iranian Journal of Science and Technology, Transactions of Electrical Engineering, 2020. 45(1): p. 1-13.
336. R. Vijay and P. Mathuria, *Complex Power Flexibility Evaluation using Energy Arbitrage between Transmission and Distribution.* Electric Power Systems Research, 2022. 203.
337. S. Riaz and P. Mancarella. *On Feasibility and Flexibility Operating Regions of Virtual Power Plants and TSO/DSO Interfaces*. in *2019 IEEE Milan PowerTech*. 2019.
338. H. Nosair and F. Bouffard, *Energy-Centric Flexibility Management in Power Systems.* IEEE Transactions on Power Systems, 2016. 31(6): p. 5071-5081.
339. S. Yamujala, et al., *Enhancing power systems operational flexibility with ramp products from flexible resources.* Electric Power Systems Research, 2022. 202.
340. M. Heleno, et al. *Estimation of the flexibility range in the transmission-distribution boundary*. in *2015 IEEE Eindhoven PowerTech*. 2015.
341. J. Aghaei, et al., *Contribution of Plug-in Hybrid Electric Vehicles in power system uncertainty management.* Renewable and Sustainable Energy Reviews, 2016. 59: p. 450-458.
342. B. Abdolmaleki, and Q. Shafiee, *Online Kron Reduction for Economical Frequency Control of Microgrids.* IEEE Transactions on Industrial Electronics, 2020. 67(10): p. 8461-8471.
343. F. Capitanescu, *OPF Integrating Distribution Systems Flexibility for TSO Real-Time Active Power Balance Management*, in *MEDPOWER 2018*. 2018: Cavtat (Croatia).
344. J. Silva, et al., *The challenges of estimating the impact of distributed energy resources flexibility on the TSO/DSO boundary node operating points.* Computers & Operations Research, 2018. 96: p. 294-304.
345. E. Dall'Anese, et al., *Optimal Regulation of Virtual Power Plants.* IEEE Transactions on Power Systems, 2018. 33(2): p. 1868-1881.
346. H. Alsalloum, et al., *Hierarchical system model for the energy management in the smart grid: A game theoretic approach.* Sustainable Energy, Grids and Networks 2020. 21: p. 100329.
347. B. Görgülü, and M.G. Baydoğan, *Randomized trees for time series representation and similarity.* Pattern Recognition, 2021. 120.
348. A. James, et al., *Unions of random trees and applications.* Discrete Mathematics, 2021. 344(3).
349. M. Sedighizadeh, et al., *Optimal distribution feeder reconfiguration and generation scheduling for microgrid day-ahead operation in the presence of electric vehicles considering uncertainties.* Journal of Energy Storage, 2019. 21: p. 58-71.
350. R. Pegado, et al., *Radial distribution network reconfiguration for power losses reduction*

based on improved selective BPSO. Electric Power Systems Research, 2019. 169: p. 206-213.
351. M. Mohammadpoor, R. Ranjkeshan, and A. Mehdizadeh, *A Multi-objective Distribution Network Reconfiguration and Optimal Use of Distributed Generation Unites by Harmony Search Algorithm*, in *Fundamental Research in Electrical Engineering*. 2019. p. 997-1008.
352. D. Anteneh, et al., *Distribution network reliability enhancement and power loss reduction by optimal network reconfiguration.* Computers & Electrical Engineering, 2021. 96.
353. B. Stojanović, T. Rajić, and D. Šošić, *Distribution network reconfiguration and reactive power compensation using a hybrid Simulated Annealing – Minimum spanning tree algorithm.* International Journal of Electrical Power & Energy Systems, 2023. 147.
354. J.-S. Pan, et al., *Dynamic reconfiguration of distribution network based on dynamic optimal period division and multi-group flight slime mould algorithm.* Electric Power Systems Research, 2022. 208.
355. S. Malekshah, et al., *Reliability-driven distribution power network dynamic reconfiguration in presence of distributed generation by the deep reinforcement learning method.* Alexandria Engineering Journal, 2022. 61(8): p. 6541-6556.
356. R. Fathi, B. Tousi, and S. Galvani, *Allocation of renewable resources with radial distribution network reconfiguration using improved salp swarm algorithm.* Applied Soft Computing, 2023. 132.
357. V.-H. Bui, and W. Su, *Real-time operation of distribution network: A deep reinforcement learning-based reconfiguration approach.* Sustainable Energy Technologies and Assessments, 2022. 50.
358. H. Teimourzadeh, and B. Mohammadi-Ivatloo, *A three-dimensional group search optimization approach for simultaneous planning of distributed generation units and distribution network reconfiguration.* Applied Soft Computing, 2020. 88.
359. R.V.A. Monteiro, et al., *Electric distribution network reconfiguration optimized for PV distributed generation and energy storage.* Electric Power Systems Research, 2020. 184.
360. T.T. Nguyen, and T.T. Nguyen, *An improved cuckoo search algorithm for the problem of electric distribution network reconfiguration.* Applied Soft Computing, 2019. 84.